BICYCLIC STRAINED ALLENES: INCORPORATION OF AN ALLENE UNIT INTO ALPHA-PINENE AND BENZONORBORNADIENE

A THESIS SUBMITTED TO
THE GRADUATE SCHOOL OF NATURAL AND APPLIED SCIENCES
OF
MIDDLE EAST TECHNICAL UNIVERSITY

BY

AKIN AZÝZOĐLU

IN PARTIAL FULFILLMENT OF THE REQUIREMENTS FOR THE DEGREE
OF
DOCTOR OF PHILOSOPHY
IN
CHEMISTRY

JUNE 2004

Approval of the Graduate School of Natural and Applied Sciences

Prof. Dr. Canan Özgen

Director

I certify that this thesis satisfies all the requirements as a thesis for the degree of Doctor of Philosophy.

Prof. Dr. Hüseyin Ýþçi

Head of Department

This is to certify that we have read this thesis and that in our opinion it is fully adequate, in scope and quality, as a thesis for the degree of Doctor of Philosophy.

Prof. Dr. Metin Balcý

Supervisor

Examining Committee Members

Prof. Dr. Ayhan S. Demir (METU, CHEM) _____

Prof. Dr. Metin Balcý (METU, CHEM) _____

Prof. Dr. Cihangir Tanyeli (METU, CHEM) _____

Prof. Dr. Canan Ünaleroðlu (HACETTEPE UNIV., CHEM) _____

Prof. Dr. Basri Atasoy (GAZÝ UNIV.,CHEM EDUC) _____

I hereby declare that all information in this document has been obtained and presented in accordance with academic rules and ethical conduct. I also declare that, as required by these rules and conduct, I have fully cited and referenced all material and results that are not original to this work.

Name, Last name : AKIN AZÝZOĐLU

Signature :

ABSTRACT

BICYCLIC STRAINED ALLENES:
INCORPORATION OF AN ALLENE UNIT INTO
ALPHA PINENE
AND
BENZONORBORNADIENE

Azizoðlu, Akýn

Ph.D., Department of Chemistry
Supervisor: Prof. Dr. Metin Balcý
June 2004, 221 pages

The first part of study describes an investigation aimed at the incorporation of an allene unit into a natural compound, being alpha-pinene, by using Doering-Moore-Skatteboel method. DFT computations show that both allene product and insertion product can be isolated if the reaction of methyllithium with 3,3-dibromo-2,7,7-trimethyl-tricyclo[4.1.1.$0^{2,4}$]octane is carried out at either low or high temperatures. One insertion product resulting from the intramolecular C-H insertion at the bridge and three allene dimers were isolated when this reaction was carried out at room temperature.

In the second part of study, *exo*- and *endo*-cyclopropylidene incorporated into benzonorbornadiene were investigated by using theoretical and experimental methods. Theoretical calculations show that the *endo*-carbene would be stable and undergo some kind of insertion and addition reactions. On the contrary, the exo-carbene is not stable and isomerizes to the corresponding allene structure during the optimization process.

For this purpose, the reaction of dibromocarbene and dichlorocarbene with 7-methoxybenzonorbornadiene was achieved to afford *gem*-dibromocyclopropane and *gem*-dichlorocyclopropane adducts, respectively. However, they suffer stereoelectronically-controlled ring opening under the reaction conditions to give the ring-expanded allylic dihalides, respectively.

On the other hand, *gem*-bromofluorocyclopropane, obtained by the treatment of 7-methoxybenzonorbornadiene with bromofluorocarbene, provided one of the four possible [2+4] allene adducts upon treatment with MeLi in furan. The exact structure of the adduct has been elucidated on the basis of NMR spectral data. This result confirms the formation of the bicyclic allene as an reactive intermediate. No products were isolated derived from the *endo*-carbene.

Keywords: Allene, Bicyclic Allene, Cyclodimerization, Carbene, Insertion, Alpha-pinene, Doering-Moore-Skattebol Method, Benzonorbornadiene, Solvolysis, Bromination, Elimination, DFT Method, Theoretical Calculations.

ÖZ

BÝSÝKLÝK GERÝLÝMLÝ ALLENLER:
ALLEN BÝRÝMÝNÝN ALFA-PÝNEN
VE
BENZONORBORNADÝEN
MOLEKÜLLERÝNE DAHÝL EDÝLMESÝ

Azizoðlu, Akýn

Doktora, Kimya Bölümü
Tez Yöneticisi: Prof. Dr. Metin Balcý
Haziran 2004, 221 sayfa

Çalýþmamýzýn birinci bölümünde, Doering-Moore-Skattebol yöntemini kullanarak, doðal bir bileþik olan alfa-pinen içerisinde allen biriminin oluþturulmasý amaçlanmýþtýr. DFT hesaplarýna göre, eðer 3,3-dibrom-2,7,7-trimetil-trisiklo[4.1.1.$0^{2,4}$]oktan ile metillityum reaksiyona sokulursa, allen ve insersiyon ürünleri izole edilecektir. Bu reaksiyon oda sýcaklýðýnda yapýldýðýnda, köprü konumunda molekül içi C-H insersiyon reaksiyonu sonucu oluºan ürün ile üç tane allen dimeri elde edilmiºtir.

Çalýþmamýzýn ikinci bölümünde ise, benzonorbornadien molekülünde oluºturulan *exo*- ve *endo*-siklopropilidenler, teorik ve deneysel olarak incelenmiºtir. Teorik hesaplar sonucunda, *endo*-karbenin kararlý olacaðý ve bazý insersiyon ve katýlma reaksiyonlarýnýn verebileceði bulunmuþtur. Bununla birlikte, *exo*-karbenin kararlý olmadýðý ve optimizasyon iþlemi esnasýnda ilgili allen yapýsýna dönüþtüðü bulunmuºtur.

Bu amaçla, 7-methoksibenzonorbornadien ile dibromkarben ve diklorkarbenin reaksiyonlarý, *gem*-dibromsiklopropiliden ve *gem*-diklorsiklopropilideni sentezlemek amacýyla gerçekleþtirilmiþtir. Fakat, reaksiyon esnasýnda bu bileþikler steroelektronik kontrollü olarak açýlmýþ ve halka geniþleyerek alilik dihalojenleri vermiºtir.

Bununla birlikte, 7-methoksibenzonorbornadien ile bromflorkarbenin reaksiyonu *gem*-bromflorsiklopropilideni vermiºtir. Elde edilen bileºik metillityum ile furan içerisinde reaksiyona sokuldu. Oluþan allen ve ortamdaki furanýn [2+4]-siklokatýlma reaksiyonun sonucu olan tek bir ürün elde edildi. Bu sonuç, bisiklik allenin reaktif ara ürün olarak oluþtuðunu göstermektedir. *Endo*-karbenden oluºan hiç bir ürün izole edilememiºtir.

Anahtar Kelimeler: Allen, Bisiklik Allen, Siklodimerleºme, Karben, Insersiyon, Alfa-pinen, Doering-Moore-Skattebol metodu, Benzonorbornadien, Solvoliz, Brominasyon, Eliminasyon, DFT metodu, Teorik hesaplar.

To my wife Nursen and my daughter Ece

ACKNOWLEDGEMENTS

I would like to express my sincere thanks to my supervisor Prof. Dr. Metin Balcý for his continuous guidance, endless support, patience and encouragement throught this work.

My extensive thanks are offered to Assist. Prof. Dr. Recep Özen for his endless help, comments and close interest as a friend.

Thanks also extended to Fatih Algý for his unique friendship, help and comments.

I wish to express my thanks to NMR specialist Fatoº Polat Doðanel for the perfect NMR spectra.

I would like to thank to Prof. Dr. Ayhan S. Demir who let us to get GC/MS spectra and his skillful assistant Ömer Reis for taking these spectra.

I also give my thanks to the members of our research group; SYNTHOR.

Finally, my special appreciation and great gratitude is devoted to my wife Nursen Azizoðlu for her endless love, patience, moral support and encouregement in every moment of our life.

TABLE OF CONTENTS

LIST OF TABLES

LIST OF FIGURES

LIST OF ABBREVIATIONS

AM1	: Austin model 1
B3LYP	: Becke 3 parameter functional and Lee, Yang, Parr correlation functional
CI	: Configuration interaction
COSY	: Correlation spectroscopy
DEPT	: Distortionless enhancement by polarization transfer
DFT	: Density functional theory
DMSO	: Dimethylsulfoxide
DPIBF	: Diphenylisobenzofuran
DZP	: Double zeta plus polarization
FORS	: Full optimized reaction space
GC/MS	: Gas chromatography and mass spectrum
HBr	: Hydrogen bromide
HMBC	: Heteronuclear multi-bond coherence
HMQC	: Heteronuclear multiple quantum coherence
Hz	: Hertz
IR	: Infrared
IUPAC	: International union of pure and applied chemistry
J	: Coupling constant
k	: Rate constant
KO*t*Bu	: Potassium *tert*-butoxide
MCSCF	: Multi-configuration self-consistent field
MeLi	: Methyllithium
MNDO	: Modified neglect of diatomic overlap
MO	: Molecular orbital
n-BuLi	: *n*-Butyllithium
NMR	: Nuclear magnetic resonance
PM3	: Parametric method number 3
PM5	: Parametric method number 5

ppm : parts per million

RE : Relative energy

SCF : Self-consistent field

T : Temperature

TCNE : Tetracyanoethylene

THF : Tetrahydrofuran

TS : Transition structure

TZP : Triple zeta plus polarization

UV : Ultra-violet

ZPVE : Zero-point vibrational energy

CHAPTER 1

INTRODUCTION

Dienes are unsaturated hydrocarbons, which contain two double bonds and there are three broad classes of them; isolated, conjugated and cumulated dienes (Figure1).

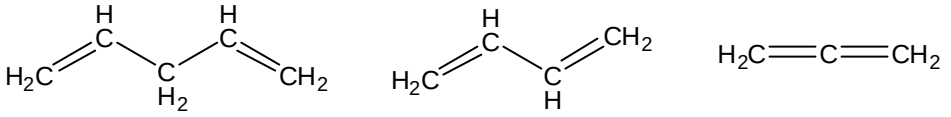

Isolated diene Conjugated diene Cumulated diene

Figure 1: Diene classes

In isolated dienes, the double bonds are separated by at least one sp^3-hybridized carbon, and each is essentially independent of the other, so that reactivity and stability are about the same as ordinary alkenes. In conjugated dienes, two double-bonded carbons, sp^2-hybridized, are directly bonded to each other. This affects stability and reactivity. Conjugated dienes are thermodynamically more stable than isolated ones, that is; equilibrium favours the conjugated isomers.

The dienes in which two double bonds share a single carbon, sp-hybridized as in alkynes, are called ‘Allenes’ or ‘Cumulenes’ and these kinds of double bonds are named as ‘Cumule double bonds’ (Figure 2). They are thermodynamically less stable than isolated dienes and often may react much more readily than ordinary alkenes. They resemble isolated and conjugated dienes only in view of chemical formulas [1].

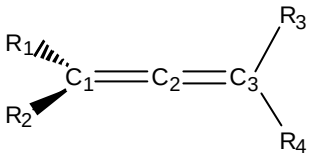

Figure 2: General structure of an allene

The normal allene linkage requires a fixed geometrical arrangement of seven atoms, with open chain allenes having a linear structure and two orthogonal π-bonds. In the π-bond structure of allene, the plane defined by R_1, R_2, C_1 and C_2 is perpendicular to that defined by R_3, R_4, C_3 and C_2. As can be seen from Figure 3, they form two orthogonal planes intersected in C_2. For that reason, these two double bonds are not in the same plane and they are not conjugated with each other [2].

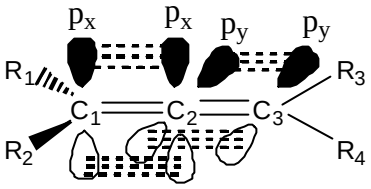

Figure 3: π-bond orbital structure of allene

The π-bond lengths of allenes are shorter than the other olefins. For instance, in ethylene the π-bond length is 1,33 Å whereas in allenes it is between 1,309 and 1,312 Å. The reason is the linear geometry arising from the sp hybridization of the central atom and the excess amount of *s* character in the hybridization [3]. These properties of allenes affect their IR and ^{13}C-NMR spectra. The vibration of π-bonds in alkenes is around 1650 cm^{-1} whereas it is between 1900-2000 cm^{-1} in allenes. The signal at 850 cm^{-1} is the characteristics of 1,1-disubstituted allenes [4,5]. Moreover, ^{13}C-NMR spectra of allenes indicate that the central carbon atom, C_2, resonates around 201-220 ppm whereas olefinic carbons resonate around 120-140 ppm [6]. These observations had been related to theory by Pople [7].

As can be seen from Figure 3, $R_1R_2C_1$ and $R_3R_4C_3$ atom groups are perpendicular to each other and they form orthogonal planes intersected in C_2. Therefore, allene gains the optical activity if one of the substituents attached to terminal carbon is different. The same is true for all cumulenes, which have an even

number of double bonds [8]. Chiral allenes are present in nature. Indeed, recently two bromoallenic aliphatic fatty acids (Figure 4) were found and isolated from lichens collected around Central Asia [9]. The C_{15} bromoallenes, dactylallene and obtusallene, were isolated from the digestive gland of the anaspidean mollusk *Aplysia dactylomela* and from the red algae *Laurencia obtuse* [9].

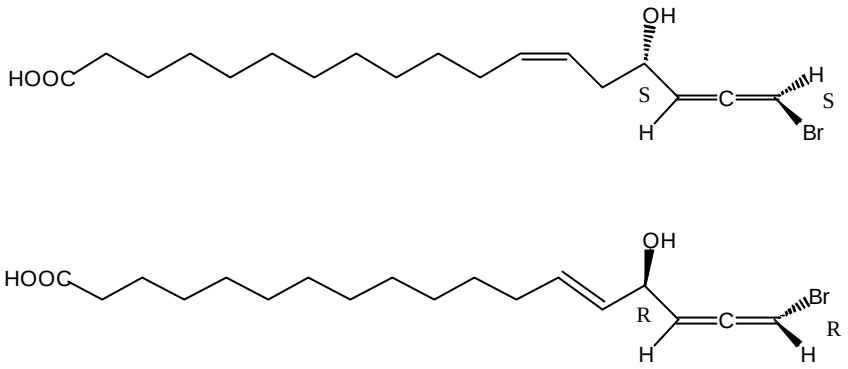

Figure 4: Chiral two bromoallenic aliphatic fatty acids

1.1 STRAINED CYCLIC ALLENES

The equilibrium geometry for allenes is linear and they are not inherently "strained". Strain implies some deviation from an ideal bonding geometry; this is not true for compounds which contain ordinary sp- and sp^2-hybridized carbons. However, the electronic structure of allenes and their ability to form stabilized intermediates do render them highly reactive and many allenes dimerize easily. As with cycloalkenes and cycloalkynes, ring constraints in cyclic allenes cause increasing angle strain as the ring size diminishes from n=6 to 1. Ring constraints bend the allene and exert torsion a planar arrangement of ligands. Bending also destroys the degeneracy of π and π^* orbitals; correlation with orbitals of planar allene. Therefore, cyclic allenes further demonstrate the remarkable tenacity of π-bonding.

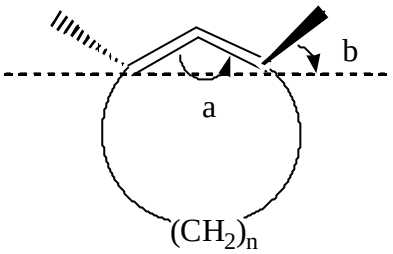

a= bending angle
b= torsional angle

Figure 5: Bending and torsional angles in cyclic allenes

Bending and torsional angles in cyclic allenes make them unisolable and highly reactive intermediates (Figure 5). Due to that, the synthesis, isolation and trapping of cyclic-strained allenes have been attracting more and more interest in the past few decades [10-12]. Besides the synthesis, these compounds have been subject of several theoretical investigations [13-29].

Molecular models suggest that allene can be included in only ten-membered or larger rings without distortion. If the ring size is decreased, it becomes necessary to deform the allene linkage in order to close the ring. In the rings of nine or fewer, there should be increasing strain as the allene becomes bent. Theoretical calculations with semiemprical [23] and ab-initio [25] methods show that the bending potential is remarkably soft for the first 20^0, resulting in only 4 kcal/mol estimated strain, but rises rapidly beyond this point. Therefore, crude strain estimations for five to eight membered ring allenes are 30, 20, 15, 10 kcal/mol, respectively. These values were first reported by Gasteiger and Dammer [26]. Because bent, planar allene should be unstrained by ring constraints, the maximum strain that might be accommodated by an allene unit must be ca. 46 kcal/mol, which corresponds to the ground state rotational barrier. Comparison of this value with ab initio predictions for the barrier in **4** and **5** permitted strain estimates of 41 and 31 kcal/mol, respectively [24, 27].

Bending angles and out of plane torsional angles calculated by MNDO method are given in Figure 6. Other calculation methods yield similar results [12].

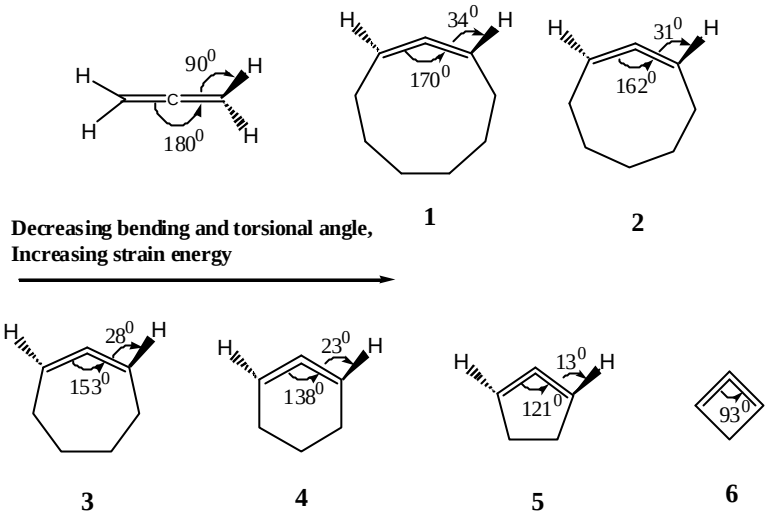

Figure 6: Predicted angles by using MNDO method

1.1.1 Cyclonona-1,2-diene and Its Derivatives

Cyclonona-1,2-diene (**1**), with its allenic chromophore bent ca. 10^0 from linearity, is the smallest unsubstituted cyclic allene which is kinetically stable at ambient temperature. It, the best studied cyclic allene, was first synthesized in 1951 by Blomquist and co-workers [30]. As later shown by Skattebøl, this compound is easily prepared in high yield by ring expansion of cyclooctene (**7**) [31]. Allene **1** dimerizes upon heating. This general two-step approach, known as "Doering-Moore-Skattebøl method" [32], continues to be widely applied to cyclic allene synthesis.

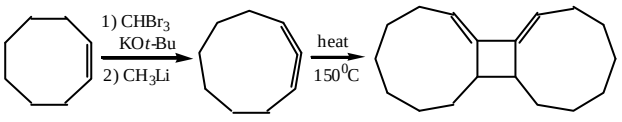

However, Christl *et al.* [33] reported that 1-phenylcyclonona-1,2-diene which has been generated by application of this method to 1-phenylcyclooctene dimerizes slowly at room temperature to give *cis*- and *trans*-**11** in a 1:1 ratio. In other word, the phenyl group decreases the stability of formed allene (**10**).

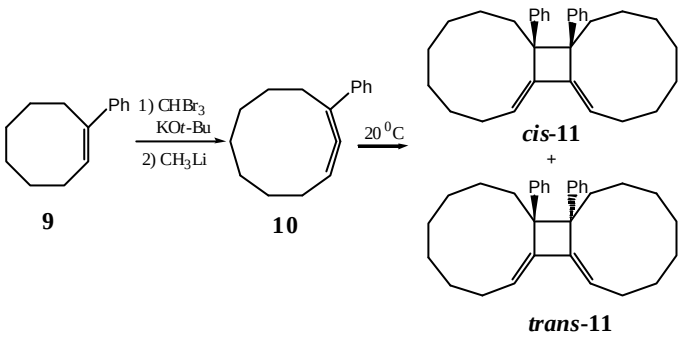

Moreover, unsaturated derivatives of **1** are more reactive. In 1976, Baird and Reese reported that allene **12** shown in Figure 7 dimerizes with a half-life of ca. 10 min. at 0 ^{0}C. Enhanced reactivity of **12** is probably due to increased ring strain caused by the additional double bonds [34].

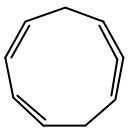

12

Figure 7: Unsaturated Derivative of Cyclonona-1,2-diene (**1**)

Stable cyclo-1,2-dienes can be converted into synthetically promising compounds. For instance, it has been demonstrated recently that the reaction of parent cyclonona-1,2-diene (**1**) with Sn_2Me_6 and [$Pd(Ph)_4$] in the absence of solvent at 80 ^{0}C provides in excellent yield *cis*- and *trans*-**13**. These compounds furnish useful doubly functionalized medium-ring cycloalkenes [35].

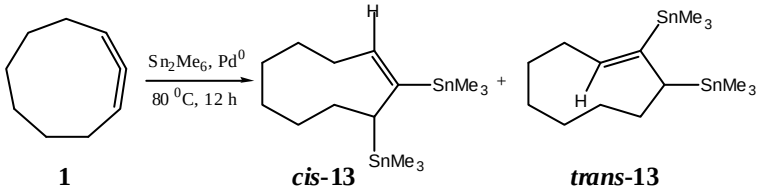

Furthermore, the photochemistry of cyclonona-1,2-diene (**1**) was studied by Ward and Karafiath [36] who showed that benzene-sensitized irradiation in the vapour phase resulted in the formation of **15** while direct irradiation furnished four C_9 isomers from which only **15** was characterized. Gilbert *et al.* [37] reported the formation of **18** and **19** in benzene solution. However, Stierman and Johnson [38]

reinvestigated the photochemical reaction of **1** and characterized other products as bicyclo[6.1.0]non-9-ene (**16**) and cyclononyne (**17**).

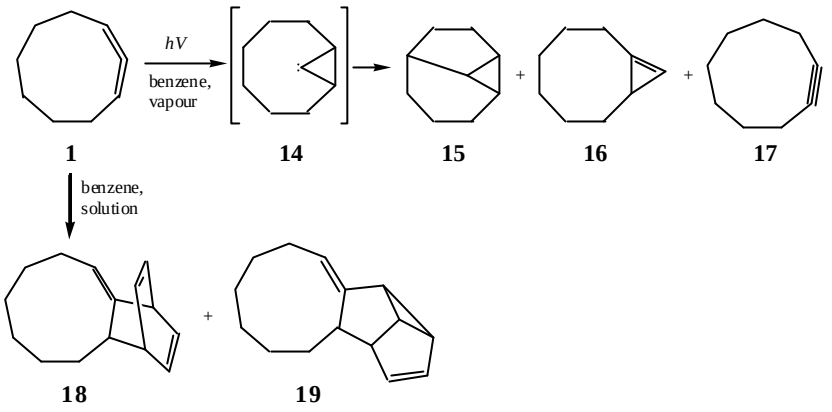

1 **14** **15** **16** **17**

18 **19**

Recently, Johnson *et al.* [39] have reported the photoreaction of 1-methylcyclonona-1,2-diene (**20**), which was synthesized by the Doering-Moore-Skattebøl method, for the determination of the substituent effect on the mechanism. Direct irradiation of **20** afforded as primary products the seven isomers **21**-**27**. In contrast to the apparently concerted reaction of **1**, methyl derivative **20** seems to favour vinylcarbene intermediates.

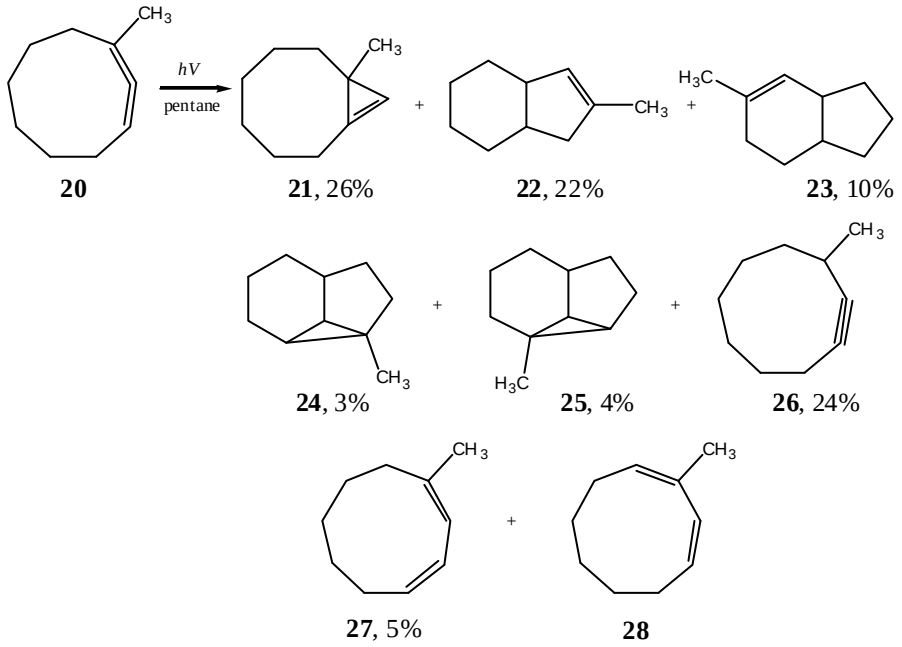

20 **21**, 26% **22**, 22% **23**, 10%

24, 3% **25**, 4% **26**, 24%

27, 5% **28**

1.1.2. Cycloocta-1,2-diene and Its Derivatives

The cycloocta-1,2-diene (**2**) was first synthesized in 1961 by Ball and Landor [40] who reported that it undergoes rapid dimerization to dimer **30** which is isolated from the dehydrohalogenation of 1-chlorocyclooctene **29**. The facile dimerization of strained allenes, such as **2**, doubtless results from twofold strain release upon C_2-C_2 bonding. Wittig [41] performed the same reaction several years later and also succeeded in trapping **2** with DPIBF to yield **33**. Marquis and Gardner have applied the carbenoid route for the syntheses of **2** with dibromocarbene adduct **42** and methylithium in high yield [42]. This strained allene readily dimerizes, but cold, dilute solutions are suitable for rapid IR and NMR spectrum analysis [43]. The IR stretching frequency is 1950 cm^{-1}, only slightly reduced from 1956 cm^{-1} in **1**. Theoretical calculations support the expectation that allene vibrational frequencies should decrease with bending [12]. Angus and Johnson [44] have also found it feasible to add dibromocarbene to **2** at low temperature. More novel approach to the synthesis of **2** has been reported by Kropp *et al.* [45]. They suggested that **2** as an intermediate in photolysis of vinyl iodide **32** in methanol.

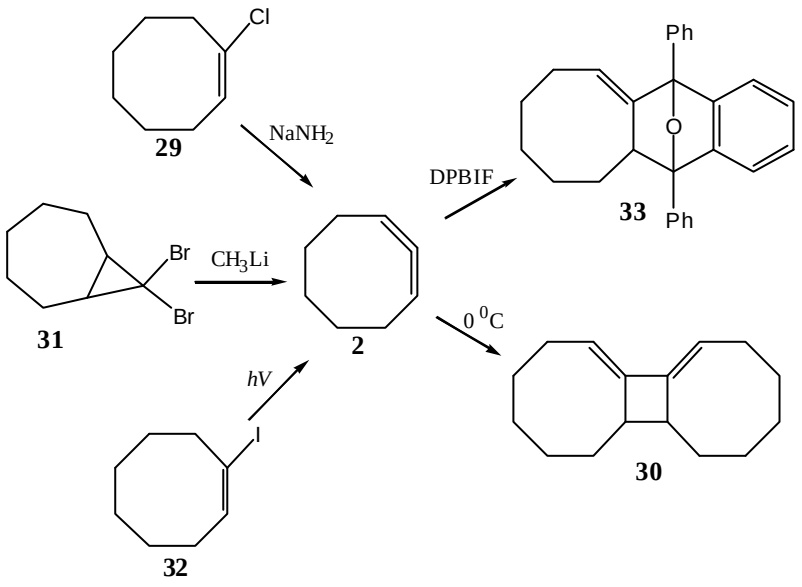

An interesting cycloocta-1,2-diene derivative is **35** that contains a propellane subunit. It was recently synthesized by Kreuzholz and Szeimies starting from the

allenic tautomer **34** in 59% yield, but an attempted distillation causes complete polymerization [46].

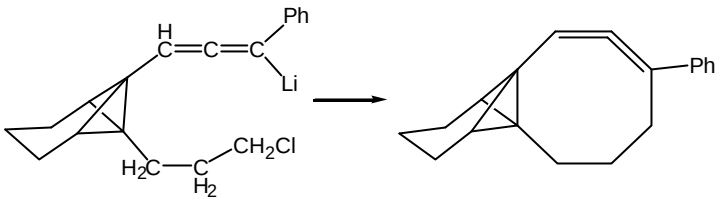

34 **35**

Other derivatives of cycloocta-1,2-diene **36** and **37** have been analysed to investigate their kinetic stabilities. The 1-methyl derivative **36** has greater stability than **2** and it dimerizes with a half-life time of 10-15 min at ambient temperature [12]. 1-*tert*-Butylcycloocta-1,2-diene (**37**) is the only eight-membered cycloallene stable at 20 ^{0}C. On the other hand, cyclic allene **37** did not dimerize, even on prolonged standing at ambient temperature [47].

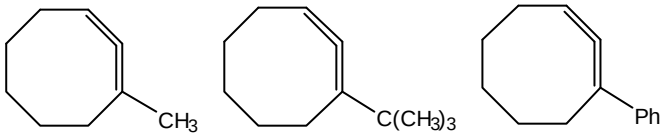

36 **37** **38**

Figure 8: Cycloocta-1,2-diene Derivatives

However, 1-phenylcycloocta-1,2-diene (**38**), generated by application of Doering-Moore-Skattebøl method to dibromocarbene adduct (1R, 7S) **39**, dimerizes in an unusual manner to yield product *trans*-**41b**. Its structure was confirmed by an X-ray analysis. It is now well established that cyclic allenes dimerize by the way of a diradical. The formation of **41b** can be rationalized by formation of the diradical **40** as the intermediate. The fast collapse of **40** to **41a** is probably resulted by the conformation of the eight-membered rings placing the reaction centers in suitable positions. When this experiment is done with racemic **39**, cis-**41b** which can be converted to trans-**41b** with its heating to 160 ^{0}C is observed [48].

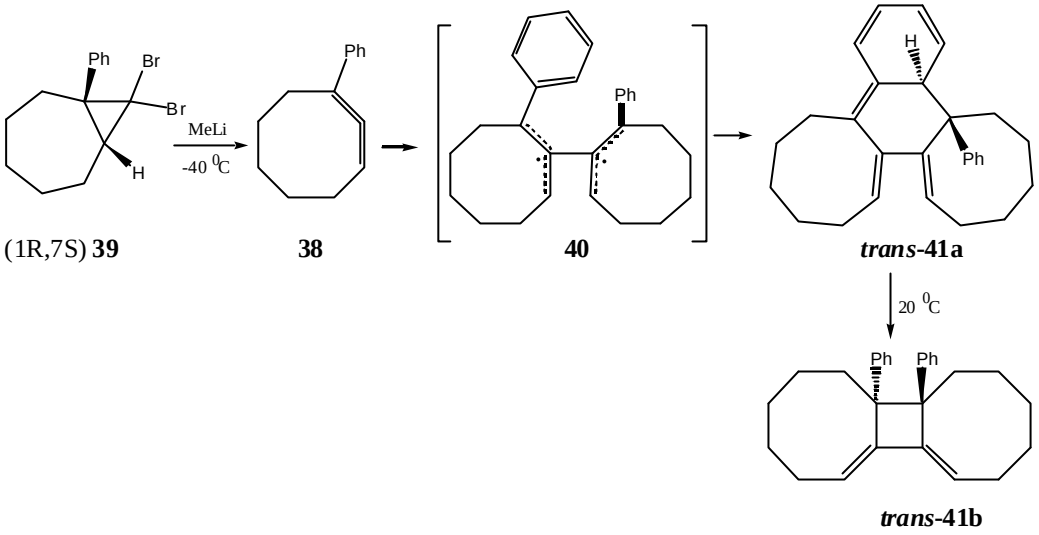

(1R,7S) **39** **38** **40** ***trans*-41a**

***trans*-41b**

Moreover, Price and Johnson [49] examined the photochemical behaviour of the stable eight-membered ring allene, 1-*tert*-Butylcycloocta-1,2-diene (**37**). Direct irradiation of **37** in pentane at 254 nm affords **42a** as the major product. Formation of this product has been explained by initial 1,2-hydrogen migration in the excited state to give a vinylcarbene, independent generation of which gave a similar product distribution. However, the triplet reaction of **37**, sensitized with benzene, afforded products of hydrogen abstraction at the *tert*-butyl group or the ring methylenes. Irradiation of **37** in oxygenated solutions gave 1-tert-butylcycloheptene, probably from extrusion of carbon monoxide form an intermediate cyclopropane.

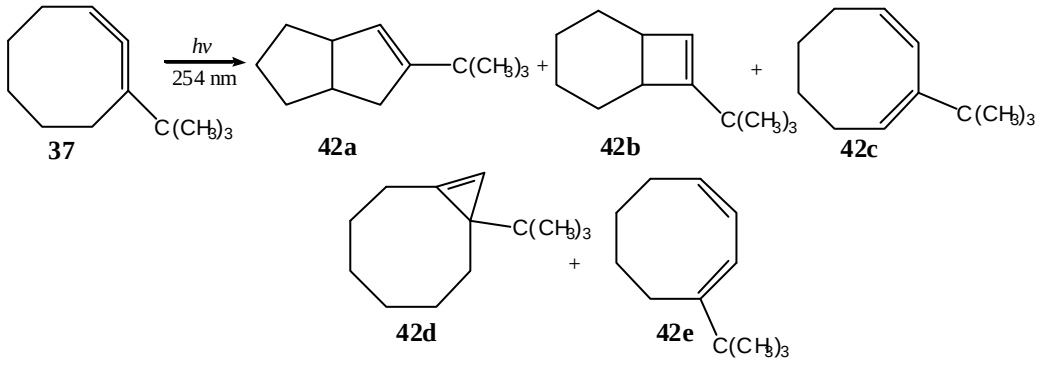

37 **42a** **42b** **42c**

42d **42e**

1.1.3 Cyclohepta-1,2-diene and Its Derivatives

Cyclohepta-1,2-diene (**3**) was first synthesized by Favorskii around 1936 with the treatment of **43** with sodium [50]. However, they did not consider the possibility

of dimerization of **3** to give the [2+2] cycloaddition dimer **47**, only they believed that they had synthesized **3**. This result remained unchallenged until 1961, when Ball and Landor [40] employed the dehydrohalogenation of 1-chlorocycloheptene (**44**) and isolated the allene dimer **47**. After that, allene **3** has proved too reactive to be isolated or even to be observed spectroscopically [51, 52]. One other approach to synthesize **3** has been photolysis of vinyl iodide **45**, a reaction reported recently by Kropp [45].

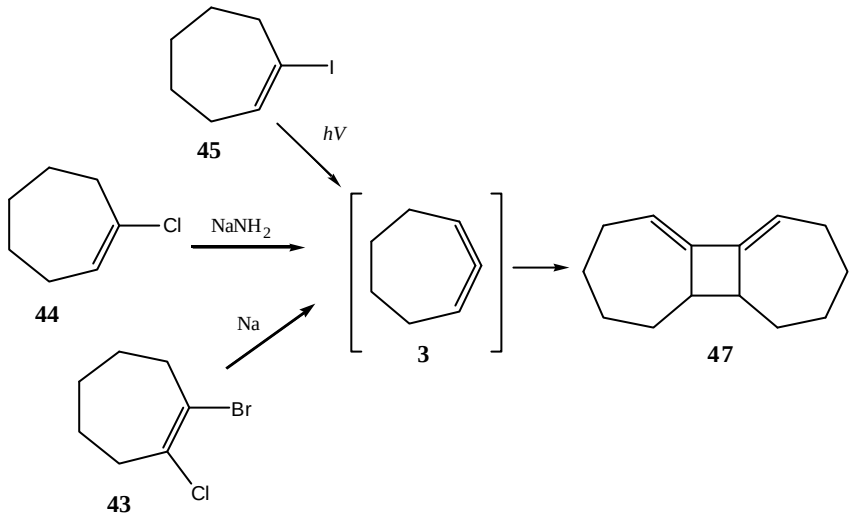

The allene has also been trapped by formation of platinum complex and free allene can be regained from this complex by ligand displacement with CS_2 at -25 ^{0}C and yielded only the allene dimer **47** [43].

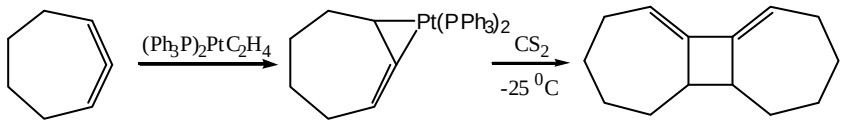

Evidence for the chirality of **3** was proved by Balci and Jones [52], who isolated optically active cycloadducts **48** and **49** by trapping of **3** with DPBIF.

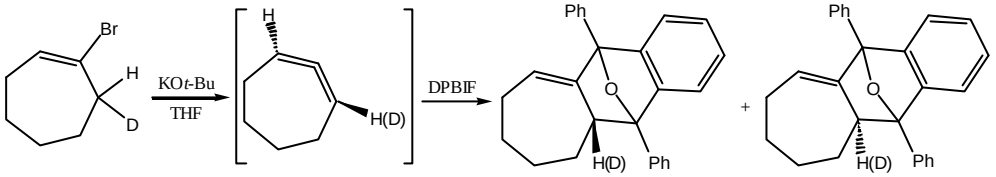

48 **49** **50** **51**

As explained before, Doering-Moore-Skattebøl method is the most often used for the generation of allene, but paradoxically, this method was not successful for the synthesis of 1,2-cycloheptadiene (**3**). Moore *et al.* [53] isolated a mixture of tricyclic hydrocarbons **54** and **55** in 40% yield from the reaction of 7,7-dibromobicyclo[4.1.0]heptane (**52**) with methyllithium. Köbrich and Goyert [54] suggested that a carbenoid structure for the reaction intermediate and free carbene was assumed to be involved in the formation of **54** and **55** in ether.

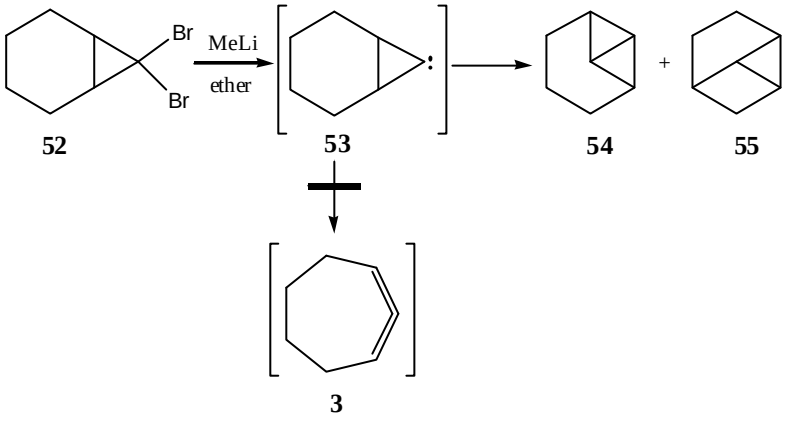

52 **53** **54** **55**

3

More recently, Schleyer *et al.* [20] have focused on the ring opening of bicyclo[4.1.0]hept-7-ylidene (**53**) by using DFT calculations and they found that the ring opening of **53** to **3** has unusually high activation energy of 14.6 kcal/mol because of the unfavourable conformational changes in the cyclohexane moiety of **53** during the reaction. However, the activation barriers for intramolecular CH-insertions to form highly strained hydrocarbons, tricyclo[4.1.0.$0^{2,7}$]heptane (**54**) and tricycle[4.1.0.$0^{3,7}$]heptane (**55**) were found to be 6.4 and 9.1 kcal/mol, respectively. They concluded that the half-chair conformation of the cyclohexane moiety in **53** must change to a chair conformation and at higher temperatures **3** is accessible, and its very fast dimerization causes the dimer of **3** to be main product.

Generally, C-H insertion in such systems is not regiospecific [55], but Creary and co-workers [56] have shown that the reaction can become so by introducing a trimethylsilyl substituent in strategic positions in the molecule. Thus, treatment of 1α, 2α, 6α-7,7-dibromo2-(trimethylsilyl)bicyclo[4.1.0]heptane (**56**) with MeLi gave one product only, 2-(trimethylsilyl)tricyclo[4.1.0.$0^{2,7}$]heptane (**57**), in 79% yield. Obviously, the trimethylsilyl group causes the C-H in the α position to be oriented in such a way that an effective 1,3-CH insertion of the cyclopropylidene can occur.

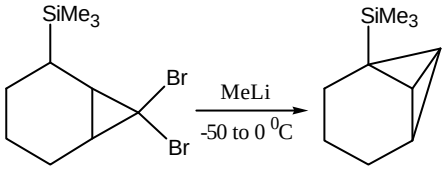

56 **57**

High-temperature thermolysis of *exo*(*endo*)-7-bromo-7-(trimethylstannyl)-bicyclo[4.1.0]heptane (**58**) in benzene gives [2+2] dimer of cyclohepta-1,2-diene (**3**). Insertion products, **54** and **55**, were not observed at this reaction. Its mechanism was established by running the reaction in different solvents and the involvement of a free carbene was postulated as the precursor for the allene formation [57].

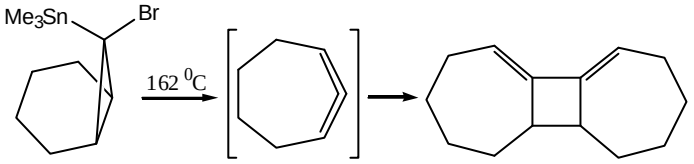

58 **3** **47**

Interestingly, Doering-Moore-Skattebøl method does succeed for the methoxy-derivative **57** at -25 ^{0}C and the dimerization product of **60** was isolated in 85% yield and its hydrolysis gives diketone **62** in acidic media [58].

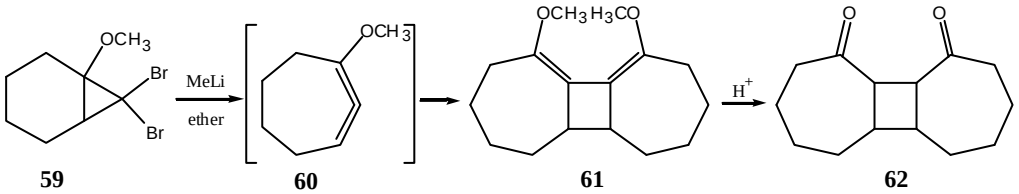

59 **60** **61** **62**

It is well established that additional unsaturation in the ring system increases the ring strain. Therefore, Christl *et al.* [59] have prepared **64** with the condition of phase transfer catalyst and applied the Doering-Moore-Skattebøl route to it. They isolated two products, one is C-H insertion product **65** in 19% yield and other is the unexpected allene dimer **66** in 20% yield. It is likely that the annulation of benzene to the seven-membered ring changes the conformation of the ring in a manner that is suitable for the ring opening of the cyclopropylidene carbene. Probably the activation barrier for the formation of allene is decreased and has a similar value to that of the insertion reaction and this is reflected by the product distribution.

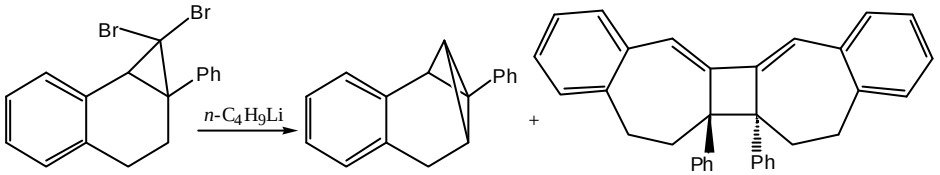

63 **64** **65**

Another study on benzannulated cycloheptadiene system was achieved by Balci *et al.* [60] who applied classical base-supported elimination using appropriate halocycloalkenes. Therefore, they synthesized vinylbromide **67** in three steps starting from the dibromocyclopropane **66**. Subsequent dehydrobromination with KO*t*-Bu base gave the dimer of **68** in 20% yield. To distinguish between the head-to-head and head-to-tail dimers, **69** were reacted with TCNE to give **70** whose structure was established by NMR and X-Ray analysis. Analogous dehydrobromination of **71** provided instead of the expected seven-membered-ring allene, **73** likely from primarily double bond isomerization followed by a rapid β-elimination.

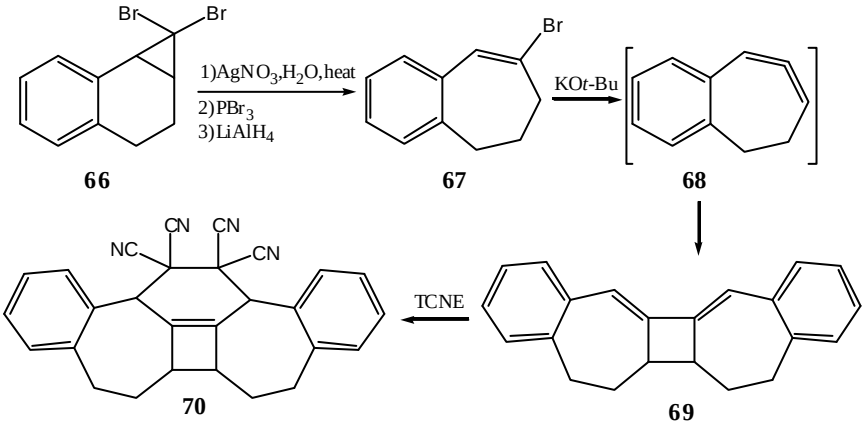

66 **67** **68** **70** **69**

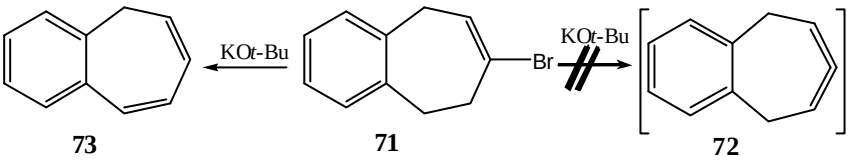

73 **71** **72**

It should also be mentioned that if 1,1-dibromocyclopropanes are treated with either MeLi or *n*-BuLi at low temperature (<-78^{0}C) and the resulting product mixture is kept at this temperature for a period of time, the stability of the corresponding 1-bromo-1-lithiocyclopropanes formed initially may increase enough to favour other reactions at the expense of allene formation [55]. This has been utilized by Banwell *et al.* [61] to convert the tricyclic *gem*-dibromocyclopropane **74** to the *syn*-cyclopropylidene dimer **75**, which after addition of dichlorocarbene, oxidation, and photolysis, affords the tube-like compound **76**. The yield of **75** was rather low (11%) because of formation of a number of other products, including *anti* analogue.

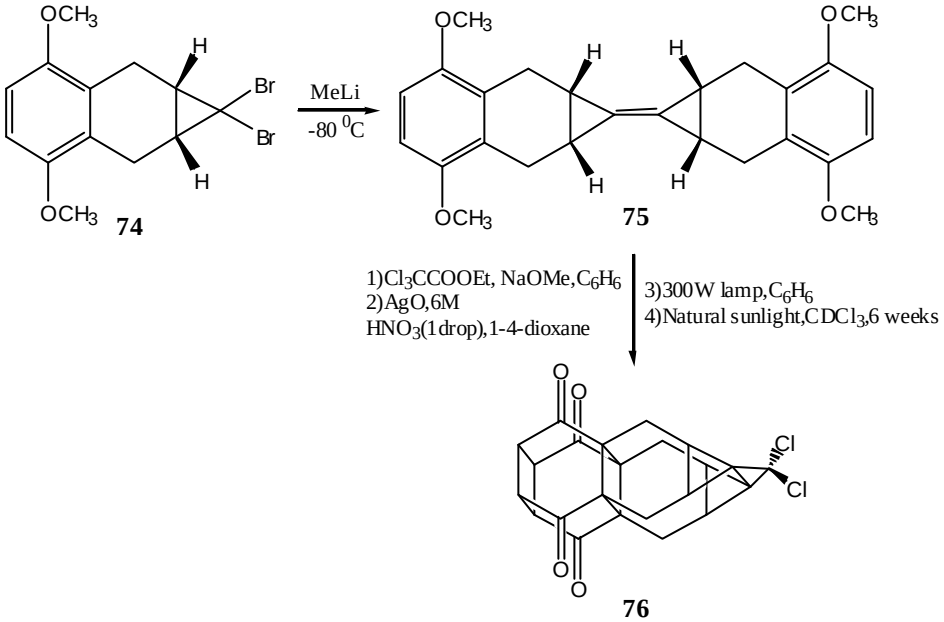

74 **75** **76**

Recently, Chapman and Abelt [62] have explained that photolysis of 2-diazabicyclo[3.2.0]hepta-3,6-diene (**78**) ,which can be prepared by pyrolysis of the tosylhydrazone sodium salt **77** at 101 ^{0}C and condensation of the volatile products with Ar onto CsI window cooled to 25 K, in an argon matrix at 10 K gives 1,2,4,6-cycloheptatetraene **80**. The identity of **80** was confirmed by comparison with an

authentic spectrum produced in the photolysis of phenyldiazomethane. Cycloheptatetraene shows absorptions at 1818, 1810, 1600, 1376, 771, 687 and 667cm^{-1}. On the other hand, Mc Mahon and Bonvallet [63] have discussed that the enigmatic allene 4,5-benzocyclohepta-1,2,4,6-tetraene (**83**), predicted by theoretical calculations to be a low-energy isomer on the $C_{11}H_8$ potential energy surface, is directly observed in an argon matrix at 10 K. IR spectrum was also reported for **83**.

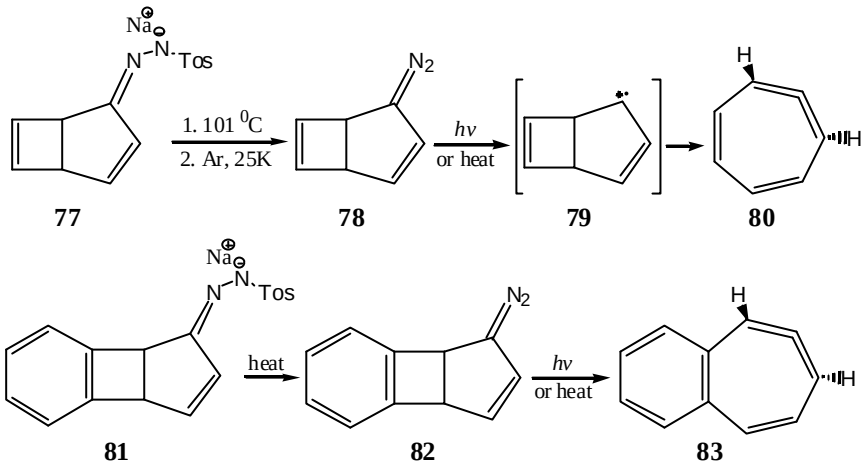

1.1.4. Cyclohexa-1,2-diene and Its Derivatives

Enormous efforts have been devoted toward the synthesis of 1,2-cyclohexadienes. There are at least ten different synthetic methods leading to cyclohexa-1,2-diene (**4**) and some of them are summarized below [12].

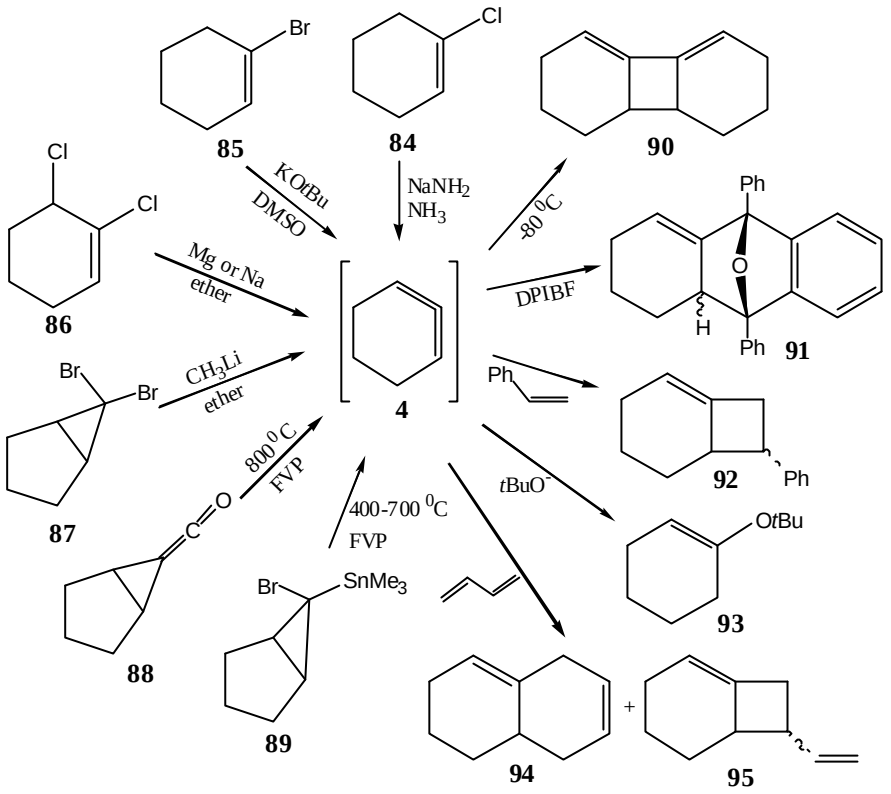

Early attempts to synthesize and isolate cyclohexa-1,2-diene and its strained isomer cyclohexyne were made around 1935 by Favorski *et al.* [50]. Treatment of dichlorocyclohexene (**86**) with sodium in ether yielded $(C_6H_8)_n$ oligomers, including a distillable tetramer. After twenty years, Ball and Landor [40] reported isolation of similar non-volatile oligomers upon the dehydrohalogenation of 1-chlorocyclohexene (**84**) with sodium amide. Perhaps, these two reactions generate transient **4**. In 1966, Wittig and Fritze [64] reported the first clear demonstration of the existence of 1,2-cyclohexadiene (**4**). Dehydrobromination of 1-bromocyclohexene (**85**) with KO*t*Bu base yielded [2+2] dimerization product **90** (7%) and the allene intermediate (**4**) was also trapped with DPBIF to give two stereoisomeric cycloadducts (**91**). Additionally, Bottini *et al.* [65] provided evidence against cyclohexyne intermediates in these reactions with the subsequent labelling studies. They also trapped the allene **4** with other reactive dienes like 2,4-hexadiene, 1,3-cyclohexadiene 2,3-dimethylbutadiene, *cis*-pentadiene, furan and 2-methylfuran. They compared their relative reactivities to cyclohexa-1,2-diene (**4**) at 60 ^{0}C and found 0.17, 1.85, 1.00, 47, 0.17, 0.12, respectively [66].

The cryogenic two matrix studies starting from **88** and **89** are not in good agreement with each other. First one is done by Wentrup *et al.* [67] who trapped pyrolitically generated cyclohexa-1,2-diene (**4**) from ketene **88** at 11 K. An intermediate allene **4** displayed an IR absorption at 1886 cm^{-1}, which is shifted only 70 cm^{-1} from that of a normal allene. Dimer **90** was formed upon warming the matrix condition. Later, Runge and Sander [68] reported that pyrolysis of **89** at 500 ^0C forms cyclohexa-1,2-diene (**4**) with IR absorption at 1829 cm^{-1}. At higher temperatures, they observed the retrograde [2+4] fragmentation to vinylacetylene and ethylene instead of pyrolysis reaction.

Between known routes to **4** summarized above, the most efficient one is by the reaction of 6,6-dibromobicyclo[3.1.0]hexane (**87**) with MeLi. This reaction was first reported by Moore and Moser [69] and yielded **92** as [2+2] cycloaddition with styrene. In a subsequent paper, they explained that allene **4** yields mostly (61%) two streoisomeric tetramers **97** at -80 ^0C, probably formed by dimerization of bisallyl intermediate **96** whereas at 35 ^0C, the major was crystalline dimer **90** with 55% yield.

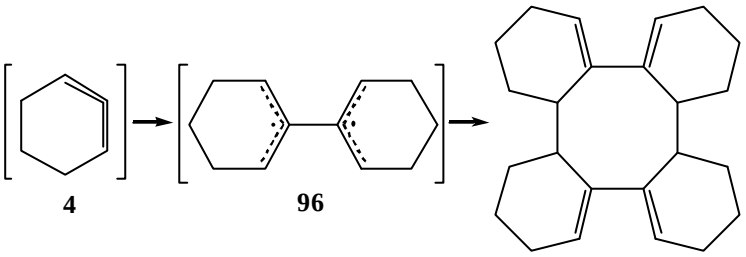

4 **96** **97**

The structure of cyclohexa-1,2-diene (**4**) has proved problematic, in part due to some mistaken ideas about the structure of planar allene. Bottini *et al.* [65] preferred initial formation of a bent, twisted allene which rapidly isomerizes to the diradical **100** that is the active agent in both [2+2] and [2+4] cycloaddition reactions [66]. Moore and Moser [70] and Greenberg and Liebman [71] proposed zwitterion **98** for cyclohexa-1,2-diene and this finding was supported with INDO semiemprical calculations by Dilon and Underwood [29].

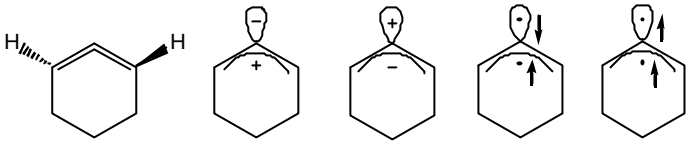

4 **98** **99** **100** **101**

On the other hand, Balci and Jones [52] provided experimental evidence that cyclohexa-1,2-diene (**4**) and cyclohepta-1,2-diene (**3**) are both chiral. In their studies, they isolated optically active cycloadducts, **104** and **105**, at different temperatures and suggested that at around 80 ^{0}C conversion of the nonplanar form of **4** into a symmetrical isomer (probably **98**) competes with its reaction with the allene trap. Recently, Johnson *et al.* [24, 25] have carried out *ab initio* SCF, MCSCF and Möller-Plesset calculations to cyclohexa-1,2-diene (**4**) and cyclopenta-1,2-diene (**5**). The former is calculated to prefer a chiral allenic structure, cf. **4** with a barrier to inversion of ca. 15 kcal/mol, whereas cyclopenta-1,2-diene (**5**) is predicted to have an inversion barrier of 2-5 kcal/mol with a chiral equilibrium geometry. Moreover, Lam and Johnson [72] have predicted the following order among the possible electronic configurations for bent planar allene: **99**>**98**>**101**>**100** (ground state); the zwitterions **6** and **7** are excited states, by using *ab initio* FORS MCSCF and CI calculations.

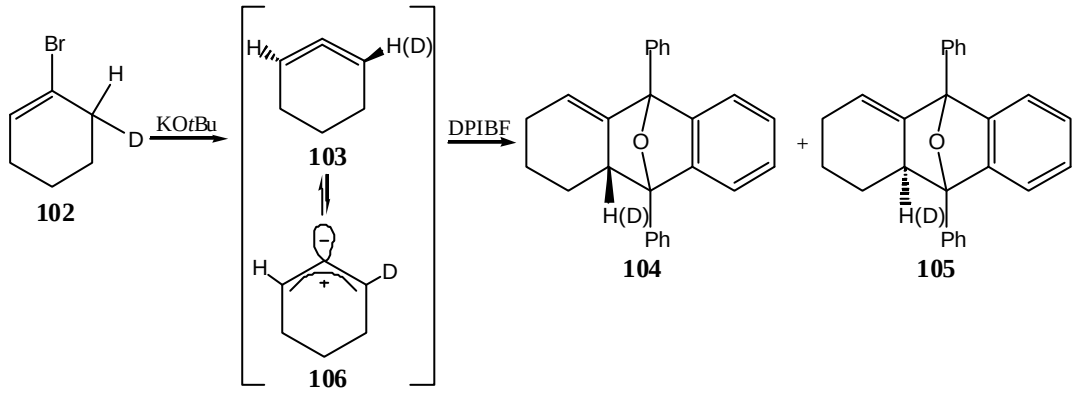

102 **103** **106** **104** **105**

Recently, Tolbert and Johnson *et al.* [73] developed a photochemical approach to strained cyclic allenes and it was applied successfully to **108 a,b** to generate the substituted six-membered-ring allenes **110 a,b** and **111 a,b** which were trapped successfully with furan and DPBIF, respectively. The structure of allene **109a** was confirmed by its independent generation from treatment of **112** with MeLi

in the presence of DPBIF. The cycloadditions of allene **109a** are regiospecific and display high stereoselectivity, despite the high reactivity and expectation of a highly nonsynchronous mechanism. Semiemprical AM1 calculations predict a chiral allenic structure, with a C1-C2-C3 angle of 134°. Frontier MO coefficients are greater at the styryl centers, which also is consistent with the observed regiospecificity.

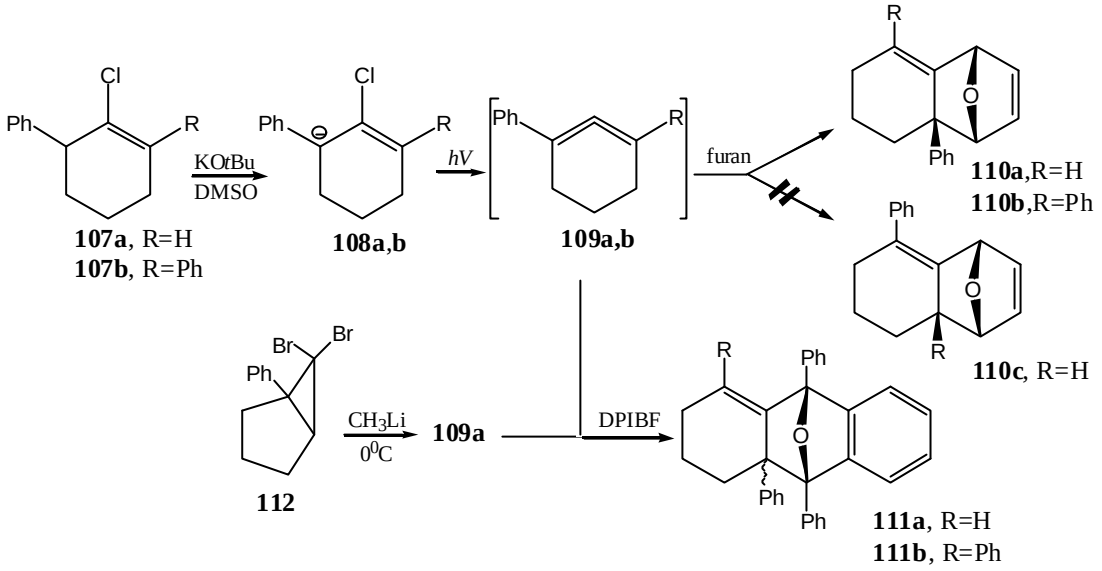

More recently, Tolbert and Houk *et al.* [74] have presented convincing theoretical evidence that even [4+2] cycloadducts of **4** with conjugated dienes such as furan proceed in two steps via a diradical intermediates. They found that alkyl cyclohexa-1,2-dienecarboxylates (**113**) yield the nonconjugated *endo* adduct as the major product. However, chiral cyclohexa-1,2-dienecarboxylates, such as *l*-menthyl and *l*-bornyl derivatives, show no diastereoselectivity in [2+4] cycloadditions.

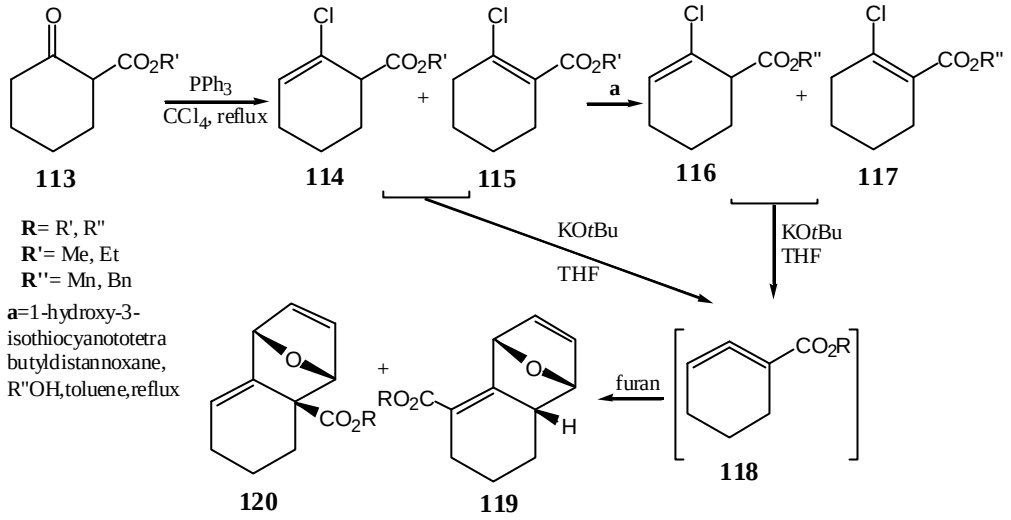

Moreover, A comparison to the calculated transition structures and intermediates at B3LYP/6-31G (d) level along the reaction paths of 1,2-cyclohexadiene with 1,3-butadiene and with furan (as well as propadiene with butadiene) show that the diradical stepwise pathways (**121**) are preferred over the concerted paths. At the same time, the concerted transition structures are extremely asynchronous [74].

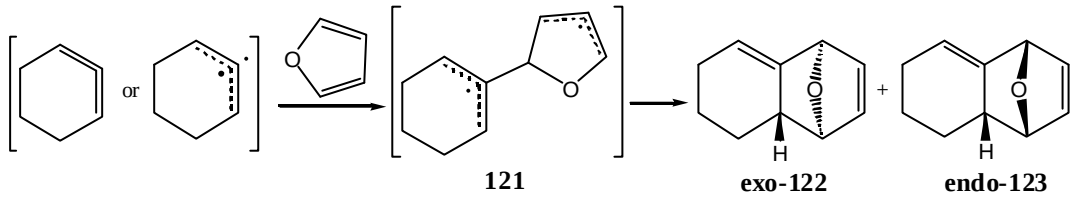

The synthesis of unusual, ring-strained isomers of benzene has been attracting increasing interest in the past few years. Besides cyclohexa-1,2,3-triene (**124**) and cyclohexa-1-en-3-yne (**125**), these species include cyclohexa-1,2,4-triene (**126**), an isobenzene or isoaromatic compound, having allene unit in its structure, that has been subject of several experimental and theoretical studies.

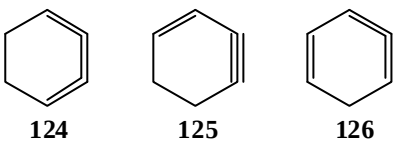

The first example of an isoaromatic molecule containing a cyclohexa-1,2,4-triene structure was reported by Miller and Shi [75]. This molecule **128** was synthesized by dehydrobromination of **127** with KO*t*Bu base in the presence of DPBIF and the cycloadducts **129** and **130** were obtained in 3:2 ratio. Reaction of **127** with KO*t*Bu base in the absence of DPIBF resulted in the formation of enol ether **131** with no evidence for the formation of the conjugated isomer.

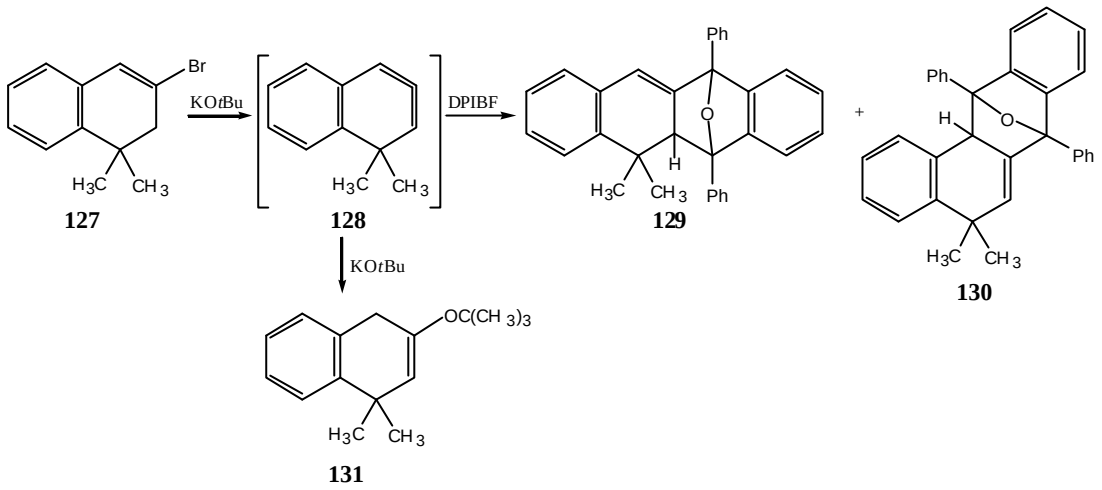

In 1992, Christl *et al.* [76] have generated cyclohexa-1,2,4-triene (**126**) and its benzo derivative (**139**) for the first time using the Doering-Moore-Skattebøl method starting from **132** and **138**, respectively.. They confirmed its existence chemically by means of trapping reactions.

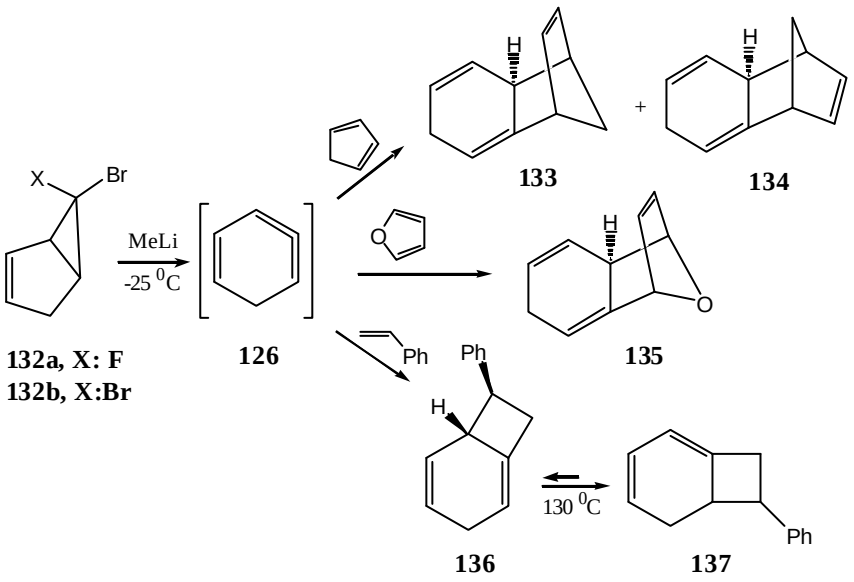

Moreover, they observed isomerization reactions at the trapping products by heating. Apparently, ring closures to yield **136** and **140** are with high selectivity under kinetic control. These products are thermodynamically less stable than their conjugated isomers **137** and **141**, respectively [76].

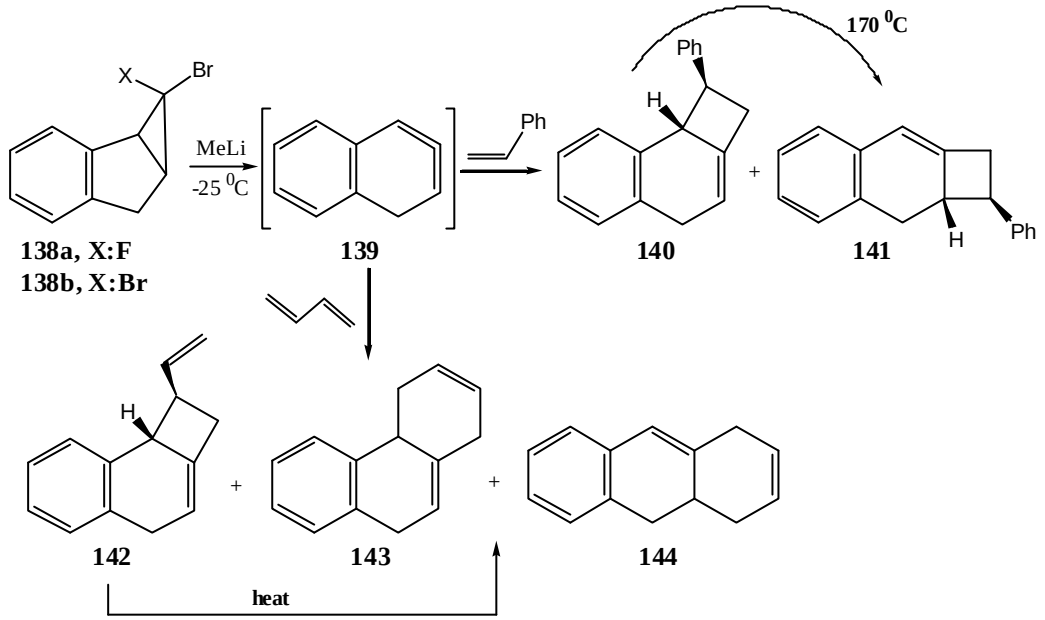

Furthermore, Johnson *et al.* [77] have described computational and experimental evidence for allene intermediates in the intramolecular cycloadditions. They found that both *ab-initio* calculations and flash thermolysis experiments support the existence of thermally activated [2+4] cycloadditions in which an enyne or diyne acts as the four-electron component and observed products are consistent with the intermediacy of strained allenes, **146** and **149**.

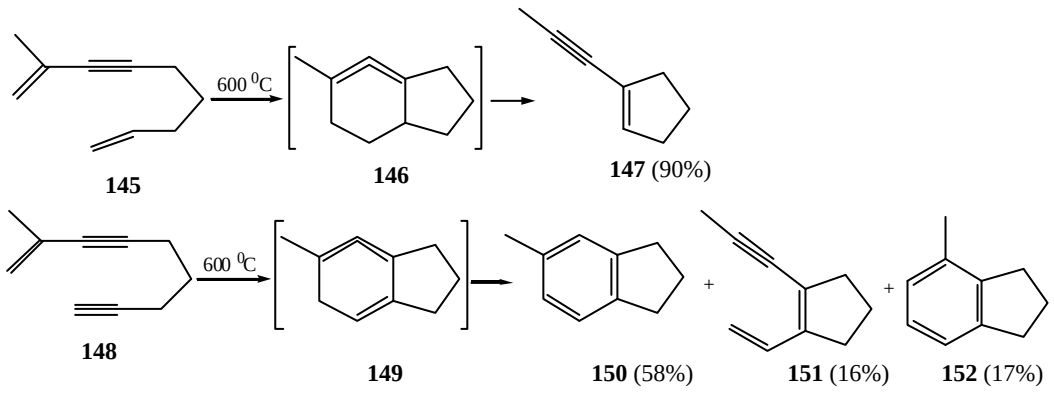

More recently, Christl *et al.* [78] have demonstrated that in the presence of furan, the treatment of **132** with MeLi and the β-elimination of hydrogen bromide from 1-bromocyclohexa-1,4-diene (**153**) furnish the same product **135**. This is good evidence for the same intermediate in both reactions, i.e. the isobenzene **126** is unassociated with fragments of the precursors. In addition, they found that the reaction conditions offer a test as to whether **126** can be transformed to the phenyl anion by deprotonation and performing the reaction in the presence of benzophenone gives rises to triphenylmethanol provides an unequivocally positive answer.

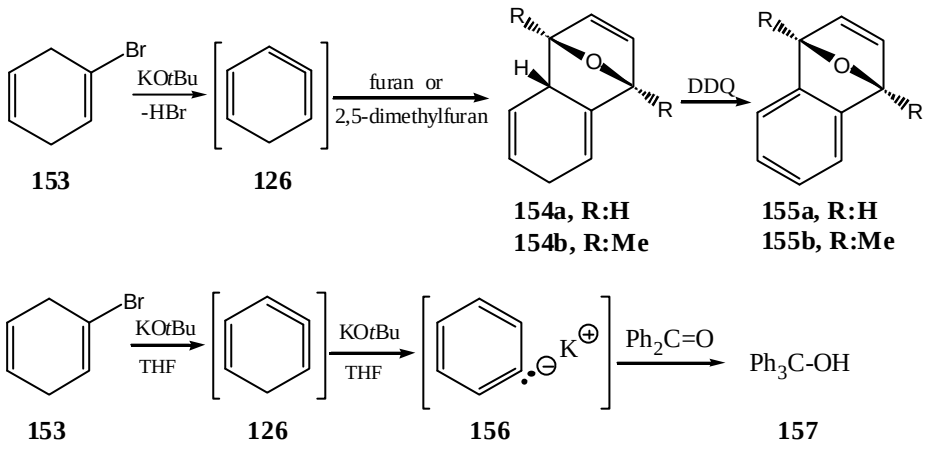

At the same year, Christl *et al.* [79] have treated 3-bromo-1,2-dihydronaphthalene (**158**) with KO*t*Bu to generate the isonapthalene intermediate **139** by the β-elimination of hydrogen bromide. They found that the treatment of **158**, dissolved in anhydrous THF, with KO*t*Bu gave a 73:22:3:2 mixture of naphthalene (**159**), 3-tert-butoxy-1,2-dihydronapthalene (**160**), 2,2′-binaphthyl (**161**) and 1,2-dihydronaphthalene (**162**) in a yield of 92%.

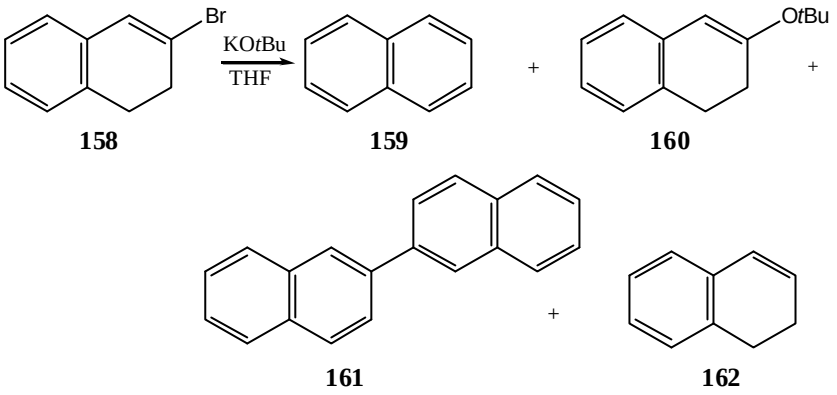

As shown below, they proposed the intermediacy of the carbanions for the formation of products; **159**, **160**, **161** and **162** [79].

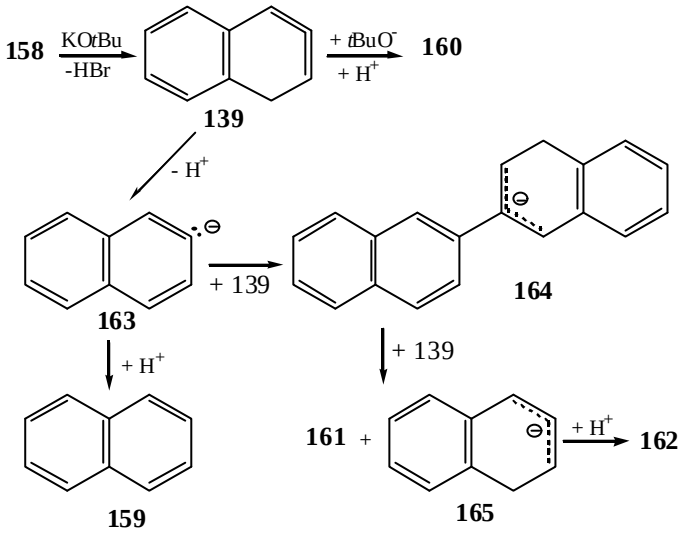

Further evidence for the intermediacy of the carbanions **163** and **165** was provided by the treatment of **158** with KO*t*Bu in the presence of benzophenone. They found that the major product was naphthalene (**159**) and also the enol ether **160** and the binaphthyl **161** were obtained, but the formation of the tertiary alcohols **166** and **167** (13 and 4% yield, respectively) prove that the carbanions **163** and **165** emerge from **158** and are intercepted by benzophenone [79].

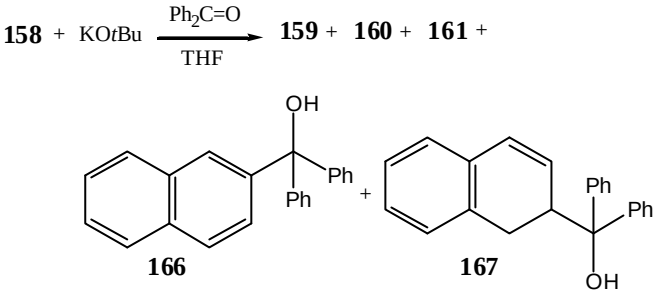

Moreover, they carried out the same reaction in the presence of different conjugated dienes; such as furan, 2,5-dimethylfuran and spiro[2,4]hepta-4,6-diene. Particularly interesting are the products, 30 and 35-37, which give evidence for [2+2] cycloadditions of a strained cycloallene with furan and spiro[2,4]hepta-4,6-diene for the first time [79].

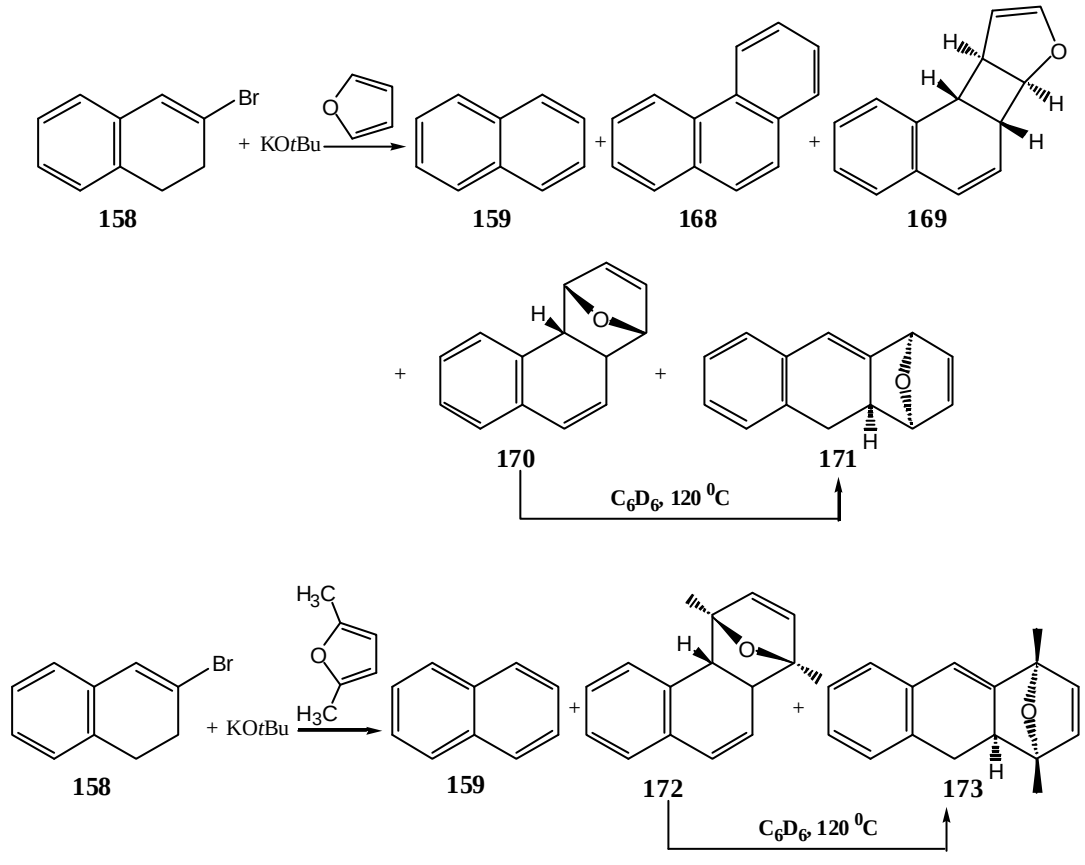

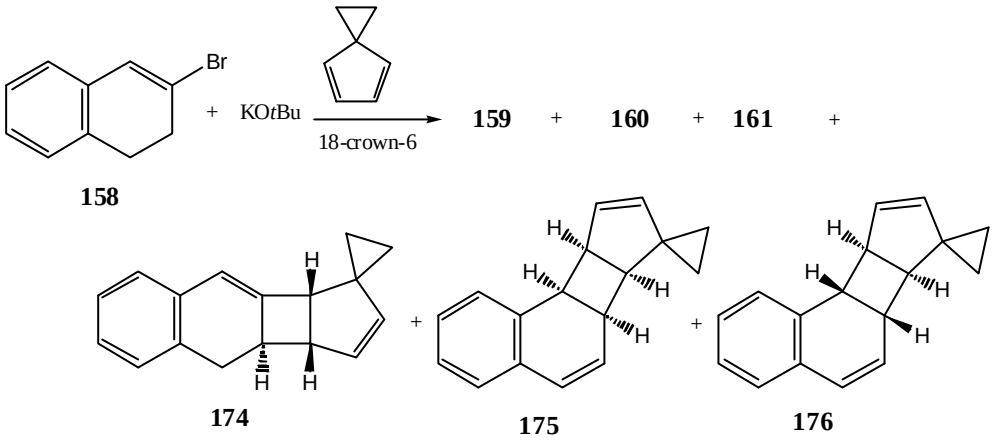

They explained the cycloaddition products that since the Woodward-Hoffmann rules favour the stepwise formation of [2+2] cycloadducts, the radical **177a** and **177b** should be the common intermediate en route to the products **169-171**. On closure of the four-membered ring, conformer **177a** furnishes **178**, which isomerizes to give **169** by deprotonation of the methylene group by KO*t*Bu and reprotonation by HO*t*Bu of the resulting allyl anion at the terminus belonging to the cyclobutane moiety [79].

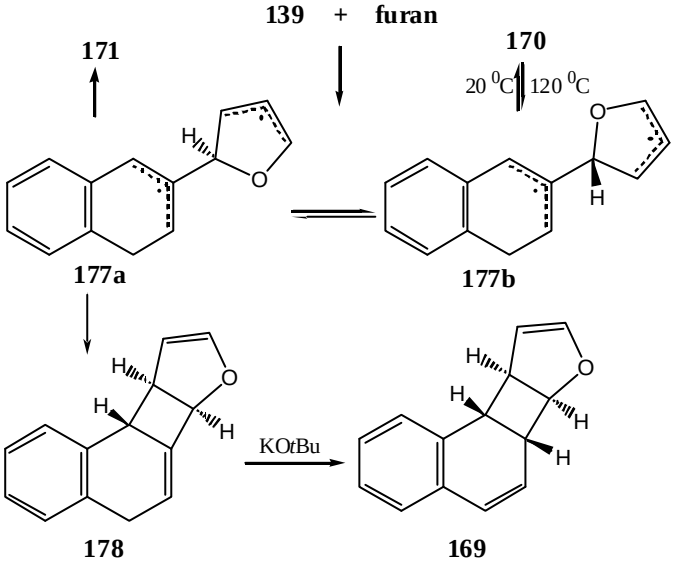

Zertuche *et al.* [80] have reported some rearrangements involving the electrocyclic ring closure of dieneynes **181a,b**. Such ring closures are envisaged to possibly give strained substituted cyclic allenes **182** which could behave as diradicals **182b**. The experimental results show that compounds such as **179** rearrange to

cyclohexadienones **183a** and **183b** through these kinds of intermediates. Theoretical calculations performed on simple models similar to the intermediates suggest that the nature of these intermediates correspond to that of cyclic allenes.

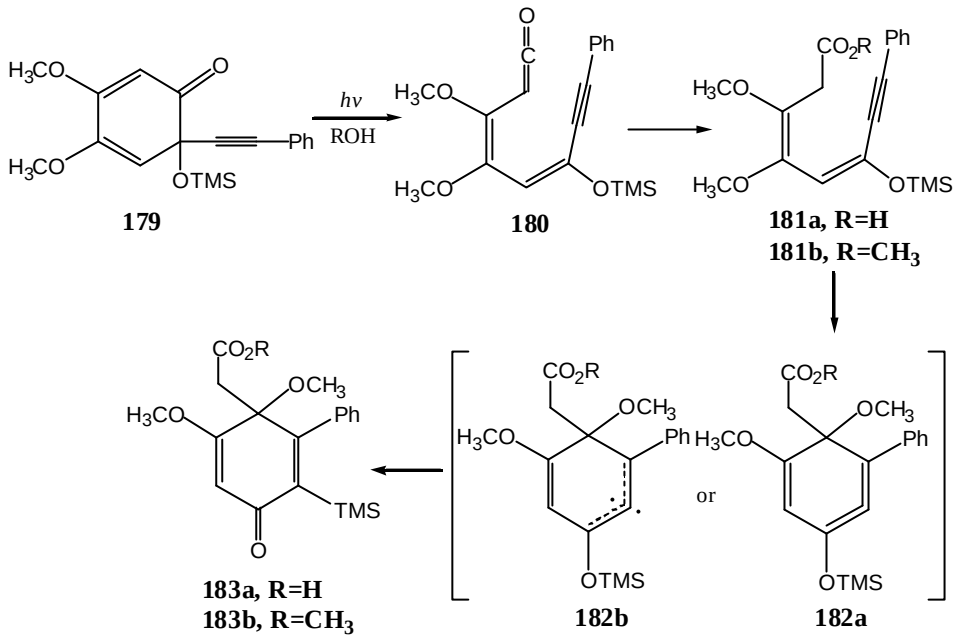

179 **180** **181a, R=H** **181b, R=CH_3** **183a, R=H** **183b, R=CH_3** **182b** **182a**

More recently, Rodriguez *et al.* [81] have explained a comprehensive theoretical and experimental investigation of dehydro Diels-Alder reactions examining the evolution of the cyclic allene intermediates under conditions for intramolecular and ionic and radical intermolecular cycloaromatization processes. Theoretical calculations, given in Table 1 showed that the most favoured intramolecular path for cycloaromatization of 1,2,4-cyclohexatriene (**126**) and its benzoannulated derivative **193**, strained cyclic allenes, consists of a pair of successive [1,2] H-shifts rather than a [1,5] H-shift. Cycloaromatization of cyclic allenes may follow both inter- and intramolecular pathways, depending on the experimental conditions (use of protic or aprotic solvents).

Table 1: Relative Energy Values (kcal/mol) of the Species Potentially Involved in Isomerization of Cyclohexa-1,2,4-triene (**126**) and Isonaphthalene (**193**) at DFT methods. (*s*: singlet state, *t*: triplet state, R.E: relative energy)

	126a	**126b^{s}**	**126b^{t}**	**184**	**185**	**186^{s}**	**186^{t}**
R.E.(B3LYP)	0.0	2.2	4.6	49.6	27.8	5.8	2.2
R.E. (CCSD(T))				48.0	31.9		
	187	**188**	**192**	**193**	**194**	**159**	
R.E. (B3LYP)	11.2	61.6	-81	0.0	17.9	-101	
R.E. (CCSD(T))			-75	0.0	23.9	-91.7	

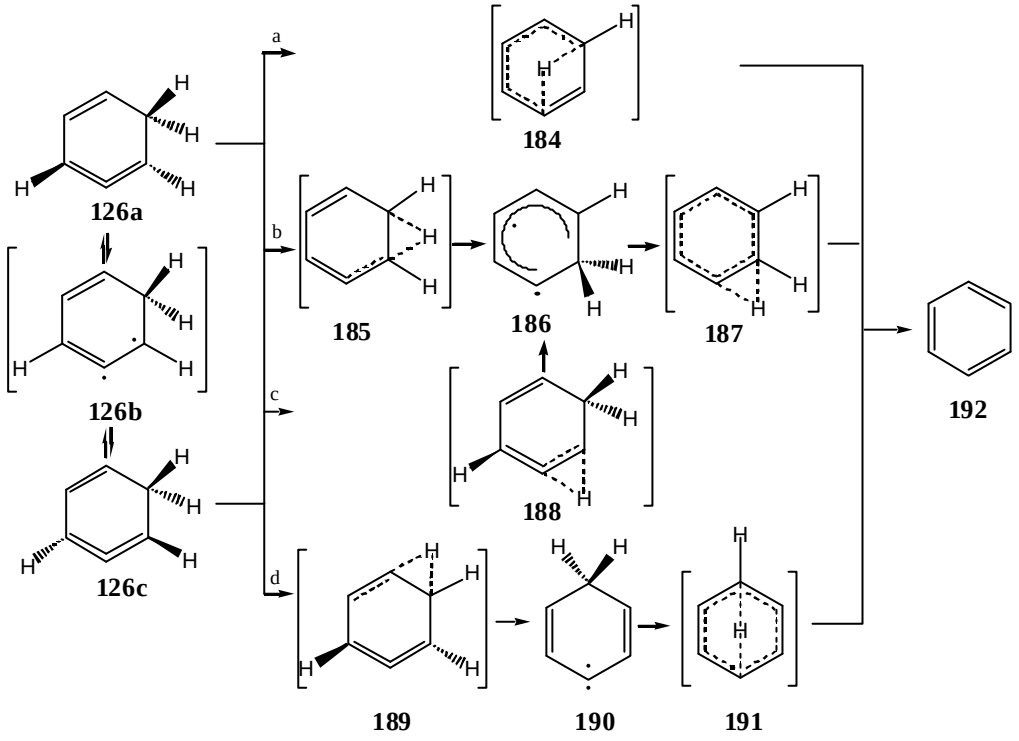

Moreover, they found that benzo[c]annulation of **126** to **193** lowers the barrier to first [1,2]hydrogen shift of path *b* by nearly 10 kcal/mol. This difference in activation enthalpy must be attributed to conjugation in transition state **194** being more extensive than in **185**, and means that intramolecular isomerization might well compete with intermolecular ionic or radical processes in the naphthalenic systems they have studied experimentally [81].

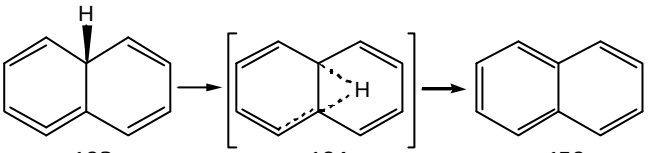

193 **194** **159**

Although six-membered carbocyclic allenes have been studied extensively, little is known about heteroatom derivatives of cyclohexa-1,2-diene (**4**). Oxa-derivatives of **4** are the best known among others. As described before, cyclic allene **4** is best generated by treatment of 6,6-bicyclo[3.1.0]hexane with methyllithium [11]. Hence, 6,6-chloro-**195** and 6,6-dibromo-2-oxabicyclo[3.1.0]hexane **196** were used as a potential precursors for **197** by Schreck and Christl [82]. They trapped it with styrene and furan to give **198** and **199**, respectively. Moreover, they suggested that because of the smaller covalent radius of the oxygen atom, the oxa derivative **197** should have a more bent allene moiety in comparison to cyclohexa-1,2-diene (**4**) and, as a consequence, should exhibit a higher strain energy. Despite this, cycloaddition products with activated alkenes are formed in similar yields as in the case of **4**. They also reported that a specific feature of **197** is the addition of the nucleophile *n*-butyllithium to give **198**.

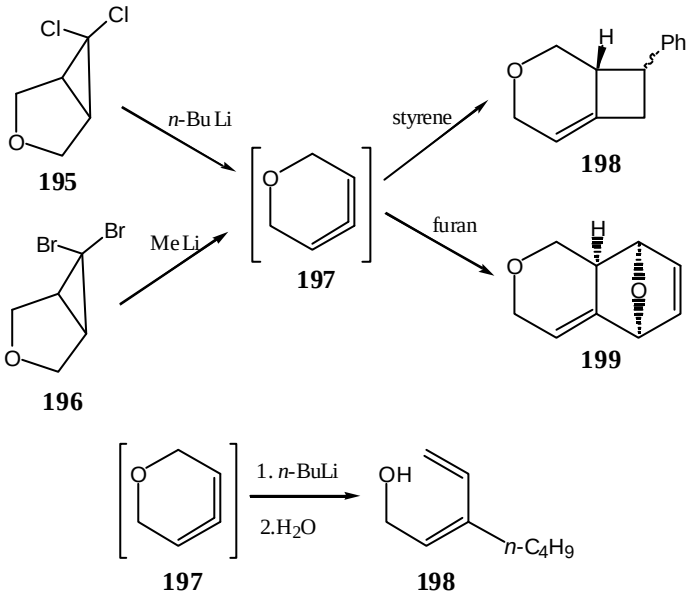

195 **196** **197** **198** **199** **197** **198**

Later, Christl and Braun [83] have obtained the best results by the treatment of *exo*-6-bromo-*endo*-6-fluoro-2-oxabicyclo[3.1.0]hexane (**199**) with methyllithium. An interesting feature of these trapping experiments was the observation of different

chemoselectivity. [2+4] cycloaddition reactions with the allene **197** take place exclusively at the double bond most remote from the oxygen atom, whereas [2+2] cycloaddition reactions prefer the enol ether double bond. In the case of the [2+4] cycloaddition reaction the electron-pure double bond, which is that more remote form the oxygen atom, will react preferentially with electron-rich dienes. For the formation of the [2+2] cycloaddition products a two-step mechanism involving diradical intermediates was offered [84,85].

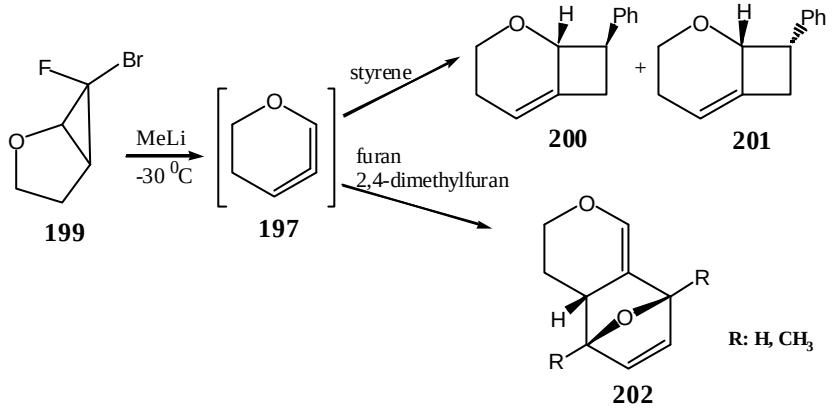

199 **197** **200** **201** **202**

1-Oxa-2,3-cyclohexadiene (**197**) was also generated by Ruzziconi *et al.* [86] independently by treatment of 5-bromo-3,4-dihydro-2*H*-pyran (**203**) with KO*t*Bu base in the presence of 18-crown-6 in DMSO as a solvent. It was trapped with various dienes and dienophiles and also observed the same stereoselectivity.

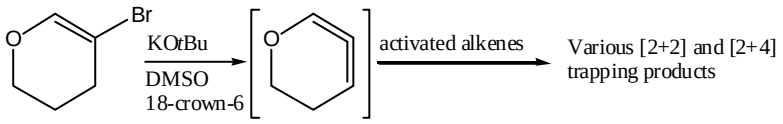

203 **197**

Furthermore, Caubere *et al.* [87, 88] have generated **197** by reacting **204** with cyclohexanone enolate as activating agent for sodium amide, and intercepted it with cyclohexanone enolate in [2+2] cycloaddition to yield **206**, **207** and **208**. They explained the formation of **207** by attack of enolate **205** to the central allene carbon atom. This methodology shows the synthetic potential of strained cyclic allenes in the synthesis of polycyclic oxygenated heterocycles.

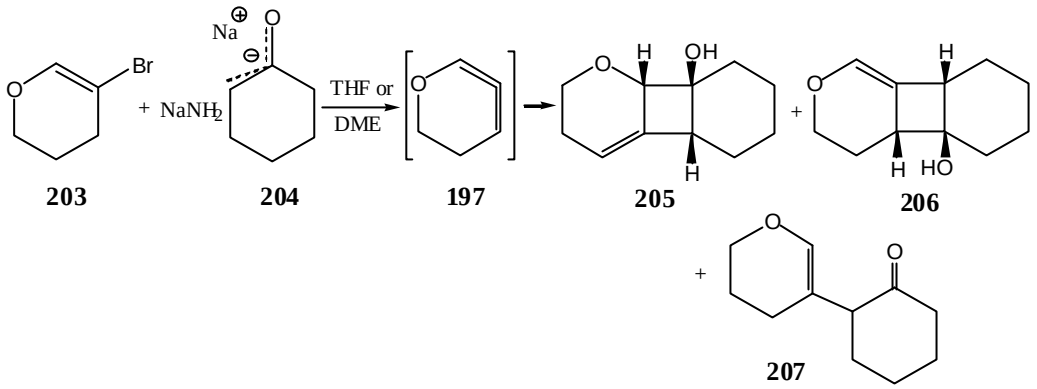

203 **204** **197** **205** **206** **207**

Christl *et al.* [89] have reported that the treatment of 3-bromo-2*H*-chromene (**208**), dissolved in furan, 2-methylfuran or 2,5-dimethylfuran, with KO*t*Bu, results in the formation of the epoxybenzo[*c*]chromene derivatives **211-213** in yields of 28-59%. Likewise, *exo*-2-phenylcyclobuta[*b*]chromene (**210**) is produced in styrene. With tetrahydrofuran as the solvent, 2-*tert*-butoxy-2H-chromene (**217**) is observed as the only product (79% yield) in the absence of activated alkenes. The epoxybenzochromenes **211-213** rearrange on heating to give the epoxyxanthene derivatives **214-216**.

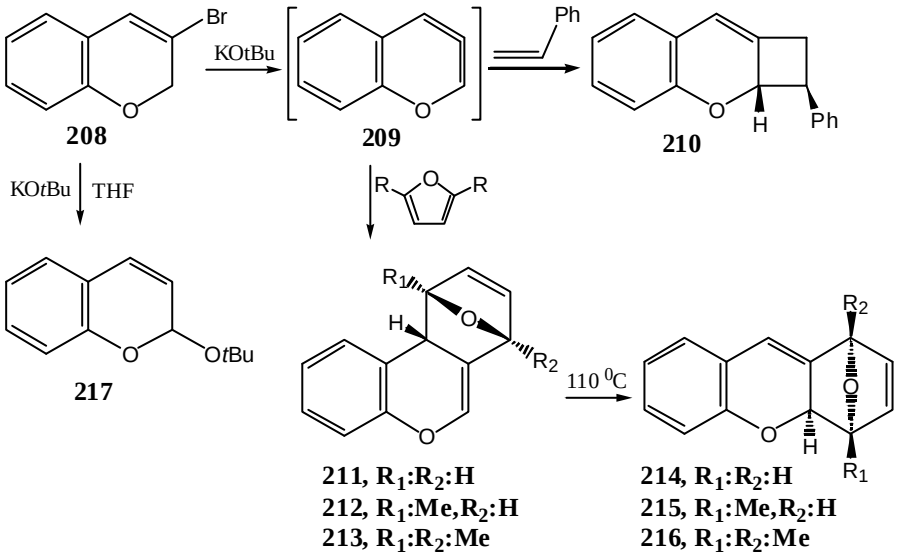

208 **209** **210**

217

211, R_1:R_2:H
212, R_1:Me,R_2:H
213, R_1:R_2:Me

214, R_1:R_2:H
215, R_1:Me,R_2:H
216, R_1:R_2:Me

Recently, Khasanova and Sheridan [90] have discovered a facile photochemical interconversion between the benzofurylcarbene **218** and highly strained didehydrobenzopyran **219**, mediated by the intercession of ring-opened quinomethide **222**. They also compared the energies of studied molecules calculated

by DFT method (Table 2). Finally, they speculated that a 1,3-aryl shift from allene **219** to the photostable benzocyclobutadiene **223** completes the process.

Table 2: Relative Energies of Studied Molecules; **218a**, **218b**, **219**, **222**, and **223** at B3LYP/6-31G** level

	218a	**218b**	**219**	**222**	**223**
Relative Energy	1.0	3.2	0.0	5.1	-13.3

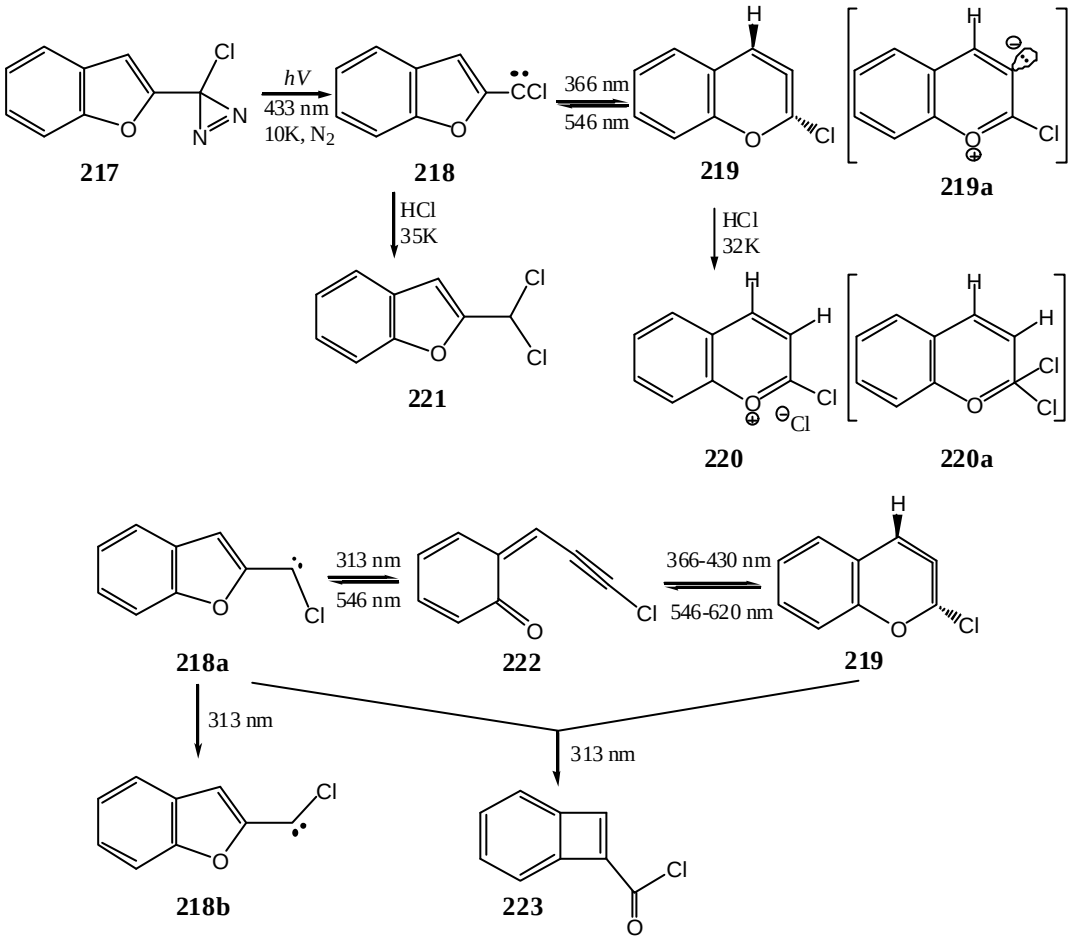

Later, Nikitina and Sheridan [91] thought that the corresponding benzooxazolycarbene system may afford the corresponding strained ketenimine. However, they found that the presence of nitrogen not only changed the photochemistry of this system significantly, but also opened an unexpected new fragmentation channel, yielding yet another carbene. In 2002, they have reported a novel transformation of a benzoxazolyl carbene **225** to a phenoxycarbene **228**, by a

way of a highly strained cyclic ketenimine **227**. Ring opening of **227** to **228**, formally a double bond cleavage to two carbenes, appears unlikely at first glance. However, pseudopericyclic nature of the fragmentation is more apparent, perhaps, when contributions from **227b** to the electronic structure are considered. They also supported their experimental results with the energies of studied molecules calculated by DFT method (Table 3).

Table 3: Relative Energies of Studied Molecules; **225a**, **225b**, **226**, **227**, **228**, and **229** at B3LYP/6-31G** level

	225a	**225b**	**226**	**227**	**228**	**229**
Relative Energy	0.7	0.0	7.7	4.3	16.7	-42.6

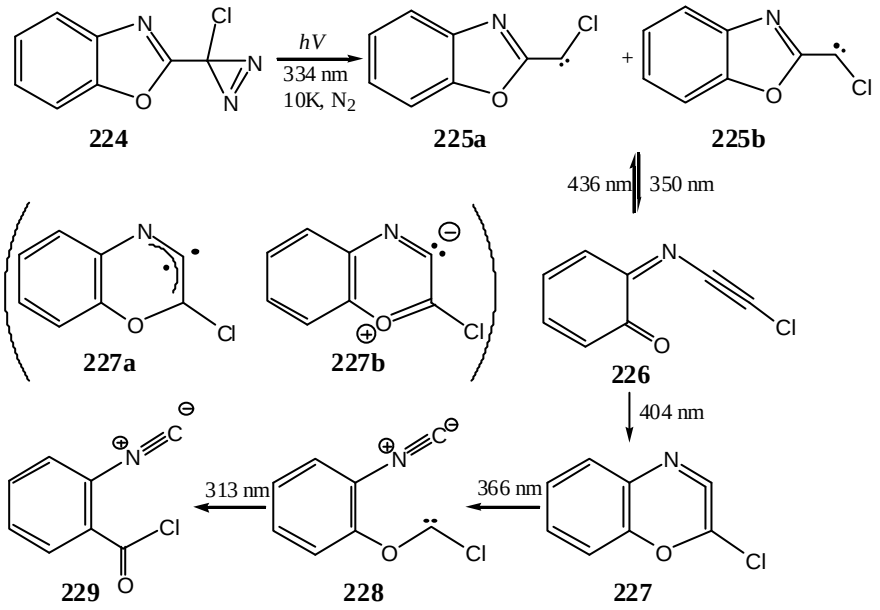

More recently, Engels *et al.* have provided the computational assessment of the electronic structures of cyclohexa-1,2,4-triene (**126**), 1-Oxacyclo-2,3,5-triene (3d^2-pyran) (**230**), their benzo derivatives, cyclohexa-1,2-diene (**4**) and also an experimental approach to 3d^2-pyran. In the cases of cyclohexa-1,2-diene (**4**), the isobenzene **126**, the isonaphthalene **139**, the most stable structures having a planar allene moiety are the diradicals **4b**, **126b**, and **139b**, representing the transition states for the racemization of **4a**, **126a**, and **139a** and being less than the latter by 14.1, 8.9, and 11.2 kcal/mol, respectively. According to the simulation of the solvent effect,

230c even becomes the ground state of **230** in tetrahydrofuran. For the first time, they have generated the pyran **230**, which is trapped. As a precursor for 4, 3-bromo-4*H*-pyran (**232**) was chosen, the synthesis of which was achieved on two routes from 4*H*-pyran. The treatment of **232** with potassium *tert*-butoxide (KO*t*Bu)/18-crown-6 gave 4-*tert*-butoxy-4*H*-pyran (**233**) as the only discernible product, whether styrene or furan was present, indicating the interception of **230** by KO*t*Bu.

Table 4: Relative free energies computed at MR-CI+Q/cc-pVDZ//DFT level for various stationary points of the isobezene **126**, the pyran **230**, the isonaphthalene **139**, and the chromene **209**. (*s*: singlet state, *t*: triplet state, R.E.: Relative Energy)

	126a	**126b^s**	**126b^t**	**126c**	**230a**	**230b^s**	**230b^t**	**230c**
R.E.	0.0	8.9	11.3	28.8	0.0	14.3	15.6	1.0
	139a	**139b^s**	**139b^t**	**139c**	**209a**	**209b^s**	**209b^t**	**209c**
R.E.	0.0	5.4	9.6	10.4	0.0	11.2	12.4	33.7

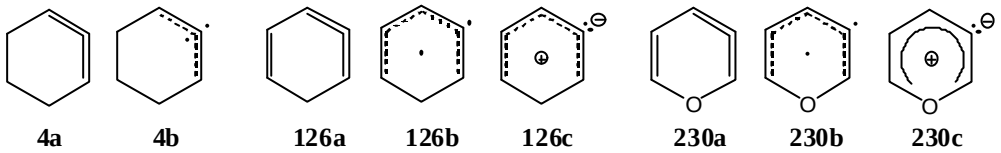

4a **4b** **126a** **126b** **126c** **230a** **230b** **230c**

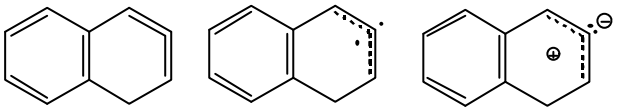

139a **139b** **139c**

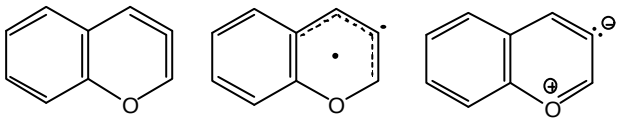

209a **209b** **209c**

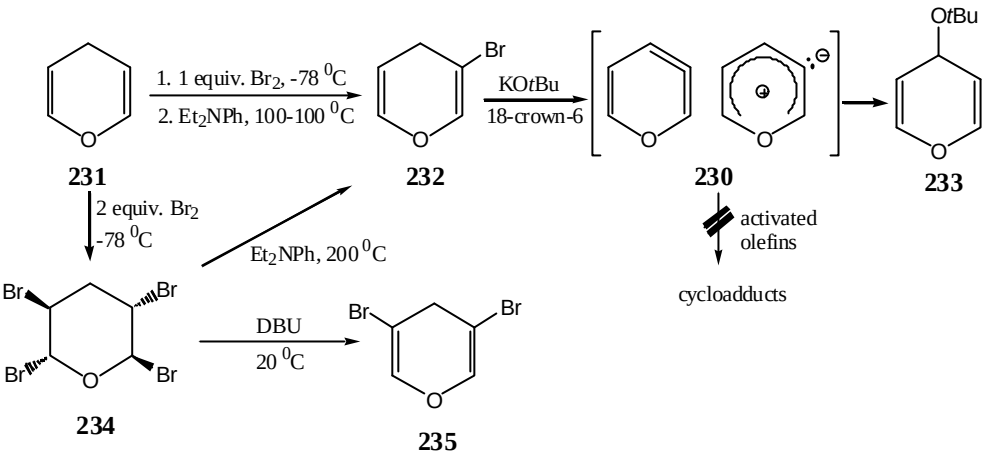

Akin to cyclohexa-1,2-diene (**4**), the isodihydropyridines can be performed by Doering-Moore-Skattebøl method. By this way, the first isodihydropyridine **237** has been recently generated from 6,6-dibromo-3-phenyl-3-azabicyclo[3.1.0]hexane (**236**) with methyllithium [92]. In the presence of buta-1,3-diene, furan, or cyclopenta-1,3-diene was trapped successfully to yield [2+4] and [2+2] cycloaddition products; **238** and **239**.

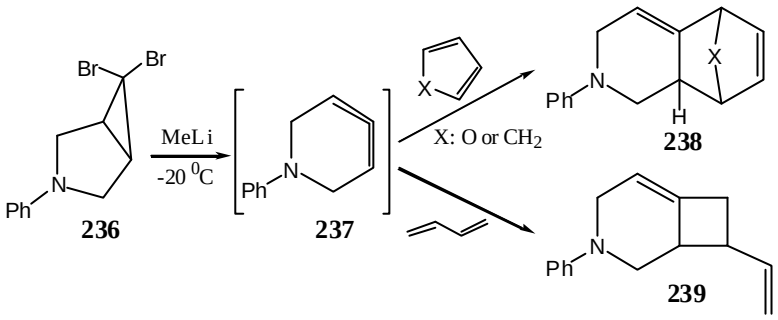

In contrast 1-azacyclohexa-3,4-dienes **240**, attempts to generate 1-methyl-1-azacyclohexa-2,3-diene (**241**) did not furnish products that proved the existence of **241**. However, the intermediacy of its borane complex **242** has been secured by the isolation of cycloadducts of **242** with furan and styrene [93].

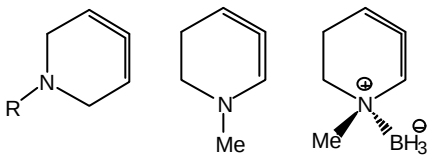

Christl *et al.* [93] reported that the compound **243** reacts rather readily with KO*t*Bu in the presence of furan, providing the hexahydroepoxyquinolines **244**-**246**, although the yield turned out to be only 13%. On replacement of KO*t*Bu by sodium bis(trimethylsilyl)amide, the yield increased to 20%, with the ratio of **244**/**245**/**246** being about 3:2:1. When styrene was used instead of furan, with $NaN(SiMe_3)_2$ as base, the hexahydrocyclobutapyridines **247**-**249** were obtained in 30% yield in a ratio of ca. 6:2:1.

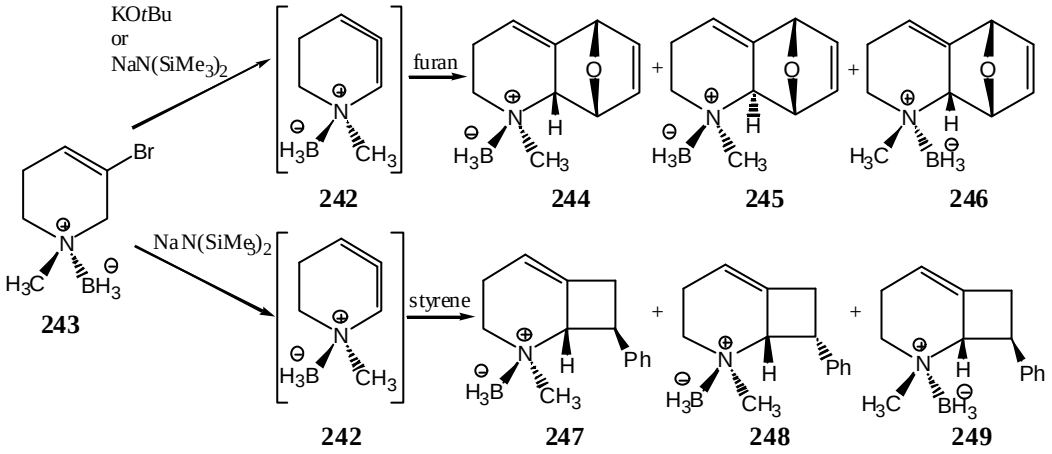

More recently, Christl and Engels *et al.* [94] have provided the generation and interception of 1-Methyl-3d^2-1H-quinoline. They treated a solution of 3-bromo-1-methyl-1,2-dihydroquinoline (**250**) and 18-crown-6 in furan or styrene with KO*t*Bu followed by hydrolsis which afforded a mixture of 1-methyl-1,2-dihydroquinolone (**251**) and 1-methyl-2-quinolone (**252**). If the reaction was performed in $[D_8]$-THF and the mixture was immediately analysed by NMR spectroscopy, 2-tert-butoxy-1-methyl-1,2- dihydroquinolone (**254**) was shown to be the precursor of **251** and **252**. The structure of **254** is evidence for the title cycloallene **253**, which arises from **250** by *b*-elimination of hydrogen bromide and is trapped by KO*t*Bu to give **254** so fast that cycloadditions of **253** with furan or styrene cannot complete.

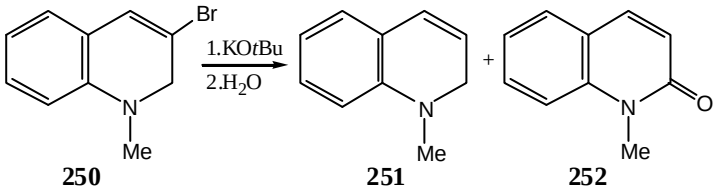

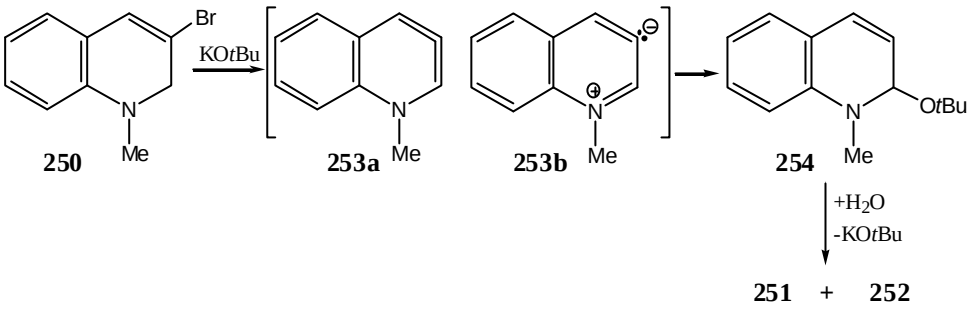

250 **253a** **253b** **254**

251 + 252

Isopyridines of types **255** and **256** have been postulated by Shevlin *et al.* [95, 96] as intermediates in reaction sequences that start with the addition of carbon atoms onto the respective pyrolles. The structure of the products as well as quantum-chemical calculations support the dipolar nature of **255** and **256**, namely, the zwitterions **255b** and **256b** are more likely to be ground state than the allenes **255a** and **256a**. More recently, Yavari *et al.* [17] have theoretically studied the zwitterionic form **256b** and the triplet diradical **256c**, but did not consider more closely the allene form **256a** and the singlet diradical **256c**.

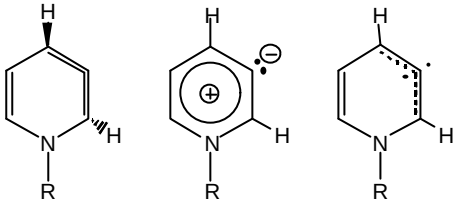

255a, R:Me **255b, R:Me** **255c, R:Me**
256a, R:H **256b, R:H** **256c, R:H**

Shevlin *et al.* [95, 96] have reported that the reaction of atomic carbon with N-methylpyrolle (**257**) at 77 K generates the N-methyl-3-hydropyridinium ylid (**255b**) which can be trapped with added hydrogen halides or carbon dioxide. The addition of carbondioxide is strong evidence for the ylid **255b** rather than cumulene **255a**.

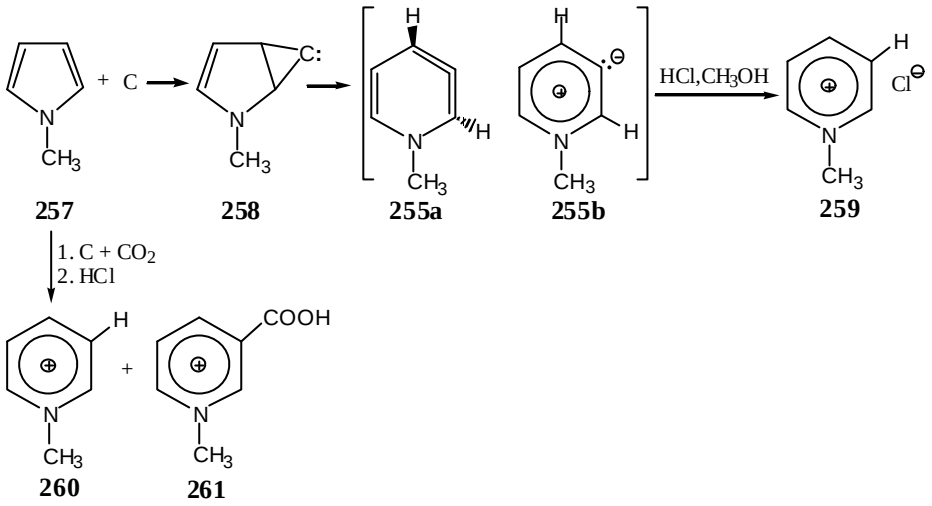

257 **258** **255a** **255b** **259**

260 **261**

Later, they have provided that the reaction of arc-generated atomic carbon with thiophene (**262**) at 77 K yielded two new products, **266** and **268**, in a ratio of 2,5:1 [97]. These forming products possibly result from the reaction of parent 262 with the carbenes **265** and **267**, which can arise from a simple C-H insertion by a carbon atom on **262**. However, the reaction of ^{13}C atoms with **262** using the same conditions revealed that **268** is labelled in the 2′- and 6-positions in a 5:1 ratio while **266** is labelled exclusively in the 6-position. These results clearly demonstrate that carbenes **265** and **267** have been produced by the 'cumulene-to-carbene' rearrangement of the initially formed allene **264**.

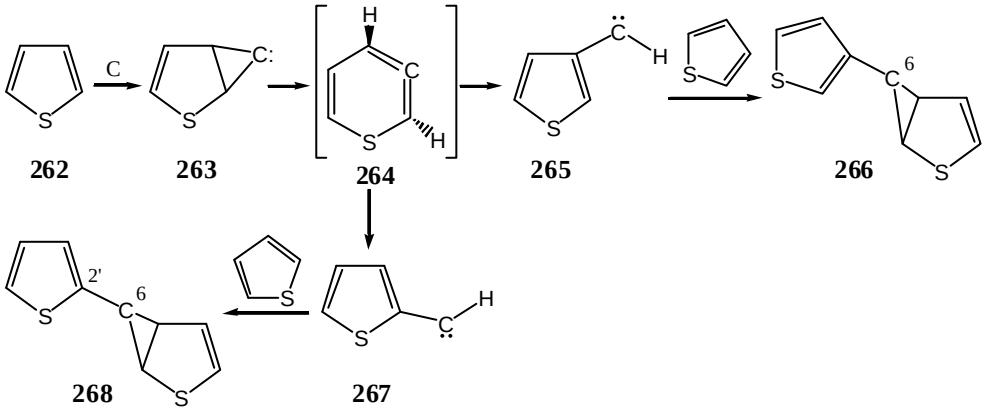

262 **263** **264** **265** **266**

268 **267**

The synthetic potential of strained cyclic heteroallenes has been nicely reported by Elliot *et al.* [98, 99]. The liberation of the cephalosporins 269 proceeds under astoundingly mild conditions and their interception, even with nonactivated olefins and acetylenes, takes place with high efficiency.

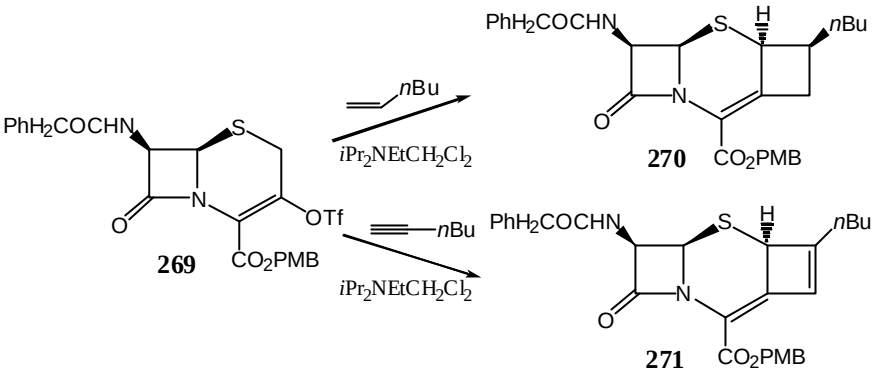

Furthermore, reactions of **273** and **276** with furan resulted in the formation of the [2+4] cycloaddition products, **274** and **277**, respectively. These reactions have rationalized by invoking the intermediacy of the six-membered cyclic hetereoallene **273** or **276**. As can be seen from reaction of 272, the [2+4] cycloadditions take place at the less electron-rich 3,4-double bond to give **274**. However, when cephalosporin α-sulfoxide triplate **275** was treated with *i*-Pr_2Net in the presence of furan, **277** was isolated in 66% yield as the sole product contrary to the reaction of **272**. The oxidation state of sulphur determines the regiochemistry of the addition. In the case of sulphide **272**, this is the 3,4-double bond, whereas in the sulfoxide **275**, the 2,3-double bond is more electron-deficient [98,99].

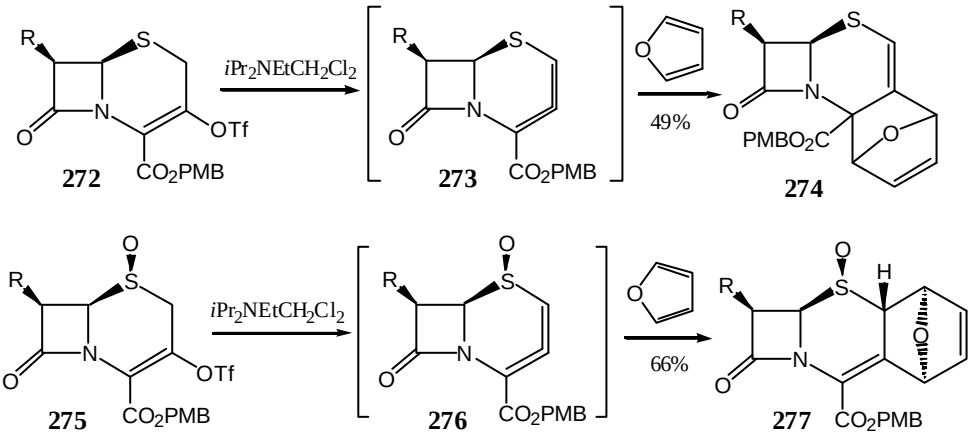

R: -NHCOCH$_2$Ph

More recently, Regitz *et al.* [100] have prepared an isolable diphosphaisobenzene **280**, the first stable cyclohexa-1,2-diene (**4**) with only two heteroatoms in the six-membered ring, starting from phosphatriafulvene (**278**) which

is reacted with the kinetically stabilized phosphaalkyne **279** at 80 ^{0}C. The forming product, isobenzene **280**, is characterized by an unexpected thermal stability and was obtained as a red oil in 77 % yield by bulb-to-bulb distillation. For unequivocal confirmation of its isobenzene structure, **280** was converted to the crystalline adduct **282** by treatment with 2,4,6-trimethylbenzonitrile oxide (**281**); this reaction proceeds chemo-, regio-, stereoselectively. A single-crystal X-ray structure analysis confirmed not only the constitution but also the relative configuration of the 5,7,8,8a-tetra-*tert*-butyl-3-(2,4,6-trimethylphenyl)-8a*H*-6δ2-[1,3]diphosphinino[1,2-*d*][1,2,4] oxazaphosphole (**282**) and thus also those of **280**.

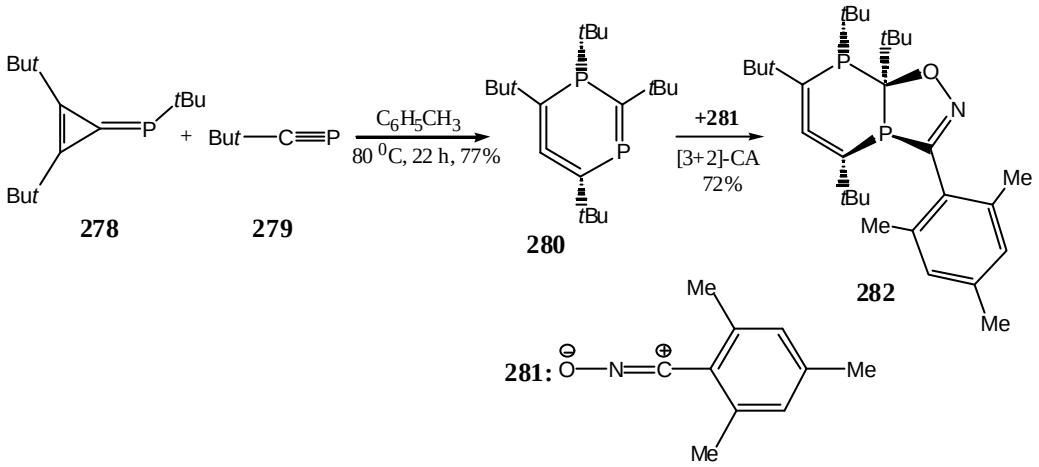

1.1.5. Cyclopenta-1,2-diene and Its Derivatives

The first attempt for the synthesis of cyclopenta-1,2-diene (**5**) was achived by Favorski around 1935. He tried to prepare this highly strained allene by method that does succeed for larger cyclic allene systems, but the sole product was cyclopenta-1,3-diene (**284**) [50].

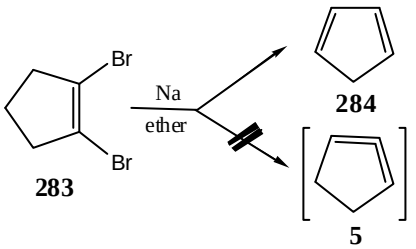

Subsequent base-promoted elimination reaction of vinyl bromide **285** resulted in the formation of cyclopentyne **286** that was trapped by suitable reagents [101].

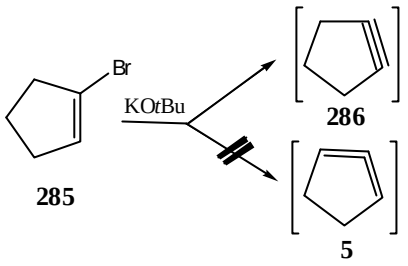

Tolbert and Johnson *et al.* [73] have tried the photodehalogenation of 1-chloro-2-phenylcyclopentene (**287**) with KO*t*Bu, a technique that does succeed for the synthesis of six-membered ring allene **109**. Suprisingly, there was no evidence that irradiation of **288** provided 1-phenyl-cyclopenta-1,2-diene (**289**); precursor **287** was recovered unchanged, along with a minor amount of dehalogenation product 1-phenylcyclopentene. It is possible that the anion does not undergo elimination due to the increased strain in **289**, or anion **288** may undergo a spontaneously reversible electron ejection or electrocyclic opening.

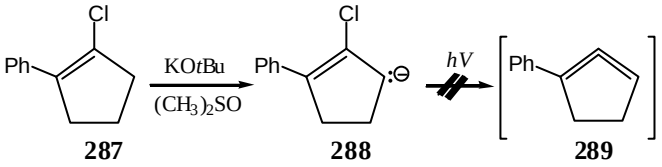

More recently, Balci and co-workers [102] have applied Doering-Moore-Skatebol method to *gem*-bromofluorocyclopropane derivative **291** and succeeded for the first time in the generation of five-membered ring allene derivative **292**. They reacted bicyclo[3.2.0]hept-6-ene **290** with bromofluorocarbene to yield 3-bromo-3-fluorotricyclo[3.3.0.$0^{2,4}$]octane (**291**) and the ring-opened product **295** in a ratio of 1:5. Treatment of a solution of **291** in ether with MeLi in the presence of furan afforded the trapping product **293**. The formation of the trapping product is consistent with the first generation of a five-membered ring allene **292** which is a reactive intermediate.

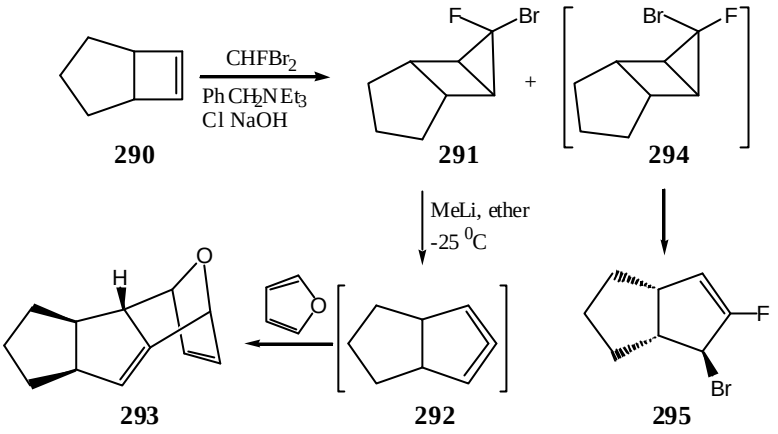

290 **291** **294** **293** **292** **295**

Later, Balci *et al.* [103] have shown that the base-promoted elimination reaction of 1-(2-iodocyclopent-1-en-1yl)benzene (**296**) with potassium *t*-butoxide results in the formation of 1-(2-phenylcyclopent-1-en-1-yl)benzene (**297a**) and 1-cyclopent-1-en-1-ylbenzene (**298**) in a ratio of 1:1. They have repeated the reaction under the same conditions in fully deuterated benzene. The same products (**297b** and **298**) were formed in the same ratio.

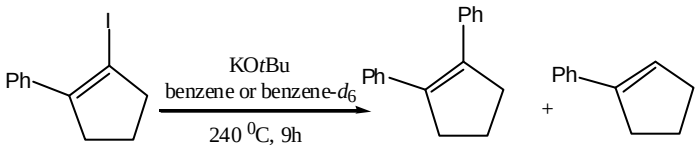

296 **297a, R:Ph** **298**
297b, R:Ph-d_5

On the basis of these results [103], they assumed that the HI elimination gave the strained five-membered ring allene **289a**, which is in equilibrium with the diradical intermediate **289b**. This radicalic intermediate is intercepted by benzene ring (benzyl radical) followed by proton abstraction to provide the diphenyl alkenes **297**.

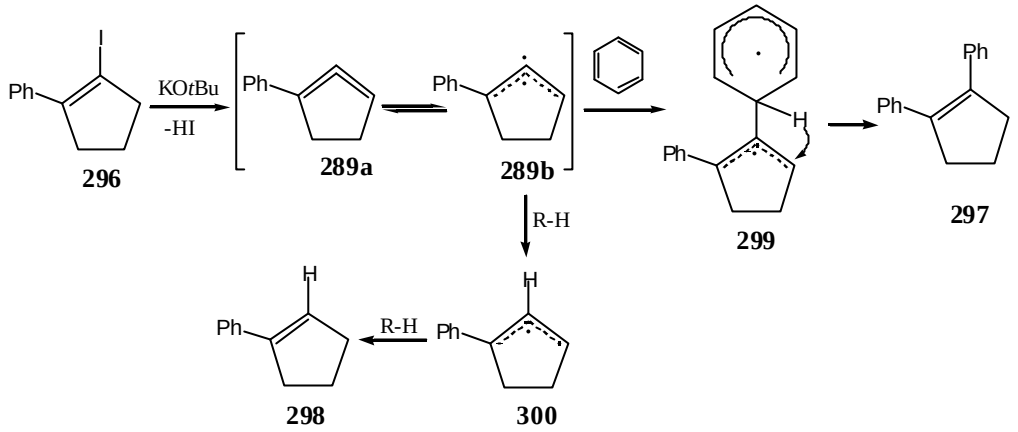

1.2 STRAINED BICYCLIC ALLENES

Although there are much more studies on cyclic allenes, the studies on bicyclic allenes are remarkably limited. One of them is related with the synthesis of bicyclo[3.2.1]octa-2,3,6-triene (**302**) which was reported by Bergman and Rajadhyaksha [104] in 1970. The dehydrobromination of **301** with KO*t*Bu gives the acetylenic compound **303** in the absence of any trapping reagent. The same compound was also observed from the thermal decomposition of **303**. They suggested that the homoaromatic zwitterionic structure **302b** as a plausible precursor of **303**. This reactive intermediate undergoes facile [3,3] sigmatropic rearrangement to alkyne **303**.

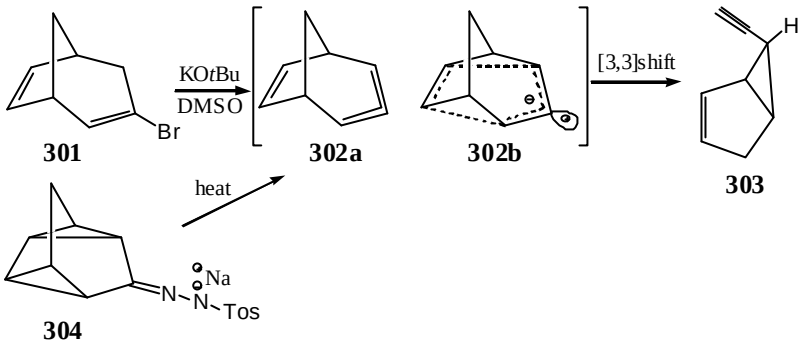

Later, Balci and Jones [105] provided the evidence for the allenic structure **302a** rather than zwitterion **302b**. They generated the strained bicyclic allene **302a** by base-promoted dehydrobromination of **301**, and trapped it with DPBIF. Four adducts, **305**-**308**, were isolated in yields of 21%, 7%, 21%, 4%. Under these conditions no trace of **303** (or its expected adduct with DPBIF) was observed. In the absence of the trap, **303** was formed, although low in yield (15%).

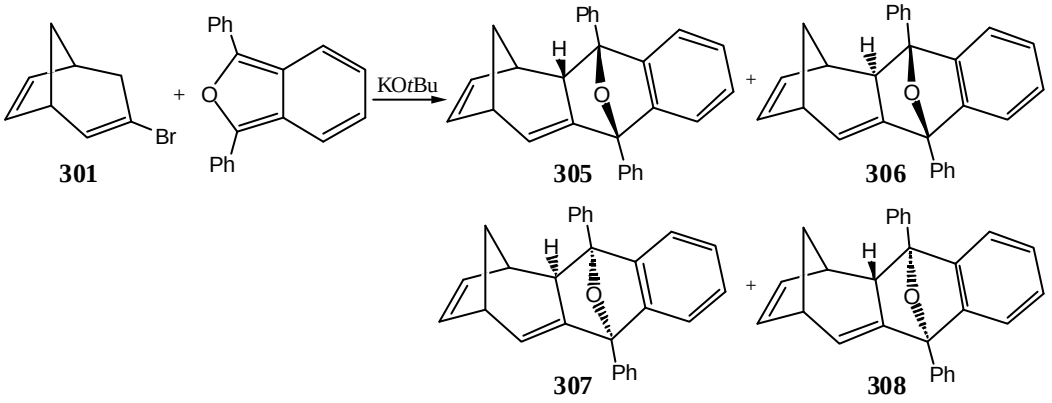

To this end, Balci and Harmandar [106] prepared 3-bromo-6,7-benzobicyclo[3.2.1] octa-2,3-diene (**309**) and subjected it to dehydrobromination with potassium *tert*-butoxide in the presence of DPBIF to investigate the fate of bicyclic allene **310** when the remote double bond in bromo-compound **301** is deactivated by benzosubtitution. Five products, **311**-**316**, were isolated from this reaction in yields of 18%, 17%, 8%, 12 %, 16%, respectively.

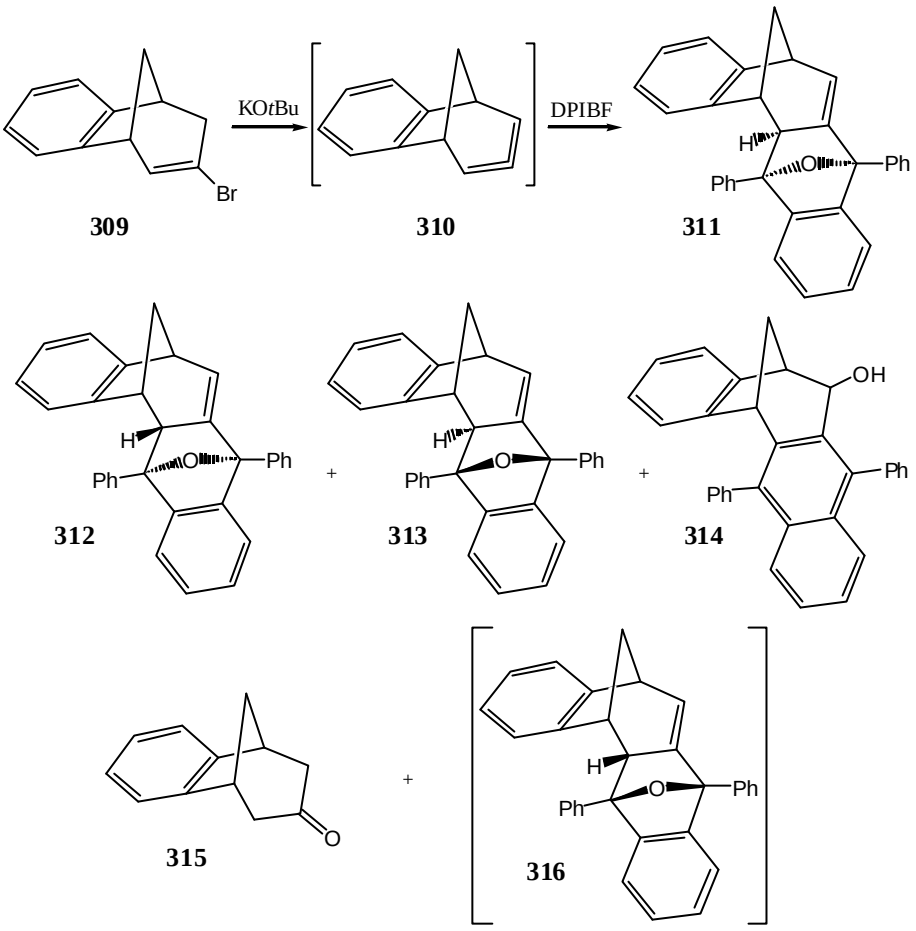

The formation of **311**, **312** and **313** is most reasonably explained by the intermediacy of the strained allene **310** which is trapped by DPBIF. There are four possible cycloadducts. Isomer **316**, which was not found among the products, would be unstable due to strong steric interaction of the two benzene rings. They believed that it underwent facile isomerization to the less strained alcohol **314**. Ketone **315** ought to stem from the addition of *tert*-butanol to allene **310** followed by hydrolysis [106].

On the basis of these results, they concluded that the dehydrobromination of **309** results in the strained bicyclic allene **310** which unlike **302** does not isomerize further to a ring-opened alkyne in the absence of DPBIF because the involvement of the remote double bond in **310** is impeded by the stability of the aromatic ring [106].

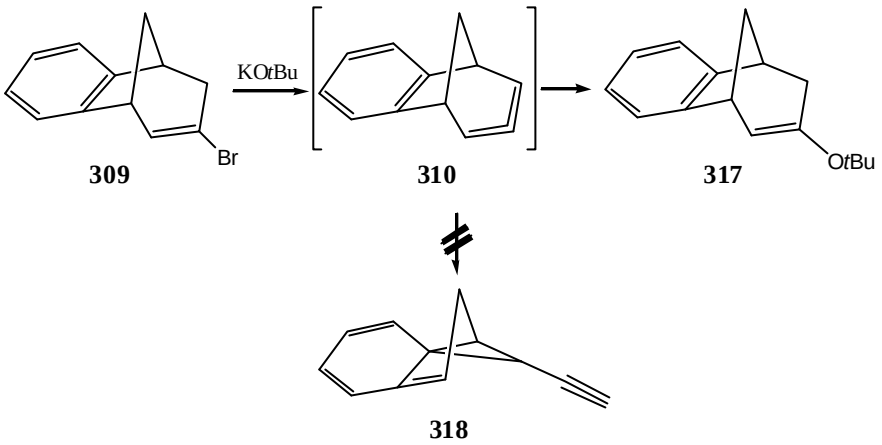

309 **310** **317**

318

However, as noticed in the same paper [106], these results were also in agreement with an alternative mechanism for the formation of cycloadducts **311**-**313**. According to this mechanism dehydrobromination of **309** can yield the bicyclic alkyne **319**, which undergoes cycloaddition reaction reaction with DPBIF to give **320**. The base-promoted isomerization of the double bond in **320** would give the observed products, **311**-**313**.

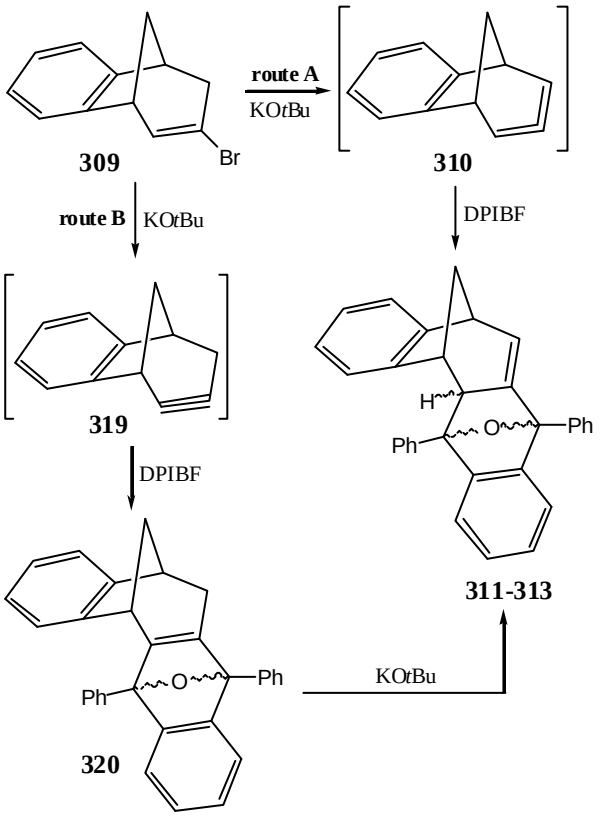

309 **310** **319** **311-313** **320**

To distinguish between these two possible mechanisms, Balci *et al.* [107] have recently investigated the generation and trapping of the alkyne **319** by two alternative procedures. The alkyne **319** was generated by treatment of dibromide **321** and with *tert*-butyllithium, and by the KO*t*Bu induced rearrangement of exocyclic bromomethylidene compound **322**. The intermediates were trapped with DPBIF to give the cycloadducts, **320a** and **320b**, which then isomerize completely to the products **311**-**313** in the presence of KO*t*Bu [108].

Since the allene intermediate can not be generated from the base-promoted reaction of **322**, it was concluded that the intermediate is the alkyne **319**. This is calculated to be 11 kcal/mol by MOPAC program and 16 kcal/mol by PCMODEL program more stable than the bicyclic allene **310** [107].

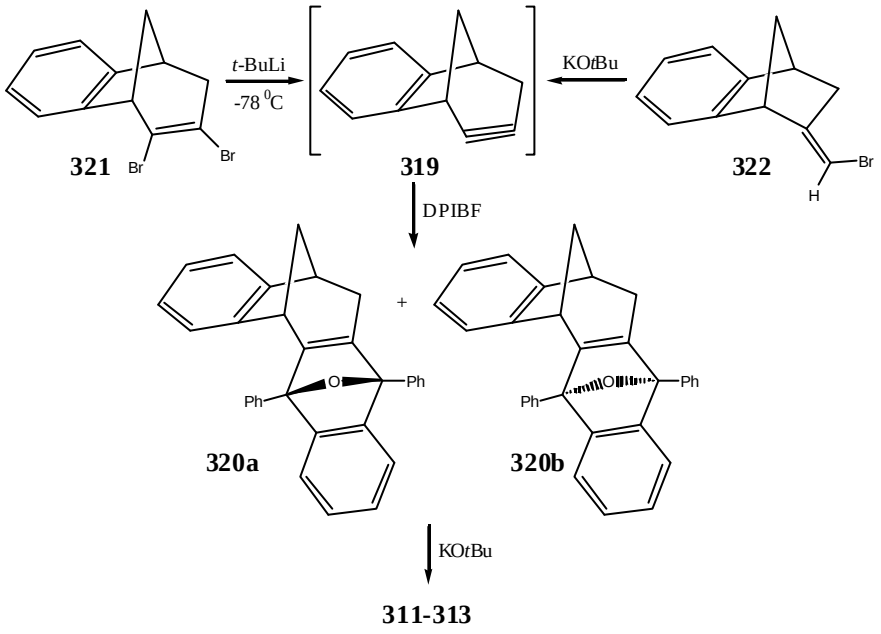

Even with these results allene formation cannot be excluded in the base-promoted reaction of **309**. To reveal whether the real intermediate in the dehydrobromination of **309** is **310** or **319** it was necessary to undertake another independent generation of alkyne **319** where the formation of allene **310** was excluded. For this reason, the chloroalkene **323** was prepared and submitted to dehydrochlorination with KO*t*Bu. However, the base-promoted reaction of **323** did not form the alkyne intermediate **319** or its derived enol ether **317** and allyl ether **324** was isolated as the sole product of reaction. They suggested that the prototropic

rearrangement of the chloro alkene **323** to the corresponding allyl chloride is followed by nucleophilic displacement of the chlorine atom by *tert*-butoxide and that this is responsible for this conversion [109].

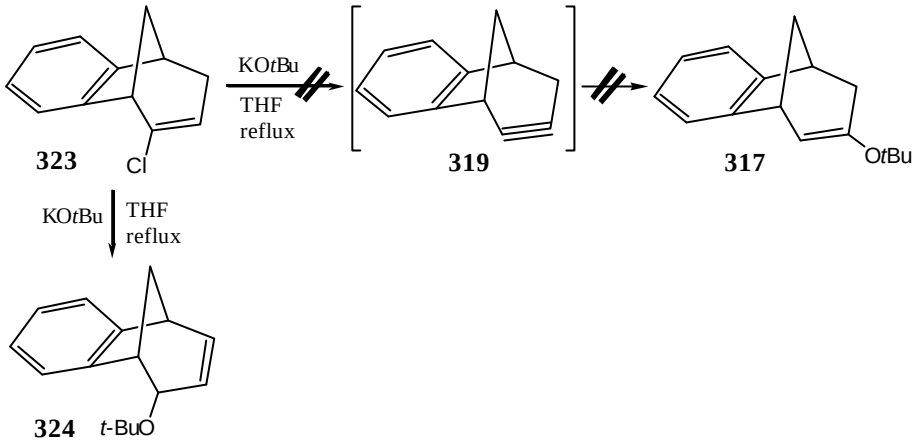

In order to solve the problem of what the real intermediate is in the base-promoted reaction of vinylbromide **309**, they decided to label the allylic position of bromocyclo alkene **309** with deuterium atoms and submitted this compound, **325**, to a dehydrobromination reaction. Formation of an allene intermediate **327** would result in the scrambling of deuterium atoms, but alkyne formation will give product **326** where deuterium is located at the double bond. Unfortunately, they explained that substrate **325** undergoes H/D exchange reaction before HBr elimination [110].

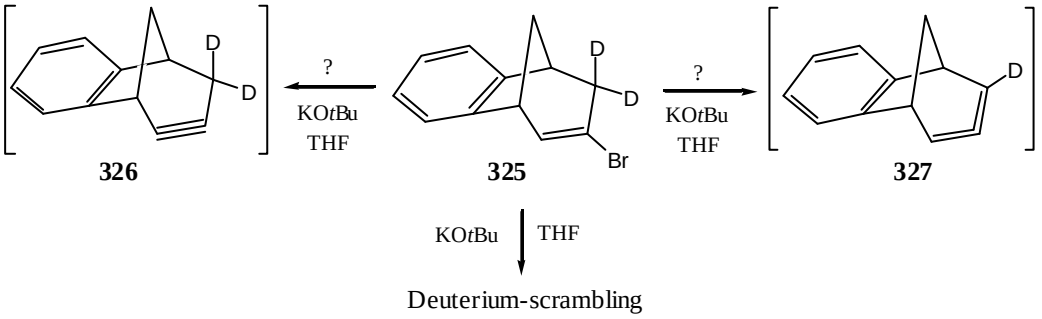

Furthermore, they have forced the system to undergo allene formation by replacing the double bond proton in **309** by a methyl group. No reaction was observed when **328** was subjected to dehydrobromination with KO*t*Bu under the same reaction for **309**. When the more drastic conditions of diglyme at 170 ^{0}C were applied, dehydrobromination occurred and the exocyclic olefin **330** was isolated;

primarily base abstracts a hydrogen atom from the methyl group. This result indicates that **328** has no tendency for dehydrobromination reaction to form allene **329** [111].

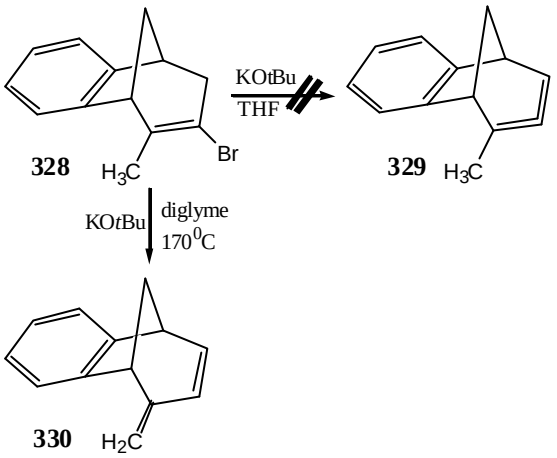

The same reaction was repeated using the phenyl derivative of **309** to prevent the proton abstraction from the methyl group. They synthesized the corresponding compound **331** and submitted it to the base-promoted dehydrobromination reaction. After the reaction, enol ether **333** was isolated in 16% yield. This result indicates the formation of allene **332** which is trapped by *tert*-butoxide ion [111].

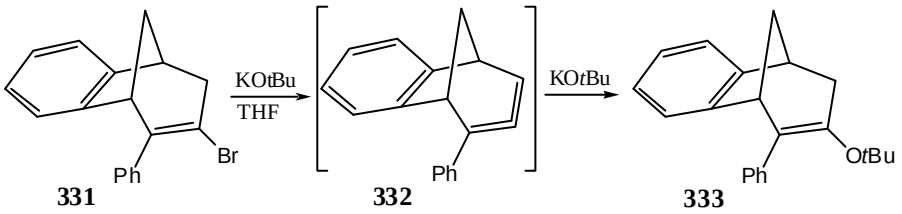

Another study to generate bicyclic allene **310** was carried out using zinc-catalysed elimination of the dibromide **334** by Balci *et al.* who isolated two isomeric Wurtz-like condensation products, **335** and **336**, in 16% yield. Not even a trace of the expected allene dimerization product was observed in this reaction [112].

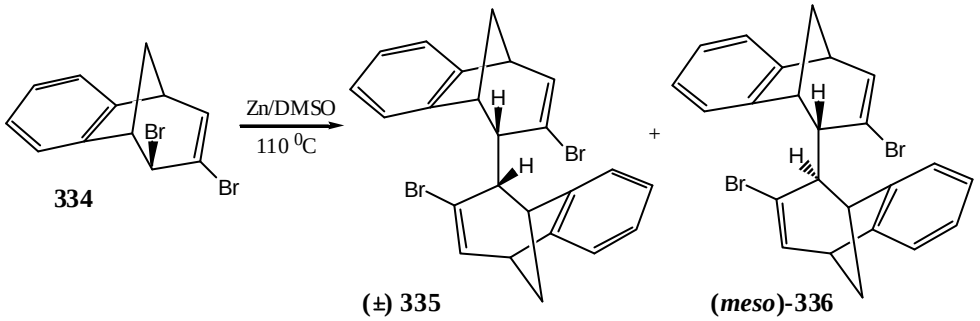

334 **(±) 335** **(*meso*)-336**

More recently, Balci and Özen [113] have succeeded to synthesize allene **310** with Doering-Moore-Skattebøl method. Addition of fluorobromocarbene, generated from $CHFBr_2$ and NaOH under phase-transfer conditions to benzonorbornadiene (**337**) afforded the *exo*-bromofluoro ring-opened product **340** and the expected addition product, the fluorobromocyclopropane **338**, in a ratio of 3:2 and in a total yield of 42%. Treatment of a solution of 10-Bromo-10-fluorotetracyclo[$6.3.1^{2,7}.0^{9,11}$] dodeca-2,4,6-triene (**338**) in ether with methyllithium in the presence of furan or styrene yielded the trapping products **342**, **343** and **341**, respectively. The formation of these trapping products confirms the formation of the bicyclic allene **310** as a reactive intermediate.

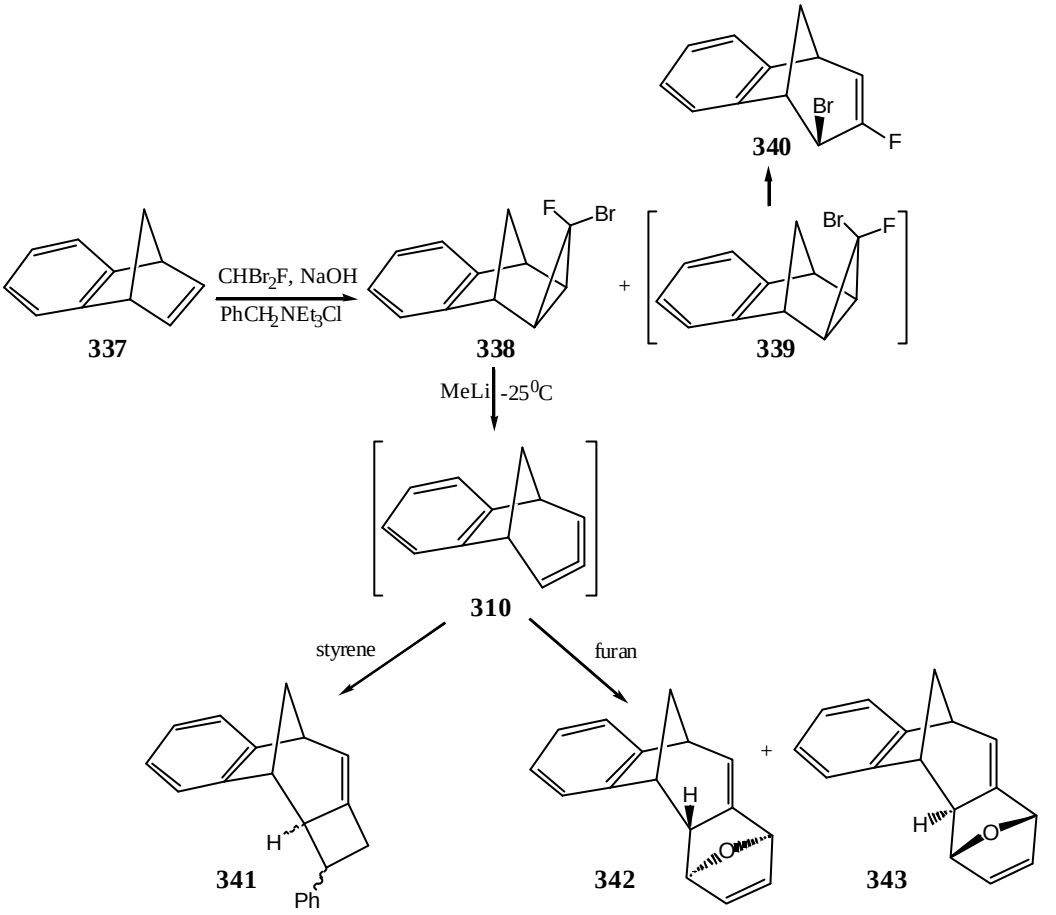

Some years ago, Mohanakrishnan *et al.* [114] reported that the base-induced dehydrobromination of **344** gives the highly strained bicyclic allene **345**, which was trapped as either enol ether **346** or its [2+2] cycloaddition product **347**. An alternate mechanism for the formation of these products was not discussed.

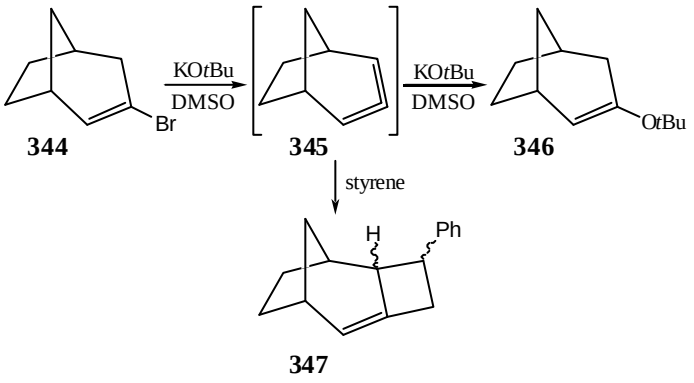

Later, Bottini and Hilton [115] reported another experimental study for bicyclo[3.2.1]octa-2,3-diene (**345**) which was generated by treatment of the corresponding dichloride **348** with magnesium in THF. It was found to undergo cycloaddition reactions with activated olefins, 2,3-dimethylbutadiene, styrene and 1,3-cyclopentadiene to form **349**, **350** and **351**, respectively.

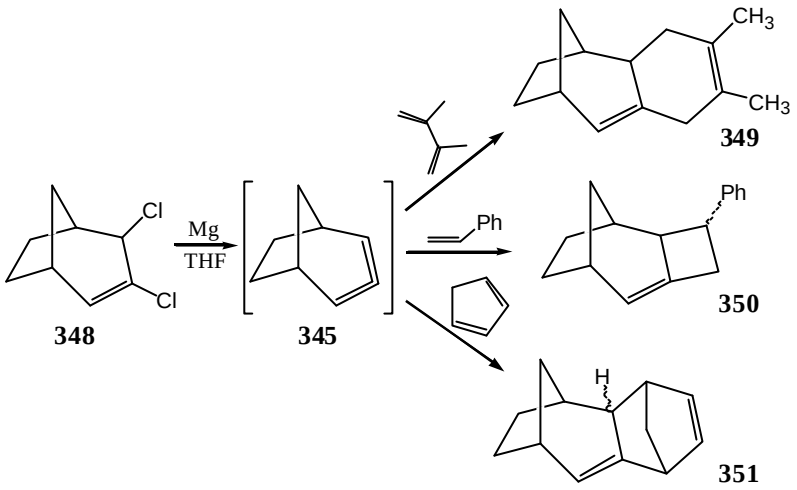

348 **345** **349** **350** **351**

More recently, Sevin and Dogan [13] have focused on the possibilities of intramolecular trapping and fragmentation products of *endo*-bicyclo[3.2.1]octa-2,3-dien-6-ol (**352**) with the concerted reaction mechanism by using quantum chemical calculations at the semiemprical PM3, PM5, and the molecular density functional, B88-PW91 and B88-LYP. The theoretical calculations show that cyclohexa-2,4-dien-1-ylacetaldehyde (**353**) and (5Z)-octa-1,5-dien-7-yn-3-ol (**354**) are competitive reactions and appear more favour than the intramolecular trapping product 2-oxatricyclo[4.2.1.$0^{3,8}$]non-4-ene (**356**).

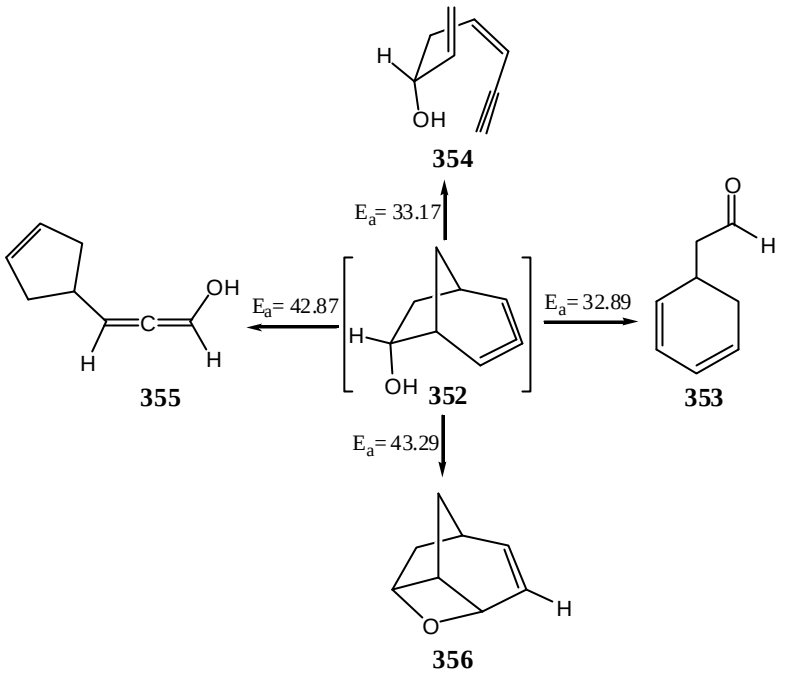

Christl and co-workers [116] have succeeded to synthesize highly strained tricyclic allene **359** which was trapped with different activated olefins.

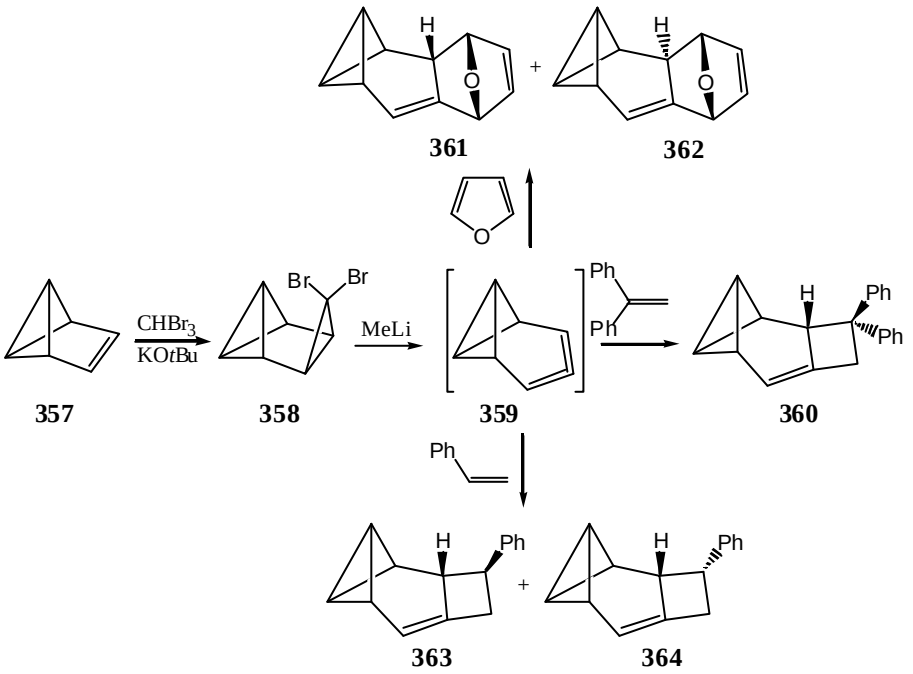

More recently, Okazaki *et al.* [117] have reported that dehalogenation of 3-bromo-4-iodo-4-homoadamantene (**365**) with *n*-BuLi, which gives rise to 3,4-homoadamantadiene (**366**), a novel tricyclic bridgehead allene. It readily dimerizes

to head-to-head and head-to-tail [2+2] cycloadducts, **367** and **368**, respectively, in a ratio of 96:4. The selectivity was much higher than that of the known bridgehead olefins. Trapping **366** with DPIBF is successful to produce the corresponding Diels-Alder adduct **369** in 79% yield.

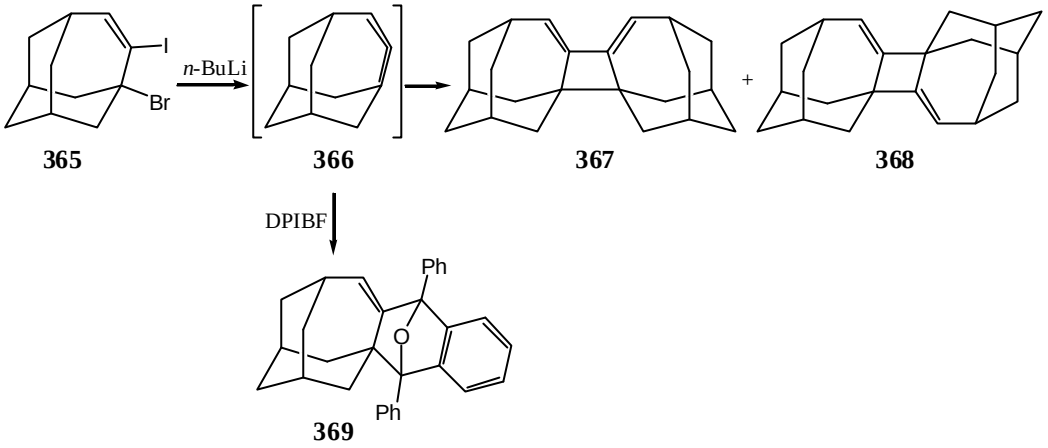

365 **366** **367** **368**

369

1.3. AIMS OF THE STUDY

The syntheses of bicyclic allenes are of considerable interest in organic chemistry because of their high strain and reactivity as mentioned before. However, the studies on bicyclic allenes are remarkably limited when compared with the cyclic allenes.

In the first part of the work, it is aimed to develop synthetic strategies leading to the synthesis of the following bicyclic strained allenes **371** and **372**, starting from α-pinene.

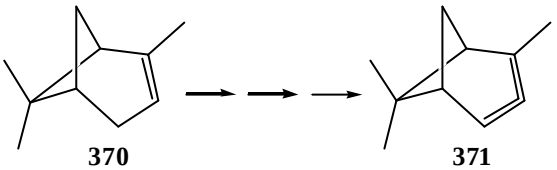

370 **371**

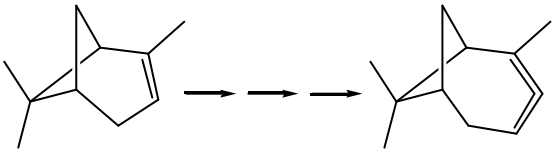

370 **372**

In the second part of the work, it is aimed to develop a synthetic strategy leading to the dihalocyclopropanes **373** and to investigate its reaction with MeLi to test the behaviour of the *endo* cyclopropylidene **374** which affords either allene or carbene addition product, **375**.

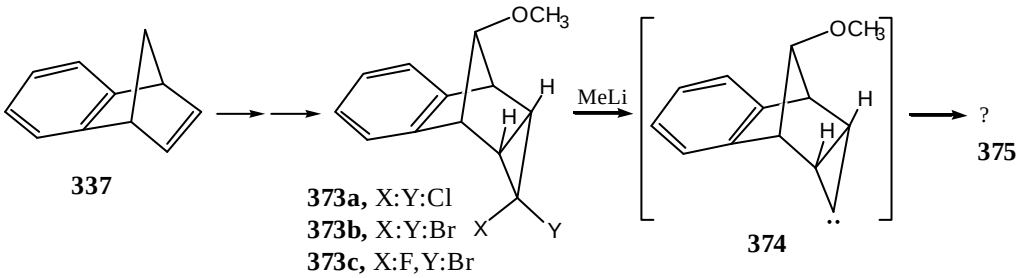

337

373a, X:Y:Cl
373b, X:Y:Br
373c, X:F,Y:Br

374

375

CHAPTER 2

RESULTS AND DISCUSSION

2.1. THE REACTION PATH FOR THE SYNTHESIS OF 2,6,6-TRIMETHYL-BICYCLO[3.1.1]HEPTA-2,3-DIENE (371)

The synthetic path for the synthesis of 2,6,6-trimethyl-bicyclo[3.1.1]hepta-2,3-diene (**371**) is summarized below. According to this path, compound **376** would be synthesized from the bromination of α-pinene. Then, it would be subjected to the elimination reaction with KO*t*Bu to yield **377**. Finally, bicyclic allene **371** would be generated by the β-elimination of hydrogen bromide from **377** with KO*t*Bu.

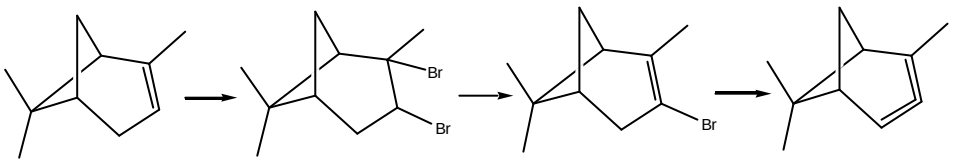

370 **376** **377** **371**

2.1.1. Bromination of 1R-(-)-a -pinene

α-Pinene (**370**), $C_{10}H_{14}$, (IUPAC Name: 2,6,6-trimethylbicyclo[3.1.1]hept-2-ene) is widely distributed in nature, being found in most essential oils of the *Coniferae*. Due to this abundance, there are much more studies starting from 19th Century on α-pinene in the literature. However, they were complicated because α-pinene readily undergoes molecular rearrangements [118]. Many rearrangements of α-pinene are of the Wagner-Meerwein type [119], which takes place via the formation of a carbonium ion.

From the bromination of α-pinene, Wallach [120] isolated two products, bornyl bromide (**378**) and a dibromide **379** which he considered to a true pinene derivative (non-arranged product, **376**), but Semmler [120] showed that the dibromide was a 2,6-dibromobornane (**379**). Later, Raymond and Walker [121] reported the stereochemistry of these products **378** and **379** with NMR spectroscopy. Hence, bromination of α-pinene at 0 ^{0}C gives the rearranged products, **378** and **379**, via Wagner-Meerwein rearrangement with accompanying alkyl migration.

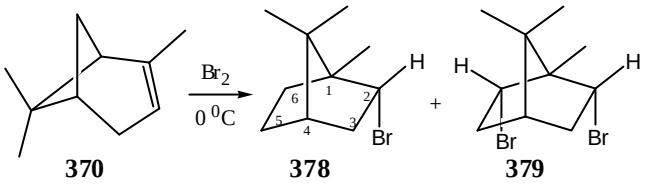

370 **378** **379**

On the other hand, Balci *et al.* [122] reported that high temperature bromination of benzonorbornadiene (**337**) resulted in the formation of small amount of **380** and non-arranged products, **381**, **382**, **383** although bromination of **337** at room and lower temperature gives the only rearranged product **380**. High temperature bromination prevents skeletal rearrangement.

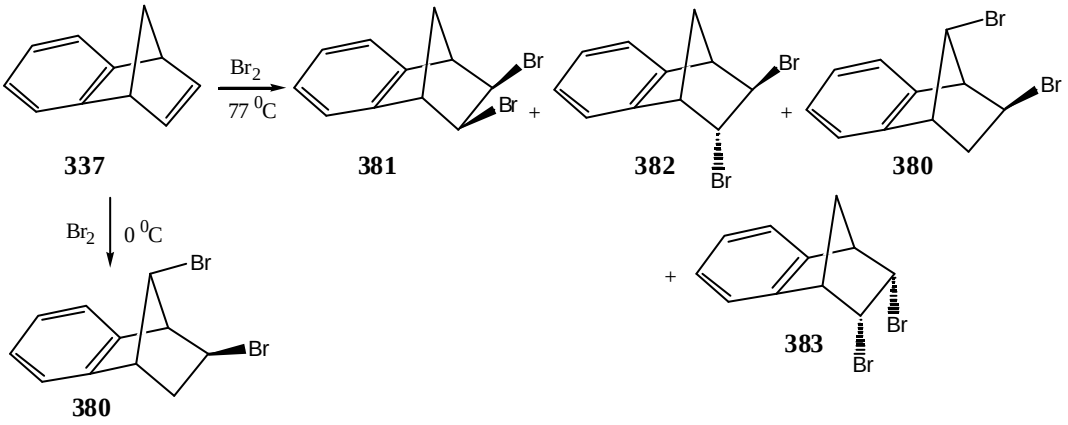

337 **381** **382** **380**

380 **383**

In the light of these literature data, the addition of bromine to α-pinene (**370**) was carried out at low (0 ^{0}C) and high (77 ^{0}C) temperature to investigate the effect of temperature on the formation of products and to synthesize the non-arranged product **376**. After performing bromination in carbontetrachloride at 0 ^{0}C, two products, **378**

and **379**, reported in the literature [120], were isolated in the yields of 18 % and 74%, respectively (Table 5).

Then, α-pinene was submitted to high temperature bromination. To a refluxing solution of α-pinene in carbontetrachloride was added a hot solution of equal amount of bromine over 1 hour period. The solution was stirred at the reaction temperature for an additional 30 min. After silica gel column chromatography, we isolated the same products, **378** and **379**, with the yields of 61 % and 10%, respectively.

Table 5: The products' yields at low and high temperature bromination of α-pinene

	378 (%)	**379(%)**
Low Temp. Bromination	18	74
High Temp. Bromination	61	10

The assignment of the structures to **378** and **379** was accomplished by ^{1}H and ^{13}C-NMR spectral data. ^{1}H-NMR spectrum of **378** consists of three singlets at 0.80, 0.82 and 0.91 ppm for three methyl group protons, doublet of doublets of doublets at 1.19-1.25 ppm for H_{5exo} proton, multiplet at 1.27-1.41 ppm for H_{6exo} proton, doublet of doublets at 1.47 ppm for H_{3exo} proton, triplet at 1.60 for H_4 proton, multiplet at 1.62-1.73 ppm for H_{5endo} proton, doublet of doublets of doublets at 1.99-2.04 ppm for H_{6endo} proton, multiplet at 2.41-2.50 ppm for H_{3endo} proton, and doublet of doublets of doublets at 4.20 ppm for H_{2exo} proton. There are ten lines in the ^{13}C-NMR spectrum of **378** at 14.2, 19.0, 21.4, 28.5, 30.8, 41.2, 45.5, 47.4, 51.2, 62.3 ppm. A signal at 62.3 ppm arises from C-2 carbon attached to bromine atom.

Moreover, ^{1}H-NMR spectrum of **379** shows two singlets at 0.91 and 0.94 ppm for three methyl group protons, triplet at 1.72 ppm for H_4 proton, doublet of doublets at 1.77 ppm for H_{3exo} and H_{5exo} protons, doublet of doublets of doublets at 2.54 ppm for H_{3endo} and H_{5endo} protons, and doublet of doublets at 4.29 ppm for H_{2exo} and H_{6exo} protons. ^{13}C-NMR spectrum consists of seven signals at 13.1, 21.1, 41.1,

44.1, 48.9, 52.8, 55.2 ppm because of the symmetry in the molecule. A signal at 55.2 ppm results from C-2 and C-6 carbons attached to bromine atoms.

As a result, the target bicyclic allene **371** could not be synthesized from the reaction path offered at the start of work.

2.2. THE REACTION PATH FOR THE SYNTHESIS OF 2,7,7-TRIMETHYL-BICYCLO[4.1.1]OCTA-2,3-DIENE (372)

The reaction path for the synthesis of 2,6,6-Trimethyl- bicyclo[3.1.1]hepta-2,3-diene (**372**) is summarized below. According to this path, compound **385** was synthesized from the reaction of dibromocarbene with α-pinene. Then, it was reacted with MeLi to generate the bicyclic allene **372**.

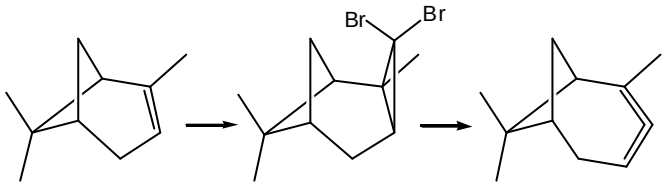

370 **385** **372**

2.2.1. Reaction of dibromocarbene with 1R-(-)-a -pinene

Carbenes are molecules containing divalent carbon atoms. Each divalent carbon has two unshared electrons, which are often shown when writing the structures of carbenes (Figure 8). However, carbenes are neutral molecules, not carbanions.

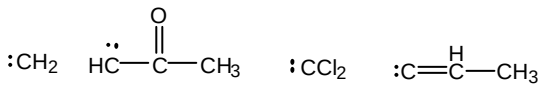

Figure 8: Some typical carbenes

The rather vague term carbenoids is used to refer to molecules in which all the carbons are tetravalent, but which have properties resembling those of carbenes.

Those properties often include the ability to transfer divalent carbons and their substituents to other molecules. Typically, carbenoids have carbon atoms that are simultaneously bonded both to metal atoms and to halogen atoms. It is often difficult to be certain whether a 'carbene' reaction in solution is actually the reaction of a free carbene or the reaction of a carbenoid [123].

Although carbenes can be formed a wide variety of reactions [124], halocarbenes are commonly prepared by reactions of strong bases with organic polyhalides that lack hydrogens on β-carbons, and therefore cannot undergo the usual β-elimination reactions [125]. Instead, the bases abstract protons from the polyhalogenated carbons. The resulting carbanions then lose halide ions to form carbenes, as shown in Figure 9.

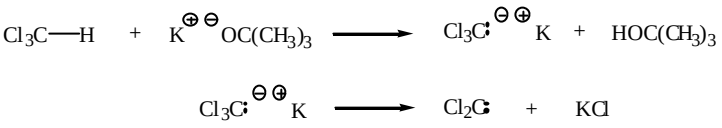

Figure 9: The formation of dihalocarbene

Polyhalides with bromine or iodine atoms can react with organolithium reagents to form α-halolithium reagents, which are frequently stable at dry ice temperatures (Figure 10). At higher temperatures, they react to yield products similar to those obtained from carbenes formed by other methods. However, the ratios of products can vary depending on the types of halogen, suggesting that the α-halolithium compounds act as carbenoids rather than dissociating to form free carbenes [126].

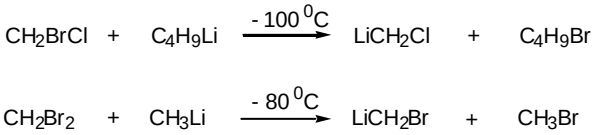

Figure 10: The formation of α-halolithium reagents

The current interest in carbene chemistry stems in large part from the demonstration by Doering and Hoffmann, in 1954, that dihalocarbenes can add to alkenes to form cyclopropane derivatives in high yields [127].

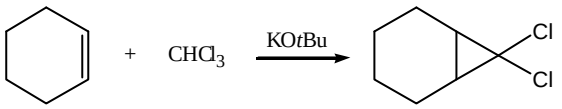

386 **387**

After that, *gem*-Dihalocyclopropanes play an important role in synthetic organic chemistry. They are valuable subtrates for the preparation of monohalocyclopropanes, cyclopropanes, cyclopropenes, benzocyclopropenes, bicyclobutanes, allenes, cumulenes and many other hydrocarbon systems, both unsubstituted and possessing useful functional groups [128].

The studies on the addition of dihalocarbene to α-pinene was firstly reported at 1970 by Arbuzov *et al.* [129] who explained that the dichlorocarbene adduct **388** was synthesized with the yield of 30% as a stable crystal. However, the dibromocarbene adduct **385** could not be isolated because it is unstable at room temperature. One year later, Muehlstaedt *et al.* [130] showed that the reaction of α-pinene with dibromocarbene results in **385** and it readily rearranges to 2,3-dibromo-2,7,7-trimethylbicyclo [4.1.1]oct-3-ene (**389**) at room temperature.

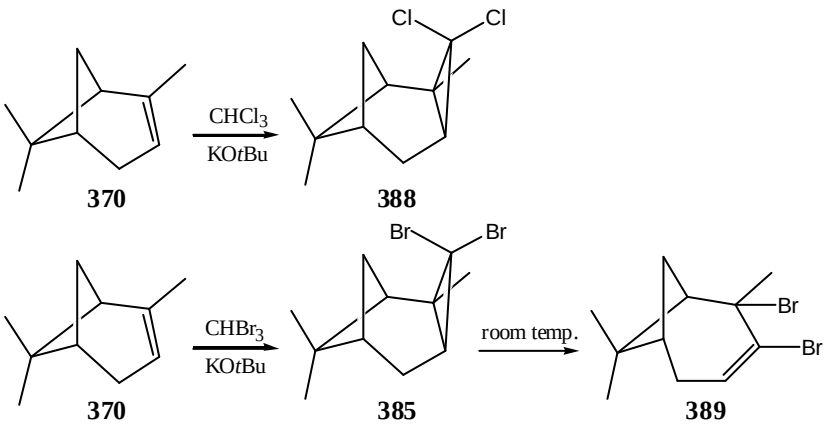

370 **388**

370 **385** **389**

At the same year, Hatem and Waegell [131] reported that **385** could not be isolated in the stable form due to its rapid ring openning to **391** and **392** with the ratio

of 8:2, respectively. Recently, they isolated **385** in the stable form, but their ^{1}H-NMR data were not sufficient to characterize the structure of **385** exactly [132].

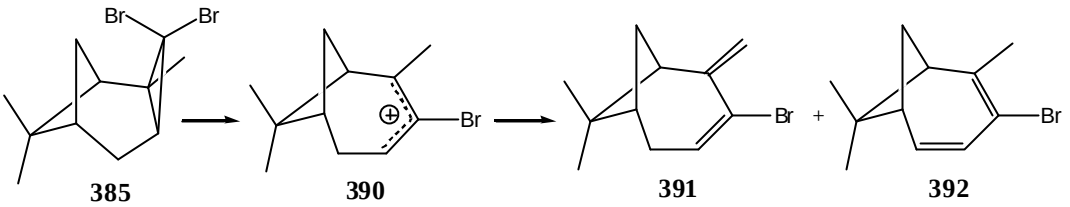

385 **390** **391** **392**

More recently, [a]enol and Balci [133] showed in their unpublished results that the dibromocarbene adduct **385** is stable in hexane for a week at room temperature and it can be synthesized up to 59% yield.

According to these literature data, a solution of α-pinene in hexane was added to a mechanically stirred suspension of potassium *tert*-butoxide in hexane, which was then pre-cooled and maintained at –10 ^{0}C with ice-salt bath under a nitrogen atmosphere. A solution of equivalent amount of bromoform in hexane was added to this suspension while maintaining the reaction mixture at –10 ^{0}C. After the addition was completed, the mixture was stirred at room temperature for two hours and hydrolyzed through the addition of water. After work-up, the residue was crystallized from hexane in the refrigerator to provide the cyclopropane adduct **385** as colorless crystals. The reaction yield was up to 71%, which is higher than the previous reported values [129-133].

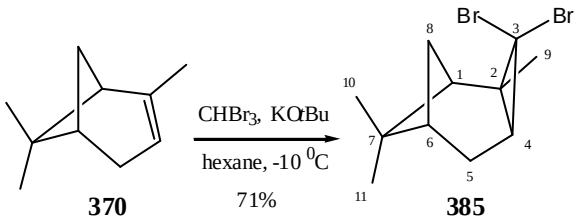

370 **385**

The characterization of **385** was based on the ^{1}H and ^{13}C-NMR spectral data, which was not reported exactly in the literature before. ^{1}H-NMR spectrum consists of three singlets at 0.84, 1.16 and 1.29 ppm for three methyl group protons, multiplet at 1.49-1.53 ppm for H_6 proton, multiplet at 1.54 ppm for H_4 proton, doublet at 1.70 ppm for H_{5b} proton, doublet of doublets of doublets at 1.76 ppm for H_{8d} proton,

triplet at 1.96 ppm for H_1 proton, multiplet at 2.06-2.13 ppm for H_{5a} proton, and doublet at 2.41 for H_{8c} proton. There are eleven signals in the ^{13}C-NMR spectrum of **385** at 22.5, 26.2, 26.7, 26.8, 27.1, 32.6, 35.0, 39.9, 43.4, 48.6, 50.8 ppm. A signal at 50.8 ppm comes from C-3 carbon bonded to two bromine atoms.

2.2.2. The heat stability of 3,3-dibromo-2,7,7-trimethyl-tricyclo[4.1.1.0^{2,4}]octane (385)

Sandler and Skell [135] explained that the strain in the [3.1.0] ring system of **87** results in greatly enhanced reactivity, **87** being 200 times as reactive as the analogous 7,7-dihalobicyclo[4.1.0]heptane which has a [6.3.0] ring system. The reactions of geminal dihalocyclopropanes cause the formation of alkenes via ring expansion. Moreover, the reactions of these compounds with electrophilic reagents and or heat results in allyl derivatives, whereas the reactions with Mg, Na, or alkyllithiums result in the formation of allenes.

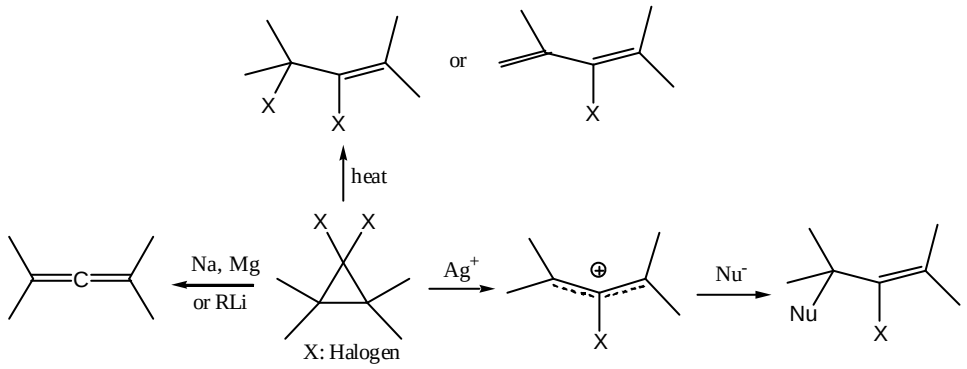

Figure 11: The reactions of geminal dihalocyclopropanes with Ag^+, heat, and Na, Mg or MeLi.

Sonnenberg and Winstein [134] reported that 6,6-dibromobicyclo [3.1.0]hexane (**87**) rearranges thermally at 150 ^{0}C for a short time to yield the dibromide **393**.

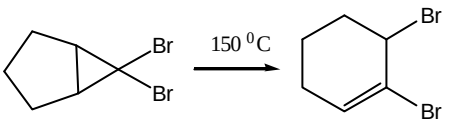

87 **393**

Sütbeyaz *et al.* [136] have isolated dibromo **396** and tetrabromo **397** from the reaction of dibromocarbene and cyclobutene **394** and they could not isolate the dibromocyclopropane adduct **395**.

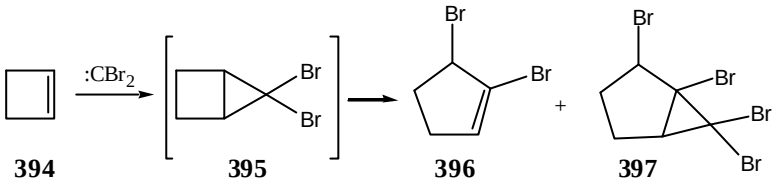

394 **395** **396** **397**

Therefore, the stability of cyclopropane ring decreases as the ring strain in the formed molecule increases. To investigate the heat stability of 3,3-dibromo-2,7,7-trimethyl-tricyclo[4.1.1.$0^{2,4}$]octane (**385**), it was refluxed in hexane. The reflux condition was checked with TLC every half-hour to determine whether **385** was consumed completely or not. After seven hours, all of **385** were converted to **391** as a sole product.

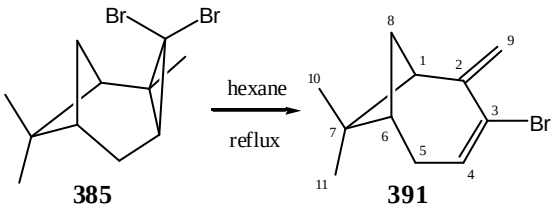

385 **391**

The structure of **391** has been elucidated on the basis of ^{1}H- and ^{13}C-NMR spectral data. ^{1}H-NMR spectrum of **391** shows two singlets at 0.64 and 1.13 ppm for two methyl group protons, doublet at 1.41 ppm for H_{8d} proton, multiplet at 1.91 ppm for H_6 proton, multiplet at 2.24 ppm for H_5 proton, doublet to triplet at 2.30 ppm for H_{8c} proton, doublet of doublets at 2.63 ppm for H_1 proton, singlet at 5.00 ppm for H_{9b} proton, singlet at 5.39 ppm for H_{9a} proton, triplet at 6.16 ppm for H_4 proton. There are eleven signals in the ^{13}C-NMR spectrum of **391** at 20.8, 26.6, 30.2, 34.2, 39.7,

40.5, 51.7, 122.0, 123.3, 133.3, 145.8 ppm. Olefinic carbons, C_9, C_3, C_4, and C_2, resonate at 122.0, 123.3, 133.3, and 145.8 ppm, respectively.

2.2.3. Reaction of 3,3-Dibromo-2,7,7-trimethyl-tricyclo[4.1.1.$0^{2,4}$]octane (385) with MeLi

As described in Chapter 1, from among the numerous synthetic approaches [10-12] to the cyclic allenes currently available, the conversion of 1,1-dihalocyclopropanes [128] to the corresponding cyclic allenes upon treatment with alkyllithium reagents discovered by Moore and co-workers [53] and Skattebol [31] has played the most important role. This part of study describes an investigation aimed at the incorporation of an allene unit into a natural product, being α-pinene, by using the above-mentioned method.

It has been reported independently by Baird *et al.* and Waegell *et al.* [137] in the literature that the reaction of dibromide **385** formed by the addition of dibromocarbene to α-pinene exclusively provides the insertion product **398** upon the treatment with methyllithium in a 94% yield. However, 2,7,7-trimethylbicyclo[4.1.1] octa-2,3-diene (**372**), was not observed.

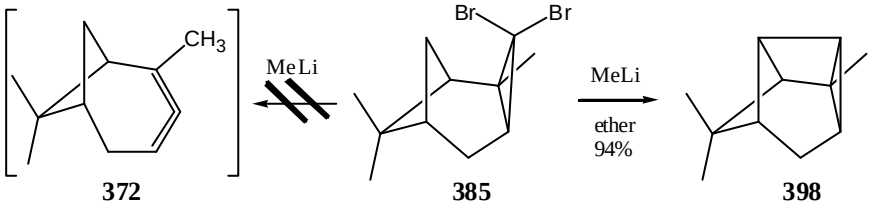

372 **385** **398**

The Doering-Moore-Skattebol method is the most efficient for the generation of cyclohexa-1,2-diene (**4**) [69], but paradoxically, this method was not successful for the synthesis of cyclohepta-1,2-diene (**3**) [53, 54, 138]. Therefore, Schleyer *et al.* have focused on the ring opening of bicyclo[4.1.0]hept-7-ylidene (**53**) by using density functional theory calculations at the B3LYP/DZP and TZP levels [20].

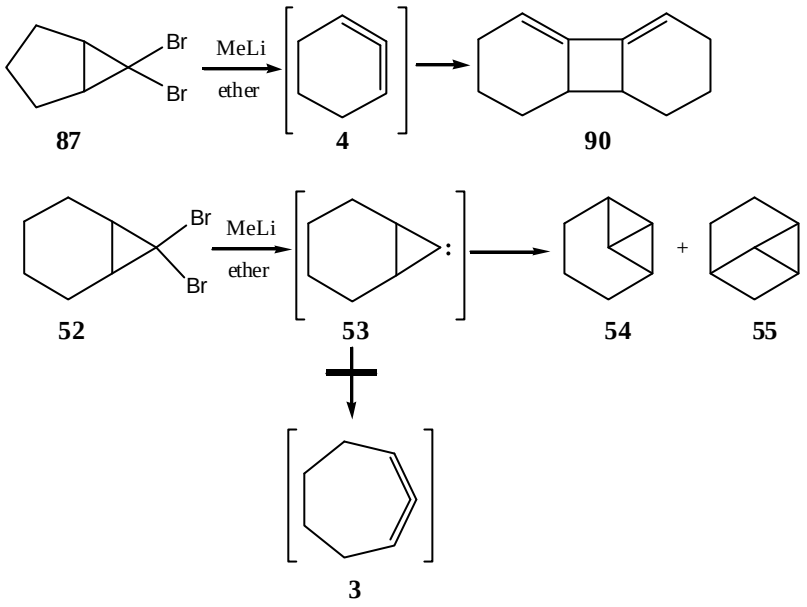

They found that the ring opening of **53** to **3** has unusually high activation energy of 14.6 kcal/mol because of the unfavorable conformational changes in the cyclohexane moiety of **53** during the reaction. However, the activation barriers for intramolecular CH-insertions to yield highly strained hydrocarbons, tricyclo[4.1.0.$0^{2,7}$]heptane (**54**) and tricyclo[4.1.0.$0^{3,7}$]heptane (**55**) were found to be 6.4 and 9.1 kcal/mol, respectively. They concluded that the half-chair conformation of the cyclohexane moiety in **3** must change to a chair conformation during the reaction [20].

Therefore, there is an important question why **399** fails to give **372** which should possess the additional strain, compared to **3** and this additional strain results from the methyl substituent and bicyclic form of **372**. To address the question of "why does 2,7,7-trimethyltricyclo[4.1.1.$0^{2,4}$]oct-3-ylidene (**399**) fail to provide the bicyclic allene **372**", we studied the ring opening of **399** with DFT computations.

The GAUSSIAN 98W [139] program was used for density functional theory (DFT) [140] calculations, employing Becke's three hybrid method [141] and the exchange functional of Lee, Yang, Parr (B3LYP) [142]. Results reported by Schleyer *et al.* for the ring opening of the unsubstituted and substituted cyclopropylidenes indicate that B3LYP should be reliable for this type of reaction [20, 143]. The geometry optimizations of all the structures were achieved at the B3LYP/6-31G(d)

level. Energies were refined by using B3LYP/6-31G(d) single point evaluations. Stationary points were characterized as minima or transition structures by way of an analytic evaluation of harmonic vibrational frequencies at the level of geometry optimization.

Table 6: The relative energy values (kcal/mol) for products of the ring opening of bicyclo[4.1.0]hept-7-ylidene (**53**) calculated by using B3LYP/6-31G(d) basis set and their literature values [20].

	Relative Energy	
	B3LYP/6-31G(d)	B3LYP/TZP
53	0.0	0.0
54	6.2	6.4
55	9.6	9.1
3	15.1	14.6

First of all we have recalculated the reported results by Schleyer et al. [20] to analyze the reliability of the chosen 6-31G(d) basis set with respect to the TZP basis set, which was used for the ring opening of bicyclo[4.1.0]hept-7-ylidene (**53**) [20]. Therefore, geometry optimizations were performed again at the chosen basis set. As can be seen in Table 6, our results are found to be consistent with reported literature values.

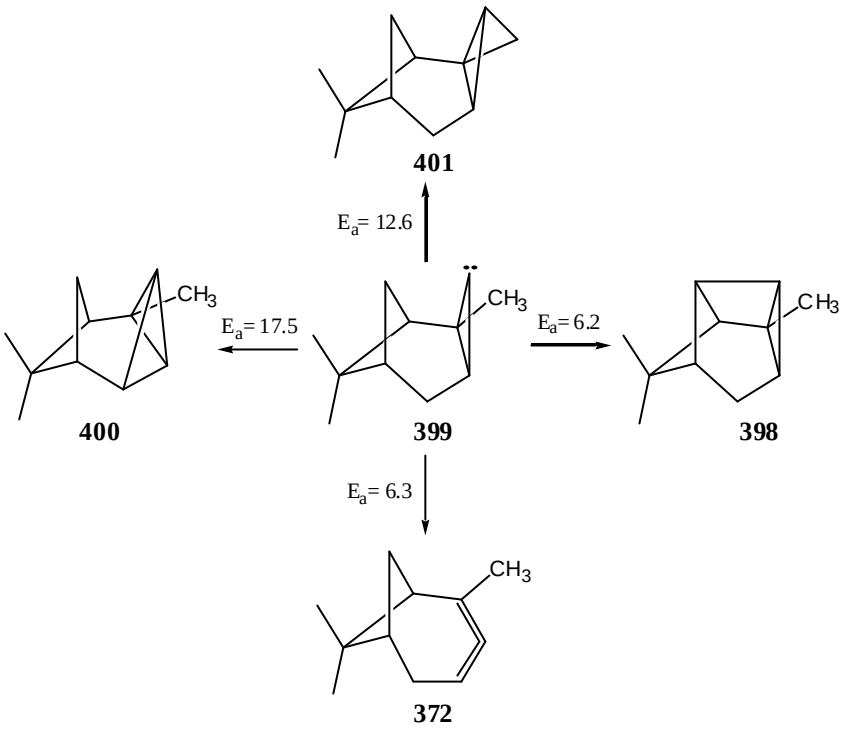

After this we turned our attention to elucidate the insertion and ring opening reactions of the carbenoid **399**. Three possible products can be considered for the intramolecular CH-insertion reactions of **399**; 3,7,7-trimethyltetracyclo-[4.2.0.0^{2,4}.0^{3,8}]octane (**398**), 2,7,7-trimethyltetracyclo[4.1.1.0^{2,4}.0^{3,5}]octane (**400**), and 8,8-dimethyltetracyclo- [5.1.1.0^{2,4}.0^{2,5}]nonane (**401**) (Scheme 3). The computed activation energy barriers for their internal CH-insertions are predicted to be 6.2 kcal.mol^{-1} (**TS1**) for **399**® **398**, 12.6 kcal.mol^{-1} (**TS3**) for **399**® **401**, and 17.5 kcal.mol^{-1} (**TS2**) for **399**® **400** (Table7). According to these results, the formation of insertion products, **400** and **401** is less likely, whereas **398** can be easily formed during the reaction due to the low activation energy barrier. On the other hand, the activation barrier for the disrotatory ring-opening reaction forming allene, **399**® **372**, is predicted to be 6.3 kcal.mol^{-1} which is as low as the insertion reaction **399**® **398**. This explains that both allene product **372** and insertion product **398** can be isolated if the reaction of **385** with MeLi is carried out at either low or high temperatures.

Table 7: Absolute energies (E, in hartree/particle), number of imaginary frequencies [in brackets], zero-point vibrational energies (ZPVE, in kcal/mol), and energies relative to the carbene ground state including zero-point corrections (in kcal/mol) for the insertion products, **398**, **400**, **401**, and the bicyclic allene **372**, and the related transition state structures (**TS1**, **TS2**, **TS3**, **TS4**).

	Energy	ZPVE	Relative Energy
399	-428.61424 [0]	150.4	**0.0**
398	-428.71827 [0]	152.3	**-63.3**
400	-428.67802 [0]	151.7	**-38.7**
401	-428.69134 [0]	152.7	**-46.0**
372	-428.69093 [0]	151.5	**-46.9**
TS1 (399 ® 398)	-428.60140 [1]	148.6	**6.2**
TS2 (399 ® 400)	-428.58417 [1]	149.0	**17.5**
TS3 (399 ® 401)	-428.59236 [1]	149.2	**12.6**
TS4 (399 ® 372)	-428.60370 [1]	150.1	**6.3**

Optimized structures of **398**, **399**, **400**, **401**, and **372** and transition structures **TS1**, **TS2**, **TS3**, and **TS4** at B3LYP/6-31G(d) level are shown in Figure12. These structures are visualized by using Molden [144] and Mercury [145] programs.

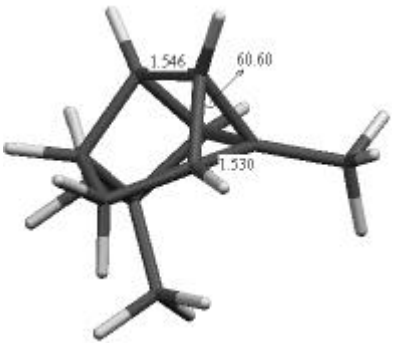

398

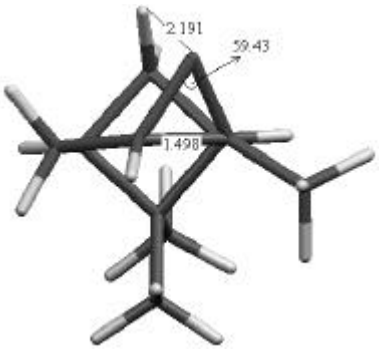

399

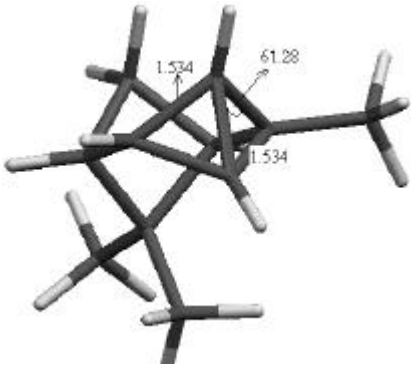

400

401

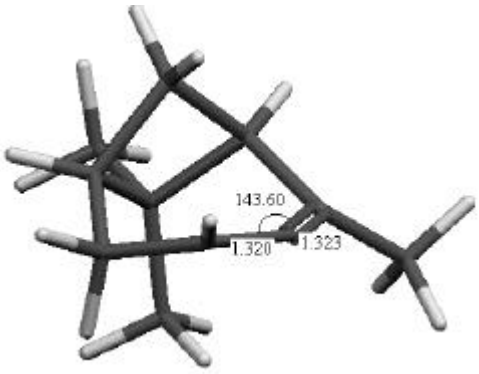

372

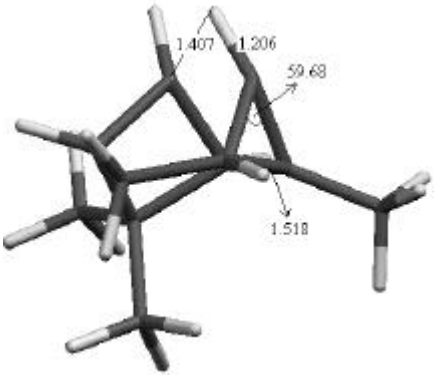

TS1 (399 ® 398)

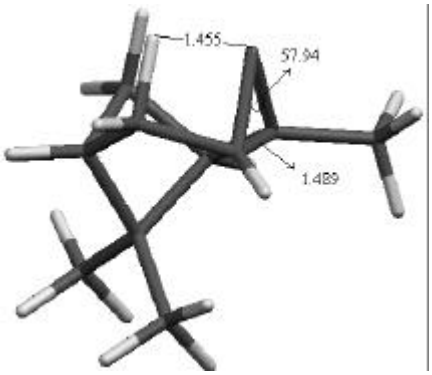

TS2 (399 ® 400)

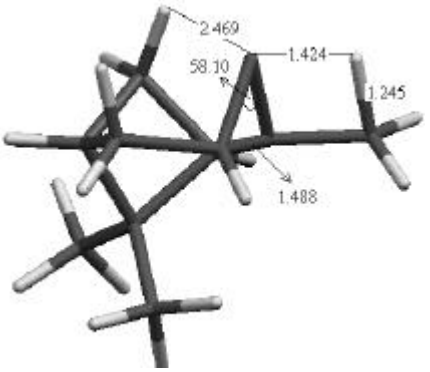

TS3 (399 ® 401)

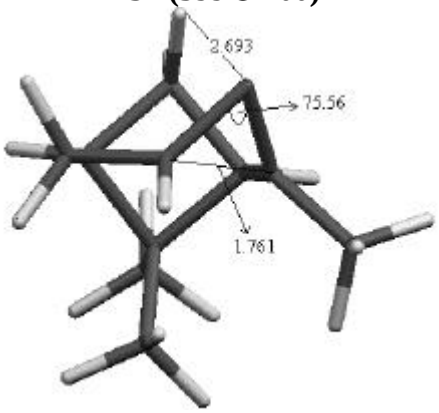

TS4 (399 ® 372)

Figure 12: Optimized structures of **398**, **399**, **400**, **401**, and **372** and transition structures **TS1**, **TS2**, **TS3**, and **TS4** at B3LYP/6-31G(d).

Moreover, the optimized geometry of bicyclic allene **372** by DFT calculations at the B3LYP/6-31G(d) level has a C_s symmetry with a bending angle of 143.60 °. This bending value is lower than seven membered cyclic allene's value, whereas this is higher than six membered cyclic allene's value (Figure 6). This means that the strain in **372** should be higher than the cyclohepta-1,2-diene (**3**) and lower than cyclohexa-1,2-diene (**4**).

After showing the possibilities of formation of **372**, which is nearly equal to that of **398** by theoretical calculations, we have repeated the reaction of dibromocarbene adduct **385** with methyllithium at various temperatures to investigate what will happen experimentally. Therefore, to a magnetically stirring solution of **385** in dry ether was added dropwise MeLi in ether at room temperature and the resulting solution was stirred for 2 hours at that temperature. The reaction mixture was quenched carefully with water. After the usual aqueous work-up procedure and vacuum distillation for the seperation of the insertion product **398**, the residue was analyzed by ^1H and ^{13}C NMR measuments, whose spectra showed the formation of three dimeric products, **403**, **404**, and **405**, with a total yield of 37%.

The structure of insertion product **398** has been also elucidated on the basis of ^1H- and ^{13}C-NMR spectral data. The ^1H-NMR spectrum of **398** shows three singlets at 0.60, 0.74, and 0.99 ppm for three methyl group protons, broad doublet at 1.20 ppm for H_4 proton, doublet of doublets at 1.66 ppm for H_{5b} proton, triplet at 1.72 ppm for H_3 proton, doublet of doublets at 1.89 ppm for H_6 proton, doublet of doublets at 1.94 ppm for H_1 proton, doublet at 2.02 ppm for H_{5a} proton, doublet of doublets of doublets at 2.57 ppm for H_8 proton. There are eleven signals in the ^{13}C-NMR spectrum of **398** at 19.5, 20.4, 26.0, 27.1, 27.5, 31.3, 32.0, 35.7, 36.8, 48.0, 49.0 ppm. Methylenic carbon resonates at 31.3 ppm and bridge-head carbons resonates at 26.0, 32.0, 36.8, 48.0, 49.0 ppm.

Column chromatography on SiO_2 and subsequent recrystallization from ethanol afforded **403** as colorless crystals, whose UV spectrum in hexane showed

absorption bands at 260 nm (Figure 13). This value indicates the existence of a conjugated butadiene structure [117].

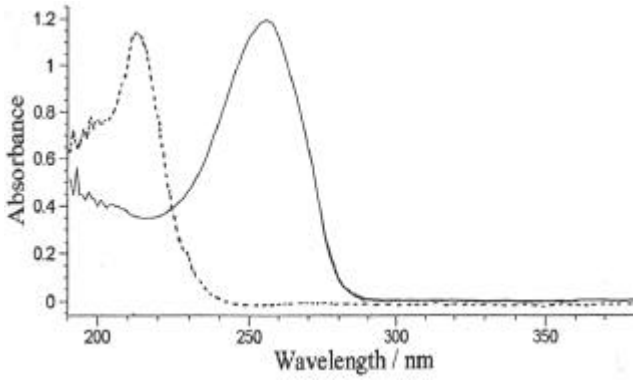

Figure 13: UV spectra for the dimeric products in hexane (**403**: solid line, 9.41×10^{-5} M, λ_{max}= 260 nm, å= 12698 $M^{-1}cm^{-1}$; **404+405**: dashed line, 7.63×10^{-5} M, λ_{max}= 212 nm, å= 15068 $M^{-1}cm^{-1}$)

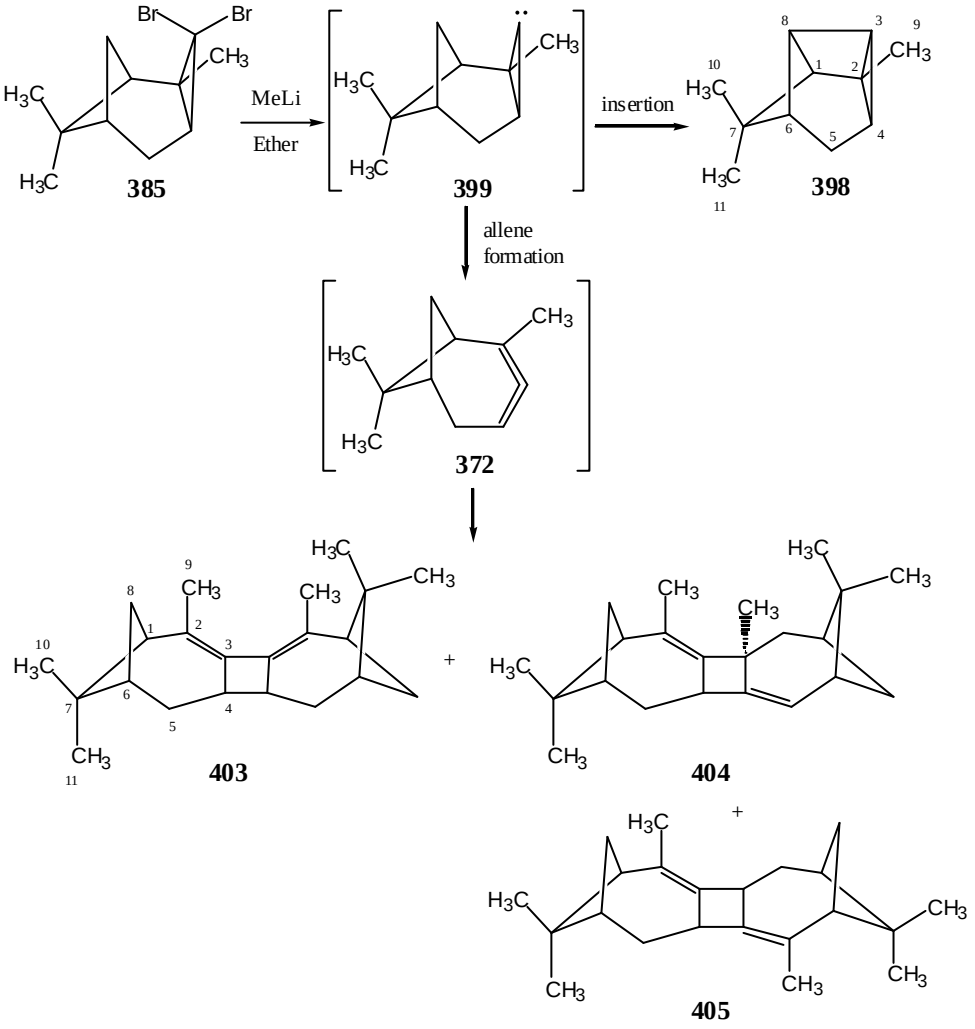

Furthermore, ^{1}H-NMR spectrum of **403** provides that there is no olefinic proton in its structure. However, ^{13}C-NMR spectrum of **403** shows the presence of olefinic carbons which resonate at 127.7 and 136.0 ppm. The 11-signals in the ^{13}C-NMR spectrum and the molecular peak of 296 (M+) in mass spectrum (GC/MS) clearly indicated the presence of an allene dimer. Moreover, X-Ray analysis of **403** was carried out to determine its exact configuration. As it can be seen from Figure 14, it is a head to head dimer and the dimethyl bridges are in the anti-position.

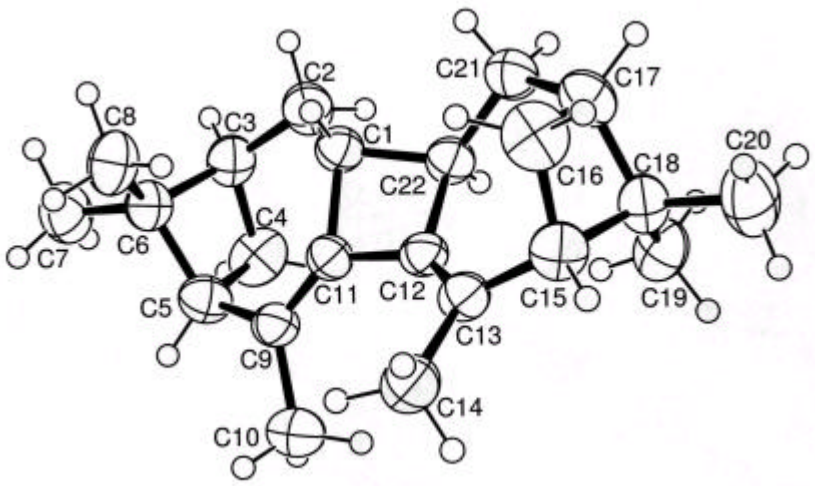

Figure 14: X-ray crystal structure of the allene dimer **403**

All efforts by using column chromatography, crystallization and distillation to separate the diastereomeric mixture consisting of **404** and **405** in a ratio of 1:1 (determined by ^{1}H-NMR spectroscopy) failed. The UV spectrum of this mixture showed an absorption band at λ= 212 nm and no distinct peaks around 260 nm. This observation indicates that both diastereomeric isomers have a non-conjugated butadiene unit. Furthermore, 31 lines ^{13}C-NMR (two lines are overlapped, a total sum of 33 lines) spectrum showed the presence of symmetrical and unsymmetrical dimerization products. Moreover, the presence of a vinyl proton resonating as a doublet at 5.18 ppm indicates the presence of a head-to-tail dimerization product **404**. The mass spectrum of the mixture showed a single peak at 296 (M^{+}), which is

equal to the molecular weight of dimer. The elemental analysis of the mixture was also in agreement with the expected structures.

As a result, the formation of these trapping products, **403**, **404**, and **405** confirms the formation of the bicylic allene **372** as a reactive intermediate from the reaction of methyllithium with 3,3-dibromo-2,7,7-trimethyl-tricyclo[4.1.1.$0^{2,4}$]-octane (**385**).

Table 8: The amount of products (in a mol unit) for the reaction between 3,3-dibromo-2,7,7-trimethyl-tricyclo[4.1.1.02,4]octane (**385**) and MeLi at different temperatures.

Temperature (^{0}C)	[**398**]	[**403**]+[**404**]+[**405**]	[**398**]/([**403**]+[**404**]+[**405**])
-80	0.0319	0.00590	5.407
-50	0.0301	0.00693	4.343
-25	0.0294	0.00807	3.643
0	0.0281	0.00863	3.256
25	0.0273	0.00951	2.871

Additionally, the amounts of products at different temperatures were investigated for the reaction of **385** with MeLi. As it is seen in Table 8, the amount of dimerization products increased at the cost of the insertion product **398** when the reaction temperature increased from -80 ^{o}C up to 25 ^{o}C. The steady-state approximation can be applied on the allene intermediate **372**. If it is done, this product ratio can be found;

$$\frac{[3]}{[16]+[17]+[18]} = \frac{k_1}{k_2}$$

where k_1 is the rate constant for appearance of **398** and k_2 is the rate constant for the formation of allene **372**. From this equation, the trend of increasing product ratio in favour of **398** as the temperature is decreased is shown by a plot of In([**398**]/{[**403**]+[**404**]+[**405**]}) versus 1/T (Figure 15). This shows that the energy

barrier for the k_2 step leading to allene **372** is larger than that for the k_1 step leading to insertion product **398**. According to Arrhenius equation, the difference in activation energy between two products **398** and **372** can be calculated from the slope of this graph and be found that it is 0.685 kcal/mol. Hence, these results are in good agreement with our theoretical results.

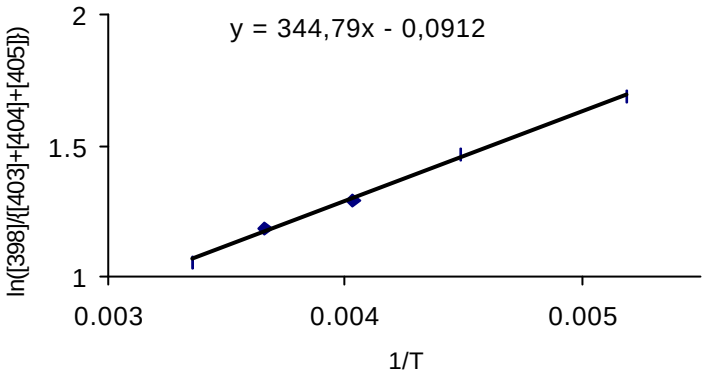

Figure 15: A graph of In([**398**]/{[**403**]+[**404**]+[**405**]}) versus 1/T

2.3. THE INITIAL EXISTENCE OF *EXO* AND *ENDO* CYCLOPROPYLIDENE INTERMEDIATE DURING THE FORMATION OF ALLENE

As mentioned before, Balci and Özen reported that the bicyclic allene **310** was synthesized by the treatment of *gem*-bromofluorocyclopropane with methyllithium. The possibility of formation of free carbene intermediate ***exo*-412** was not discussed in their paper.

338 ***exo*-412** **310**

To determine whether free carbene intermediate is initially formed or not, the theoretical calculations were carried out by using density functional theory at B3LYP/6-31(d) level. As can be understood from Table 9 and Figure 16, we could not find any minima for the structure of carbene ***exo*-412**, which readily isomerize to the corresponding allene structure **310** during the optimization process. This means that there is no free carbene intermediate ***exo*-412** for the formation of allene **310**.

Table 9: Electronic energies (E, in hartree/particle), number of imaginary frequencies [in brackets], zero-point vibrational energies (ZPVE, in kcal/mol), and sum of electronic and zero-point vibrational energies (in hartree/particle) for the molecules given in Figure 15. (* means that there is no minima for this structure)

	Energy	ZPVE	Energy + ZPVE
310	-463.174935 [0]	113.68	-462.993771
***exo*-412**	*	*	*
***endo*-412**	-463.103156 [0]	112.38	-462.924058
TS5 (*exo*-412 ® 310)	*	*	*
TS6 (*endo*-412 ® 310)	-463.103046 [1]	112.28	-462.924121

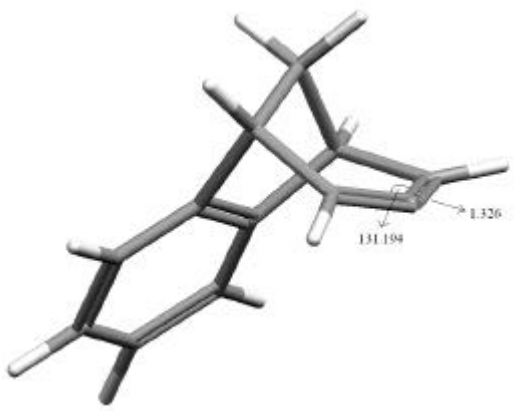

310

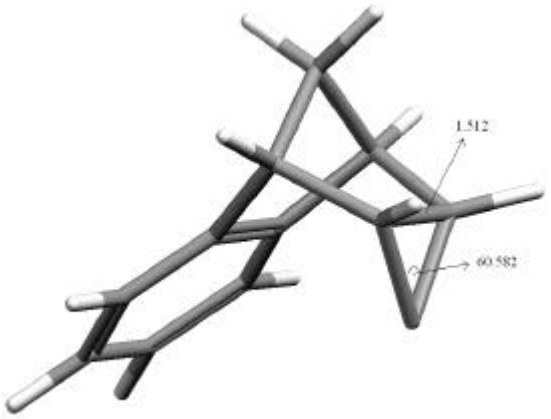

***endo*-412**

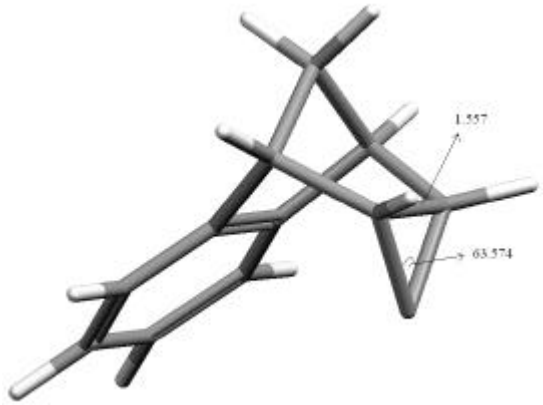

TS6 (*endo*-412 ® 310)

Figure 16: Optimized structures of **310**, ***endo*-412** and transition structure **TS6 (*endo*-412 ® 310)** at B3LYP/6-31G(d)

At this point, we were curious about the stability of *endo*-cyclopropylidene ***endo*-412** that was not discussed in the literature before. The computations were achieved by using the same methodology. Suprisingly, ***endo*-412** were optimized as a free carbene. To calculate the activation energy barrier for their isomerization to the corresponding allene **310** transition structures of ***endo*-412** were investigated. However, all attempts to find the allene transition structure failed and computations gave the free carbene transition structure **TS6 (*endo*-412 ® 310)**. This means that this carbene ***endo*-412** does not isomerize to the bicyclic allene **310** during the reaction. It is expected that ***endo*-412** would undergo some kind of insertion or carbene addition

reactions. In order to study the behaviour of ***endo*-412** and compare the results with those obtained by the theoretical calculations we have undertaken the synthesis of ***endo*-412**.

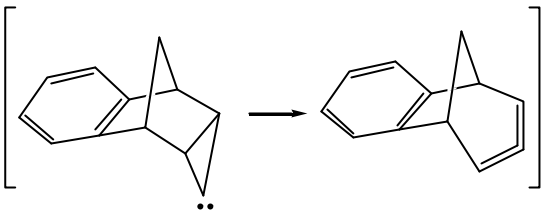

***endo*-412** **310**

Normally, the addition of dihalocarbene proceeds predominantly from the *exo* face of benzonorbornadiene. To hinder this reaction, the *exo* face of benzonorbornadiene was protected with the methoxy group as shown below.

2.4. THE REACTION PATH FOR THE SYNTHESIS OF 10-EXOBROMO-10-FLUOROTRICYCLO-[6.3.1.$0^{2,7}$.$0^{9,11}$]DODECA-2,4,6-TRIENE (408)

The synthetic path for the synthesis of **408** is summarized below. According to this path, the dibromo **380** can be synthesized from the bromination of benzonorbornadiene (**337**). Then, it can be treated with the suitable base to afford **406**. If bromine group at 7-position of benzonorbornadiene is exchanged with methoxy group to yield **407**, the bromofluorocarbene adduct **408** can be synthesized by using the carbene addition procedure.

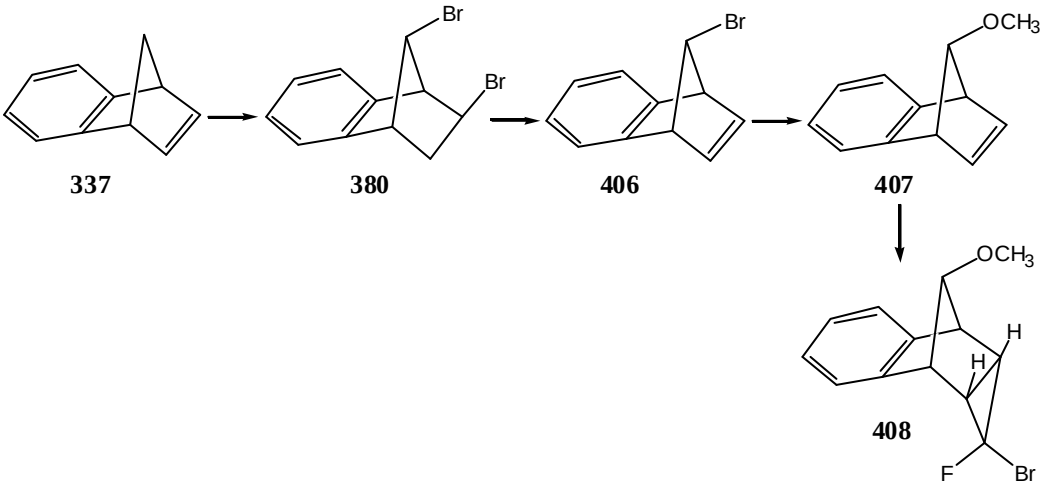

337 **380** **406** **407** **408**

2.4.1. The synthesis of benzonorbornadiene (337)

When a solution of *iso*-amylnitrite in methylene chloride is heated to reflux, the decomposition of the diazonium salt can be monitored by observing gas evolution as the solution of acetone, anthranilic acid, and cyclopentadiene is added. After the addition is complete, the entire mixture is refluxed until gas evolution ceases. This usually takes 2-5 hours. Then, solvent is removed under reduced pressure. Suitable work-up and vacuum distillation procedure afforded benzonorbornadiene (**337**) with 40% yield [146].

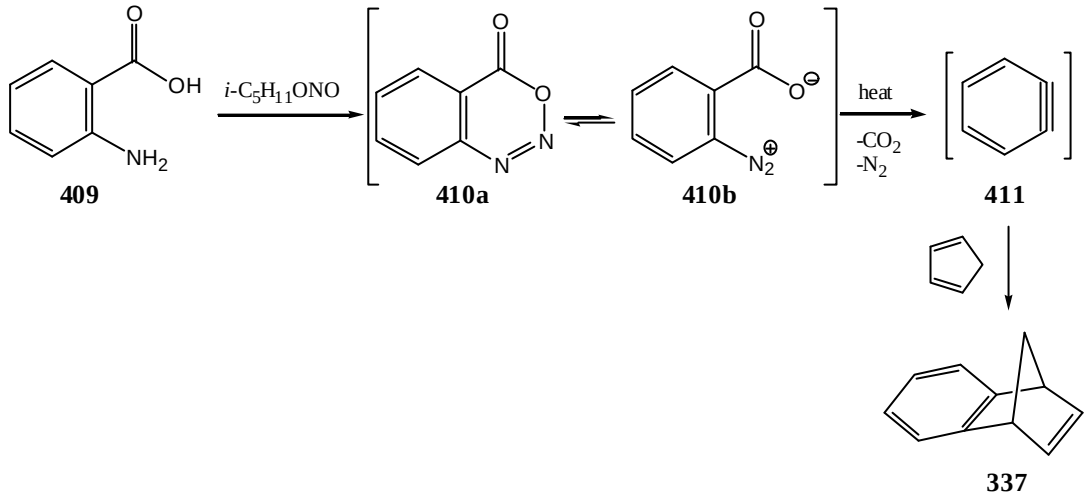

409 **410a** **410b** **411** **337**

Characterization of benzonorbornadiene (**337**) was based on the ^{1}H- and ^{13}C-NMR spectral data, which was also consistent with the literature data [147].

2.4.2. The synthesis of 2-exo-7-anti-Dibromobenzonorborn-5-ene (380)

Benzonorbornadiene (**337**) affords the possibilities of several mechanistically interesting investigations as explained before in the low and high temperature bromination of benzonorbornadiene (**337**) [122]. The electrophilic addition of bromine to benzonorbornadiene (**337**) gives a dibromide **380** in quantitative yield at 10 ^{0}C, which was first reported by Wittig and Knauss [148]. According to this literature, to a magnetically stirred solution of **337** in carbon tetrachloride cooled to $0^{0}C$ was added dropwise a solution of bromine in carbontetrachloride. After

completion of the addition, the solution allowed to warm to room temperature. The solvent removed under reduced pressure. The residue was cryctallized from ethanol to give Wagner-Meerwein rearranged dibromide **380**. The crude yield of reaction was 99%.

.

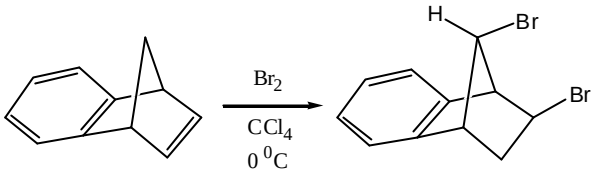

337 **380**

Characterization of 2-exo-7-anti-dibromobenzonorborn-5-ene (**380**) was based on the ^{1}H- and ^{13}C-NMR spectral data, which was also consistent with the literature data [122, 147].

2.4.3. The synthesis of *anti*-7-Bromobenzonorbornadiene (406)

Wilt *et al.* reported that dehydrobromination of **380** in DMSO gives *anti*-7-bromobenzonorbornadiene (**406**) with 67 % yield [148]. However, a dibromide **380** in freshly distilled THF over sodium was added portionwise to mechanically stirring potassium *t*-butoxide in the same solvent at reflux under nitrogen atmosphere. After the addition, heating was continued for two hours. Then, the cooled solution was poured into water and extracted with three portions of chloroform. The oily residue was crystallized in hexane to give **406** as a colorless crystal with 91 % yield.

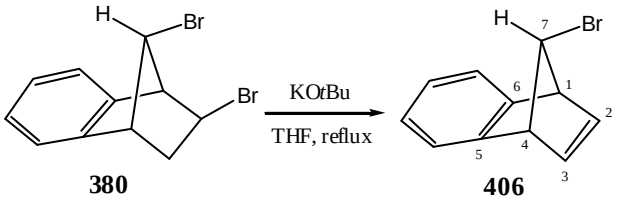

380 **406**

Characterization of *anti*-7-bromobenzonorbornadiene (**406**) was based on the ^{1}H- and ^{13}C-NMR spectral data, which was also consistent with the literature data [148]. ^{1}H-NMR spectrum of **406** shows singlet at 4.08 for bridge-head protons, singlet at 4.39 for bridge proton, singlet at 6.73 for olefinic protons, AA′BB′ system

at 7.01-7.23 for aromatic protons. ^{13}C-NMR spectrum of **406** consists of six signals at 57.7, 74.3, 122.3, 125.9, 139.8, 147.5 ppm.

2.4.4. Reaction of dibromocarbene and dichlorocarbene with *anti*-7-bromobenzonorbornadiene (406)

Alkenes are normally planar structure. However, a number of strained olefins that prefer non-planar structures have received extensive theoretical and experimental attention due to the fact that double bond pyramidalization plays an important role on the π-facial stereoselectivity in addition reactions. Remarkable exceptions are observed if double bonds are included in strained cyclic systems, in which cases considerable deviation from planarity of the double bond can occur [149]. As a consequence of the double bond pyramidalization, the two faces of double bond are no longer equivalent. This extraordinary geometrical feature causes the very noticable π-facial stereoselectivity in addition reactions to carbon double bonds [150]. The degree of pyramidalization is influenced by the electron density of the alkenyl π-bond [151].

Theoretical calculations on norbornene (**413**), norbornadiene (**414**), and benzonorbornadiene (**337**) show that the double bond in norbornene (**413**) is slightly pyramidalized in the *endo* direction (out of plane angle of 7°). Norbornadiene (**414**) and benzonorbornadiene (**337**) is bent to a smaller extent in the *endo* direction, the pyramidalization angle being approximately 2-4° [152].

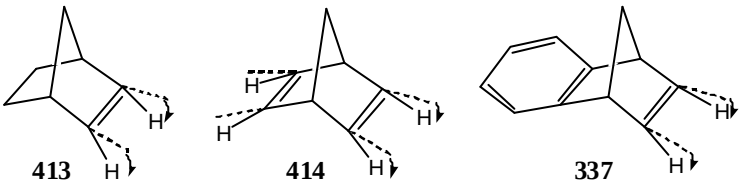

413 **414** **337**

Therefore, their two π-faces are chemically non-equivalent and they are attacked by a variety of reagents preferentially from the *exo* face of the double bond [153].

The addition of dihalocarbenes to norbornene (**413**), norbornadiene (**414**), and benzonorbornadiene (**337**) provides the most direct route to compounds containing the bicyclo[3.2.1]octyl ring system [154]. Kitahonoki *et al.* reported [155] that the reaction involves addition of the carbene to the *exo* face of benzonorbornadiene (**337**) to give initially a *gem*-dibromocyclopropane **415**, which under the reaction conditions usually undergoes ring opening to afford a rearranged, ring-expanded dihalide **417**.

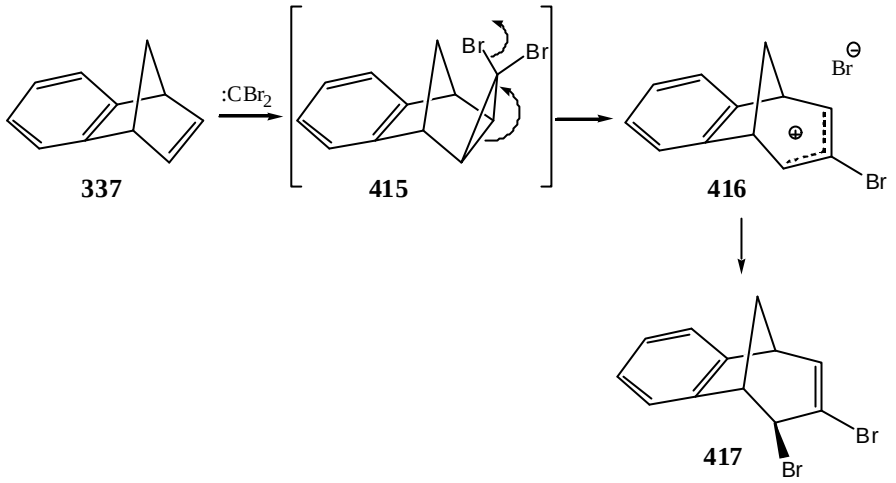

Woodward-Hoffman explained that the stereochemical outcome of *gem*-dihalocyclopropane ring opening has been rationalized in terms of orbital symmetry constraints [156]. The reaction involves cyclopropyl to allyl cation interconversion with participation of the cyclopropyl bonding electrons from the face of the cyclopropyl ring opposite to that of the departing halide ion **416**, then affords the allylic halide **417**, of defined stereochemistry. In a converse argument, for those cases in which the *gem*-dihalocyclopropane can not be isolated or detected, the sterochemistry of the allylic halide defines the stereochemistry of carbene addition: *exo* halogen orientation implies *exo* addition of dihalocarbene.

Recently, Wege [157] reported that the addition of dichlorocarbene to benzonorbornadiene (**337**) at 0 ^{0}C permitted the isolation of the *exo* adduct **418**, which underwent isomerization to the *exo* allylic chloride **419** only upon prolonged storage, or upon distillation. All previous reports of the addition of dichlorocarbene to **337** have only recorded the direct isolation of the rearranged material **419**.

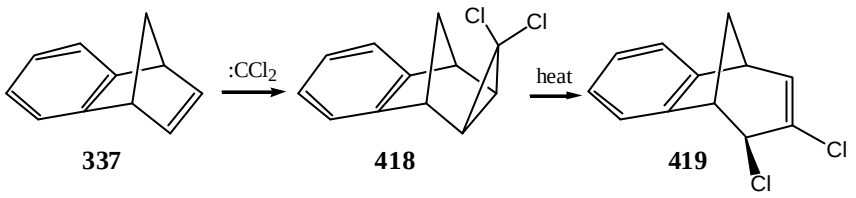

337 **418** **419**

Moreover, Wege [157] explained the addition of dichlorocarbene to 7,7-dimethoxy benzonorbornadiene (**420**) in which a substituent shields the *exo* face of the double bond. The dichloride **422** was isolated as the only product, which results from the ring opening of an adduct **421** under the reaction conditions.

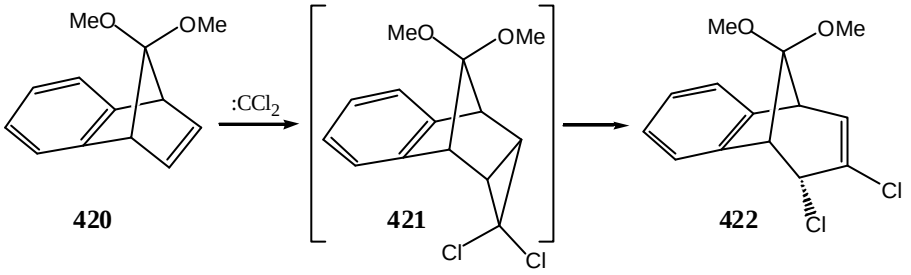

420 **421** **422**

α-Elimination of a hydrogen halide from a haloform remains the most important and the most frequently used method for generating dihalocarbenes. However, in 1969 Makosza [158] showed that α-elimination as well as addition of dichlorocarbene to an alkene can be performed in a two-phase system using the concentrated aqueous NaOH as a base in the presence of a quanternary ammonium salt acting as a phase-transfer catalyst (Figure 17). Usually high yiels of the *gem*-dichlorocyclopropanes are obtained, even from alkenes of low nucleophilicity. Hydrolysis of the carbene does not proceed to a significant extent, even though the reaction of the carbene with water and hydroxide anions is known to proceed at a high rate, and despite the fact that these reactions are carried out in the presence of a great excess of aqueous NaOH. These reactions indicate that there is very little contact between the dihalocarbene and the water and hydroxide anions in the PTC system [128].

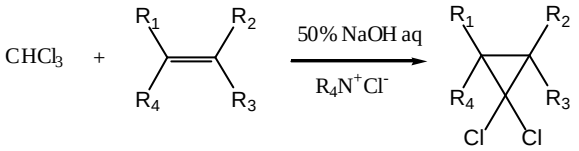

Figure 17: General representation of Makosza Reaction

In the light of these literature data, the addition of dibromo and dichloro carbene to *anti*-7-bromobenzonorbornadiene (**406**) was carried out to isolate the *endo* adducts **423** and **425** at various temperatures.

For this purpose, a mixture of *anti*-7-bromobenzonorbornadiene (**406**), bromoform, 50% sodium hydroxide and benzyltriethylammonium chloride as a phase transfer catalyst was vigorously stirred at 0 ^{0}C for 6 hours. The reaction did not occur at that temperature. Hence, reaction temperature increased to 50 ^{0}C. After work-up, *anti*-7-bromobenzonorbornadiene, which reacted with dibromocarbene, was detected with ^{1}H-NMR spectrum. Unreacted alkene was recovered by distillation, and the distillation residue was saved. The recovered alkene was resubmitted to the reaction conditions, using the same quantities of bromoform, sodium hydroxide and phase-transfer catalyst. The combined distillation residues were crystallized from hexane to give **424** as the only product with the total yield of 53% (based on unrecovered starting material after two sequential reactions).

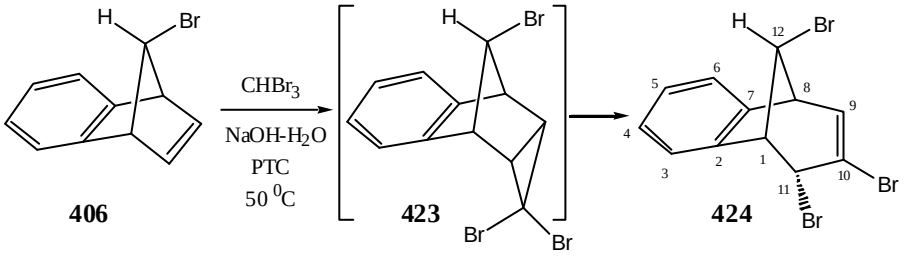

Characterization of **424** was based on the ^{1}H- and ^{13}C-NMR spectra. The *endo* orientation of the bromo substituent in **424** was apparent from the value $J_{1,11}$= 4.5 Hz for the bridgehead H_1 proton to bromomethine H_{11} proton coupling constant. The corresponding coupling constant for the *exo* derivative **417** obtained from dibromocarbene addition to benzonorbornadiene (**337**) was 1.5 Hz [157]. ^{1}H-NMR spectrum also shows doublet of doublets at 3.53 ppm for H_8 proton, triplet at 3.65

ppm for H_1, triplet at 4.59 ppm for H_{12} proton, doublet at 5.24 ppm for H_{11} proton, doublet at 6.48 ppm for H_9 proton, multiplet at 7.12-7.44 ppm for aromatic protons. There are twelve lines in the ^{13}C-NMR spectrum of **424** at 48.7, 53.6, 53.7, 54.1, 121.1, 121.9, 127.4, 128.1, 128.8, 134.9, 139.0, 147.1 ppm.

Addition of dichlorocarbene, to *anti*-7-bromobenzonorbornadiene (**406**) afforded the *endo*-chloro derivative **426** as the only product in a total yield of 61% (based on unrecovered starting material after two sequential reactions).

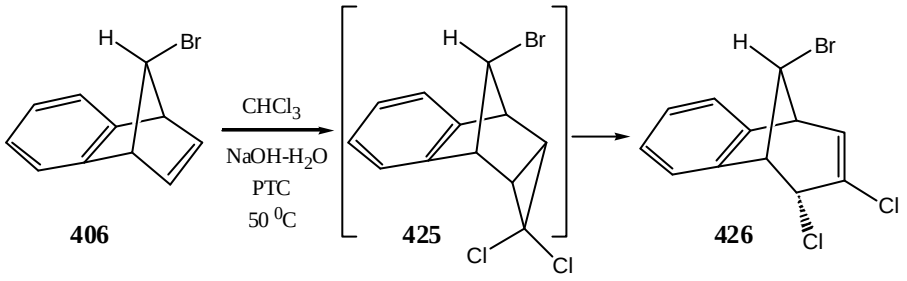

Characterization of **426** was based on the ^{1}H- and ^{13}C-NMR spectra. The *endo* orientation of the chloro substituent in **426** was apparent from the value $J_{1,11}$= 4.7 Hz for the bridgehead H_1 proton to chloromethine H_{11} proton coupling constant. ^{1}H-NMR spectrum of **426** also shows doublet of doublets at 3.50 ppm for H_8 proton, triplet at 3.55 ppm for H_1, triplet at 4.52 ppm for H_{12} proton, doublet at 4.94 ppm for H_{11} proton, doublet at 6.18 ppm for H_9 proton, multiplet at 7.05-7.32 ppm for aromatic protons. There are twelve signals in the ^{13}C-NMR spectrum of **426** at 47.6, 52.9, 54.3, 59.5, 121.9, 127.6, 128.1, 128.8, 129.9, 131.2, 138.3, 147.8 ppm.

As a result, it is evident that in the addition of dibromocarbene and dichlorocarbene to *anti*-7-bromobenzonorbornadiene (**406**), attack of the carbene occurs exclusively at the *endo* face of the π-bond, leading to the adducts **423** and **425**, respectively. However, they suffer stereoelectronically-controlled ring opening under the reaction conditions to give the dibromide **424** and the dichloride **426**. This predominant *endo* addition is a consequence of shielding of the *exo* face by the bromine substituent at C7 position in compound **406**.

2.4.5. The Synthesis of *anti*-7-methoxybenzonorbornadiene (407)

Wilt and Chenier studied the solvolysis reaction of halogenated benzonorbornadienes extensively [159]. The authors reported that both *syn*- and *anti*-7-bromobenzonorbornadienes (**427** and **406**) solvolyze in aqueous dioxane with the retention of configuration to yield **428** and **429**, respectively. They explained these experimental results in terms of the contrast in π-participation between aromatic and olefinic abilities to stabilize homoallylic cationic centers formed by ionization of **427** and its anti epimer **406** as shown below. Cristol and Nachtigall [160] also reported similar results in the acetolysis of chloro derivatives of **427** and **406**.

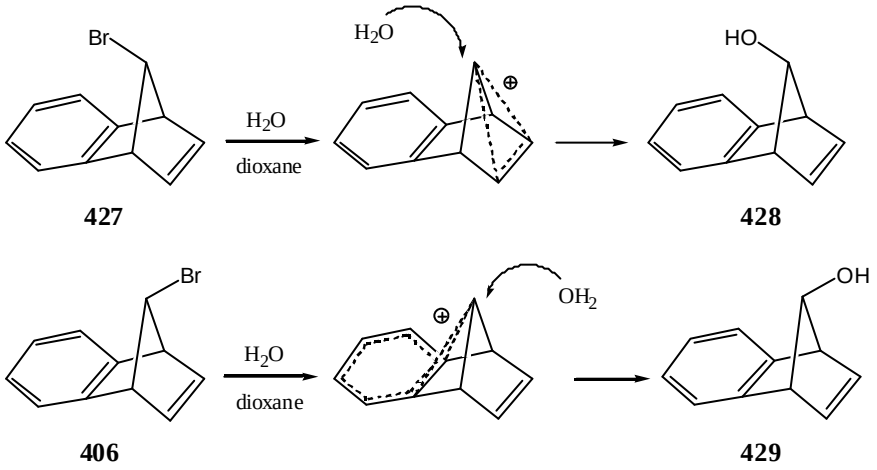

Therefore, we tried to solvolyze *anti*-7-bromobenzonorbornadiene (**406**) in methanol and dioxane solution. We expected the formation of *anti*-7-methoxy-benzonorbornadiene (**407**). However, after the reaction mixture was refluxed about 24 hours, there was no evidence for the formation of **407** observed with ^{1}H-NMR spectra. The same reaction was repeated in the sealed tube. Again, no reaction was observed.

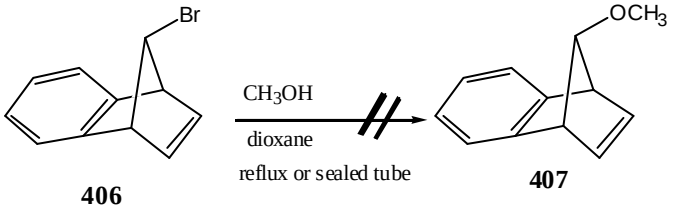

We thought that the solyvolysis of **406** in methanol should require the assistance of a Lewis acid, such as silver ion. Hence, *anti*-7-bromobenzonorbornadiene (**406**) in methanol was mechanically stirred at 0 ^{0}C. Then, silver nitrate in methanol was dropwise added to the stirring solution. Resulting mixture was stirred about four hours at room temperature. After suitable work-up, the residue was subjected to silica gel column eluting with hexane to give *anti*-7-nitroxybenzonorbornadiene (**430**) with the yield of 52%. The second fraction eluting with hexane-ethylacetate (10:1) was the desired compound **407** with a yield of 48%.

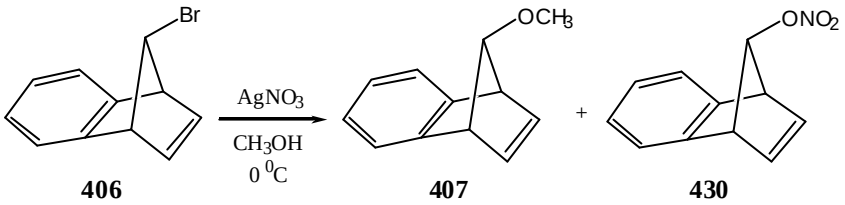

406 **407** **430**

Characterization of the unexpected product **430** was based on the ^{1}H- and ^{13}C-NMR, and Mass spectra. ^{1}H-NMR spectrum shows singlet at 4.14 ppm for bridge-head protons, singlet at 4.90 ppm for bridge proton, singlet at 6.66 ppm for olefinic protons, AA′BB′ system at 7.13-7.34 ppm for aromatic protons. There are seven lines in the ^{13}C-NMR spectrum of **430** at 52.5, 52.6, 101.7, 123.2, 126.4, 138.1, 146.0 ppm.

Characterization of compound **407** was based on the ^{1}H- and ^{13}C-NMR spectra, and Mass Spectra. ^{1}H-NMR spectrum shows singlet at 3.31 ppm for bridge-head protons, singlet at 3.98 ppm for bridge proton, singlet at 6.63 ppm for olefinic protons, AA′BB′ system at 7.02-7.24 ppm for aromatic protons. There are seven lines in the ^{13}C-NMR spectrum of **407** at 53.8, 57.0, 107.4, 122.7, 125.5, 137.8, 147.7 ppm.

As a result, *anti*-7-bromobenzonorbornadiene (**406**) afforded these two products, **407** and **430**, with the retention of configuration due to the π-participation by the benzene ring and the non-classical structure of the carbonium ion intermediate after this solvolytic reaction with the help of Lewis acid, silver ion.

2.4.6. Reaction of dibromocarbene and dichlorocarbene with *anti*-7-methoxybenzonorbornadiene (407)

In this part, the addition of dibromo and dichloro carbene to *anti*-7-methoxybenzonorbornadiene (**407**) was carried out to isolate the *endo* adducts, **432** and **434**.

For this purpose, a mixture of *anti*-7-methoxybenzonorbornadiene (**407**), bromoform, 50% sodium hydroxide and benzyltriethylammonium chloride as a phase transfer catalyst was vigorously stirred at 50 ^{0}C for 6 hours. Unreacted alkene was recovered by distillation, and the distillation residue was saved. The recovered alkene was resubmitted to the reaction conditions, using the same quantities of bromoform, sodium hydroxide and phase-transfer catalyst. The combined distillation residues were crystallized from hexane to give **433** as the only product with the total yield of 57 % (based on unrecovered starting material after two sequential reactions).

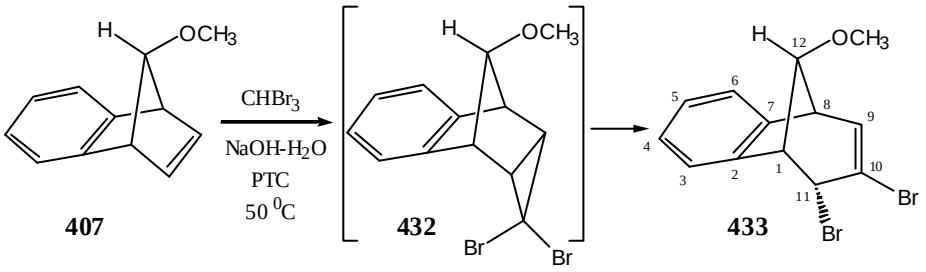

Characterization of **433** was based on the ^{1}H- and ^{13}C-NMR spectra. The *endo* orientation of the bromo substituent in **433** was apparent from the value $J_{1,11}$= 4.6 Hz for the bridgehead H_5 proton to bromomethine H_6 coupling constant. Moreover, ^{1}H-NMR spectrum of compound **433** shows singlet at 3.45 ppm for methyl protons (overlapped with the bridge-head proton H_8 proton), triplet at 3.67 ppm for H_1 proton, triplet at 4.04 ppm for H_{12} proton, doublet at 5.09 ppm for H_{11} proton, doublet at 6.43 ppm for H_9 proton, multiplet at 7.13-7.46 ppm for aromatic protons. There are thirteen lines in the ^{13}C-NMR spectrum of **433** at 44.9, 51.7, 53.7, 57.3, 86.3, 121.9, 122.3, 127.1, 128.3, 128.5, 132.4, 139.2, 146.6 ppm.

Moreover, addition of dichlorocarbene, generated from chloroform and sodium hydroxide under phase-transfer conditions explained before, to *anti*-7-methoxybenzonorbornadiene (**407)** afforded the *endo*-chloro derivative **435** as the only product in a total yield of 63% (based on unrecovered starting material after two sequential reactions).

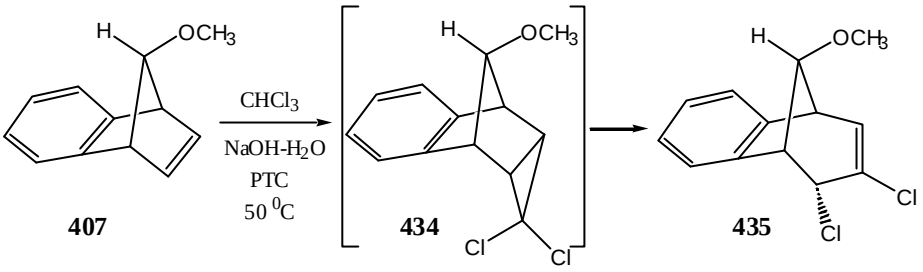

The structure of compound **435** has been elucidated on the basis of ^{1}H- and ^{13}C-NMR spectra. The *endo* orientation of the chloro substituent in **435** was apparent from the value $J_{1,11}$= 4.6 Hz for the bridgehead H_1 proton to chloromethine H_{11} proton coupling constant. ^{1}H-NMR spectrum also shows singlet at 3.46 ppm for methyl protons, doublet of doublets at 3.54 ppm for H_8 proton, triplet at 3.66 ppm for H_1 proton, triplet at 4.10 ppm for H_{12} proton, doublet at 4.89 ppm for H_{11} proton, doublet at 6.22 ppm for H_9 proton, multiplet at 7.16-7.45 ppm for aromatic protons. There are thirteen signals in the ^{13}C-NMR spectrum of **435** at 43.7, 50.9, 57.3, 59.0, 86.6, 122.3, 127.2, 128.2, 128.5, 128.6, 130.6, 138.3, 147.3 ppm.

As a result, in the addition of dibromocarbene and dichlorocarbene to *anti*-7-methoxybenzonorbornadiene (**407**), the attack of carbene occurs exclusively at the *endo* face of the π-bond, leading to the adducts **432** and **434**, respectively. However, they suffer stereoelectronically-controlled ring opening under the reaction conditions to give the dibromide **433** and the dichloride **435**. This *endo* addition is a consequence of shielding of the *exo* face by the methoxy substituent at 7-position.

2.4.7. Reaction of bromofluorocarbene with *anti*-7-methoxybenzonorbornadiene (407)

After the failure of the isolation of *gem*-dihalocyclopropanes, **432** and **434**, which isomerizes to the *endo*-bromo **433** and *endo*-chloro **435** derivative, respectively, we decided to achieve the reaction of bromofluorocarbene with *anti*-7-methoxybenzonorbornadiene (**407**) to prevent the ring opening.

However, *gem*-bromofluorocyclopropanes are often unstable, so there is a limited amount of information available concerning their generation and applications despite their potential usefulness in organic chemistry [128]. For the preparation of *gem*-bromofluorocyclopropanes, the reaction of dibromofluoromethane and a base (aqueous NaOH/PTC catalyst [161] or KO*t*Bu [162]) with an olefin, or the thermal decomposition of dibromofluoromethyl(phenyl)mercury in the presence of an olefin [163], is used. The mercury precursor is rather unstable, which allows the addition of bromofluorocarbene to alkenes, including electrophilic ones, to be performed even at room temperature or at 80 ^{0}C within a very short time.

Jefford and Hill reported the addition of bromofluorocarbene to the bicyclic olefin, norbornene for the first time [164]. They isolated three products, **436**, **437**, and **438**, by fractional distillation and thin layer chromatography. Compound **436** is suprisingly stable; heating to 110 ^{0}C for 4 hours is without effect, so the rearranged product **437** undoubtedly arise spontaneously from the epimeric adduct **439**. The unexpected formation of the dibromo product **438** results from the presence of some undetected bromoform in difluorobromomethane.

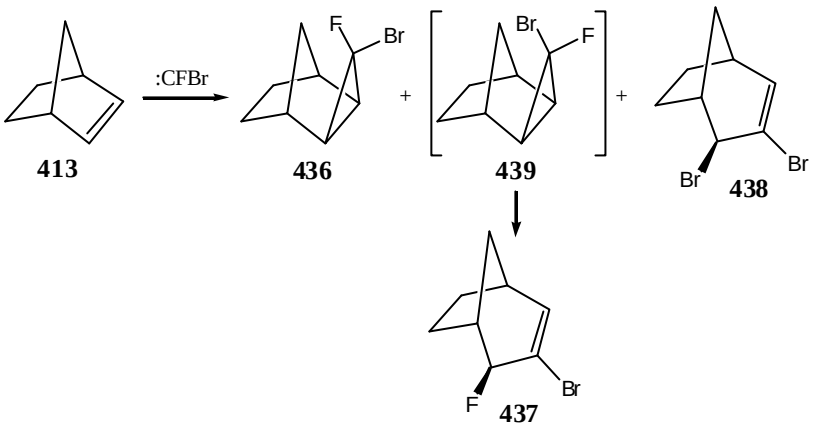

More recently, Balci and co-workers [102, 113] have reported that the addition of bromofluorocarbene, which is generated from dibromofluoromethane under PTC conditions in methylenechloride, to benzonorbornadiene (**337**) and bicyclo[3.2.0]hept-6-ene (**290**) affords unrearranged bromofluorocyclopropane, **338** and **291**, in addition to the *exo*-bromofluoro ring-opened product, **340** and **295**, respectively.

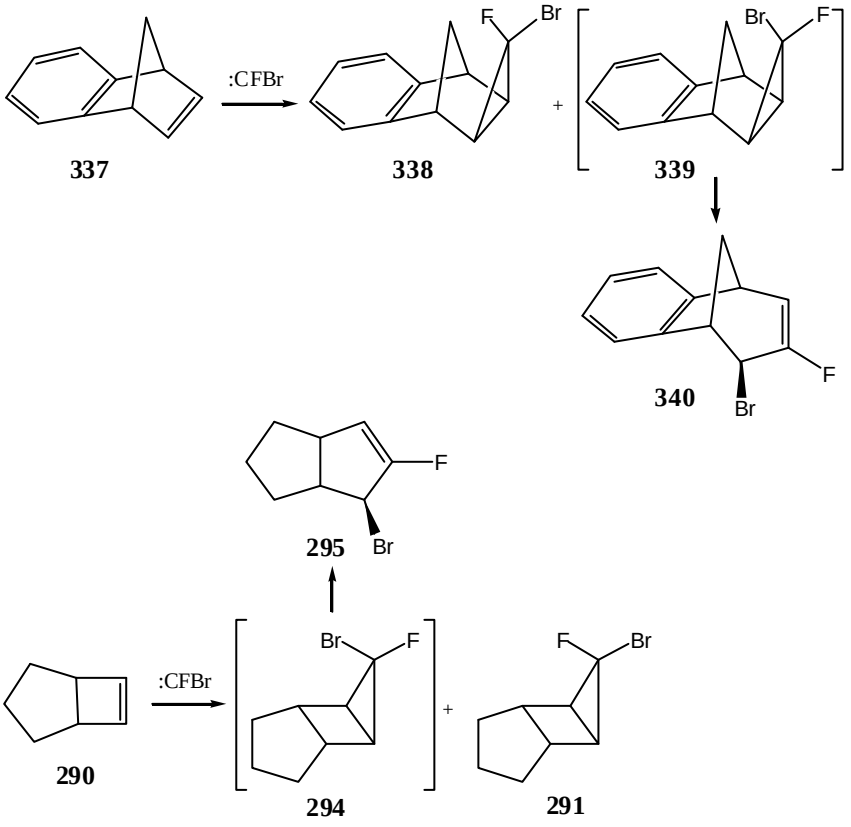

In the light of these literature data, the addition of bromofluorocarbene to *anti*-7-methoxybenzonorbornadiene (**407**) was achieved to isolate the *endo*-adduct **408**.

First of all, dibromofluoromethane, precursor of bromofluorocarbene, should be prepared, because this reagent was not available. According to the literature [165], it can be obtained from the reaction of antimony trifluoride with bromoform under the nitrogen atmosphere with 35 % yield. The careful distillation is needed to remove any impurities, such as bromoform, which would give dibromocarbene with bases if it were present in the dibromofluoromethane.

Later, bromofluorocarbene was generated with the Doering-Hoffmann route. Dibromofluoromethane was slowly added to stirred slurry of potassium *tert*-butoxide and *anti*-7-methoxybenzonorbornadiene (**407**) in hexane at 0 ^{0}C. After work-up, the residue was analyzed with TLC and ^{1}H-NMR spectrum, and there are no products formed in this reaction.

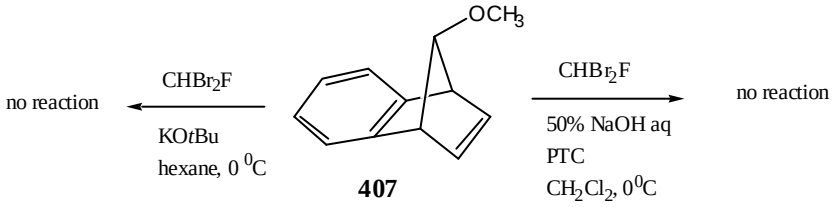

After that, the bromofluorocarbene, which were generated from $CHBr_2F$ and sodium hydroxide under phase transfer conditions reacted with *anti*-7-methoxybenzonorbornadiene (**407**) in methylenechloride at 0 ^{0}C. The suitable work-up procedure was applied to the reaction mixture. The analysis of the reaction mixture by NMR spectra did not reveal the formation of the addition product.

After two unsuccessful attempts, we thought that incresing temperature of reaction and dibromofluoro taken as a solvent would affect the formation of products expected from the reaction of fluorobromocarbene and an alkene **407**. Therefore, the addition of fluorobromocarbene, generated from $CHBr_2F$ and sodium hydroxide under phase-transfer conditions, to *anti*-7-methoxybenzonorbornadiene (**407**) at 50^{0}C

afforded the two addition products, **408** and **440**, and the *endo*-bromofluoro ring-opened product **441** in a ratio of 3:1:2 and in a total yield of 18 %. During the reaction, the temperature should be kept at 50 ^{0}C, because the yield of products decreases drastically above or below this temperature. Other important point is the selection of suitable phase-transfer catalytst. At the start of work, benzyltriethylammonium chloride was used as a PTC and the yield of this reaction was 10%. On the contrary, the reaction yield increased up to 18% when benzyltributylammonium chloride was used instead of it.

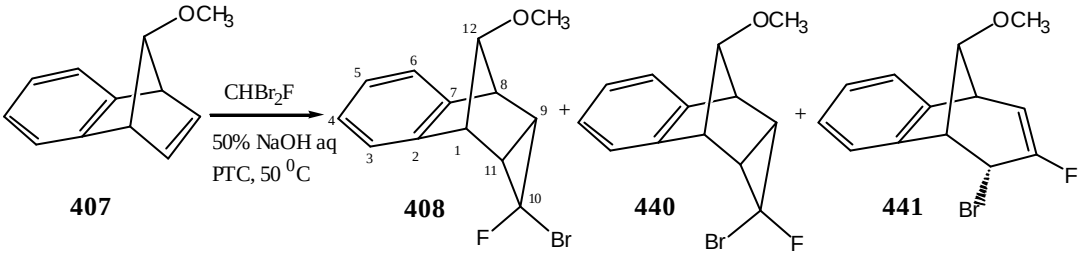

Structural assignments of **408**, **440**, and **441** were made on the basis of the ^{1}H-NMR, ^{13}C-NMR, and Mass spectra. ^{1}H-NMR spectrum of compound **408** shows triplet at 2.57 ppm for H_9 and H_{11} protons, singlet at 3.37 ppm for methyl protons, doublet at 3.70 ppm for H_1 and H_8 protons, singlet at 3.83 ppm for H_{12} proton, AA′BB′ system at 7.12-7.16 ppm for aryl protons. In particular, the observation of eight signals in the ^{13}C-NMR spectrum at 37.3 (d, J=13.2), 48.6, 56.7, 93.0 (d, J=340), 107.0 (d, J=4.6), 122.9, 127.3, 141.7 (d, J=3.4) ppm, as required by the symmetry in molecule **408**, are in good aggrement with the structure. The spin multiplicities between the fluorine and carbon atom are also given in parentheses with the coupling constants (Hz).

^{1}H-NMR spectrum of compound **440** consists of singlet at 1.87 ppm for H_9 and H_{11} protons, singlet at 3.19 ppm for H_{12} proton, singlet at 3.20 ppm for methyl protons, singlet at 3.81 ppm for H_1 and H_8 protons, AA′BB′ system at 7.06-7.19 ppm for aromatic protons. There are eight lines in the ^{13}C-NMR spectrum of **440** at 42.0 (d, J=16.0), 48.9 (d, J=2.0), 56.9, 86.6, 97.4 (d, J=351), 122.4, 126.7, 146.5 ppm due to the symmetry in compound **440**. The spin multiplicities between the fluorine and carbon atom are also given in parentheses with the coupling constants (Hz).

^{1}H-NMR spectrum of compound **441** shows doublet of doublets of doublets at 3.49 ppm for H_8 proton, doublet of doublets at 3.64 ppm for H_1 proton, broad singlet at 3.95 ppm for H_{12} proton, doublet at 5.07 ppm for H_{11} proton, doublet of doublets at 5.63 ppm for H_9 proton, multiplet at 7.15-7.45 ppm for aryl protons. There are thirteen signals in the ^{13}C-NMR spectrum of **441** at 40.6 (d, J=6.3), 45.1 (d, J=45.1), 50.0 (d, J=4.3), 56.7, 85.8, 106.7 (d, J=14.3), 121.9, 126.4, 127.8, 127.9, 138.2, 147.1, 153.8 (d, J=259) ppm. The spin multiplicities between the fluorine and carbon atom are also given in parentheses with the coupling constants (Hz).

To decide how the rearranged product **441** forms from the reaction of bromofluorocarbene with **407**, the *endo* adducts, **408** and **440**, was refluxed in toluene seperately. Compound **408** was suprisingly stable, refluxing for five days was without effect. However, compound **440** was not stable to heat and it rearranged completely to the ring-opened product **441** after three hours. These results validate the Woodward-Hoffman rules relating with the stereochemical outcome of *gem*-dihalocyclopropane ring opening rationalized in terms of orbital symmetry constraints [156]. Hence, this reaction involves the cyclopropyl to allyl cation interconversion with participation of cyclopropyl bonding electrons from the face of cyclopropyl ring opposite to that of the departing bromine anion. Collapse of the resulting ion pair, **442**, then affords the allylic halide, **441**.

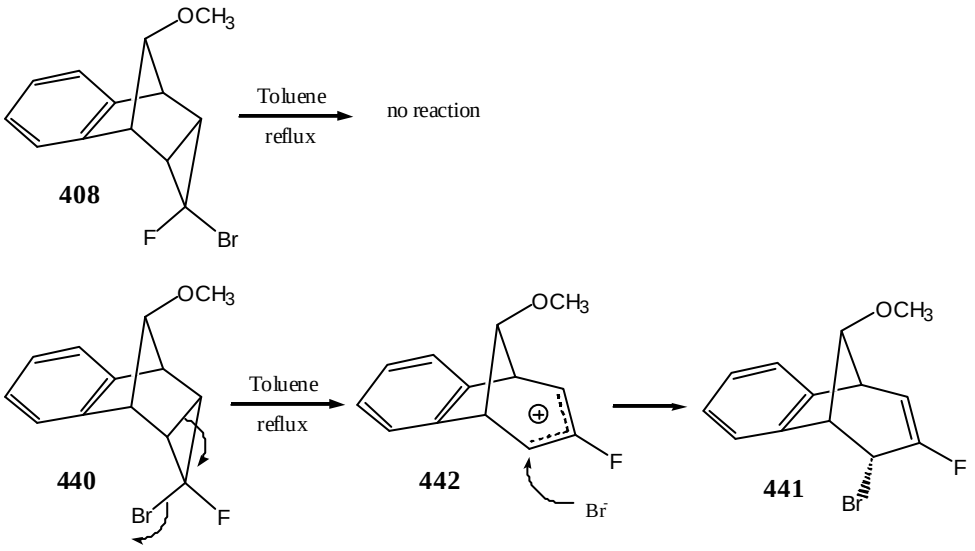

As a result, it was observed in this part that the addition of bromofluorocarbene to *anti*-7-methoxybenzonorbornadiene (**407**) under phase-transfer catalysis conditions permitted the isolation of the desired compound, **408**, which does not underwent isomerization to the *endo* allylic molecule **441**. Some of the epimeric *endo* adduct **440** rearranges to **441** during the reaction.

2.5. The reaction of the bromofluorocyclopropane 408 with methyllithium

To investigate the reaction of the *endo* carbenoid, bromofluorocyclopropane **408** was submitted to the last step of Doering-Moore-Skatebøl reaction. Therefore, to a magnetically stirring solution of bromofluorocyclopropane **408** in dry ether was added dropwise MeLi in ether at –25 ^{0}C in the presence of the freshly distilled furan, as the trapping reagent. After the resulting solution was stirred for half-hour at that temperature, it was allowed to warm to room temperature by itself. Then, it was quenched carefully with water. After the usual work-up procedure, the residue was analyzed by ^{1}H and ^{13}C NMR measurements, whose spectra showed the formation of trapping product **446** as the only product. The formation of this trapping product **446** confirms the formation of the bicyclic allene **445** as a reactive intermediate. To purify **446**, it was chromatographed on neutral aluminum oxide.

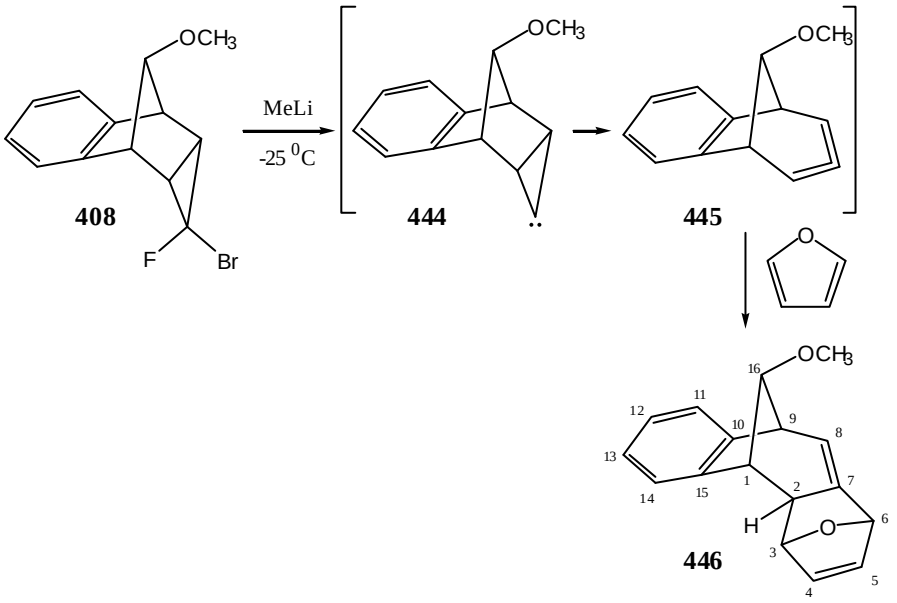

The structure of compound **446** has been elucidated on the basis of ^{1}H-NMR, ^{13}C-NMR, and Mass Spectra. ^{1}H-NMR spectrum of **446** shows triplet at 2.46 ppm for H_2 proton, singlet at 3.15 ppm for methyl protons, broad singlet at 3.16 ppm for H_{16} proton, doublet of doublets at 3.57 ppm for H_1 proton, triplet at 3.86 ppm for H_9 proton, broad singlet at 5.02 ppm for H_6 proton, doublet at 5.04 for H_3 proton, doublet of doublets at 5.78 ppm for H_8 proton, doublet of doublets at 6.09 ppm for H_4 proton, doublet of doublets at 6.28 ppm for H_5 proton, multiplet at 7.04-7.21 ppm for aromatic protons. There are seventeen lines in the ^{13}C-NMR spectrum of compound **446** at 41.0, 42.7, 44.4, 55.5, 80.3, 81.8, 84.2, 117.3, 122.1, 123.2, 126.7, 127.1, 130.5, 134.7, 142.6, 144.1, 146.4 ppm. Mass spectra shows M^{+} signal at 252.1, which is equal to the molecular weight of **446**. The configurations of the proton (H_2) and the *oxo* bridge were determined by achieving theoretical calculations and measuring the coupling constant between H_1 and H_2, H_2 and H_3 protons.

The addition of furan to the forming allene **445** may result in the formation of four possible isomers which can be represented as; syn-*exo* isomer **446a**, anti-*exo* isomer **446b**, syn-*endo* isomer **446c**, anti-*endo* isomer **446d** as shown in Figure 18.

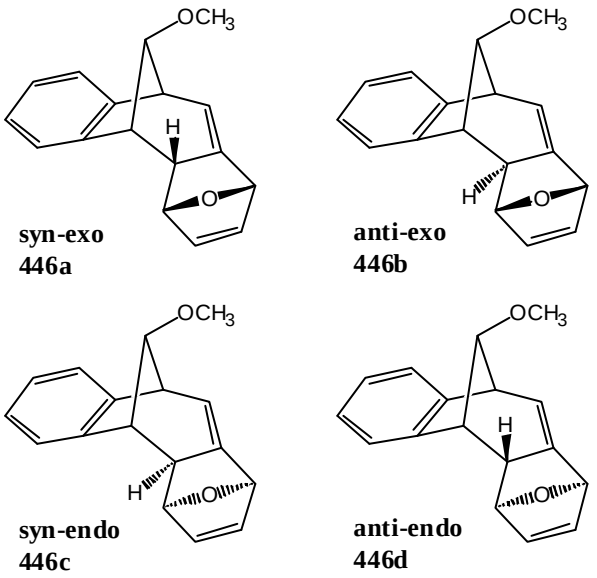

Figure 18: Possible isomers of the allene adduct **446** that afford from the reaction of **408** with MeLi in the presence of furan

To determine which isomer energetically the most stable one, the theoretical calculations were carried out by using Gaussian 98W program [139]. The geometry optimizations of all the structures, **446a**-**446d**, were achieved at the B3LYP/6-31G(d) level. Energies were refined by using B3LYP/6-31G(d) single point evaluations. Stationary points were characterized as minima or transition structures by way of an analytic evaluation of harmonic vibrational frequencies at the level of geometry optimization. The results of calculations summarized in Table 10 showed that **446a** is the lowest one in energy, including zero point correction.

Table 10: Absolute energies (E, in hartree/particle), zero-point vibrational energies (ZPVE, in kcal/mol), and energies relative to the isomer that has a lowest energy, including zero-point corrections (in kcal/mol) for the isomers, **446a**, **446b**, **446c**, and **446d**.

	Energy	**ZPVE**	**Relative Energy**
446a	-807.786115	182.50	0.00
446b	-807.777506	182.40	5.30
446c	-807.779517	182.43	4.07
446d	-807.783646	182.51	1.56

Optimized structures of **446a**, **446b**, **446c**, and **446d** at B3LYP/6-31G(d) level are shown in Figure 19. These structures are visualized by using Molden [144] and Mercury [145] programs.

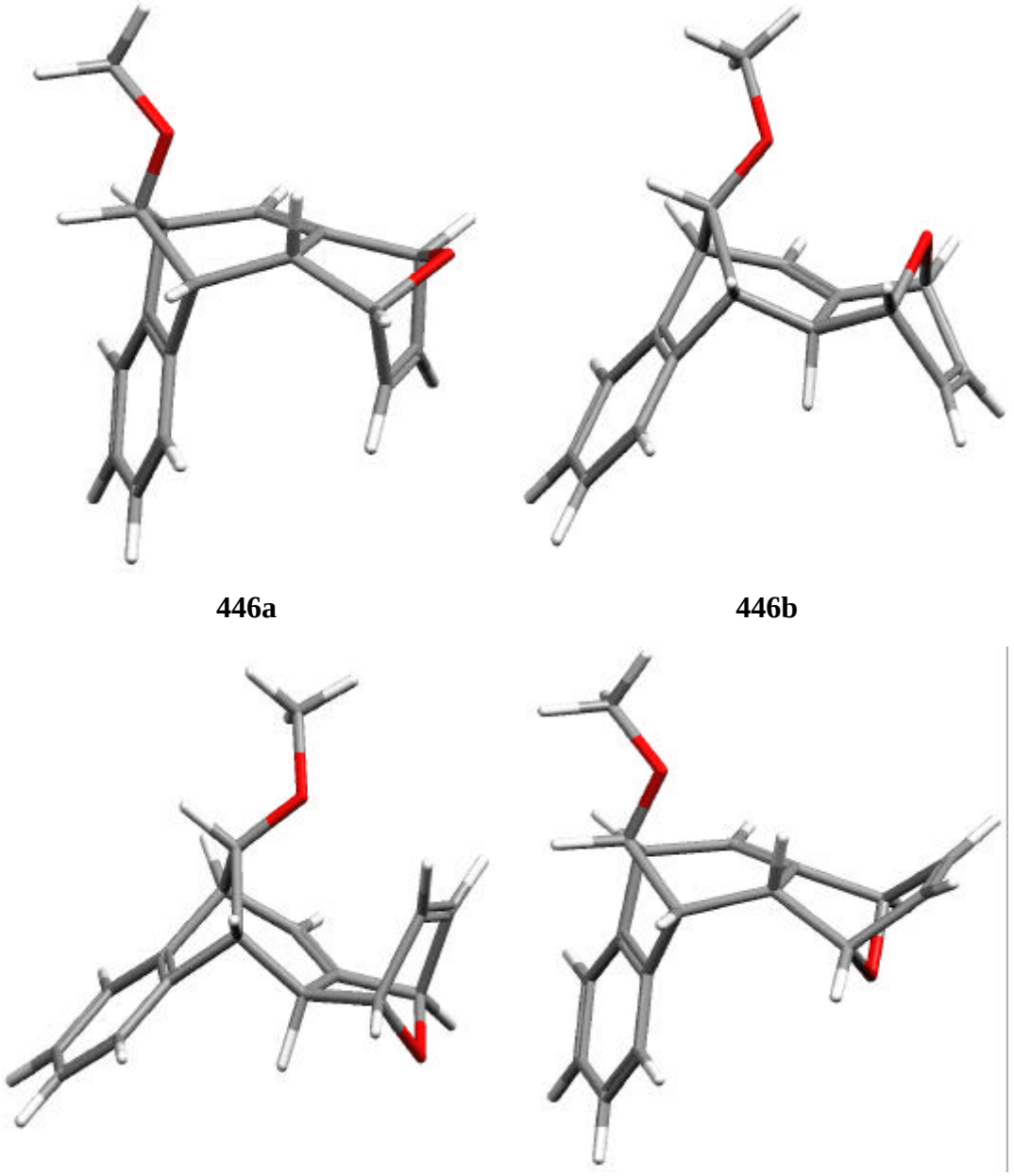

446a **446b**

446c **446d**

Figure 19: Optimized structures of **446a**, **446b**, **446c**, and **446d** at B3LYP/6-31G(d) level

On the basis of the geometry optimized structures of **446a-d** shown in Figure 19, the dihedral angles between H_1-H_2, H_2-H_3, H_3-H_4, H_8-H_9 protons were found to be as given in Table 11.

Table 11: The dihedral angles between H_1-H_2, H_2-H_3, H_3-H_4, H_8-H_9 protons for **446a**, **446b**, **446c**, and **446d** molecules from the geometry optimization at B3LYP/6-31G(d) level.

	H_1-H_2	H_2-H_3	H_3-H_4	H_8-H_9
446a	-58.88 °	51.98 °	33.68 °	-32.04 °
446b	89.25 °	-96.87 °	32.65 °	-2.40 °
446c	90.83 °	-53.23 °	-33.32 °	-6.91 °
446d	-58.25 °	95.83 °	-32.93 °	-36.23 °

From ^{1}H-NMR spectrum of **446**, the coupling constant (J_{12}) between H_1 and H_2 protons was found to be around 4.0 Hz. Karplus-Conroy graph [166] indicates that in the case of both isomers, **446b** and **446c**, this coupling constant value should be nearly zero due to the dihedral angle that is approximately 90 °. Therefore, it is likely that the trapped isomer is neither **446b** nor **446c** in this case.

On the other hand the coupling constant (J_{23}) between H_2 and H_3 protons is around 4.0 Hz. The angle between these two protons is 95.83 ° in the case of **446d** isomer and this coupling constant is unlikely to arise from this isomer. Hence, compound **446a** is most likely isomer to afford from the reaction of **408** with metyhllithium in the presence of furan.

After that, we concluded that the reaction of *gem*-bromofluorocyclopropane **408** with methyllithium gives the bicyclic allene **445** as a reactive intermediate trapping with furan. However, we were not sure about the structure of initially formed intermediate whether it is a carbene or carbenoid. During the reaction, no products were isolated derived from any carbene insertion reaction. To understand these intermediates, theoretical calculations were achieved by Gaussian 98W-program [139]. The geometry optimizations of all the structures were achieved at the B3LYP/6-31G(d) level (Singlet State). Energies were refined by using B3LYP/6-31G(d) single point evaluations. Stationary points were characterized as minima or transition structures by way of an analytic evaluation of harmonic vibrational frequencies at the level of geometry optimization.

To determine the energy barriers for the isomerization of carbene to allene, the geometry of carbene structures, **444** and **449**, (Figure 20) in their singlet state were optimized firstly at B3LYP/6-31G(d) level and their energy results were summarized in Table12.

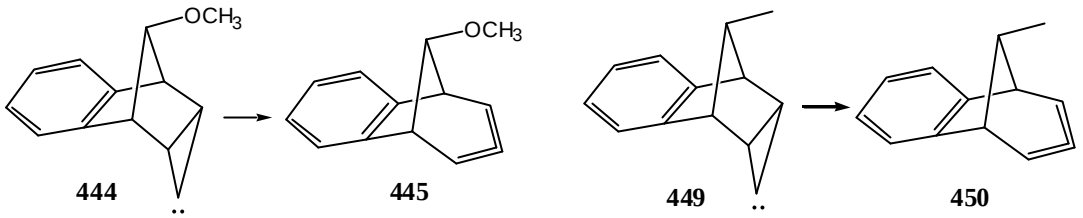

Figure 20: Isomerization of the carbenes to the corresponding allenes **444® 445**, **449® 450**.

As can be seen from Figure 21 and Table 12, we could not find any minima for the structures of carbene **444**, which readily isomerize to the corresponding allene structure **445**. This means that there is no carbene intermediate **444** for the formation of allene intermediate **445**. We suggested that the α-halolithium compounds act as carbenoids rather than dissociating to form free carbenes when the reaction of *gem*-dihalocyclopropane with methyllithium was carried out in these situations.

Table 12: Electronic energies (E, in hartree/particle), number of imaginary frequencies [in brackets], zero-point vibrational energies (ZPVE, in kcal/mol), and sum of electronic and zero-point vibrational energies (in hartree/particle) for the molecules given in Figure 19. (* means that the structure could not be optimized)

	Energy	ZPVE	Energy + ZPVE
444	*	*	*
445	-577.688734 [0]	134.03	-577.475147
449	-502.418643 [0]	129.89	-502.211648
450	*	*	*
TS7 (444® 445)	*	*	*
TS8 (449® 450)	-502.414459 [1]	129.68	-502.207797

On the contrary, the *endo*-cyclopropylidenes **449** were optimized in the free carbene form at B3LYP/6-31G(d) level (Figure 21). To calculate the energy barriers for their isomerization to the corresponding allene **450**, transition structures of this carbene were investigated, but all efforts to find the allene transition structures failed. Theoretical calculations showed that this carbene **449** does not isomerize to the corresponding allene **450**. Hence, they may undergo intra- or intermolecular insertion and addition reactions, depending on the molecular structure if they are synthesized experimentally.

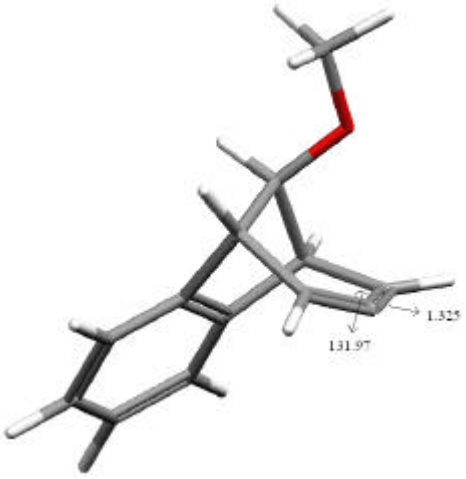

445

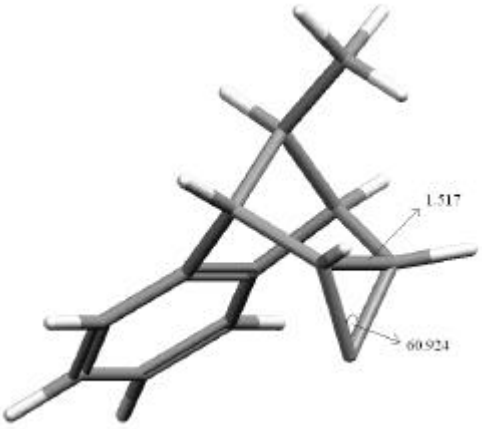

449

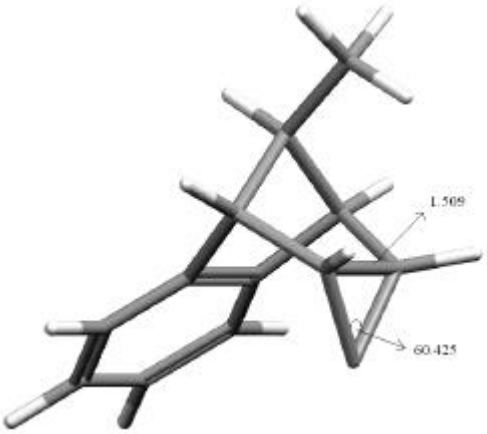

TS8 (449 ® 450)

Figure 21: Optimized structures of **445**, **449** and transition structure **TS8 (449 ® 450)** at B3LYP/6-31G(d)

Finally, the methoxy group at 7-position of benzonorbornadiene destabilizes the formation of *endo*-carbene **444** during the reaction of methyllithium with **408** arising the bicyclic allene **445** directly, whereas the methyl group at this position stabilizes the formation of *endo*-carbene **449**, which does not isomerizes to the corresponding allene **450** with respect to the result of theoretical calculations.

CHAPTER 3

CONCLUSION

The synthesis of cyclic-strained allenes has been attracting more and more interest in the past few decades as explained in Chapter 1.

For this purpose, the incorporation of an allene unit into α-pinene, being natural compound, was aimed by using β-elimination method in the fist part of study. The target allene **371** would be synthesized from compound **377** by dehydrobromination with potassium *tert*-butoxide, but the precursor of **377,** the dibromide **376** could not be isolated from the bromination of α-pinene at low and high temperature, because it is not a heat stable compound, which rearranges easily to compound **378** by hydrogen bromide elimination during the bromination reaction.

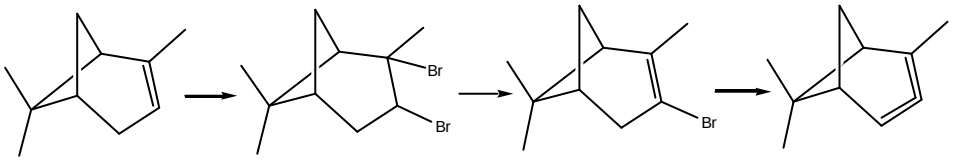

370 **376** **377** **371**

From among the synthetic approaches to the cyclic allenes currently available, the conversion of 1,1-dihalocyclopropanes to the corresponding cyclic allenes upon treatment with alkyllithium reagents discovered by Moore and co-workers and Skattebol has played the most important role.

This part describes an investigation aimed at the incorporation of an allene unit into a natural product, being α-pinene, by using the above mentioned method. It has been indepently reported by Baird *et al.* and Waegell *et al.* in the literature that the reaction of methyllithium with 3,3-dibromo-2,7,7-

trimethyltricyclo[4.1.1.$0^{2,4}$]octane (**385**) formed by the addition of dibromocarbene to α-pinene exclusively provides the insertion product **398** in a 94% yield. However, they did not observe the bicyclic allene **372**, whose bond is located in a seven membered ring.

The activation energy barriers for all possible C-H insertion products **398**, **400**, **401**, and the allene **372** were investigated by using density functional theory computations at B3LYP/6-31G(d) level. It was found that the activation barriers for the formation of **398** and **372** (6.2 and 6.3 kcal/mol) are much lower than that for the insertion products **400** and **401** (17.5 and 12.6 kcal/mol), respectively. This explains that both allene **372** and insertion product **398** can be isolated if the reaction of the dibromide **385** with methyllithium is carried out.

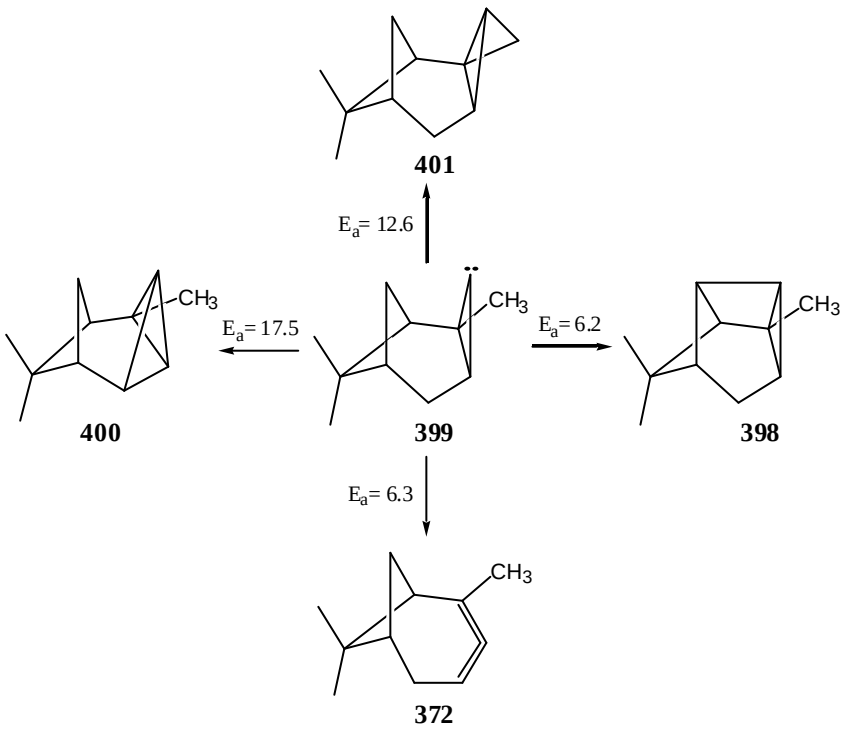

Therefore, 3,3-dibromo-2,7,7-trimethyltricyclo[4.1.1.$0^{2,4}$]octane (**385**) was synthesized from α-pinene via the dibromocarbene addition by treatment with bromoform and potassium *tert*-butoxide in hexane. The obtained dibromocyclopropane **385** was reacted with methyllithium in dry ether at room temperature. After the usual aqueous workup procedure and vacuum distillation for the separation of the insertion product, the residue was analyzed by ^{1}H- and ^{13}C-

NMR measurements, whose spectra showed the formation of three dimeric products, **403**, **404**, and **405**, with a total yield of 37 %. The formation of these dimeric products confirms the formation of the bicyclic allene **372** as a reactive intermediate. These results are in agreement with our theoretical results.

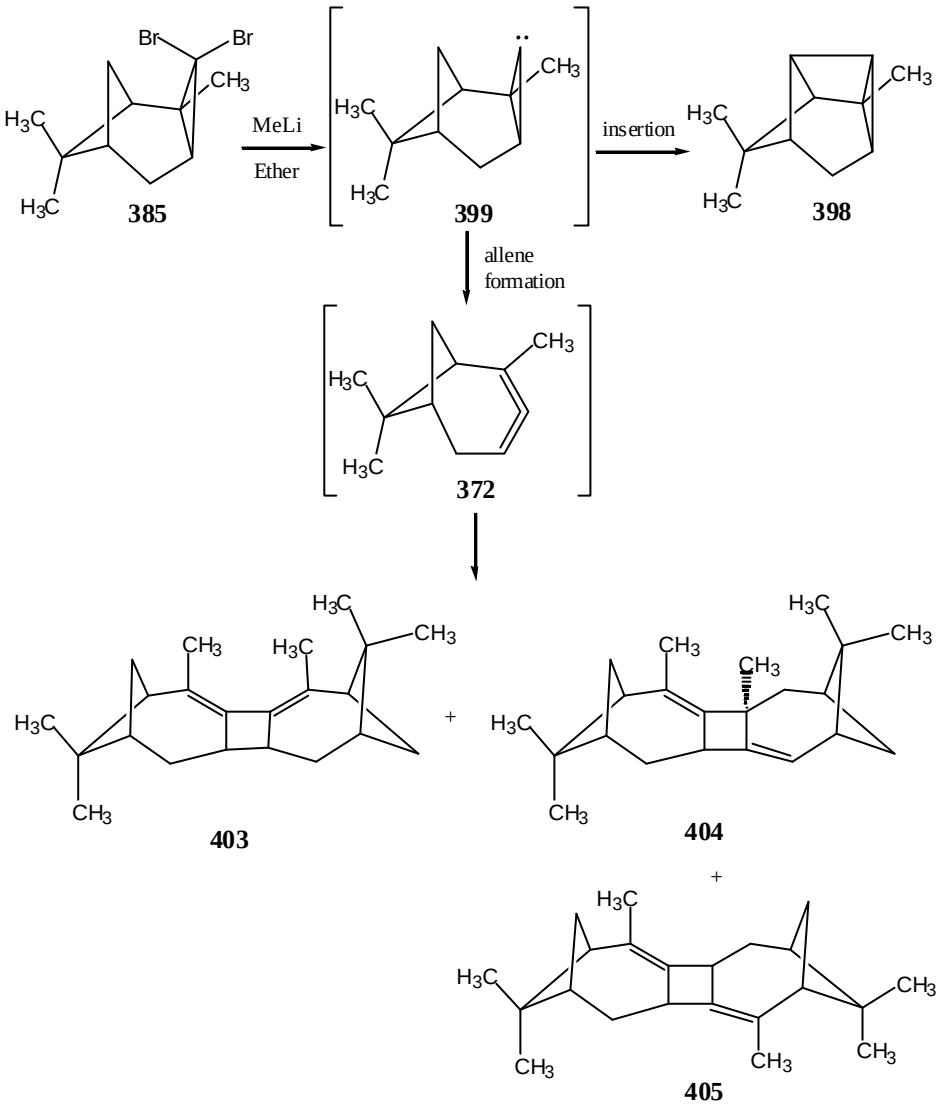

In the second part of study, the *endo* addition of dihalocarbene to anti-7-bromobenzonorbornadiene (**406**) and anti-7-methoxybenzonorbornadiene (**407**) was aimed to isolate the *gem*-dihalocyclopropane, which under the reaction conditions does not undergoe the ring opening to afford a rearranged, ring-expanded dihalide. For this purpose, the synthetic route, starting from the bromination of benzonorbornadiene (**337**), led to the formation of anti-7-bromobenzonorbornadiene (**406**) via the hydrogen bromide elimination with potassium *tert*-butoxide. Then, the

addition of dibromocarbene and dichlorocarbene to **406** provides the *endo*-bromo derivative **424** and the *endo*-chloro derivative **426**, respectively. The *endo*-orientation of the halo substituent was determined from the coupling constant value, almost 5Hz, between the bridgehead H_1 proton and halomethine H_{11} proton. However, the *gem*-dibromocyclopropane **423** and the *gem*-dibromocyclopropane **425** could not be isolated due to the ring expansion to yield **424** and **426**, respectively.

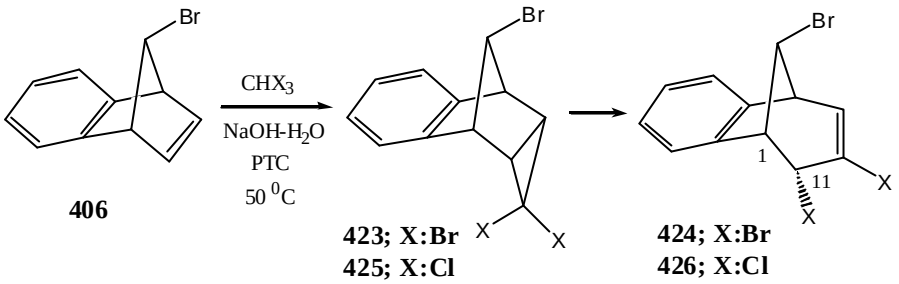

anti-7-Bromobenzonorbornadiene (**406**) were converted to anti-7-methoxybenzonorbornadiene by the treatment of **406** with silvernitrate in methanol, because the bromine group of **406** would react with methyllithium if its the *gem*-dihalocyclopropane derivatives were synthesized from the above mentioned reactions.

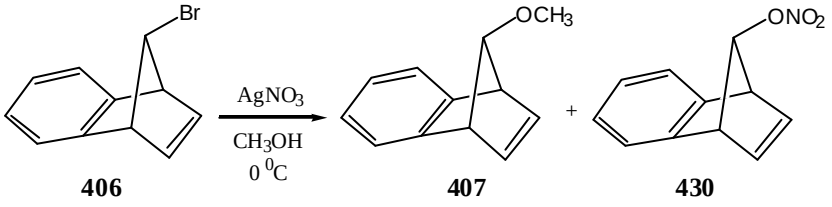

Then, the addition of dibromocarbene and dichlorocarbene to **408** was achieved to afford the *gem*-dibromocyclopropane **432** and the *gem*-dichlorocyclopropane **434**. However, the ring-expanded dihalides, **433** and **435**, were isolated from these reactions as shown below.

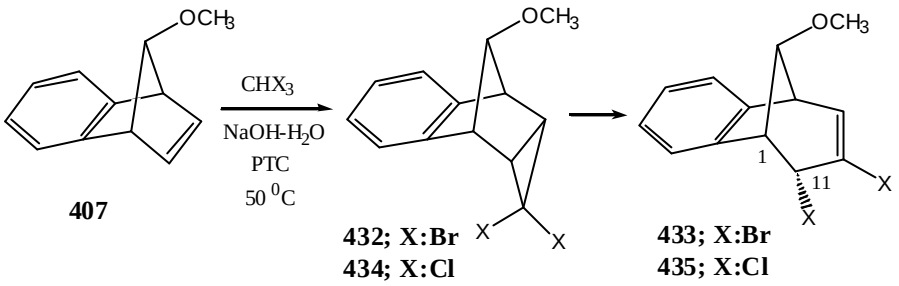

The dibromocarbene and dichlorocarbene addition reactions could not yield the desired *gem*-dihalocyclopropane. Therefore, the addition of fluorobromocarbene to **407** was carried out under the phase-transfer conditions. Three products, **408**, **440**, and **441**, were isolated in a total yield of 18%. The desired compound **408** was suprisingly so stable that the reflux in toluene for 28 hours does not decompose it. However, compound **440** was not heat stable and it rearranges completely to the ring-opened product **441** after three hours reflux in toluene. This result validate the Woodward-Hoffman rules relating with the stereochemical outcome of *gem*-dihalocyclopropane ring opening rationalized in terms of orbital symmetry constraints.

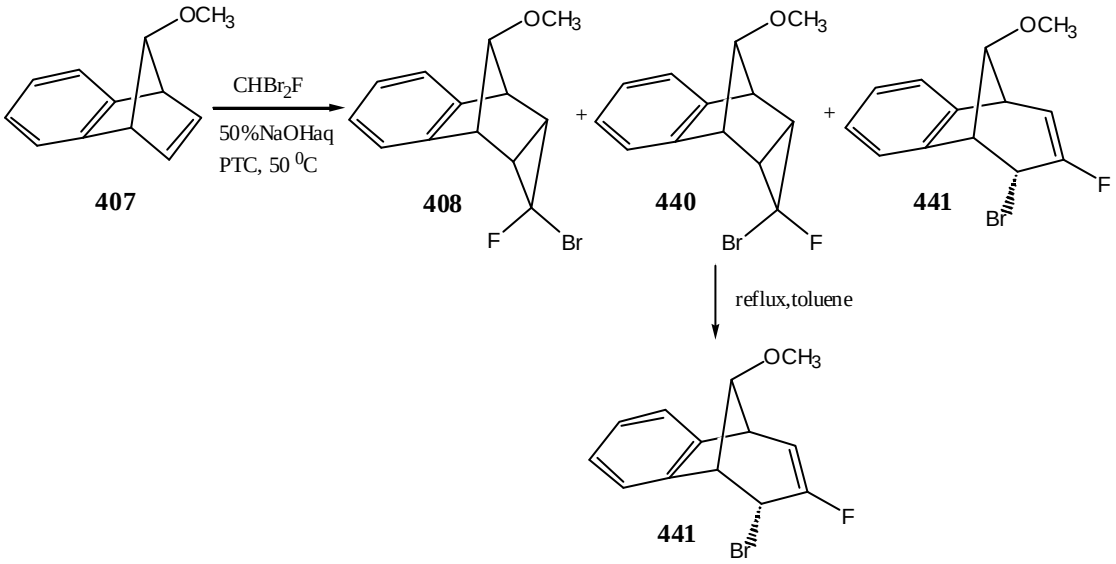

After providing the *gem*-bromofluorocyclopropane **408**, it was treated with methyllithium at low temperatures in furan. One of the four possible isomers of [2+4] cycloadduct **446**, which confirms the formation of the bicyclic allene **445** as an reactive intermediate, was isolated as a sole product. The exact structure of **446** has

been elucidated on the basis of both NMR spectral data and theoretical calculations at B3LYP/6-31G(d) level.

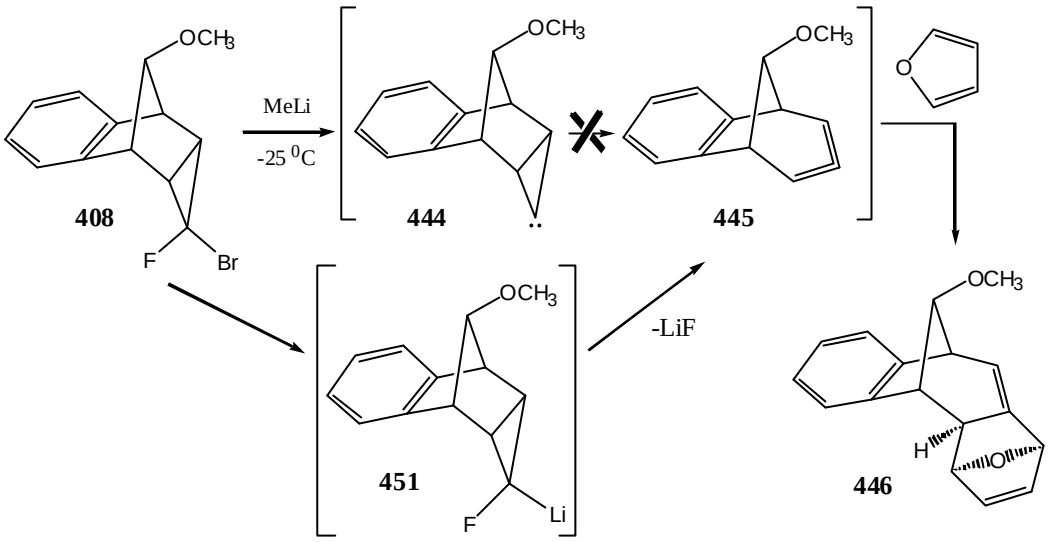

Finally, theoretical calculations at B3LYP/6-31G(d) level were achieved to prove the formation of free carbene structure **444**, which isomerize to the bicyclic allene **445**. However, the results showed that the structure of **444** could not be optimized in the free carbene form, because its optimization gave directly the bicyclic allene structure **445** as a minima. This means that the free carbene form is not an intermediate during the reaction of methyllithium with compound **408**. We suggested that the α-halolithium compounds act as carbenoids rather than dissociating to form free carbenes when the reaction of *gem*-bromofluorocyclopropane with methyllithium was carried out in these situations.

As a result, the methoxy group at 7-position of benzonorbonadiene destabilizes the formation of *endo*-carbene **444**, whereas the methyl group at this position stabilizes the formation of *endo*-carbene **449**, which does not isomerizes to the corresponding allene **450** with respect to the result of theoretical calculations.

CHAPTER 4

EXPERIMENTAL

4.1. General Experimental Techniques

Nuclear Magnetic Resonance (^{1}H, ^{13}C) spectra were recorded on a Bruker Spectrospin Avance DPX-400, Ultra Shield 400 MHz, High Performance digital FT-NMR spectrometer. Chemical shifts are reported in parts per million (δ) downfield from an internal tetramethylsilane ($SiMe_4$) reference and deuterochloroform ($CDCl_3$) as the solvent. Coupling constants (*J*) are reported in hertz (Hz). Spin multiplicities are mentioned as: s (singlet), d (doublet), dd (doublet of doublets), t (triplet), q (quartet), m (multiplet).

Infrared Spectra were recorded on a Mattson model 1000 FT-IR spectrometer and a Perkin Elmer 1600 series FT-IR spectrometer. Band positions were reported in reciprocal centimeters (cm^{-1}). GC/Mass spectra obtained by Thermo Quest Trace Finnigan Automass Multi instrument were reported in electron impact mode (70eV).

Melting points were determined on a capillary melting apparatus and are uncorrected. Elemental Analyses were performed by the way of TUBITAK Test and Analyses center, Besevler, Ankara.

Commercially available reagents were of reagent-grade quality and used as received from Merck and Fluka company. Column chromatography was conducted on Fluka Silicagel (60-200 mesh) and TLC was carried out on Merck 0.2 mm silica gel 60 F254 analytical plates.

Anhydrous solvents were prepared according to the standard methodologies [165]. All extracts were dried over anhydrous magnesium sulfate ($MgSO_4$) and solvents were concentrated under reduced pressure by using rotary evaporator.

4.2. Bromination of 1R-(-)-a -Pinene (370) at 0 ^{0}C

To a magnetically stirred solution of 1R-(-)-α-Pinene (**370**) (850 mg, 6.24 mmol) in 30 ml of chloroform cooled to 0 ^{0}C was added dropwise a solution of bromine (1.04 g, 6.48 mmol) in 10 ml chloroform during 15 minutes. After the completion of the addition, the solution was allowed to warm to room temperature. The solvent was removed under reduced pressure. The oily residue was chromatographed on silica gel (120 g) eluting with hexane to afford *endo*-2-bromobornane (**378**); white solid, m.p. 89 ^{0}C, (240 mg, 18%), and then *endo*-2,*endo*-6-dibromobornane (**379**); colorless crystals, m.p. 171 ^{0}C, (1.37 g, 74%).

378: ^{1}H NMR (400 MHz, $CDCl_3$) δ 4.20 (ddd, J=3.6, 6.7, 13.8, 1H, H_{2exo}), 2.41-2.50 (m, J=10.4, 1H, H_{3endo}), 1.99-2.04 (ddd, J= 4.3, 9.6, 13.4, 1H, H_{6endo}), 1.62-1.73 (m, 1H, H_{5endo}), 1.60 (t, J= 4.3, 1H, H_4), 1.47 (dd, J= 4.3, 13.8, 1H, H_{3exo}), 1.27-1.41 (m, 1H, H_{6exo}), 1.19-1.25 (ddd, J= 4.3, 9.8, 13.1, 1H, H_{5exo}), 0.91 (s, 3H, H_8), 0.83 (s, 3H, H_9), 0.80 (s, 3H, H_{10}); ^{13}C NMR (100 MHz, $CDCl_3$) δ 62.3 (C_2), 51.2 (C_1), 47.3 (C_7), 45.5 (C_4), 41.2 (C_3), 30.8 (C_6), 28.5 (C_5), 21.4 (C_8), 19.0 (C_9), 14.2 (C_{10}),; IR (KBr, cm^{-1}) 2942, 2878, 1473, 1391, 1373, 1294, 1225, 1161, 1083, 899, 841, 768, 661.

379: ^{1}H NMR (400 MHz, $CDCl_3$) δ 4.29 (dd, J= 5.5, 10.5, 2H, H_{2exo} and H_{6exo}), 2.54 (ddd, J= 4.7, 10.3, 13.4, 2H, H_{3endo} and H_{5endo}), 1.77 (dd, J= 5.3, 13.2, 2H, H_{3exo} and H_{5exo}), 0.94 (s, 3H, H_{10}), 1.72 (t, J= 4.7, 1H, H_4), 0.91 (s, 6H, H_8 and H_9); ^{13}C-NMR (100 MHz, $CDCl_3$) δ 55.2 (C_2 and C_6), 52.8 (C_1), 48.8 (C_7), 44.1 (C_4), 41.1 (C_3 and C_5), 21.1 (C_8 and C_9), 13.1 (C_{10}); IR (KBr, cm^{-1}) 2955, 2946, 2907, 1446, 1428, 1276, 1223, 1071, 1048, 985, 912, 871, 693.

4.3. Bromination of 1R-(-)-a -Pinene (370) at 77 ^{0}C

1R-(-)-α-Pinene (**370**) (850 mg, 6.24 mmol) was dissolved in 30 ml of CCl_4 in a 100 ml flask which was equipped with the reflux condenser. The solution was heated until carbontetrachloride started to reflux while stirring magnetically. To this refluxing solution was added a hot solution of bromine (1.69 g, 10.6 mmol) in 20 ml CCl_4 in one portion. The color of bromine disappeared immediately. The resulting reaction mixture was heated for 5 min. at that temperature. After being cooled to room temperature, the solvent was removed under reduced pressure. The oily residue was chromatographed on silica gel (120 g) eluting with hexane to afford **378**, (826 mg, 61%), and then **379**, (185 mg, 10%).

4.4. The synthesis of 3,3-Dibromo-2,7,7-trimethyl-tricyclo[4.1.1.0^{2,4}]octane (385)

A solution of 69.0 g (0.5 mol) of 1*R*-(+)-α-pinene in 100 ml hexane was added to a mechanically stirred suspension of potassium-*tert*-butoxide (65.1 g, 0.58 mole) in hexane (400 ml) which was pre-cooled and maintained at –10 ^{0}C under the nitrogen atmosphere. A solution of bromoform (131.4 g, 0.52 mole) in hexane (150 ml) was then introduced to this suspension during four hours while maintaining the reaction mixture at –10 ^{0}C. After the addition was completed, the mixture was stirred at room temperature for three hours and hydrolyzed through the addition of water (200 ml). The organic layer was washed with a saturated NaCl solution (200 ml) and dried over $MgSO_4$. After the removal of the solvent, the residue was crystallized from hexane at the refrigerator to provide the cyclopropane adduct **385** as colorless crystals (109.4 g, 71%): mp 67.2-68.7 ^{o}C.

385: ^{1}H NMR (400 MHz, $CDCl_3$) δ 2.41 (d, *J* = 11.5 Hz, 1H, H_{8c}) 2.06-2.13 (m, 1H, H_{5a}), 1.96 (t, *J* = 5.5 Hz, 1H, H_1), 1.76 (ddd, *J* = 11.4, 5.5, 2.1 Hz, 1H, H_{8d}), 1.70 (d, *J* = 14.7 Hz, 1H, H_{5b}), 1.54 (m, 1H, H_4), 1.49-1.53 (m, 1H, H_6), 1.29 (s, 3H, H_9), 1.16 (s, 3H, H_{10}), 0.84 (s, 3H, H_{11}); ^{13}C NMR (100 MHz, $CDCl_3$) δ 50.8 (C_3) , 48.6 (C_1), 43.4 (C_2), 39.9 (C_6), 35.0 (C_4), 32.6 (C_7), 27.1 (C_9), 26.8 (C_{10}), 26.7 (C_5), 26.2 (C_8), 22.5 (C_{11}); IR (KBr, cm^{-1}) 2975, 2907, 1447, 1368, 1274, 1222, 1177, 1109, 1011,

942, 892, 836. Elemental Anal. Calcd. for $C_{11}H_{16}Br_2$: C, 42.89; H, 5.24. Found: C, 42.73; H, 5.08.

4.5. The synthesis of 3-Bromo-7,7-dimethyl-2-methylene-bicyclo[4.1.1]oct-3-ene (391)

3,3-Dibromo-2,7,7-trimethyl-tricyclo[4.1.1.$0^{2,4}$]octane (**385**) (1.72 g, 5.58 mmol) was dissolved in 40 ml of dry hexane in a 100 ml flask which was equipped with the reflux condenser. The solution was heated until hexane started to reflux while stirring magnetically. The refluxing solution was checked with thin-layer chromatography every half hour. After seven hours, all of **385** were converted to 3-Bromo-7,7-dimethyl-2-methylene-bicyclo[4.1.1]oct-3-ene (**391**) as a sole product (5.47 g, 99%).

391: ^{1}H NMR (400 MHz, $CDCl_3$) δ 6.16 (t, J= 4.4, 1H, H_4), 5.39 (s, 1H, H_{9a}), 5.00 (s, 1H, H_{9b}), 2.63 (dd, J= 3.95, 7.61, 1H, H_1), 2.30 (dt, J= 7.8, 11.5, 1H, H_{8c}), 2.24 (m, 1H, H_5), 1.91 (m, 1H, H_6), 1.41 (d, J= 11.5, 1H, H_{8d}), 1.13 (s, 3H, H_{10}), 0.64 (s, 3H, H_{11}); ^{13}C NMR (100 MHz, $CDCl_3$) δ 145.8 (C_2), 133.3 (C_4), 123.3 (C_3), 122.0 (C_9), 51.7 (C_1), 40.5 (C_6), 39.7 (C_7), 34.2 (C_5), 30.2 (C_{10}), 26.6 (C_8), 20.8 (C_{11}); IR (KBr, cm^{-1}) 2948, 1679, 1593, 1461, 1378, 1239, 1101, 982, 913, 859, 794.

4.6. Reaction of 3,3-Dibromo-2,7,7-trimethyl-tricyclo[4.1.1.$0^{2,4}$]octane (385) with MeLi

To a solution of **385** (15.40 g, 50.0 mmol) in dry ether (100 ml) was added dropwise 1.6 M MeLi in ether (37.5 ml, 60 mmol) at room temperature and the resulting solution was stirred for 2 h. The reaction mixture was quenched carefully with water. The mixture was extracted with ether, and the organic layer was washed with saturated NaCl and dried over $MgSO_4$. After the removal of the solvent (20 ^oC, 15 torr), the product mixture (8.77 g) was distilled at 38^oC (5 torr) to provide the insertion product, 3,7,7-trimethyltetracyclo[4.2.0.$0^{2,4}$.$0^{3,8}$]octane (**398**) (4.04 g, 54%), colorless liquid, b.p. .

398: ^{1}H-NMR (400 MHz, $CDCl_3$) δ 2.57 (ddd, *J* = 11.8, 4.6, 3.4 Hz, 1H, H_8), 2.02 (d, *J* = 12.0 Hz, 1H, H_{5a}), 1.94 (dd, *J* = 10.6, 4.8 Hz, 1H, H_1), 1.89 (dd, *J* = 10.1, 4.6 Hz, 1H, H_6), 1.72 (t, *J* = 3.5 Hz, 1H, H_3), 1.66 (dd, *J* = 11.8, 6.9, 1H, H_{5b}), 1.20 (br. d, *J* = 4.2 Hz, 1H, H_4), 0.99 (s, 3H), 0.74 (s, 3H), 0.60 (s, 3H) ; ^{13}C NMR ($CDCl_3$, 100 MHz) δ 49.0 (CH), 48.0 (CH), 36.8 (CH), 35.7 (C), 32.0 (CH), 31.3 (CH_2), 27.5 (CH_3), 27.1 (C), 26.0 (CH), 20.4 (CH_3), 19.5 (CH_3); IR (NaCl, cm^{-1}) 2998, 2936, 2861, 1454, 1364, 1267, 1147, 1125, 918, 865, 778; MS *m/z* 148 (M^+, 23%), 133 (100), 115 (37), 115 (37), 105 (100), 91 (100), 77 (98), 69 (100), 65 (61), 51 (56), 42 (34). Elemental Anal. Calcd. for $C_{11}H_{16}$: C, 89.12; H, 10.88. Found: C, 89.02, H, 10.91.

The residue was passed through silica gel (100 g) eluting with hexane to yield head-to-head allene dimer, 1*R*,6*R*,8*S*,10*R*,11*R*,13*S*-2,5,7,7,14,14-hexamethylpentacyclo [11.1.1.1^{6,8}.0^{3,11}.0^{4,10}]hexadeca-2,4-diene **(403)**. Recrystallization from ethanol provided pure **403** as colorless crystals (1.62 g, 22%): mp 122.5-123.0 ^{o}C.

403: ^{1}H-NMR (400 MHz, $CDCl_3$) δ 2.80 (dd, *J* = 8.4, 17.6, 2H, H_1); 2.72 (br. s, 2H, H_4), 2.28-2.15 (m, 6H, H_{8c}, H_{5a}, H_6), 1.81 (s, 6H), 1.66 (dd, *J* = 13.8, 4.6, 2H, H_{8d}), 1.37 (s, 6H), 1.25 (d, *J* = 10.5, 2H, H_{5b}); 1.12 (s, 6H); ^{13}C NMR (100 MHz, $CDCl_3$) δ 136.0 (C), 127.7 (C), 52.4 (CH), 51.4 (CH), 44.1 (CH), 42.0 (C), 38.5 (CH_2), 34.4 (CH_2), 32.3 (CH_3), 30.1 (CH_3), 22.9 (CH_3); IR (KBr) 2960, 2912, 2858, 1448, 1363, 1273, 1235, 1220, 1038, 918, 778 cm^{-1}; MS *m/z* 296 (M^+, 12%), 255 (12), 227 (17), 197(6), 183 (11), 171 (17), 157 (26), 143 (27), 128 (30), 115(20), 105(26), 91 (44), 77 (31), 69 (72), 55 (36), 41 (100). Elemental Anal. Calcd. for $C_{22}H_{32}$: C, 89.12; H, 10.88. Found: C, 88.91; H, 10.83.

The second fraction was the oil of a diastereomeric mixture of head-to-tail dimer 7,7,9,11,14,14-hexamethylpentacyclo[11.1.1.1^{6,8}.0^{3,11}.0^{4,10}]hexadeca-2,9-diene (**404)** and head-to-head allene dimer 2,7,7,9,14,14-hexamethylpentacyclo-[11.1.1.1^{6,8}.0^{3,11}.0^{4,10}]- hexadeca-2,9-diene **(405),** (1.19 g, 15%).

404 and **405**: ^{1}H-NMR (400 MHz, $CDCl_3$) δ 5.19 (d, *J* = 7.6 Hz, 1H), 2.68 (br s, 1H), 2.61 (t, *J* = 7.8 Hz, 1H), 2.3-2.15 (m, 3H), 2.05- 1.75 (m, 7H), 1.61 – 1.65 (m, 2H),

1.51 (s, 3H), 1.24 – 1.32 (m, 1H), 1.12 (s, 3H), 1.10 (s, 3H), 0.89 (s, 3H), 0.75 (s, 3H), 0.67 (s, 3H); The ^{13}C-NMR data of the isomers **404** and **405** was extracted from the NMR mixture with the help of COSY, HMQC, HMBC and DEPT spectra. **405:** 137.0 (C), 127.0 (C), 52.0 (CH), 47.7 (CH) 42.5 (2x CH), 31.5 (CH_2, 30.9 (CH_3), 25.6 (CH_2), 23.3 (CH_3), 21.0 (CH_3). ^{13}C-NMR data of **404**: 146.7 (C), 140.1 (C), 126.2 (C), 116.4 (CH), 51.98 (C), 51.5 (CH), 49.5 (CH), 44.7 (CH), 43.9 (C), 43.2 (C), 42.8 (CH), 42.5 (CH), 41.4 (C), 32.2 (CH_3), 30.1 (CH_2), 26.4 (CH_2), 25.3 (CH_3), 24.2 (CH_2), 23.8 (CH_2), 21.2 (CH_3), 21.0 (2xCH_3), 20.14 (CH_3); IR (NaCl) 2963, 2902, 1450, 1382, 1364, 1227, 1129, 1068, 844, 825 cm^{-1}; (**404** and **405**) MS *m/z* 296 (M^+,12%), 255 (13), 227 (22), 183 (18), 169 (22), 157 (36), 128 (53), 91 (78), 69 (89), 41 (100). Elemental Anal. Calcd. for $C_{22}H_{32}$: C, 89.12; H, 10.88. Found: C, 88.85; H, 10.79.

4.7. The synthesis of benzonorbornadiene (337) [146]

In a 2 liters three-necked flask equipped with stirrer, condenser, and addition funnel was placed a solution of 64.35 g (0.55 mole) *i*-amylnitrite and 800 ml of methylene chloride. A solution of 68.5 g (0.50 mole) anthranilic acid, 33.0 g (0.50 mole) freshly cracked cyclopentadiene, and 300 ml of acetone was added to the stirred solution over a 1 hour period. The reaction was heated at the start until the methylene chloride started to reflux and gas evolution was observed. If the solution was not heated initially, a white solid would begin to separate on one occasion. As soon as the reaction progressed, sufficient heat was evolved to maintain gentle reflux. After the addition was complete, the reaction was refluxed for four hours and cooled by permitting it to stand overnight at room temperature. The solvents were removed under reduced pressure and the black oil diluted with 900 ml of *n*-hexane and 700 ml of saturated $NaHCO_3$ solution in 2 liters beaker. After considerable CO_2 evolution, the layers were seperated and the aqueous layer extracted with *n*-hexane two times. The combined hexane layers were washed three times with 150 ml portions of saturated $NaHCO_3$ solution, twice with saturated NaCl solution, and dried over anhydrous $MgSO_4$. Removal of the hexane at reduced pressure and distillation through a 10-in. Vigreux column afforded *i*-amyl alcohol, b.p. 45 ^{0}C/10 mm, and 28.50 g benzonorbornadiene (**337**), b.p. 72-81 ^{0}C/10 mm, 40% yield.

337: ^{1}H NMR (400 MHz, $CDCl_3$) δ 7.58-7.25 (AA′BB′ system, 4H, aryl), 7.15 (t, J=1.8, 2H, olefinic), 4.25 (t, J= 1.7, 2H, bridge-head protons), 2.71 (dd, A part of AB system, J= 1.5, 7.0, 1H, H_{7syn}), 2.63 (d, B part of AB system, J= 7.0, 1H, H_{7anti}); ^{13}C-NMR (100 MHz, $CDCl_3$) δ 152.0 (C_2 and C_3), 143.5, 124.7, 122.0 (aryl carbons), 70.6 (C_7), 50.9 (C_1 and C_4).

4.8. The synthesis of 2-*exo*-7-*anti*-dibromobenzonorborn-5-ene (380)

To a magnetically stirred solution of benzonorbornadiene (**337**) (3.4 g, 23.94 mmol) in 100 ml carbontetrachloride cooled to 10 ^{0}C was added dropwise a solution of bromine (3.92 g, 24.53 mmol) in 30 ml carbontetrachloride during 15 minutes. After completion of the addition, the solution was allowed to warm to room temperature. The solvents were removed under reduced pressure. The residue was crystallized from ethanol to give the dibromo compound **380** as colorless crystals, (7.16 g, 99%); m.p. 76.4-77.2 ^{0}C.

380: ^{1}H NMR (400 MHz, $CDCl_3$) δ 7.15-7.04 (m, 4H, aryl), 4.04 (s, 1H, H_7), 3.69 (dd, J= 4.7, 7.9, 1H, H_2), 3.66 (s, 1H, H_1), 3.43 (s, 1H, H_4), 2.79 (A-part of AB system, dt, J= 4.2, 13.3, 1H, H_{3exo}), 2.13 (B-part of AB system, dd, J=8.0, 13.2, 1H, H_{3endo}); ^{13}C NMR (100 MHz, $CDCl_3$) δ 144.0, 143.6, 128.2, 127.7, 122.2, 121.7 (aryl carbons), 56.9 (C_7), 55.7 (C_1), 51.6 (C_4), 45.0 (C_2), 37.1 (C_3).

4.9. The synthesis of *anti*-7-bromobenzonorbornadiene (406)

To a magnetically stirred solution of 5.13 g (16.98 mmol) of 380 in dry and freshly distilled THF (80 ml) was added a solution of 1.92 g (17.12 mmol) of potassium *tert*-butoxide in 40 ml of dry and fresly distilled THF. The resulting mixture was refluxed for one hour and then cooled to room temperature. The mixture was diluted with water, and the aqueous phase was extracted with ether, washed with water, and dried over $MgSO_4$. The solvents were removed under reduced pressure. The residue was crystallized from hexane to yield *anti*-7-bromo-benzonorbornadiene (**406**) as colorless crystals, (3.45 g, 92%), m.p. 53.2-53.6 ^{0}C, b.p. 99.5 ^{0}C / 5 mm.

406: ^{1}H NMR (400 MHz, $CDCl_3$) δ 7.23-7.00 (AA′BB′ system, 4H, aryl), 6.73 (s, 2H, olefinic protons), 4.39 (s, 1H, bridge proton), 4.08 (s, 2H, bridge-head protons); ^{13}C NMR (100 MHz, $CDCl_3$) δ 147.5 (C_2 and C_3), 139.8, 125.9, 122.3 (aromatic parts), 74.3 (C_7), 57.7 (C_1 and C_4).

4.10. Addition of Dibromocarbene to *anti*-7-bromobenzonorbornadiene (406)

A mixture of *anti*-7-bromobenzonorbornadiene **(406)** (6.1 g), bromoform (25 ml), 50 % sodium hydroxide solution (30 ml), and benzyltriethylammonium chloride (1.0 g) was vigorously stirred at 50 ^{0}C for five hours. The mixture was diluted with water and thorougly extracted with ether, and the combined extracts were washed with water, dried, and evaporated. Unreacted *anti*-7-bromobenzonorbornadiene **(406)** was recovered by distillation (99-101 ^{0}C / 5 mm), and the distillation residue was saved. The recovered *anti*-7-bromobenzonorbornadiene **(406)** was resubmitted to the reaction conditions, using the same quantities of $CHBr_3$, NaOH, and phase-transfer catalyst. Workup as before and distillation afforded unchanged *anti*-7-bromo-benzonorbornadiene **(406)** (2.9 g). The combined distillation residues were submitted to rapid silica filtration using silica gel (60 g) and eluting with hexane-CH_2Cl_2 (10:2) to yield 6,7,10-Tribromo-6,9-dihydro-5H-5,9-methano-benzocycloheptene (**424**) as the only product, which crystallized from hexane-CH_2Cl_2 as colorless crystals, m.p. 147.5 ^{0}C. The yield of **424** was 3.01 g (53%, based on unrecovered starting material).

424: ^{1}H NMR (400 MHz, $CDCl_3$) δ 7.44-7.12 (m, 4H, aryl), 6.48 (d, J= 7.1, 1H, H_9), 5.24 (d, J= 5.0, 1H, H_{11}), 4.59 (t, J= 4.06, 1H, H_{12}), 3.65 (t, J= 4.5, 1H, H_1), 3.53 (dd, J= 3.9, 6.9, 1H, H_8); ^{13}C NMR (100 MHz, $CDCl_3$) δ 147.1, 139.0, 134.9, 128.8, 128.1, 127.4, 121.9, 121.1, 54.1, 53.7, 53.6, 48.7; IR (KBr) 3053, 2986, 1598, 1465, 1236, 1151, 1047, 972, 885, 793, 766, 725; Elemental Anal. Calcd. for $C_{12}H_9Br_3$: C, 36.68; H, 2.31. Found: C, 36.9; H, 2.16.

4.11. Addition of Dichlorocarbene to *anti*-7-bromobenzonorbornadiene (406)

A mixture of **406** (6.3 g), chloroform (30 ml), 50 % NaOH solution (30 ml), and benzyltriethylammonium chloride (1 g) was vigorously stirred at 40 ^{0}C for five hours. The mixture was diluted with water and worked up by ether extraction in the usual manner. Distillation gave the unreacted alkene **406** (99-101 ^{0}C / 5 mm), and the distillation residue was saved. The recovered *anti*-7-bromobenzonorbornadiene **(406)** was resubmitted to the reaction conditions, using the same quantities of $CHCl_3$, NaOH, and phase-transfer catalyst. Workup as before and distillation afforded unchanged *anti*-7-bromo-benzonorbornadiene **(406)** (3.2 g). The combined distillation residues were submitted to rapid silica filtration using silica gel (60 g) and eluting with hexane-CH_2Cl_2 (10:2) to yield 10-Bromo-6,7-dichloro-6,9-dihydro-5H-5,9-methano-benzocycloheptene (**426**) as the only product, which crystallized from hexane-CH_2Cl_2 as colorless crystals, m.p. 114.7 ^{0}C. The yield of **426** was 2.6 g (61%, based on unrecovered starting material).

426: ^{1}H NMR (400 MHz, $CDCl_3$) δ 7.32-7.05 (m, 4H, aryl), 6.18 (d, J= 7.0, 1H, H_9), 4.94 (d, J= 5.0, 1H, H_{11}), 4.52 (t, J= 4.0, 1H, H_{12}), 3.55 (t, J= 4.7, 1H, H_1), 3.50 (dd, J= 4.1, 6.9, 1H, H_8); ^{13}C NMR (100 MHz, $CDCl_3$) δ 147.8, 138.3, 131.2, 129.9, 128.8, 128.1, 127.6, 121.9, 59.5, 54.3, 52.9, 47.6; IR (KBr) 3059, 2990, 2963, 1621, 1466, 1242, 1205, 989, 890, 812, 768, 726, 685; MS *m/z* 304 (M^+,96%), 269 (13), 225 (100), 188 (99), 161 (35), 153 (100), 127 (93), 115 (94), 98 (72), 93 (94), 86 (80), 75 (99), 62 (87), 49 (85); Elemental Anal. Calcd. for $C_{12}H_9BrCl_2$: C, 47.41; H, 2.98. Found: C, 47.86; H, 2.71.

4.12. The reaction of 7-*anti*-bromobenzonorbornadiene (406) with silver nitrate

To a magnetically stirred solution of $AgNO_3$ (1.8 g, 10.6 mmol) in 100 ml of methanol cooled to 0 ^{0}C was added dropwise a solution of 7-*anti*-bromobenzonorbornadiene (**406**) (2.3 g, 10.4 mmol) in 50 ml of methanol during 1 hour. After the addition was completed, the solution was allowed to warm to room temperature and stirred for five hours at that temperature. Then, the silver bromide

was filtered off and washed well with ether. Water was added to the filtrate, followed by ether. The ether extracts were combined with the silver bromide washings, made neutral, dried, and evaporated. The oily residue was passed through silica gel (75 g) eluting with *n*-hexane to yield *anti*-7-nitroxybenzonorbornadiene (**430**), colorless liquid, (1.1 g, 52%). The second fraction eluting with hexane-ethylacetate (10:1) was *anti*-7-methoxybenzonorbornadiene (**407**), colorless solid, (0.86 g, 48%), m.p. , b.p. 98 ^{0}C / 5 mm.

430: ^{1}H NMR (400 MHz, $CDCl_3$) δ 7.34-7.13 (AA′BB′ system, 4H, aryl), 6.66 (s, 2H, olefinic protons), 4.90 (s, 1H, bridge proton), 4.14 (s, 2H, bridge-head protons); ^{13}C NMR (100 MHz, $CDCl_3$) δ 146.0 (C_2 and C_3), 138.1, 126.4, 123.2 (aromatic carbons), 101.7 (C_7), 52.6 (C_1 and C_4); IR (NaCl) 3076, 3007, 2898, 1712, 1635, 1455, 1357, 1309, 1284, 1181, 1021, 987, 919, 867, 795, 750, 704, 620; MS *m/z* 156 (M^+,88%), 128 (100), 101 (30), 87 (21), 75 (49), 63 (46), 51 (50); Elemental Anal. Calcd. for $C_{11}H_9NO_3$: C, 65.02; H, 4.46; N, 6.89, Found: C, 65.9; H, 3.93; N, 6.47.

407: ^{1}H NMR (400 MHz, $CDCl_3$) δ 7.24-7.02 (AA′BB′ system, 4H, aryl) , 6.63 (s, 2H, olefinic protons), 3.98 (s, 1H, bridge proton), 3.31 (s, 2H, bridge-head protons); ^{13}C NMR (100 MHz, $CDCl_3$) δ 147.7 (C_2 and C_3), 137.8, 125.5, 122.7 (aromatic carbons), 107.4 (C_7), 57.0 (methyl carbon), 53.8 (C_1 and C_4); IR (KBr) 3071, 2985, 2930, 2881, 2826, 1632, 1568, 1455, 1361, 1361, 1310, 1232, 1213, 1003, 899, 829, 789, 745, 693; MS *m/z* 171 (M^+,73%), 155 (19), 141 (100), 129 (100), 115 (79), 102 (56), 77 (47), 63(47), 51(48); Elemental Anal. Calcd. for $C_{12}H_{12}O$: C, 83.69; H, 7.02. Found: C, 83.51; H, 6.94

4.13. Addition of Dibromocarbene to *anti*-7-methoxybenzonorbornadiene (407)

A mixture of *anti*-7-methoxybenzonorbornadiene (**407**) (3.1 g), $CHBr_3$ (15 ml), 50 % NaOH solution (20 ml), and benzyltriethylammonium chloride (0.5 g) was vigorously stirred at 50 ^{0}C for five hours. The mixture was diluted with water and thorougly extracted with ether, and the combined extracts were washed with water, dried, and evaporated. Unreacted alkene was recovered by distillation (97-99 ^{0}C / 5 mm), and the distillation residue was saved. The recovered alkene **407** was

resubmitted to the reaction conditions, using the same quantities of $CHBr_3$, NaOH, and phase-transfer catalyst. Workup as before and distillation afforded unchanged *anti*-7-methoxybenzonorbornadiene (**407**) (0,8 g). The combined distillation residues were submitted to rapid silica filtration using silica gel (60 g) and eluting with hexane-ethylacetate (10:1) to yield 6,7-Dibromo-10-methoxy-6,9-dihydro-5H-5,9-methano-benzocycloheptene (**433**) as the only product, which crystallized from hexane-CH_2Cl_2 as colorless crystals, m.p. 165.4 ^{0}C. The yield of **433** was 2.62 g (57%, based on unrecovered starting material).

433: ^{1}H NMR (400 MHz, $CDCl_3$) δ 7.46-7.13 (m, 4H, aryl), 6.43 (d, J= 6.96, 1H, H_9), 5.09 (d, J= 4.95, 1H, H_{11}), 4.04 (t, J= 4.0, 1H, H_{12}), 3.67 (t, J= 4.6, 1H, H_1), 3.48 (overlapping with methyl protons, 1H, H_8), 3.45 (s, 3H, methyl protons); ^{13}C NMR (100 MHz, $CDCl_3$) δ 146.6, 139.2, 132.4, 128.5, 128.3, 127.1, 122.3, 121.9, 86.3, 57.3, 53.7, 51.7, 44.9; IR (KBr) 2957, 2924, 2879, 2825, 1638, 1451, 1338, 1301, 1261, 1202, 1144, 1107, 1019, 993, 963, 946, 843, 795, 755 ; MS *m/z* 344 (M^+,3%), 263 (79), 219 (39), 184 (100), 169 (48), 140 (83), 115 (53), 88 (19), 75 (29), 62 (31); Elemental Anal. Calcd. for $C_{13}H_{12}Br_2O$: C, 45.38; H, 3.52. Found: C, 45.26; H, 3.37.

4.14. Addition of Dichlorocarbene to *anti*-7-methoxybenzonorbornadiene (407)

A mixture of **407** (3.4 g), chloroform (15 ml), 50 % NaOH solution (20 ml), and benzyltriethylammonium chloride (0.5 g) was vigorously stirred at 40 ^{0}C for five hours. The mixture was diluted with water and worked up by ether extraction in the usual manner. Distillation gave the unreacted alkene **407** (97-99 ^{0}C / 5 mm), and the distillation residue was saved. The recovered alkene **407** was resubmitted to the reaction conditions, using the same quantities of $CHCl_3$, NaOH, and phase-transfer catalyst. Workup as before and distillation afforded unchanged *anti*-7-methoxy-benzonorbornadiene **(407)** (1.0 g). The combined distillation residues were submitted to rapid silica filtration using silica gel (60 g) and eluting with hexane-ethylacetate (10:1) to yield 6,7-Dichloro-10-methoxy-6,9-dihydro-5H-5,9-methano-benzocyclo-heptene (**435**) as the only product, which crystallized from hexane-CH_2Cl_2 as colorless crystals, m.p. 128.3 ^{0}C. The yield of **435** was 3.56 g. (63%, based on unrecovered starting material).

435: ^{1}H NMR (400 MHz, $CDCl_3$) δ 7.45-7.16 (m, 4H, aryl), 6.22 (d, J=7.1, 1H, H_9), 4.89 (d, J= 5.1, 1H, H_{11}), 4.10 (t, J= 4.01, 1H, H_{12}), 3.66 (t, J= 4.6, 1H, H_1), 3.54 (dd, J= 4.2, 6.6, 1H, H_8), 3.46 (s, 3H, methyl protons); ^{13}C NMR (100 MHz, $CDCl_3$) δ 147.3, 138.3, 130.6, 128.6, 128.5, 128.2, 127.2, 122.3, 86.6, 59.0, 57.3, 50.9, 43.7; IR (KBr) 2951, 2932, 2834, 1620, 1466, 1348, 1211, 1117, 1011, 891, 794, 762, 695; MS *m/z* 254 (M^+,39%), 219 (100), 203 (32), 187 (60), 177 (100), 162 (75), 152 (100), 139 (100), 127 (38), 115 (98), 102 (20), 89 (40), 75 (51), 63 (60), 45 (44); Elemental Anal. Calcd. for $C_{13}H_{12}Cl_2O$: C, 47.41; H, 2.98. Found: C, 47.49; H, 2.84.

4.15. Preparation of dibromofluoromethane [167]

A 250 ml two-necked flask, equipped with a condenser and nitrogen stream system, was charged with 57 g (225 mmol) of $CHBr_3$ and 15 g of (84 mmol) SbF_3, which was dried in vacuo at the reflux temperature of xylene for six hours before starting the experiment. The reaction flask was immersed in an oil bath at 120 ^{0}C, the mixture was stirred for five minutes and then 3 ml of bromine was added. After a short while, the dark red became homogeneous and a mixture of the dibromofluoromethane and bromine began to distil into the receiving flask cooled with an ice bath. The initial exotherm resulted in a head temperature of 100 ^{0}C, but most of the distillate came over at 60-80 ^{0}C. The distillate was washed with 10 % Na_2SO_3 solution until the color of bromine disappeared. Lower organic phase was washed with water, dried over $CaCl_2$, and distilled carefully to give $CHBr_2F$ as colorless liquid. The yield was 12 g (35 %), b.p. 66-67 ^{0}C.

4.16. Addition of Bromofluorocarbene to *anti*-7-Methoxybenzonorbornadiene (407)

To magnetically stirred solution of *anti*-7-methoxybenzonorbornadiene **(407)** (5.8 g), benzyltributylammonium chloride (1.0 g) and dibromofluoromethane (10 g) heated to 50 ^{0}C was added dropwise a solution of 50% NaOH (20 ml) during four hours. After the completion of addition, the reaction mixture was stirred for two hours. Then, the solution was allowed to cool to room temperature. The mixture was

diluted with water and thorougly extracted with methylene chloride, and the combined extracts were washed with water, dried, and evaporated. Unreacted alkene was recovered by distillation (97-99 ^{0}C / 5 mm), and the distillation residue was saved. The recovered alkene **407** was resubmitted to the reaction conditions, using the same quantities of $CHBr_2F$, NaOH, and phase-transfer catalyst. Workup as before and distillation afforded unchanged *anti*-7-methoxybenzonorbornadiene (**407**) (3,9 g). The combined distillation residues were submitted to rapid silica filtration using silica gel (120 g) eluting with hexane-ethylacetate (10:1). Four products were isolated; **408** (0.28 g, 9%), **440** (0.094 g, 3%), **441** (0.19 g, 6%) and starting material **407** in that order from the column chromatography.

408: colorless liquid: ^{1}H NMR (400 MHz, $CDCl_3$) δ 7.16-7.12 (AA′BB′ system, 4H, aryl), 3.83 (s, 1H, H_{12}), 3.70 (d, J= 1.6, 2H, H_1 and H_8), 3.37 (s, 3H, methyl protons), 2.57 (t, J= 2.2, 2H, H_9 and H_{11}); ^{13}C NMR (100 MHz, $CDCl_3$) δ 141.7 (d, J= 3.4, C_2 and C_7), 127.3 (C_3 and C_6), 122.9 (C_4 and C_5), 107.0 (d, J=4.6, C_{12}), 93.0 (d, J= 340, C_{10}), 56.7 (C_{13}), 48.6 (C_1 and C_8), 37.3 (d, J= 13.2, C_9 and C_{11}); IR (NaCl) 2985, 2928, 2826, 1642, 1561, 1458, 1357, 1211, 1106, 1041, 994, 798, 718, 592.; MS *m/z* 282 (M^+,7%), 264 (23), 247.1 (33), 239.1 (10), 219.1 (24), 203.1 (39), 189.1 (12), 171.1 (80), 159.1 (100), 139.1 (49), 128.1 (85), 115.2 (26), 95.1 (43), 81.1 (37), 67.1 (19); Elemental Anal. Calcd. for $C_{13}H_{12}BrFO$: C, 55.15; H, 4.27. Found: C, 55.09; H, 4.15.

440: colorless liquid: ^{1}H NMR (400 MHz, $CDCl_3$) δ 7.19-7.06 (AA′BB′ system, 4H, aryl), 3.81 (s, 2H, H_1 and H_8), 3.20 (s, 3H, methyl protons), 3.19 (s, 1H, H_{12}), 1.87 (s, 2H, H_9 and H_{11}); ^{13}C NMR (100 MHz, $CDCl_3$) δ 146.5 (C_2 and C_7), 126.7 (C_3 and C_6), 122.4 (C_4 and C_5), 97.4 (d, J=351, C_{10}), 86.6 (C_{12}), 56.9 (C_{13}), 48.9 (d, J= 2, C_1 and C_8), 42.0 (d, J= 16, C_9 and C_{11}); IR(NaCl) 3030, 2975, 2927, 2872, 2825, 1642, 1466, 1396, 1371, 1250, 1217, 1195, 1015, 997, 949, 894, 802, 755, 722; MS *m/z* 284.5 (M^+,4%) 219.86 (3), 203.80 (15), 159.44 (100), 133.16 (23), 115.11 (7); Elemental Anal. Calcd. for $C_{13}H_{12}BrFO$: C, 55.15; H, 4.27. Found: C, 55.07; H, 4.18.

441: colorless crystals, m.p. 132.8 ^{0}C: ^{1}H NMR (400 MHz, $CDCl_3$) δ 7.45-7.15 (m, 4H, aryl), 5.63 (dd, J= 7.3, 12.4, 1H, H_9), 5.07 (d, J= 5.2, 1H, H_{11}), 3.95 (br.s, 1H,

H_{12}), 3.64 (dd, J= 5.2, 11.9, 1H, H_1), 3.49 (ddd, J= 3.5, 7.1, 10.5, 1H, H_8); ^{13}C NMR (100 MHz, $CDCl_3$) δ 153.8 (d, J= 259, C_{10}) , 147.1 (C_7), 138.2 (C_2), 127.9 (C_6), 128.8 (C_3), 126.4 (C_5) 121.9 (C_4), 106.7 (d, J= 14.3, C_9), 85.8 (d, J= 1.3, C_{12}), 56.7 (C_{13}), 50.0 (d, J= 4.3, C_1), 45.1 (d, J= 21.3, C_{11}), 40.6 (d, J= 6.3, C_8); IR (KBr) 2981, 2922, 2761, 1643, 1504, 1361, 1119, 997, 827, 754, 698; MS *m/z* 284.8 (M^+,56%), 237.56 (9), 219.58 (16), 203.43 (100), 171.09 (81), 132.94 (37), 114.89 (13), 102.88 (7); Elemental Anal. Calcd. for $C_{13}H_{12}BrFO$: C, 55.15; H, 4.27. Found: C, 55.13; H, 4.21.

4.17. Thermal rearrangement of 10-endobromo-10-fluorotricyclo-[6.3.1.$0^{2,7}$.$0^{9,11}$]dodeca-2,4,6-triene (440)

Compound **440** (100 mg, 0.35 mmol) was dissolved in 20 ml of dry toluene in a 50 ml flask which was equipped with the reflux condenser. The solution was heated until toluene started to reflux while stirring magnetically.The refluxing mixture was checked with thin-layer chromatography every half hour. After three hours, the solution was allowed to cool to room temperature. The solvent was removed under reduced pressure. The oily residue was chromatographed on 10 g of silica eluting with hexane-ethylacetate (10:1) to afford **441** (97 mg, 97%).

4.18. The synthesis of 16-Methoxy-17-oxapentacyclo-[7.6.1.1^{3,6}.$0^{2,7}$.$0^{10,15}$]-heptadeca-4,7,10,12,14-pentaene (446)

To magnetically stirring solution of **408** (0.83 g, 2.93 mmol) in ether was added dropwise a solution of 1.6 M MeLi (7.20 mmol, 4.5 ml) in ether over ten minutes at –25 ^{0}C under nitrogen atmosphere. Then, furan (0.2 g, 3 mmol) was added dropwise over five minutes at the same temperature. The reaction mixture was stirred continually and allowed to warm to room temperature over four hours. The reaction mixture was quenched carefully with water. The mixture was extracted with ether, and the organic layer was washed with saturated NaCl, dried over $MgSO_4$, and concentrated under reduced pressure. The oily residue was submitted to neutral aluminum oxide column (100 g, Grade III) eluting with hexane-ethlyacetate (10:1) to give **446** as the only product (0.17 g, 23%), colorles crsytals, m.p. 93.5-94.7.

446: ^{1}H NMR (400 MHz, $CDCl_3$) δ 7.21-7.04 (m, 4H, aryl), 6.28 (dd, J= 1.5, 5.6, 1H, H_5), 6.09 (dd, J= 1.3, 5.6, 1H, H_4), 5.78 (dd, J= 2.3, 7.1, 1H, H_8), 5.04 (d, J= 3.7, 1H, H_3), 5.02 (br. s, 1H, H_6), 3.86 (t, J= 3.9, 1H, H_9), 3.57 (dd, J= 4.0, 7.1, 1H, H_1), 3.16 (br. s, 1H, H_{16}), 3.15 (s, 3H, methyl protons), 2.46 (t, J= 3.1, 1H, H_2); ^{13}C NMR (100 MHz, $CDCl_3$) δ 146.4, 144.1, 142.6,.134.7, 130.5, 127.1, 126.7, 123.2, 122.1, 117.3, 84.2, 81.8, 80.3, 55.5, 44.4, 42.7, 41.0; IR (KBr) 2975, 2931, 2866, 2732, 1731, 1653, 1501, 1372, 1125, 1009, 833, 778, 748, 704; MS *m/z* 252.1 (M^+,8%), 220.1 (38), 191.2 (100), 178.2 (62), 165.1 (46), 152.1 (22), 128.1 (11), 115.1 (19), 95.1 (15), 81.1 (17), 67.1 (10); Elemental Anal. Calcd. for $C_{17}H_{16}O_2$: C, 80.93; H, 6.39. Found: C, 80.81; H 6.28.

REFERENCES

[1] Fischer, H., '*The Chemistry of Allenes*', Patai, S. (Ed.), Interscience Publishers Inc. London, **1964**.

[2] Hoffman, R., *Tetrahedron*, **1966**, 22, 521-538.

[3] Taylor, D.R., *Chem. Rev*., **1967**, 67, 317-359.

[4] Wotiz, J.H., Mancuso, D.E., *J. Org. Chem.*, **1957**, 22, 207-211.

[5] Simmons, H.E., Blanchard, E.P., Hartzler, H.D., *J. Org. Chem.*, **1966**, 31, 295-301.

[6] Friedel, R.A., Retcofsky, H.L., *J. Am. Chem. Soc.*, **1963**, 85, 1300-1306.

[7] Pople, J.A., *Discussions Faraday Soc.*, **1962**, 37, 7-14.

[8] a. Rossi, R., Diversi, P., *Synthesis*, **1973**, 1, 25-36.

b. Nakagawa, M., Shingu, K., Naemura, K., *Tetrahedron Lett.*, **1961**, 2, 802-806.

[9] a. Rode, J.E., Dobrowolski, J.Cz., *J. Mol. Struct. (Theochem),* **2003**, 635, 151-159.

b. Rezanka, T., Dembitsky, V.M., *Phytochemistry*, **2001**, 56, 869-874.

[10] Sydnes, L.K., *Chem. Rev*., **2003**, 103, 1133-1150.

[11] Balci, M., Taºkesenligil, Y., In *Advances in Strained and Interesting Organic Molecules*, Halton, B., Ed., JAI Press Inc., Stamfort, CT, **2000**, Vol.8, pp. 43-81.

[12] Johnson, R.P., *Chem. Rev*., **1989**, 89, 1111-1124.

[13] Sevin, F., Doðan, M., *J. Mol. Struct*., **2003**, 661-662, 265-270

[14] Musch, P.W., Scheidel, D., Engels, B., *J. Phys. Chem. A.*, **2003**, 107, 11223-11230

[15] Ananikov, V.P., *J. Phys. Org. Chem.*, **2003**, 16, 253-263.

[16] Engels, B., Schoneboom, J.C., Münster, A.F., Groetsch, S., Christl, M., *J. Am. Chem. Soc.*, **2002**, 124, 287-297.

[17] Yavari, I., Nourmohammadian, F., Tahmassebi, D., *J. Mol. Struct. (Theochem),* **2001**, 542, 199-206.

[18] Martin-Santamaria, S., Rzepa, H.S., *J. Chem. Soc. Perkin Trans.2*, **2000**, 2372-2377.

[19] Hughes, T.S., Carpenter, B.K., *J. Chem. Soc. Perkin Trans.2*, **1999**, 2291-2298

[20] Bettinger, H.F., Schleyer, P.v.R., Schreiner, P.R., Schaefer III. H.F., *J. Org. Chem.*, **1997**, 62, 9267-9275.

[21] Yavari, I., Baharfar, R., Nori-Shargh, D., *J. Mol. Struct. (Theochem)*, **1997**, 393, 167-170.

[22] Dewar, M.J.S., Merz, K.M.Jr., *J. Am. Chem. Soc.*, **1986**, 108, 5142-5145.

[23] Andres, J., Cardenas, R., Tapia, O., *J. Chem. Soc. Perkin Trans.2*, **1985**, 363-366.

[24] Angus, R.O.Jr., Schmidt, M.W., Johnson, R.P., *J. Am. Chem. Soc.*, **1985**, 107, 532-535.

[25] Schmidt, M.W., Angus, R.O.Jr., Johnson, R.P., *J. Am. Chem. Soc.*, **1982**, 104, 6838-6839.

[26] Gasteiger, J., Dammer, O., *Tetrahedron*, **1978**, 34, 2939-2945.

[27] Seeger, R., Krishman, R., Pople, J.A., Schleyer, P.v.R., *J. Am. Chem. Soc.*, **1977**, 99, 7103-7105.

[28] Dillon, P.W., Underwood, G.R., *J. Am. Chem. Soc.*, **1977**, 99, 2435-2446.

[29] Dillon, P.W., Underwood, G.R., *J. Am. Chem. Soc.*, **1974**, 96, 779-787.

[30] Blomquist, A.T., Burge, R.E.Jr., Liu, L.H., Bohrer, J.C., Sucsy, A.C., Kleis, J., *J. Am. Chem. Soc.*, **1951**, 73, 5510-5511.

[31] a. Skattebøl, L., *Tetrahedron Lett.*, **1961**, 2, 167-172.

b. Skattebøl, L., Solomon, S., *Organic Synthesis*, **1969**, 49, 35-38.

[32] a. Doering, W.v.E., LaFlamme, P.M., *Tetrahedron*, **1958**, 2, 75-79.

b. Moore, W.R., Ward, H.R., *J. Org. Chem.*, **1960**, 25, 2073.

c. Moore, W.R., Ward, H.R., Merritt, R.F., *J. Am. Chem. Soc.*, **1961**, 83, 2019-2020.

d. Skattebøl, L., *Acta Chem. Scand.*, **1963**, 17, 1683-1693.

[33] Christl, M., Moigno, D., Peters, E.M., Peters, K., Schnering, H.G.v., *Liebigs Ann./Recueil*, **1997**, 8, 1791-1796.

[34] Baird, M.S., Reese, C.B., *Tetrahedron*, **1976**, 32, 2153-2156.

[35] Kwetkat, K., Riches, B.H., Ropsset, J.M., Brecknell, D.J., Byriel, K., Kennard, C.H.L., Young, D.J., Schneider, U., Mitchell, T.N., Kitching, W., *J. Chem. Soc. Chem. Commun.*, **1996**, 6, 773-774.

[36] Ward, H.R., Karafiath, E., *J. Am. Chem. Soc.*, **1969**, 91, 7475-7480.

[37] Berridge, J.C., Forrester, J., Foulger, B.E., Gilbert, A.J., *J. Chem. Soc. Perkin Trans.1*, **1980**, 2425-2434.

[38] Stierman, T.J., Johnson, R.P., *J. Am. Chem. Soc.*, **1985**, 107, 3971-3980.

[39] Stierman, T.J., Shakespeare, W.C., Johnson, R.P., *J. Org. Chem.*, **1990**, 107, 3971-3980.

[40] a. Ball, W.J. Landor, S.R., *Proc. Chem. Soc., London*, **1961**, 143-144.
b. Ball, W.J. Landor, S.R., *J. Chem. Soc.*, **1962**, 2298-2304.

[41] Wittig, G., Dorsch, H.L., Meske-Schuller, J., *Justus Liebigs Ann. Chem.*, **1968**, 711, 55-64.

[42] Marquis, E.T., Gardner, P.D., *Tetrahedron Lett.*, **1966**, 7, 2793-2798.

[43] Wisser, J.P., Ramakers, J.E., *J. Chem. Soc. Chem. Commun.*, **1972**, 178.

[44] Angus, R.O.Jr., Johnson, R.P., *J. Org. Chem.*, **1984**, 49, 2880-2883.

[45] Kropp, P.J., McNeely, S.A., Davis, R.D., *J. Am. Chem. Soc.*, **1983**, 105, 6907-6915.

[46] Kreuzholz, R., Szeimies, G., *Liebigs Ann./Recueil*, **1997**, 1131-1134.

[47] Price, J.P., Johnson, R.P., *Tetrahedron Lett.*, **1986**, 27, 4679-4682.

[48] Christl, M., Rudolph, M., Peters, E.M., Petrs, K., Schnering, H.G.v., *Angew. Chem. Int. Ed. Engl.*, **1995**, 34, 2730-2732.

[49] Price, J.D., Johnson, R.P., *J. Org. Chem.*, **1991**, 56, 6372-6376.

[50] a. Favorski, A.E., *J. Gen. Chem. USSR (Eng. Trans.)*, **1936**, 6, 720-731.
b. Favorski, A.E., *Bull. Soc. Chim. Fr.*, **1936**, 3, 1727-1732.

[51] Wittig, G., Meske-Schuller, J., *Justus Liebigs Ann. Chem.*, **1968**, 711, 76-81.

[52] Balci, M., Jones, W.M., *J. Am. Chem. Soc.*, **1980**, 102, 7607-7608

[53] Moore, W.R., Ward, H.R., Merritt, R.F., *J. Am. Chem. Soc.*, **1961**, 83, 2019-2020.

[54] Köbrich, G., Goyert, W., *Tetrahedron*, **1968**, 24, 4327-4342.

[55] Backes, J., Brinker, U.H., *Methoden der Organischen Chemie (Houben-Weyl)*, Regitz, M. Ed.; Thieme-Verlag, Stuttgart, Germany, **1989**, Vol.E 19b, pp391-510.

[56] Creary, X., Jiang, Z., Butchko, M., McLean, K., *Tetrahedron Lett.*, **1996**, 37, 579-582.

[57] Warner, P.M., Herold, R.D., Chu, I.S., Lessman, J., *J. Org. Chem.*, **1988**, 53, 942-950.

[58] Taylor, K.G., Hobbs, W.E., Clark, M.S., Chancy, J., *J. Org. Chem.*, **1972**, 37, 2436-2443.

[59] Jelinek-Fink, H., Christl, M., Peters, E.-M., Peters, K., von Schnering, H.G., *Chem. Ber.*, **1991**, 124, 2569-2575.

[60] Yildiz, Y.K., Seçen, H., Krawiec, M., Watson, W.H., Balci, M., *J. Org. Chem.*, **1993**, 58, 5355-5359.

[61] a. Banwell, M.G., Hockless, D.c.R., Walter, J.M., *J. Chem. Soc. Chem. Commun.*, **1996**, 1469-1470.

b. Banwell, M.G., Hockless, D.C.R., Longmore, R.W., Walter, J.M., *Aust. J. Chem.*, **1997**, 50, 457-462.

[62] Chapman, O.L., Abelt, C.J., *J. Org. Chem.*, **1987**, 52, 1218-1221.

[63] Bonvallet, P.A., McMahon, R.J., *J. Am. Chem. Soc.*, **2000**, 122, 9332-9333.

[64] Wittig, G., Fritze, P., *Angew. Chem. Int. Ed. Engl.*, **1966**, 78, 846-905.

[65] Bottini, A.T., Corson, F.P., Fitzgerald, R., Frost, K.A., *Tetrahedron*, **1972**, 28, 4883-4904.

[66] Bottini, A.T., Hilton, L.L., Plott, J., *Tetrahedron*, **1975**, 31, 1997-2001.

[67] Wentrup, C., Gross, G., Maquestiau, A., Flammang, R., *Angew. Chem. Int. Ed. Engl.*, **1983**, 22, 542-543.

[68] Runge, A., Sander, W., *Tetrahedron Lett.*, **1986**, 27, 5835-5838.

[69] Moore, W.R., Moser, W.R., *J. Org. Chem.*, **1970**, 35, 908-912.

[70] Moore, W.R., Moser, W.R., *J. Am. Chem. Soc.*, **1970**, 92, 5469-5474.

[71] Greenberg, A., Liebman, J.L., *Strained Organic Molecules*, Academic Press, New York, **1978**, p.126.

[72] Lam, B., Johnson, R.P., *J. Am. Chem. Soc.*, **1983**, 105, 7479-7483.

[73] Tolbert, L.M., Islam, Md.N., Johnson, R.P., Loiselle, P.M., Shakespeare, W.C., *J. Am. Chem. Soc.*, **1990**, 112, 6416-6417.

[74] Nendel, M., Tolbert, L.M., Herring, L.E., Islam, Md.N., Houk, K.N., *J. Org. Chem.*, **1999**, 64, 976-983.

[75] Miller, B., Shi, X., *J. Am. Chem. Soc.*, **1987**, 109, 578-579.

[76] Christl, M., Braun, M., Müller, G., *Angew. Chem. Int. Ed. Engl.*, **1992**, 31, 473-476.

[77] Burrell, R.C., Daoust, K.J., Bradley, A.Z., DiRico, K.J., Johnson, R.P., *J. Am. Chem. Soc.*, **1996**, 118, 4218-4219.

[78] Christl, M., Groetsch, S., *Eur. J. Org. Chem.*, **2000**, 1871-1874.

[79] Groetsch, S., Spuziak, J., Christl, M., *Tetrahedron*, **2000**, 56, 4163-4171.

[80] Zertuche, M.F., Lamoneda, R.H., Solis, A.R., *J. Org. Chem.*, **2000**, 65, 5207-5211.

[81] Rodriguez, D., Navarro-Vazquez, A., Castedo, L., Dominguez, D., Saa, C., *J. Org. Chem.*, **2003**, 68, 1938-1946.

[82] Schreck, M., Christl, M., *Angew. Chem. Int. Ed. Engl.*, **1987**, 26, 690-692.

[83] Christl, M., Braun, M., *Chem. Ber.*, **1989**, 122, 1939-1946.

[84] Christl, M., Braun, M., In *Strain and Its Implication in Organic Chemistry*, Meijere, A., Blechert, S., Ed., Kluwer Academic Press, Dordrecht, **1989**, p.121.

[85] Harnos, S., Tivakornpannarai, S., Waali, E.E., *Tetrahedron Lett.*, **1986**, 27, 3701-3704.

[86] Ruzziconi, R., Naruse, Y., Schlosser, M., *Tetrahedron*, **1991**, 47, 4603-4610.

[87] Jamart-Gregoire, B., Grand, V., Lanelli, S., Nardelli, M., Caubere, P., *Tetrahedron Lett.*, **1990**, 31, 7603-7606.

[88] Jamart-Gregoire, B., Mercier-Girardo, S., Grand, V., Lanelli, S., Nardelli, M., Caubere, P., *Tetrahedron Lett.*, **1995**, 36, 1973-1976.

[89] Christl, M., Drinkuth, S., *Eur. J. Org. Chem.*, **1998**, 237-241.

[90] Khasanova, T., Sheridan, R.S., *J. Am. Chem. Soc.*, **2000**, 122, 8585-8586.

[91] Nikitina, A., Sheridan, R.S., *J. Am. Chem. Soc.*, **2002**, 124, 7670-7671.

[92] Christl, M., Braun, M., Wolz, E., Wagner, W., *Chem. Ber.*, **1994**, 127, 1137-1142.

[93] Drinkuth, S., Groetsch, S., Peters, E.M., Peters, K., Christl, M., *Eur. J. Org. Chem.*, **2001**, 2665-2670.

[94] Schöneboom, J.C., Groetsch, S., Christl, M., Engels, M., *Chem. Eur. J.*, **2003**, 9, 4641-4649.

[95] Emanuel, C.J., Shevlin, P.B., *J. Am. Chem. Soc.*, **1994**, 116, 5991-5992.

[96] Pan, W., Shevlin, P.B., *J. Am. Chem. Soc.*, **1997**, 119, 5091-5094.

[97] Pan, W., Balci, M., Shevlin, P.B., *J. Am. Chem. Soc.*, **1997**, 119, 5035-5036.

[98] Elliott, R.L., Nicholson, N.H., Peaker, F.E., Takle, A.K., Tyler, J.W., White, J., *J. Org. Chem.*, **1994**, 59, 1606-1607.

[99] Elliott, R.L., Nicholson, N.H., Richardson, C.M., Takle, A.K., White, J., Pearson, M.J., *J. Org. Chem.*, **1997**, 62, 4998-5016.

[100] Hofmann, M.A., Bergstraber, U., Reib, G.J., Nyulaszi, L., Regitz, M., ., *Angew. Chem. Int. Ed. Engl.*, **2000**, 39, 1261-1263.

[101] Wittig, G., Heyn, J., *Justus Liebigs Ann. Chem.*, **1972**, 756, 1-13.

[102] Algi, F., Özen, R., Balci, M., *Tetrahedron Lett.*, **2002**, 43, 3129-3131.

[103] Ceylan, M., Yalçin, S., Seçen, H., Sütbeyaz, Y., Balci, M., *J. Chem. Res. S.*, **2003**, 21-23.

[104] Bergman, R.G., Rajadbyaksha, V.J., *J. Am. Chem. Soc.*, **1970**, 92, 2163-2164.

[105] Balci, M., Jones, W.M., *J. Am. Chem. Soc.*, **1981**, 103, 2874-2876.

[106] Balci, M., Harmandar, M., *Tetrahedron Lett.*, **1984**, 25, 237-240.

[107] Taskesenligil, Y., Kashyap, R.P., Watson, W.H., Balci, M., *J. Org. Chem.*, **1993**, 58, 3216-3218.

[108] Tümer, F., Taskesenligil, Y., Balci, M., *J. Org. Chem.*, **2001**, 66, 3806-3810.

[109] Tümer, F., Taskesenligil, Y., Dastan, A., Balci, M., *Aust. J. Chem.*, **1996**, 49, 599-603.

[110] Taskesenligil, Y., Tümer, F., Kazaz, C., Balci, M., *Turk. J. Chem.*, **1999**, 23, 115-122.

[111] Tümer, F., *Ph.D. Thesis*, Atatürk University, Erzurum, **2000**.

[112] Tümer, F., Taskesenligil, Y., Balci, M., *Turk. J. Chem.*, **1995**, 19, 305-312.

[113] Özen, R., Balci, M., *Tetrahedron*, **2002**, 58, 3079-3083.

[114] Mohanakrishnan, P., Tayal, S.R., Vaidyanathhaswamy, R., Devaprabhakara, D., *Tetrahedron Lett.*, **1972**, 2871-2874.

[115] a. Bottini, A.T., Hilton, L.L., *Tetrahedron*, **1975**, 31, 2003-2006.
b. Bottini, A.T., Anderson, B., *Tetrahedron Lett.*, **1973**, 14, 3321-3324.

[116] Christl, M., Lang, R., Lechner, M., *Justus Liebigs Ann. Chem.*, **1980**, 980.

[117] Ogawa, K., Okazaki, T., Kinoshita, T., *J. Org. Chem.*, **2003**, 68, 1579-1581.

[118] Berson, J.A., *Carbonium Rearrangements in Bridged Bicyclic Systems, In Molecular Rearrangements*, Mayo, De P. (Ed.), Interscience Inc., New York, **1964**, Vol. 1.

[119] a. Wagner, G., Brickner, W., *Ber.*, **1899**, 32, 2302.
b. Meerwein, H., Emster, Van K., Joussen, J., *Ber.*, **1922**, 55, 2500-2528.

[120] Simonsen, J., Owen, L.N., *The Terpenes; The Dicyclic Terpenes and Their Derivatives*, Cambridge Univ. Press, London, **1957**, Vol. 2, 168-169.

[121] Carman, R.M., Walker, G.J., *Aust. J. Chem.*, **1977**, 30, 1393-1396.

[122] Dastan, A., Demir, Ü., Balci, M., *J. Org. Chem.*, **1994**, 59, 6534-6538.

[123] Miller, B., *Advanced Organic Chemistry; Reactions and Mechanisms*, Second Edition, Pearson Education Inc., New Jersey, **2004**.

[124] Regitz, M. (Ed.), *Methoden der Organischen Chemie (Houben Weyl)*, Fourth Edition, Thieme Verlag, Stuttgart, **1989**, Vol.E 19a.

[125] Nair, V., *Comprehensive Organic Chemistry*, Trost, B.M. (Ed.), Pergamon Press, New York, **1991**, Vol. 4, 999-1006.

[126] a. Dilling, W.L., Edamura, F.Y., *J. Org. Chem.*, **1967**, 32, 3492-3499.
b. Koebrich, G., Fischer, R.H., *Tetrahedron*, **1968**, 24, 4343-4346.

[127] Doering, W.von E., Hoffmann, A.K., *J. Am. Chem. Soc.*, **1954**, 76, 6162.

[128] Fedorynski, M., *Chem. Rev*., **2003**, 103, 1099-1132.

[129] Vereshchagin, A.N., Vul'fson, S.G., Gubkina, N.I., Arbuzov, B.A., *Seriya Khimicheskaya*, **1970**, 11, 2467-2473.

[130] Graefe, J., Lam, Q.T., Muehlstaedt, M., *Zeitschrift fuer Chemie*, **1971**, 11, 252-253.

[131] Hatem, J., Waegell, B., *Tetrahedron Lett.*, **1971**, 23, 2069-2072.

[132] Hatem, J., Waegell, B., *Tetrahedron*, **1990**, 46, 2789-2806.

[133] [a]enol, Z., *M.Sc. Thesis*, Trakya University, Edirne, **2000**.

[134] a. Skell, P.S., Sandler, S.R., *J. Am. Chem. Soc.*, **1958**, 80, 2024-2025.
b. Sandler, S.R., *J. Org. Chem.*, **1967**, 32, 3876-3881.

[135] Sonnenberg, J., Winstein, S., *J. Org. Chem.*, **1962**, 27, 748-751.

[136] Ceylan, M., *M.Sc. Thesis*, Atatürk University, Erzurum, **1989**.

[137] Baird, M.S., Sadler, P., Hatem, J., Zahra, J.-P., Waegell, B., *J. Chem. Soc. Chem. Commun.*, **1979**, 452-453.

[138] Paquette, L.A., Taylor, R.T., *J. Am. Chem. Soc.*, **1977**, 99, 5708-5715.

[139] Frisch, M. J., Trucks, G. W., Schlegel, H. B., Scuseria, G. E., Robb, M. A., Cheeseman, J. R., Zakrzewski, V. G., Montgomery, Jr., J. A., Stratmann, R. E., Burant, J. C., Dapprich, S., Millam, J. M., Daniels, A.D., Kudin, K. N., Strain, M. C., Farkas, O., Tomasi, J., Barone, V., Cossi, M., Cammi, R., Mennucci, B., Pomelli, C., Adamo, C., Clifford, S., Ochterski, J., Petersson, G. A., Ayala, P. Y., Cui, Q., Morokuma, K., Malick, D. K., Rabuck, A. D., Raghavachari, K., Foresman, J. B., Cioslowski, J., Ortiz, J. V., Baboul, A. G., Stefanov, B. B., Liu, G., Liashenko, A., Piskorz, P., Komaromi, I., Gomperts, R., Martin, R. L., Fox, D. J., Keith, T., Al-Laham, M. A., Peng, C. Y., Nanayakkara, A., Challacombe, M., Gill, P. M. W., Johnson, B., Chen, W., Wong, M. W., Andres, J. L., Gonzalez, C., Head-Gordon, M., Replogle E. S., Pople, J. A. Gaussian 98W, Revision A.11.4, Gaussian, Inc., Pittsburgh PA, **2002**.

[140] Parr, R.G., Yang, W., *Density Functional Theory of Atoms and Molecules*, Oxford Univ. Press, Oxford, **1989**.

[141] Becke, A.D., *J. Chem. Phys.*, **1993**, 98, 5648-5652.

[142] Lee, C., Yang, W., Parr, R.G., *Phys. Rev. B.*, **1988**, 37, 785-789.

[143] Bettinger, H.F., Schreiner, P.R., Schleyer, P.v.R., Schaefer, H.F.III., *J. Phys. Chem.*, **1996**, 100, 16147-16154.

[144] a. Schaftenaar, G., Noordik, J.H., *J. Comp. -Aided Mol. Design.*, **2000**, 14, 123-124.

b. http://www.cmbi.kun.nl/~schaft/molden

[145] a. Bruno, J., Cole, J.C., Edgington, P.R., Kessler, M.K., Macrae, C.F., Cabe, Mc.P., Pearson, J., Taylor, R., *Acta Crystallogr. B.*, **2002**, 58, 289-397.

b. Taylor, R., Macrae, C.F., *Acta Crystallogr. B.*, **2001**, 57, 815-817.

c. http://www.ccdc.cam.ac.uk/products/csd-system/mercury

[146] Mich, T.F., Nienhouse, E.J., Farina, T.E., Tufariello, J.I., *J. Chem. Educ.*, **1968**, 45, 272

[147] Dastan, A., *PhD Thesis*, Atatürk University, Erzurum, **1990**.

[148] Wilt, J.W., Gutman, G., Ranus, W.J., Zigman, A.R., *J. Org. Chem.*, **1967**, 32, 893-901.

[149] Bordon, W.T., *Chem. Rev.*, **1989**, 89, 1095-1109.

[150] a. Paquette, L.,*in Stereochemistry and Reactivity of Systems Containing p-Electrons*, Watson, W.H.(Ed.), Verlag Chemie International, Florida, **1983**, 41-73.

b. Barlett, P.D., Blakeney, A.J., Combs, G.L., Galloy, J., Roof, A.A.M., Subramanyam, R., Watson, W.H., Winter, W.J., Wu, C., *in Stereochemistry and Reactivity of Systems Containing p-Electrons*, Watson, W.H.(Ed.), Verlag Chemie International, Florida, **1983**, 75-104.

c. Gleiter, R., Böhm, M.C., *in Stereochemistry and Reactivity of Systems Containing p-Electrons*, Watson, W.H.(Ed.), Verlag Chemie International, Florida, **1983**, 105-146.

[151] Houk, K.N., *in Stereochemistry and Reactivity of Systems Containing p-Electrons*, Watson, W.H.(Ed.), Verlag Chemie International, Florida, **1983**, 1-40.

[152] a. Can, H., Zahn, D., Balci, M., Brickmann, J., *Eur. J. Org. Chem.*, **2003**, 1111-1117.

b. Menzek, A., *PhD Thesis*, Atatürk University, Erzurum, **1991**.

[153] Rondon, N.G., Paddon-Row, M.N., Caramella, P., Mareda, J., Mueller, P.H., Houk, K.N., *J. Am. Chem. Soc.*, **1982**, 104, 4974-4976.

[154] a. Jefford, C.W., Mahajan, S., Waslyn, J., Waegell, B., *J. Am. Chem. Soc.*, **1965**, 87, 2183-2190.

b. Moore, W.R., Moser, W.R., LaPrade, J.E., *J. Org. Chem.*, **1963**, 28, 2200-2205.

c. Tanida, H., Tori, K., Kitahonoki, K., *J. Am. Chem. Soc.*, **1967**, 89, 3212-3224.

d. Sustmann, R., Gellert, R.W., *Chem. Ber.*, **1978**, 111, 42-55.

[155] Kitahonoki, K., Takano, Y., Matsuura, A., Kotera, K., *Tetrahedron*, **1969**, 25, 335-353.

[156] Woodward, R.B., Hoffmann, R., *The Conservation of Orbital Symmetry*, Verlag-Chemie, Academic Press, Weinheim, **1970**, 46-48.

[157] Wege, D., *J. Org. Chem.*, **1990**, 55, 1667-1670.

[158] Makosza, M., Wawrzyniewicz, M., *Tetrahedron Lett.*, **1969**, 10, 4659-4662.

[159] a. Wilt, J.W., Chenier, P.J., *J. Am. Chem. Soc.*, **1968**, 90, 7366-7367.
b. Wilt, J.W., Chenier, P.J., *J. Org. Chem.*, **1970**, 35, 1562-1570.
c. Wilt, J.W., Chenier, P.J., *J. Org. Chem.*,**1970**, 35, 1571-1576.

[160] a. Cristol, S.J., Nachtigall, G.W., *J. Am. Chem. Soc.*, **1968**, 90, 7132.
b. Cristol, S.J., Nachtigall, G.W., *J. Am. Chem. Soc.*, **1968**, 90, 7133-7134.

[161] a. Müller, C., Stier, F., Weyerstahl, P., *Chem. Ber.*, **1977**, 110, 124-137.
b. Reinhard, D., Weyerstahl, P., *Chem. Ber.*, **1977**, 110, 138-145.

[162] Molchanov, A.P., Kostikov, R.R., *Zh. Org. Khim*., **2001**, 37, 784-786.

[163] Seyferth, D., Hopper, S.P., *J. Organomet. Chem.*, **1973**, 51, 77-87.

[164] Jefford, C.W., Hill, D.T., *Tetrahedron Lett.*, **1969**, 1957-1960.

[165] Furniss, B.S., Hannaford, A.C., Smith, G.S.W., Tatchell, A.R., *Vogel's Textbook of Practical Organic Chemistry*, Fifth edition, John&Wiley Inc., **1991-1994**.

[166] Balci, M., *Nükleer Manyetik Resonans Spektroskopisi*, METU Press, Ankara, **2000**.

[167] Schlosser, M., Heinz, G., *Chem. Ber.*, **1971**, 104, 1934-1941.

APPENDIX A

NMR, MASS AND IR SPECTRUMS OF THE STUDIED MOLECULES

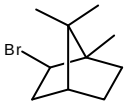

378

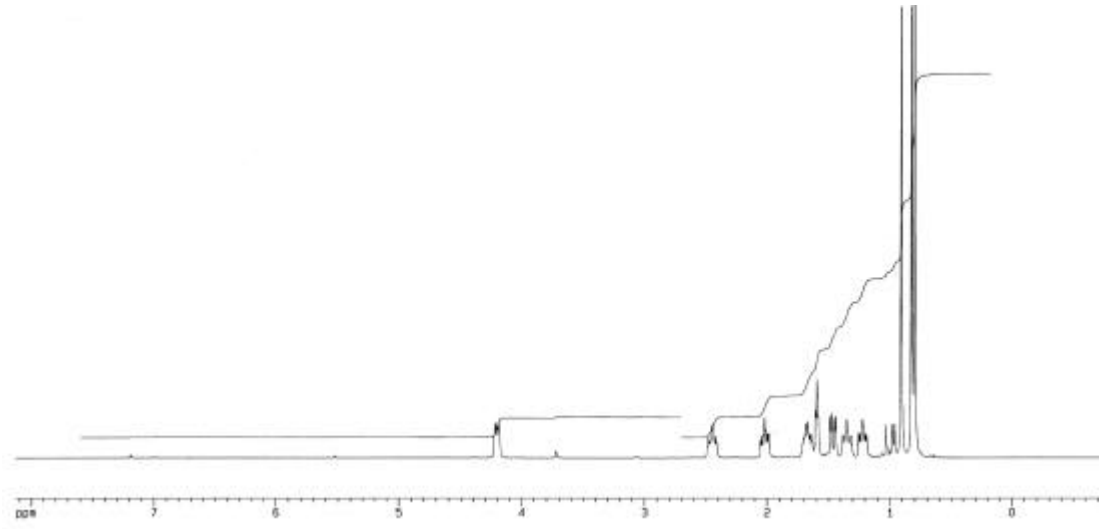

Figure A.1: ^{1}H-NMR spectrum of **378**

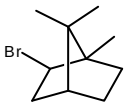

378

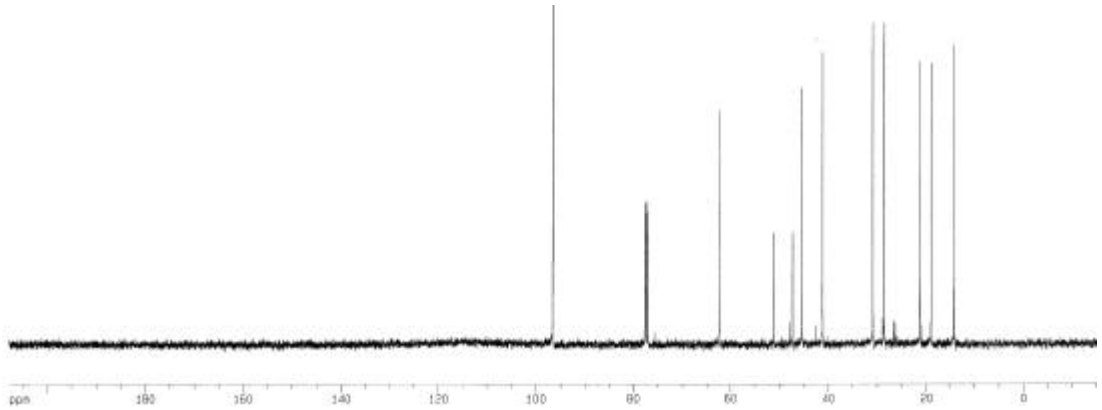

Figure A.2: ^{13}C-NMR spectrum of **378**

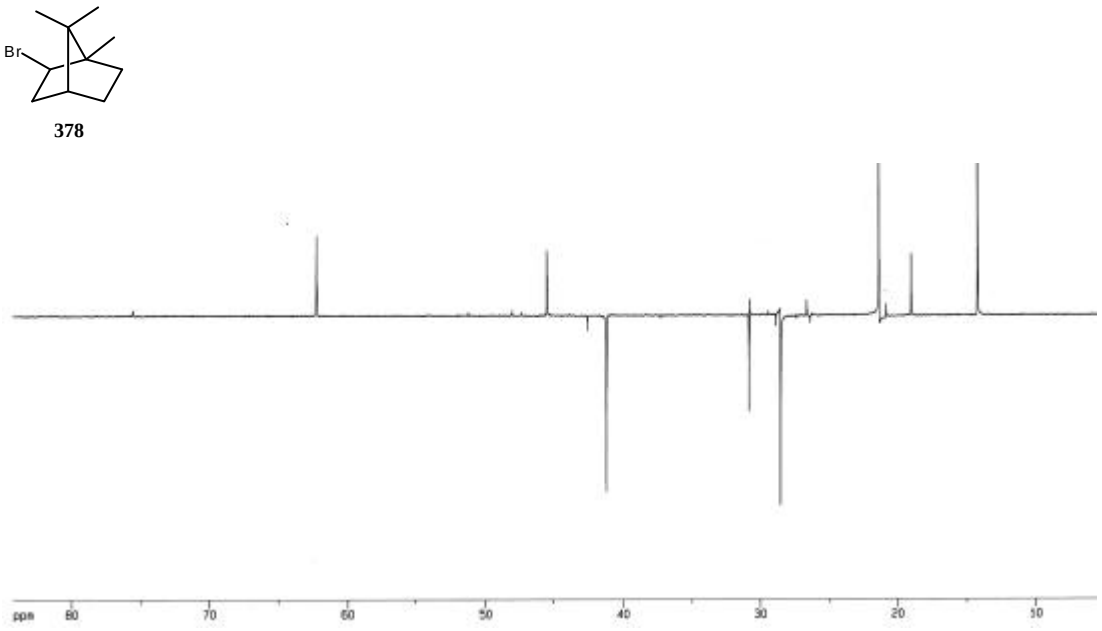

378

Figure A.3: DEPT-135 spectrum of **378**

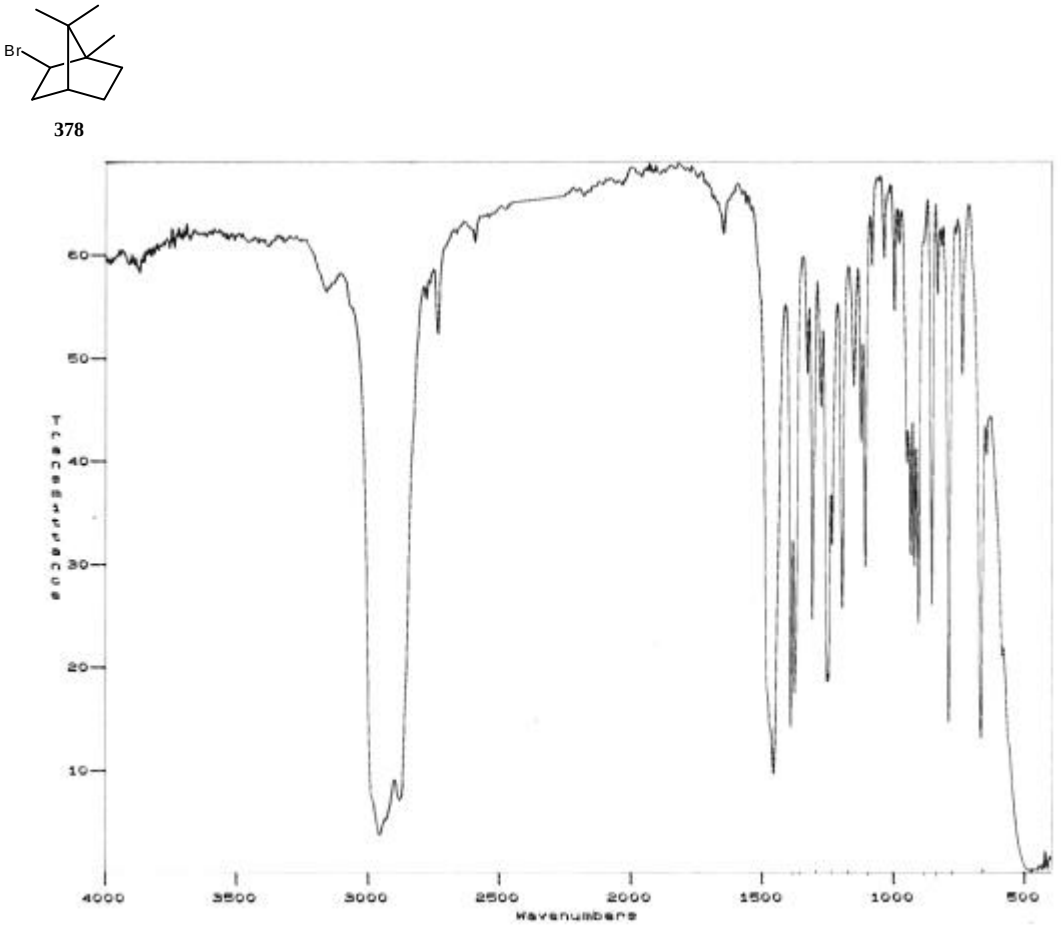

378

Figure A.4: IR-spectrum of **378**

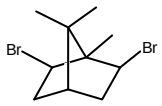

379

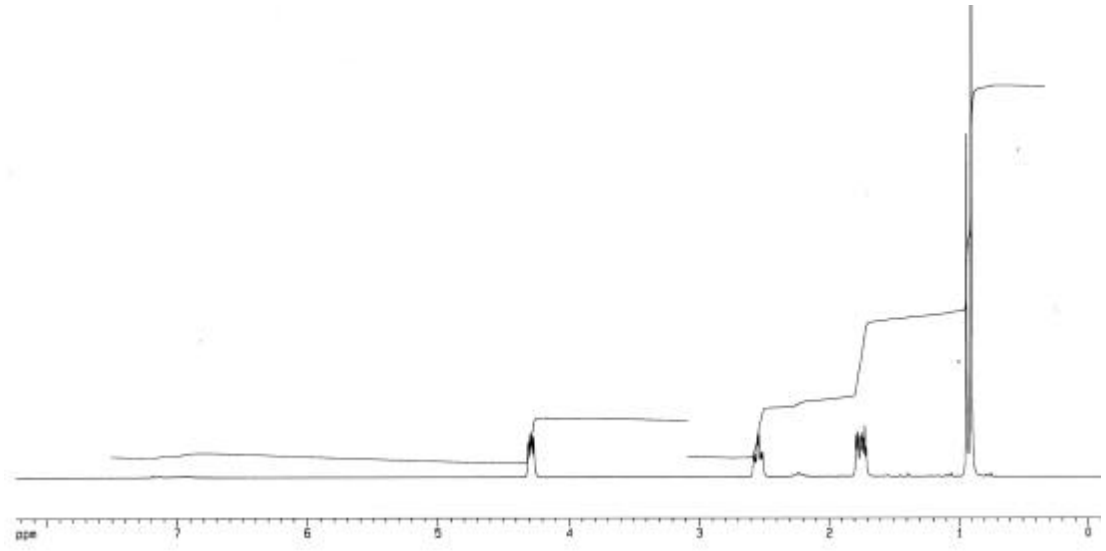

Figure A.5: ^{1}H-NMR spectrum of **379**

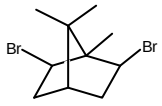

379

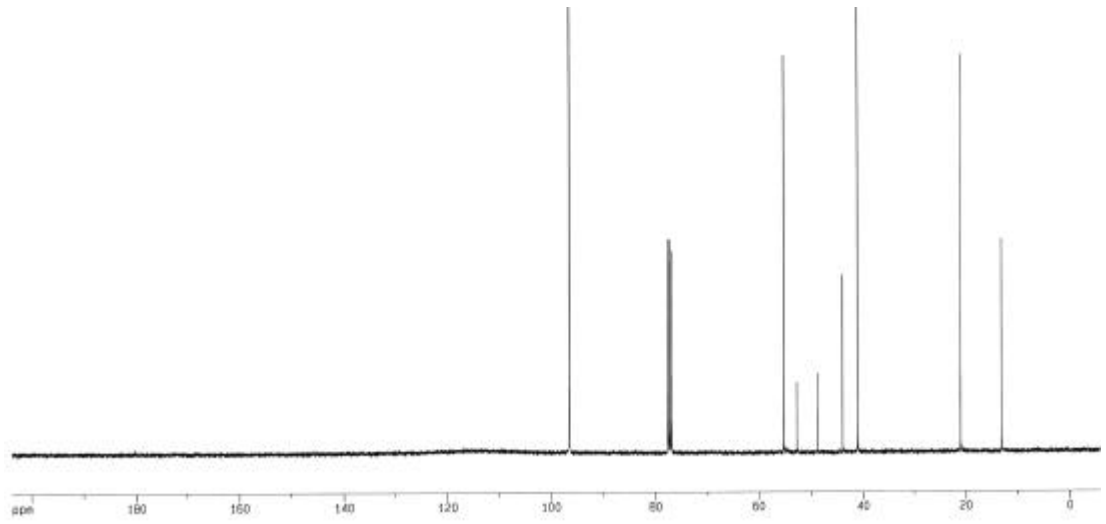

Figure A.6: ^{13}C-NMR spectrum of **379**

379

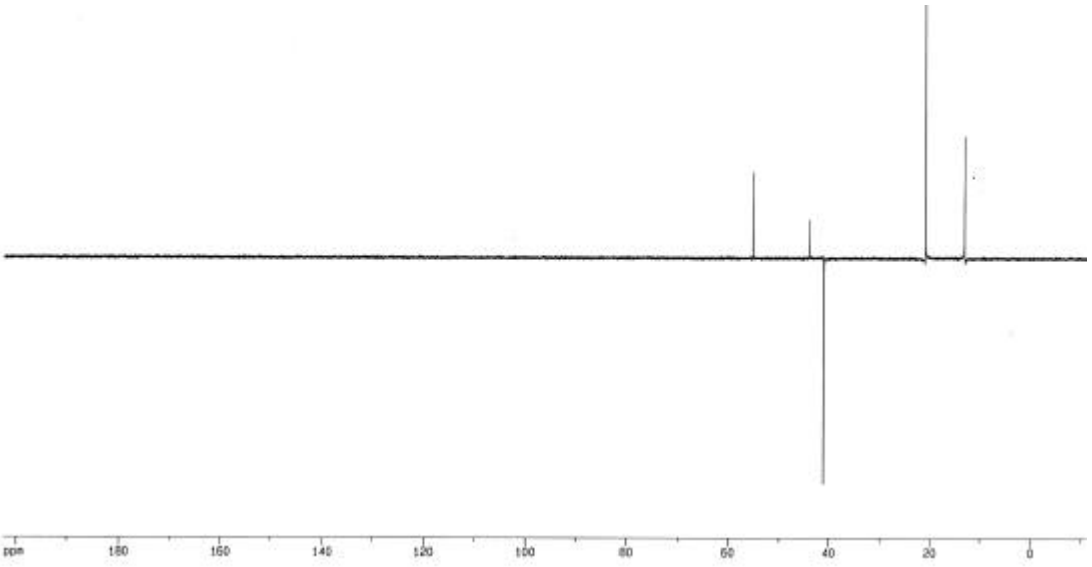

Figure A.7: DEPT-135 spectrum of **379**

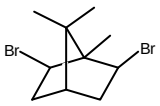

379

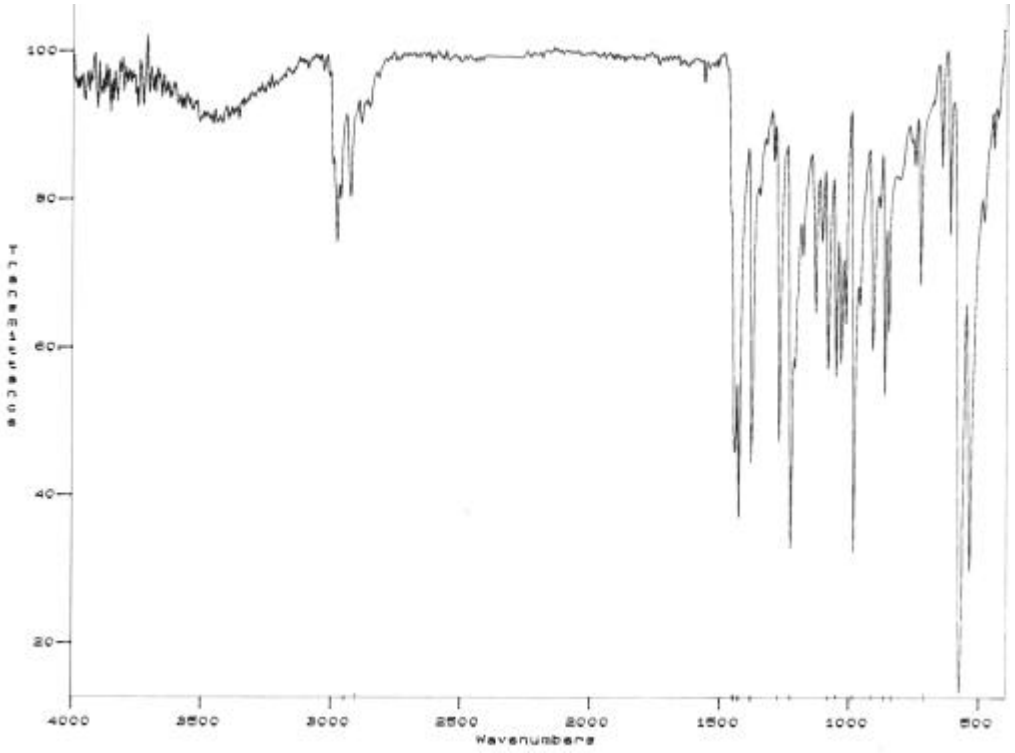

Figure A.8: IR-spectrum of **379**

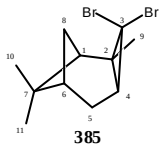

385

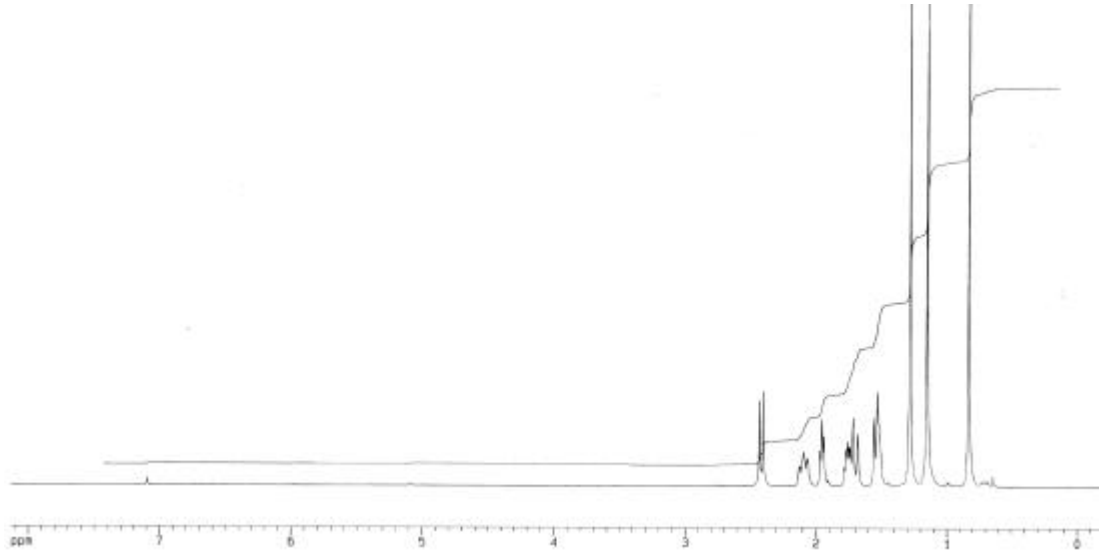

Figure A.9: ^{1}H-NMR spectrum of **385**

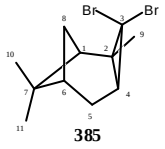

385

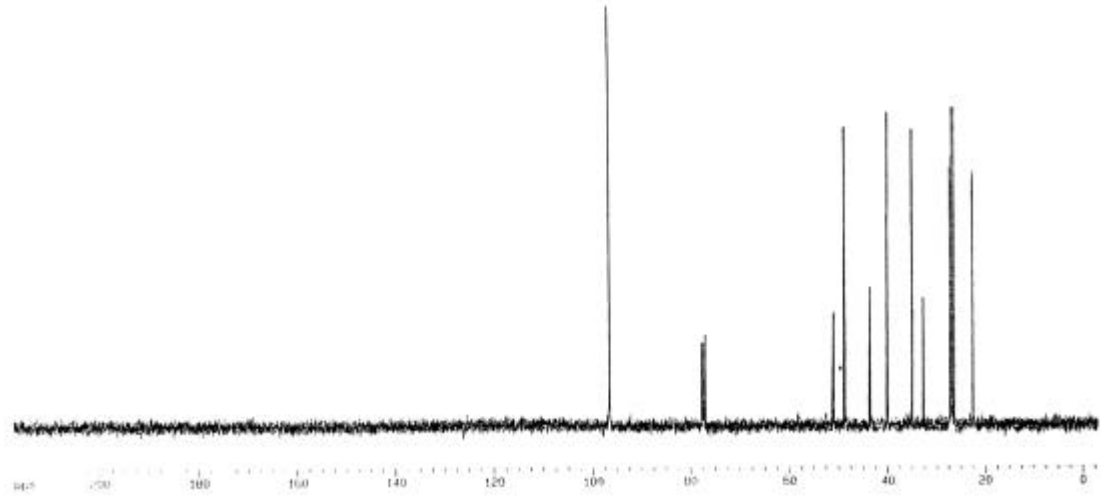

Figure A.10: ^{13}C-NMR spectrum of **385**

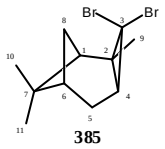

385

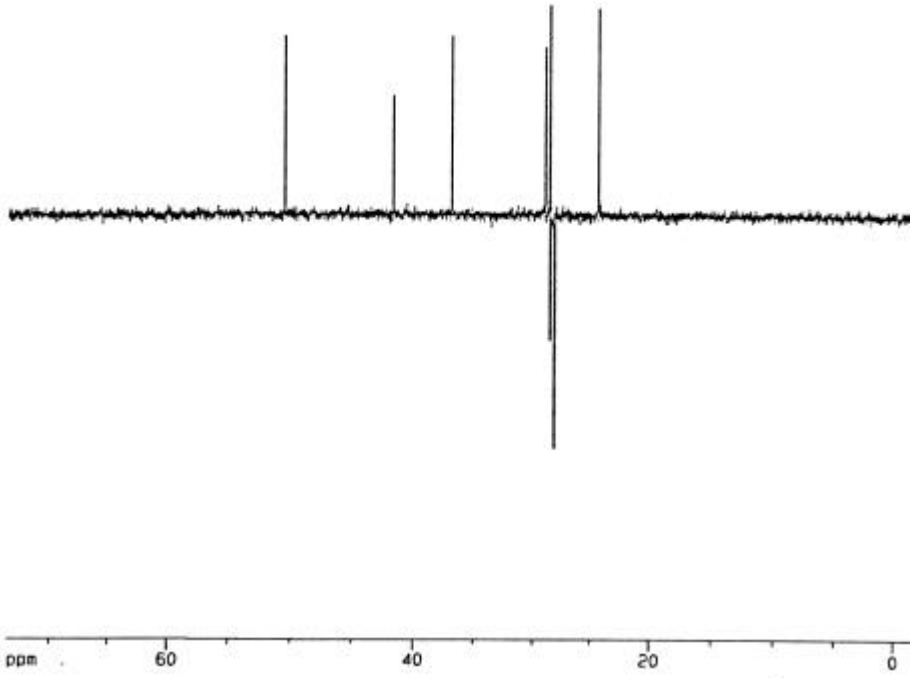

Figure A.11: DEPT-135 spectrum of **385**

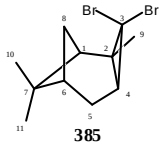

385

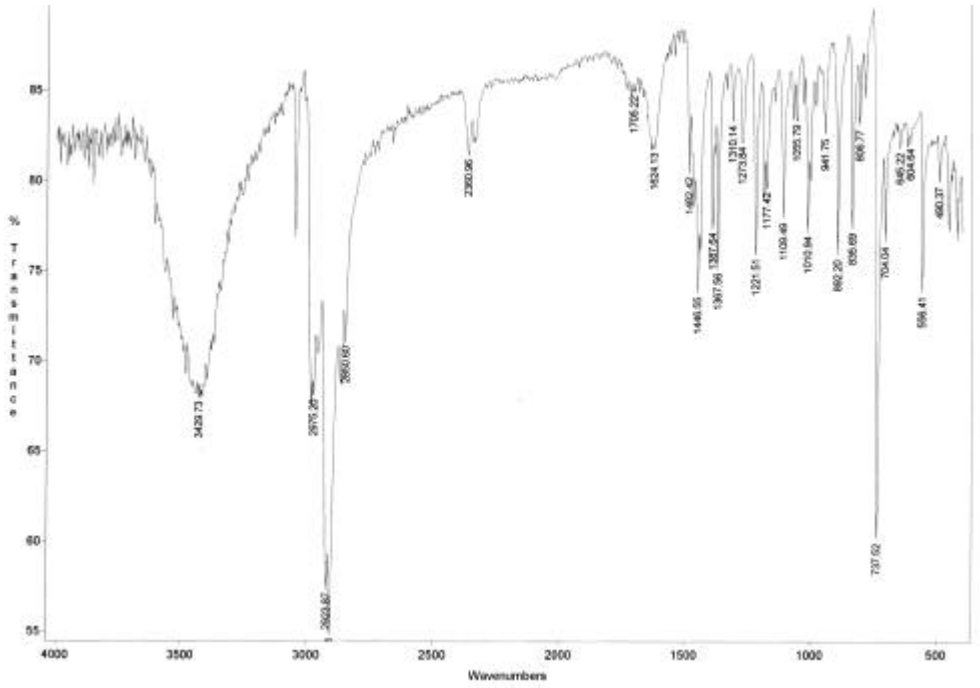

Figure A.12: IR-spectrum of **385**

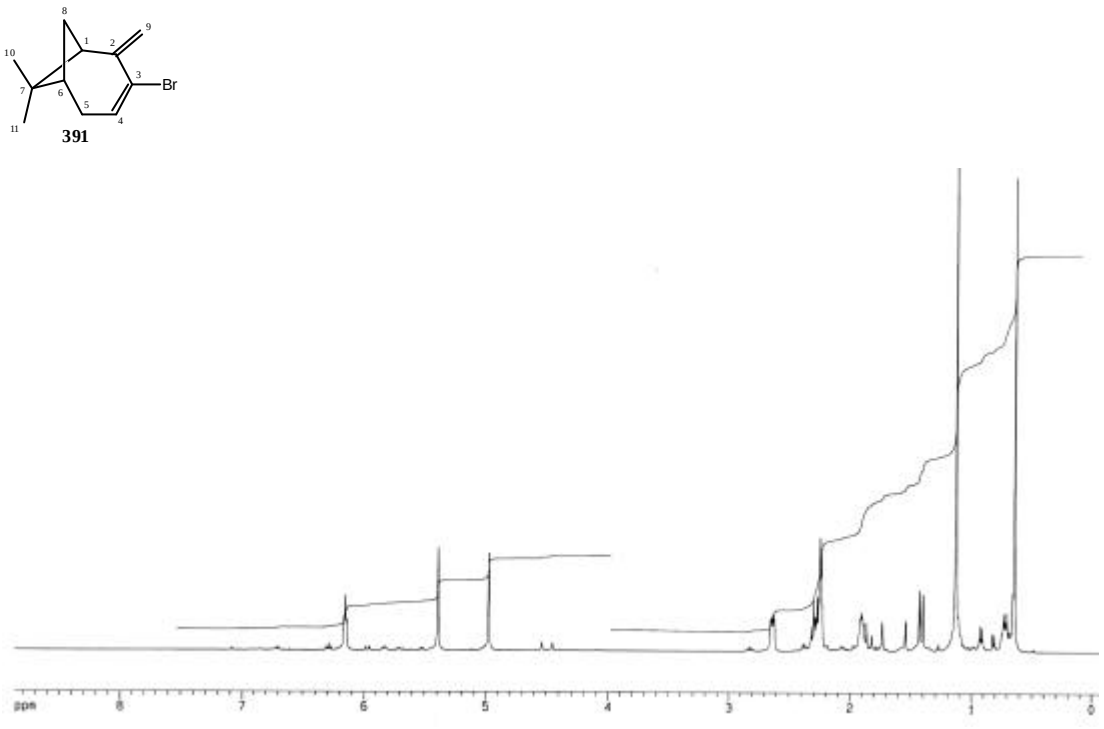

Figure A.13: ^{1}H-NMR spectrum of **391**

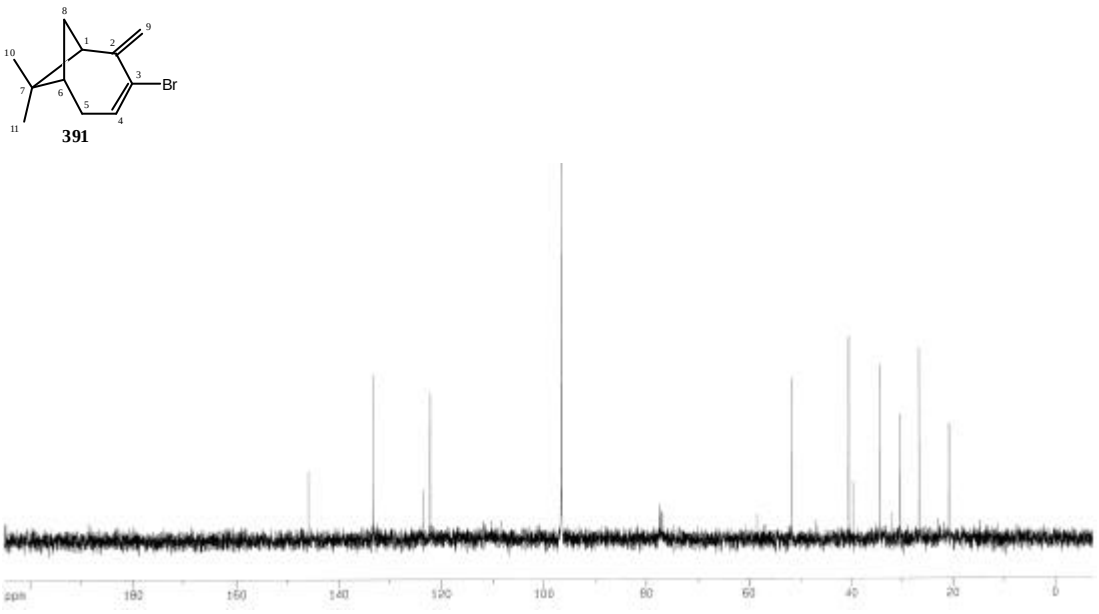

Figure A.14: ^{13}C-NMR spectrum of **391**

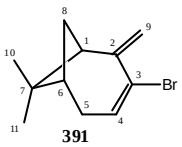

391

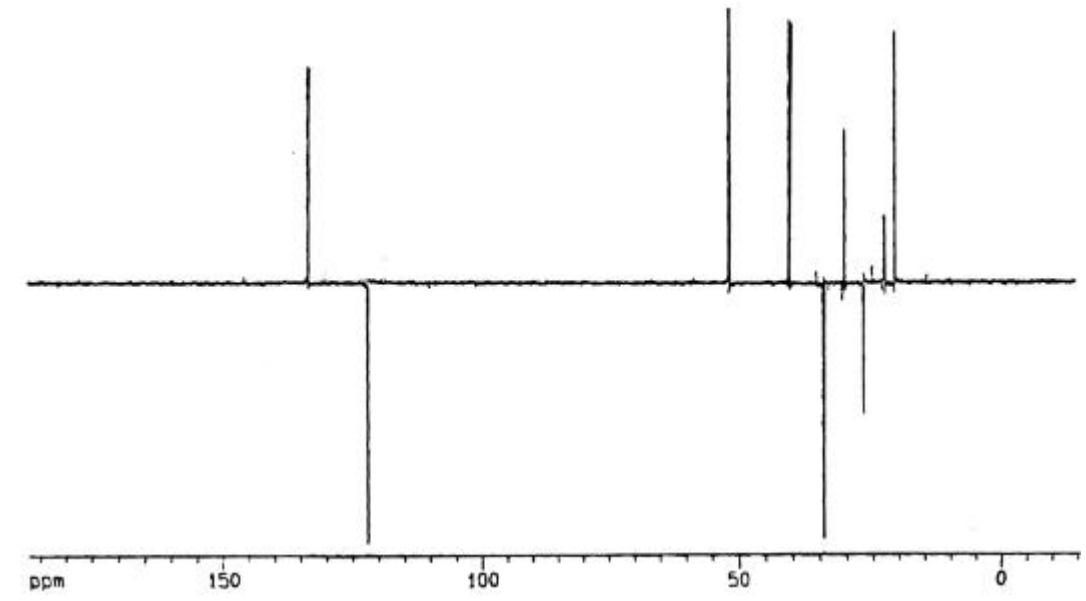

Figure A.15: DEPT-135 spectrum of **391**

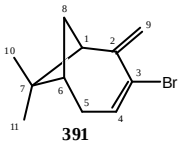

391

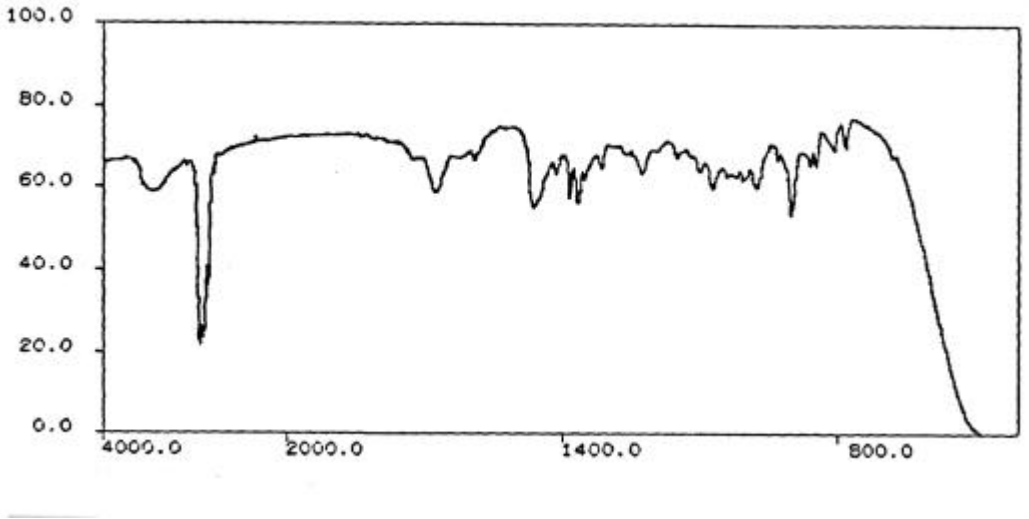

Figure A.16: IR-spectrum of **391**

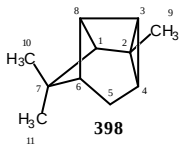

398

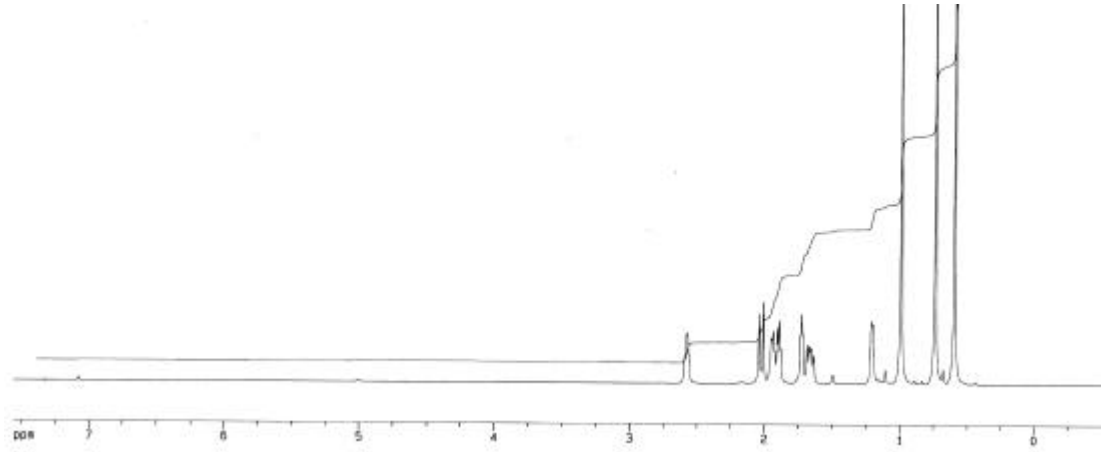

Figure A.17: ^{1}H-NMR spectrum of **398**

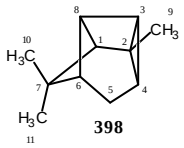

398

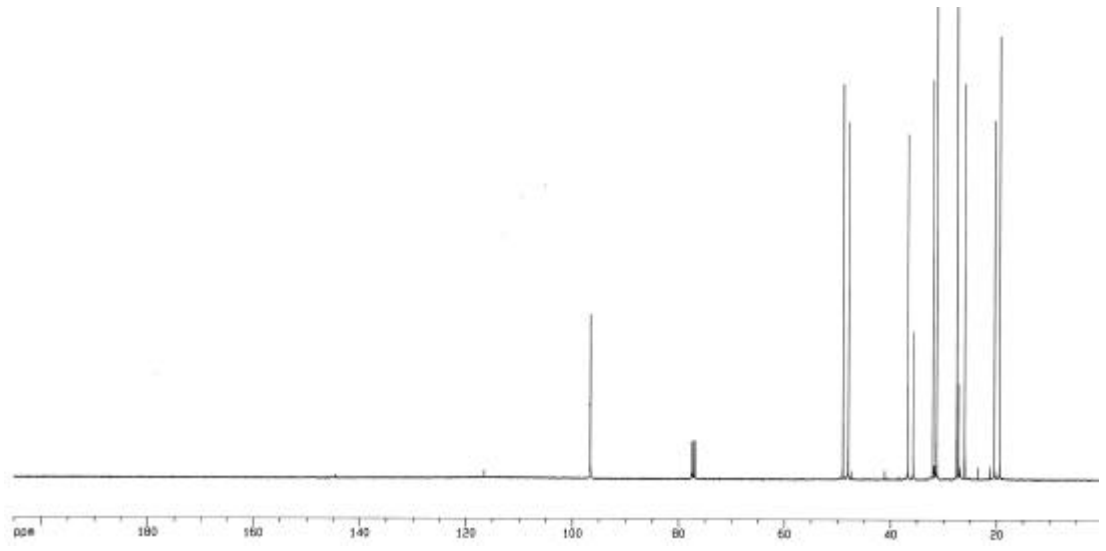

Figure A.18: ^{13}C-NMR spectrum of **398**

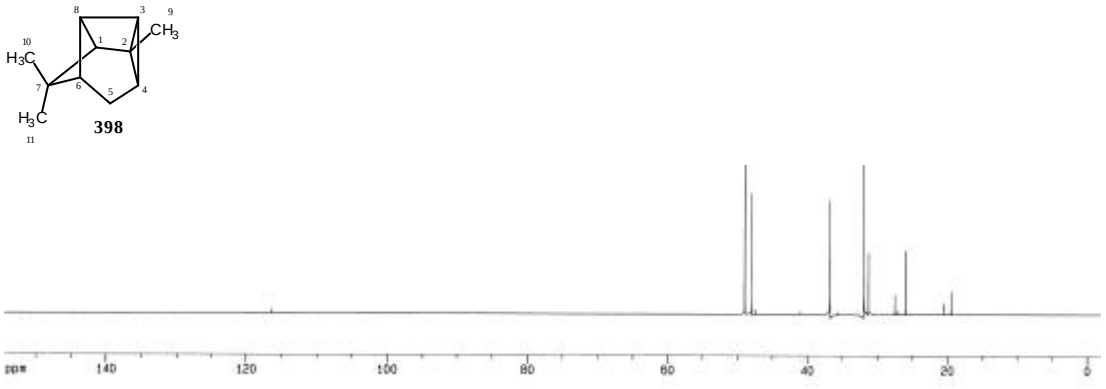

Figure A.19: DEPT-90 spectrum of **398**

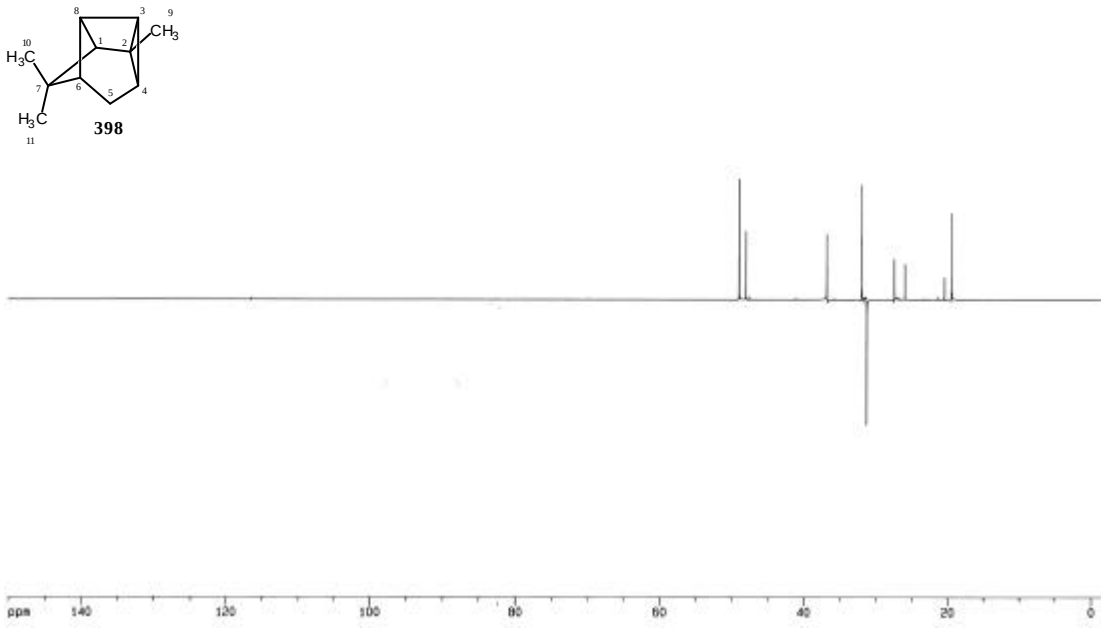

Figure A.20: DEPT-135 spectrum of **398**

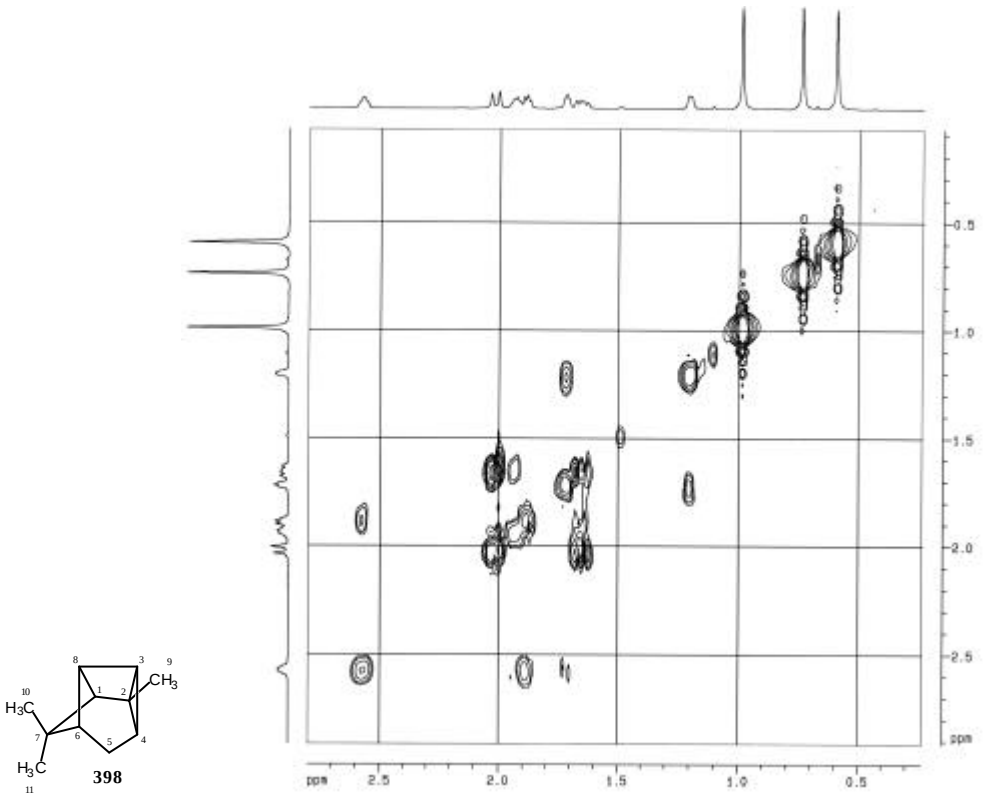

Figure A.21: COSY spectrum of **398**

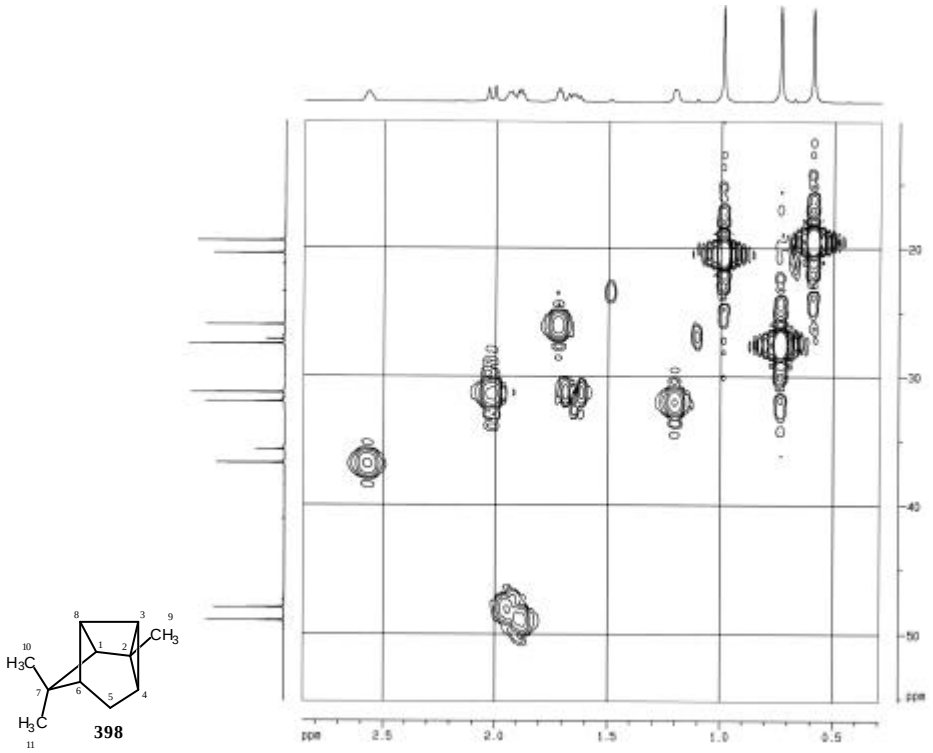

Figure A.22: HMQC spectrum of **398**

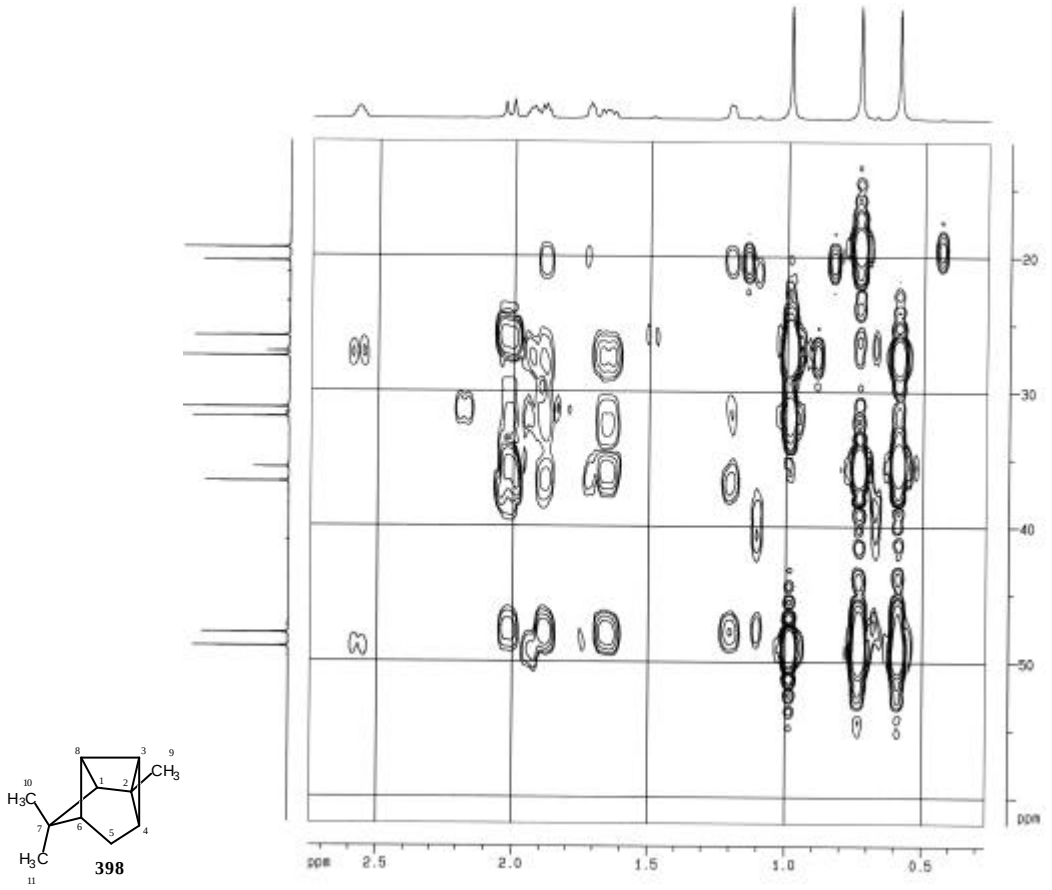

Figure A.23: HMBC spectrum of **398**

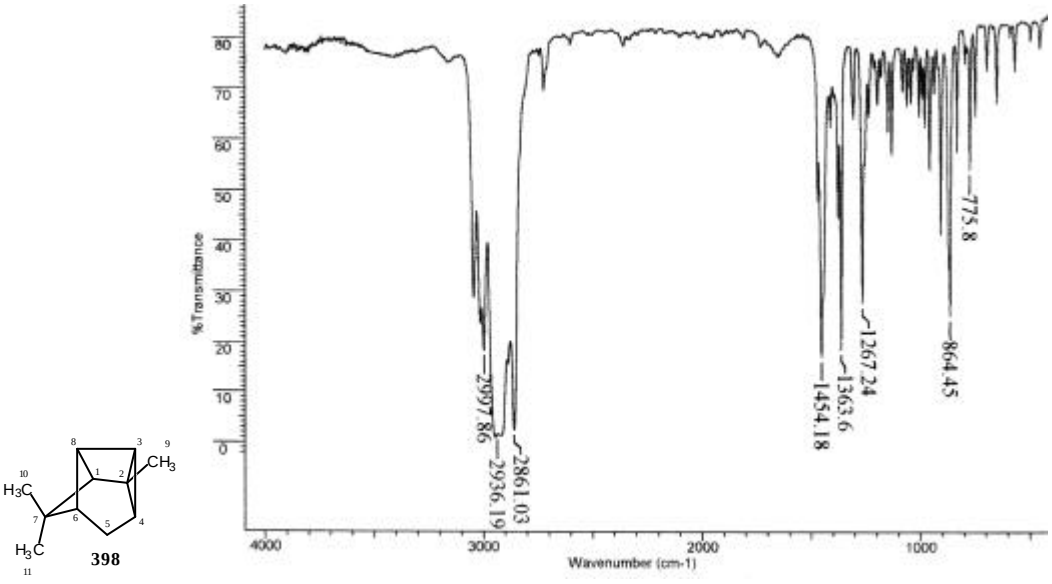

Figure A.24: IR-spectrum of **398**

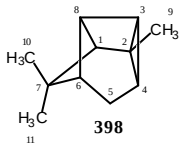

398

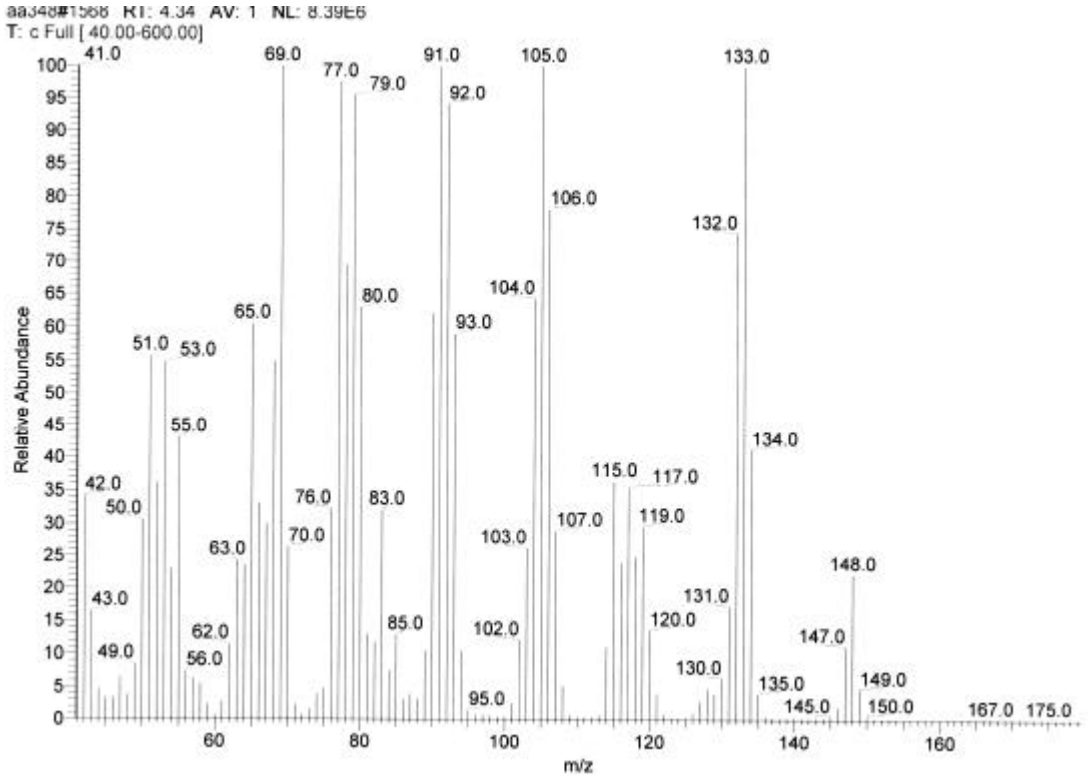

Figure A.25: GC/MS spectrum of **398**

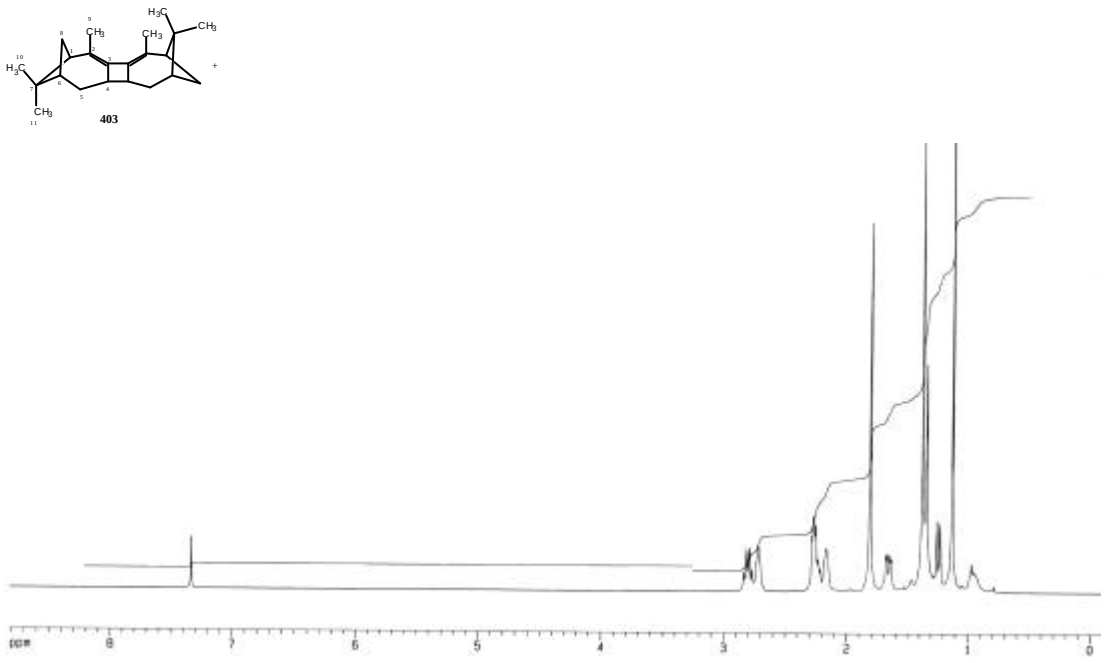

Figure A.26: ^{1}H-NMR spectrum of **403**

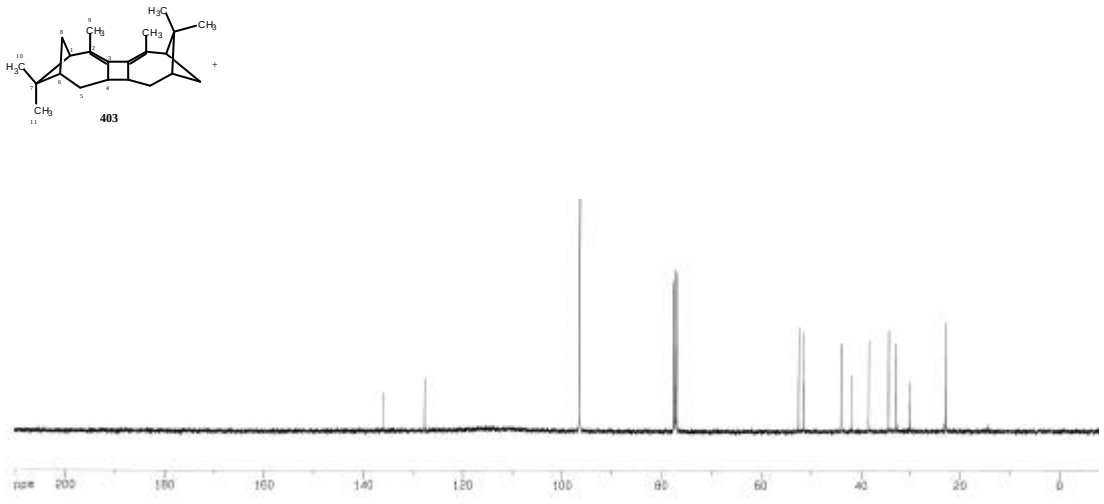

Figure A.27: ^{13}C-NMR spectrum of **403**

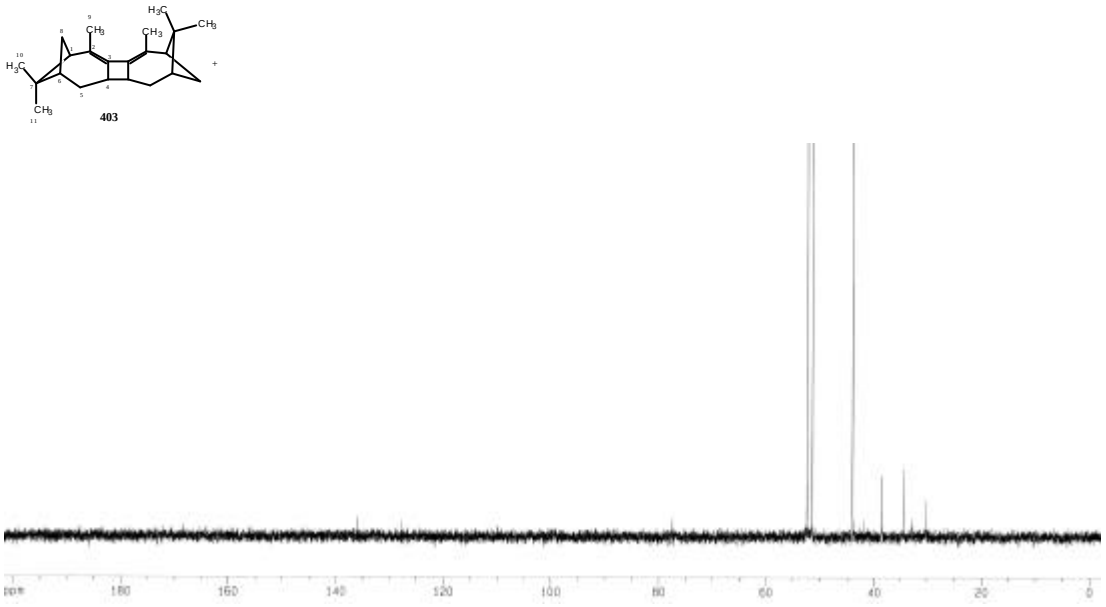

Figure A.28: DEPT-90 spectrum of **403**

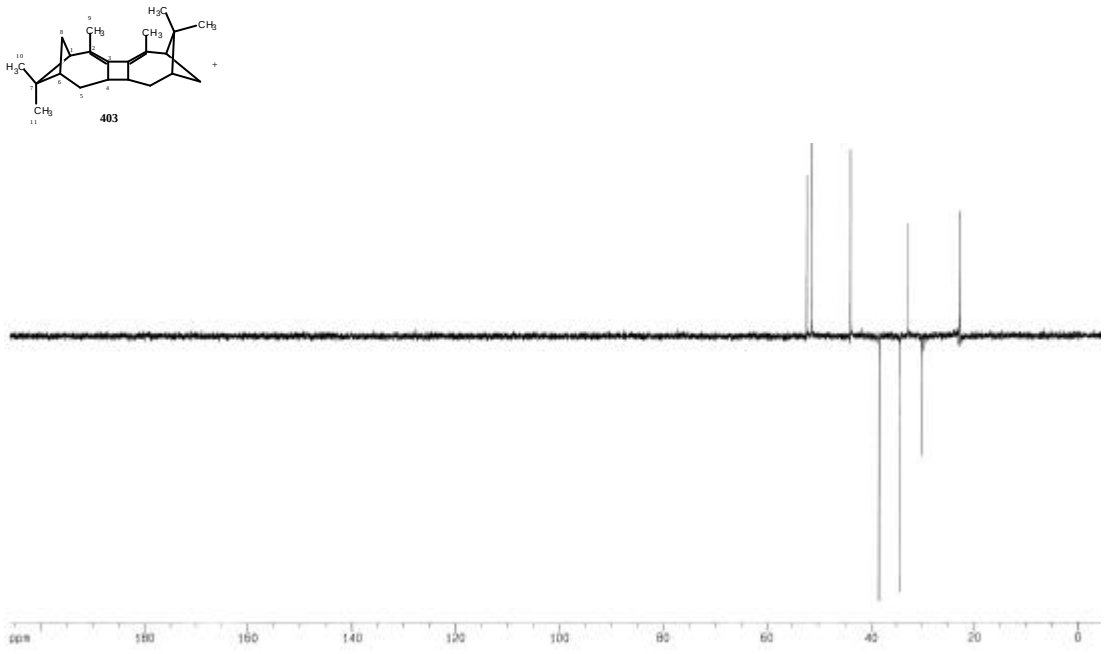

Figure A.29: DEPT-135 spectrum of **403**

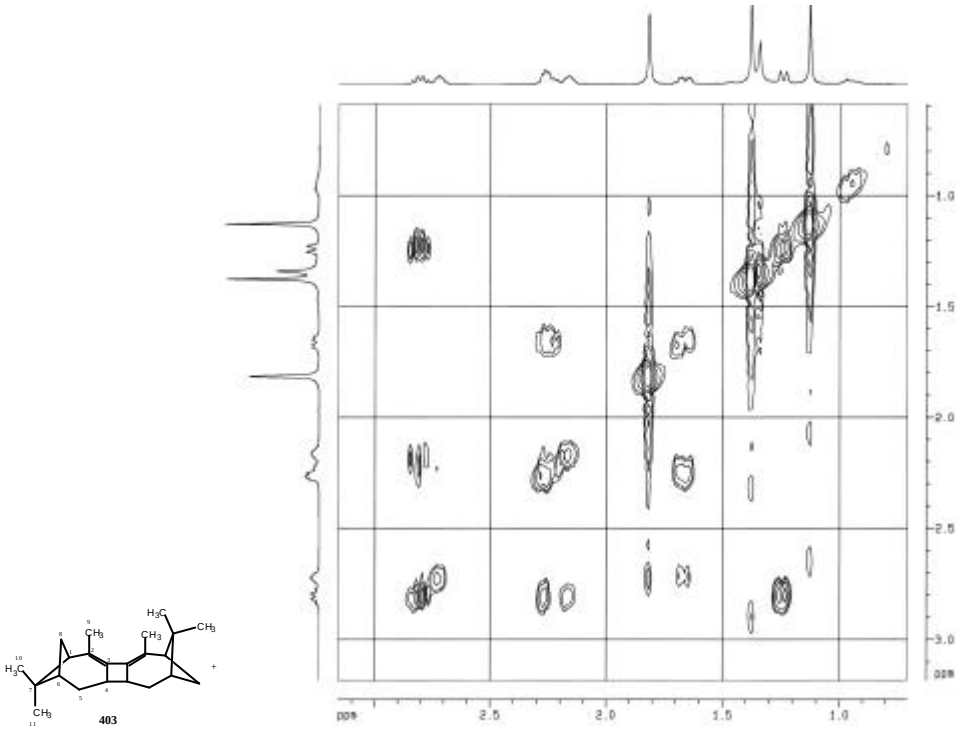

Figure A.30: COSY spectrum of **403**

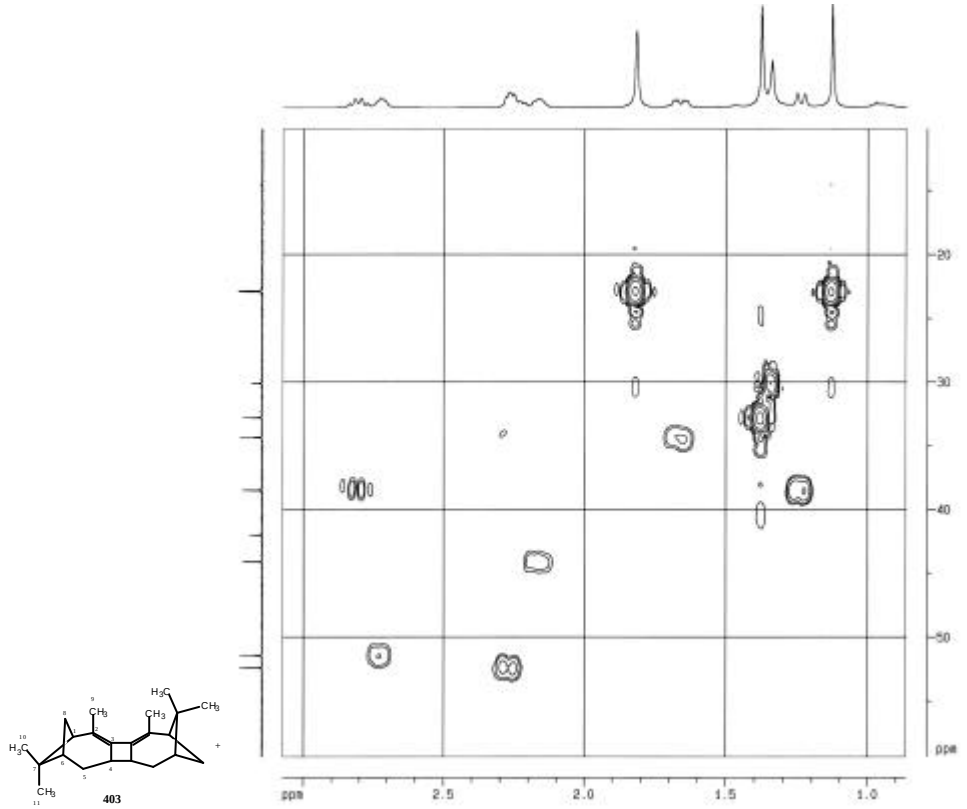

Figure A.31: HMQC spectrum of **403**

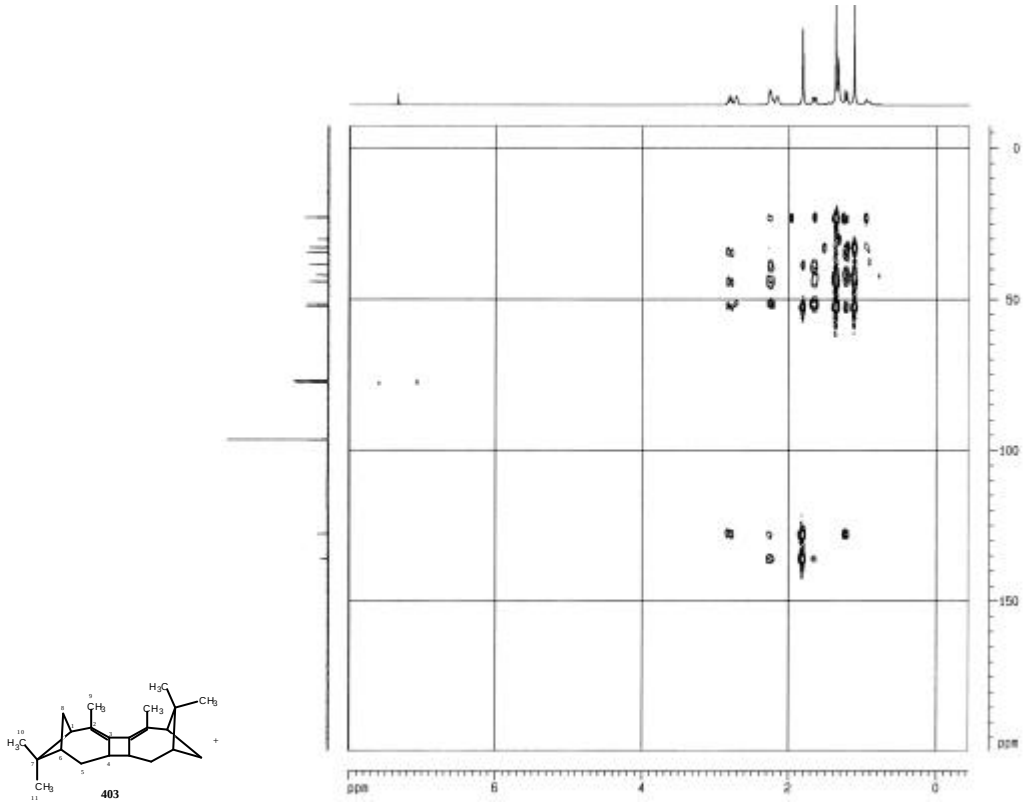

Figure A.32: HMBC spectrum of **403**

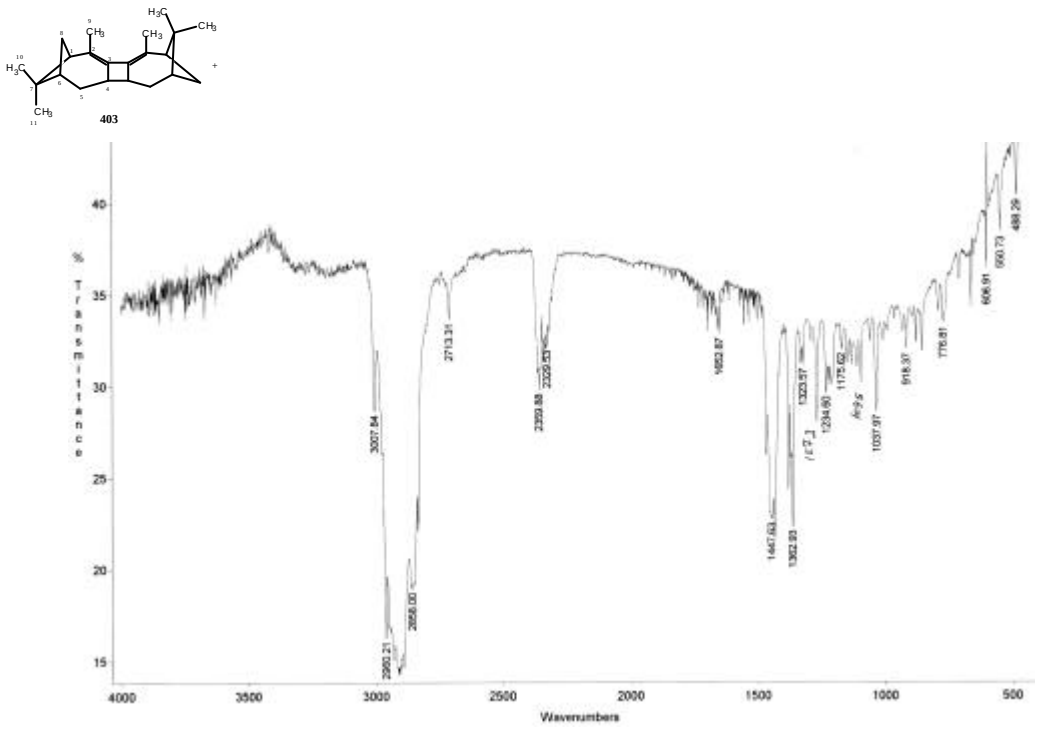

Figure A.33: IR-spectrum of **403**

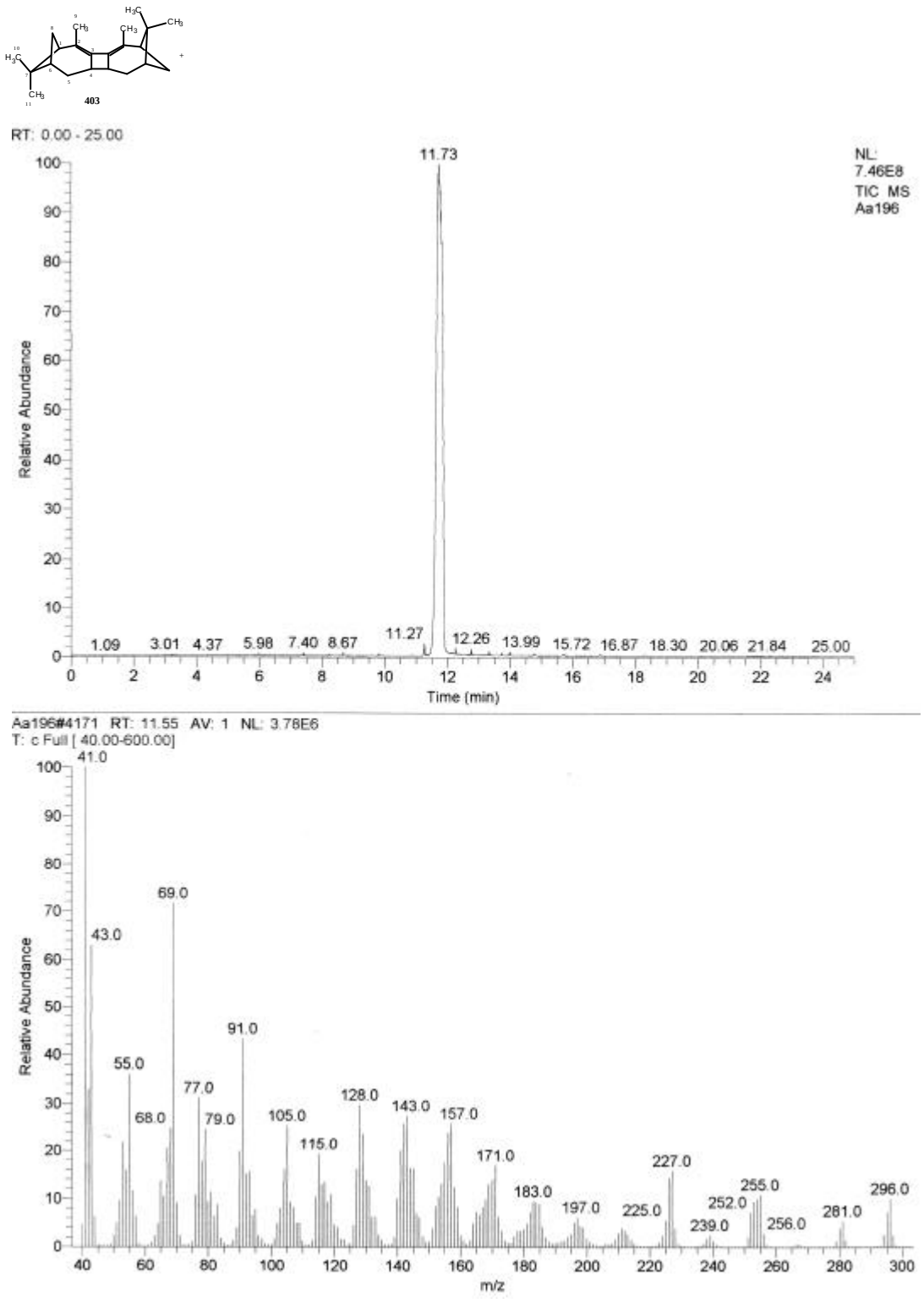

Figure A.34: GC/MS spectrum of **403**

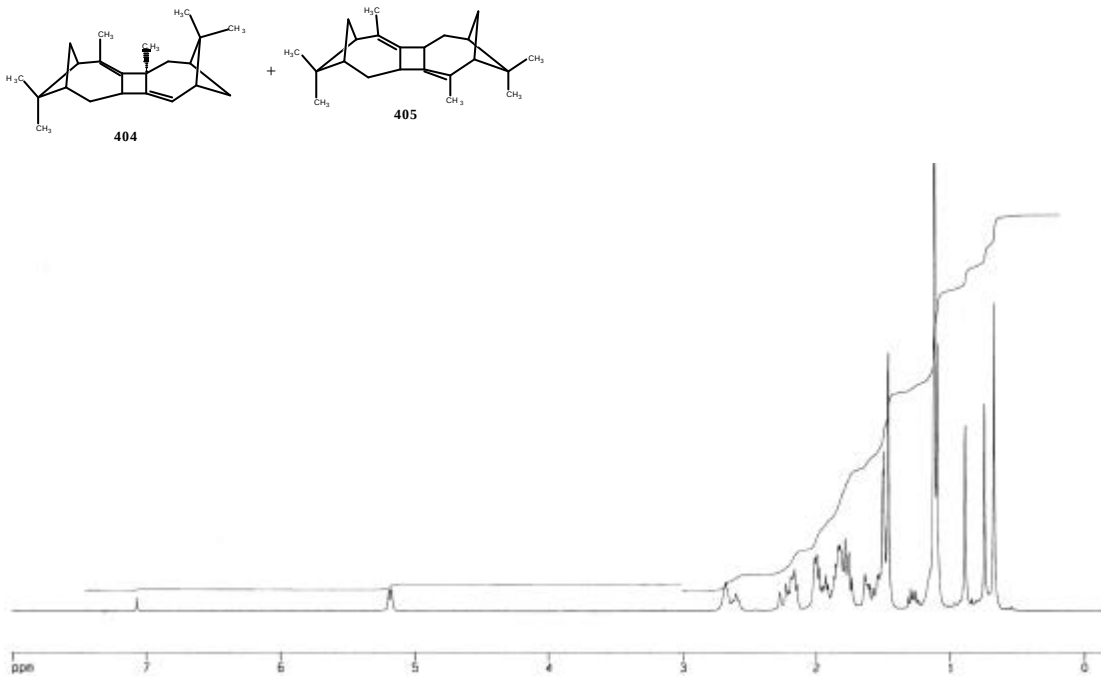

Figure A.35: ^{1}H-NMR spectrum of **404+405**

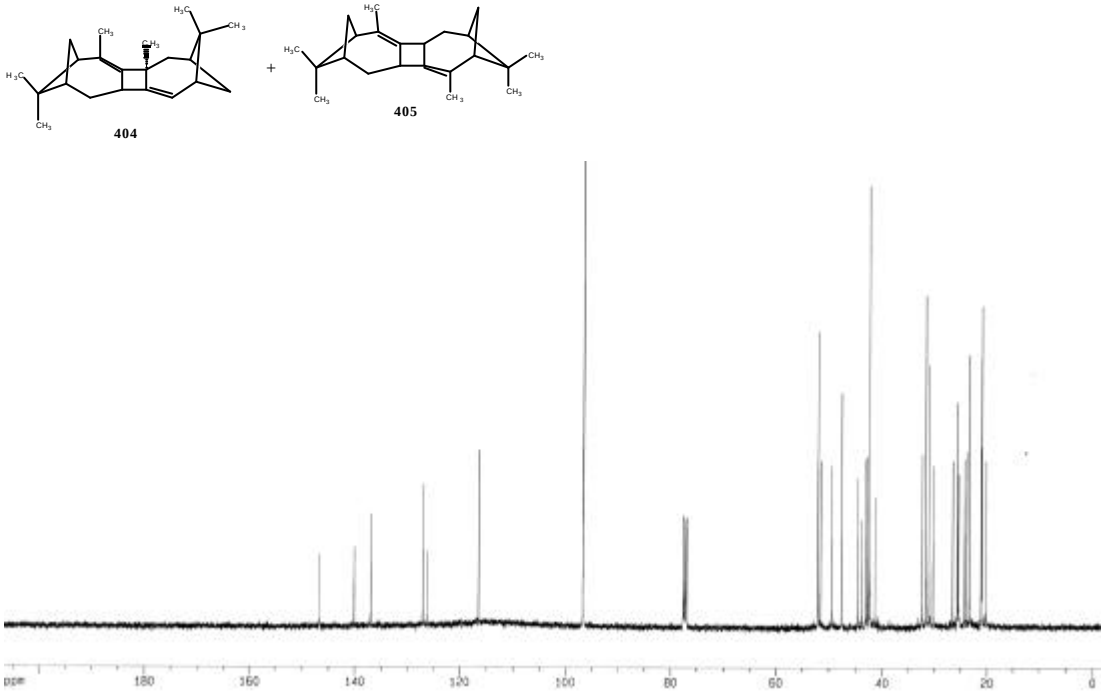

Figure A.36: ^{13}C-NMR spectrum of **404+405**

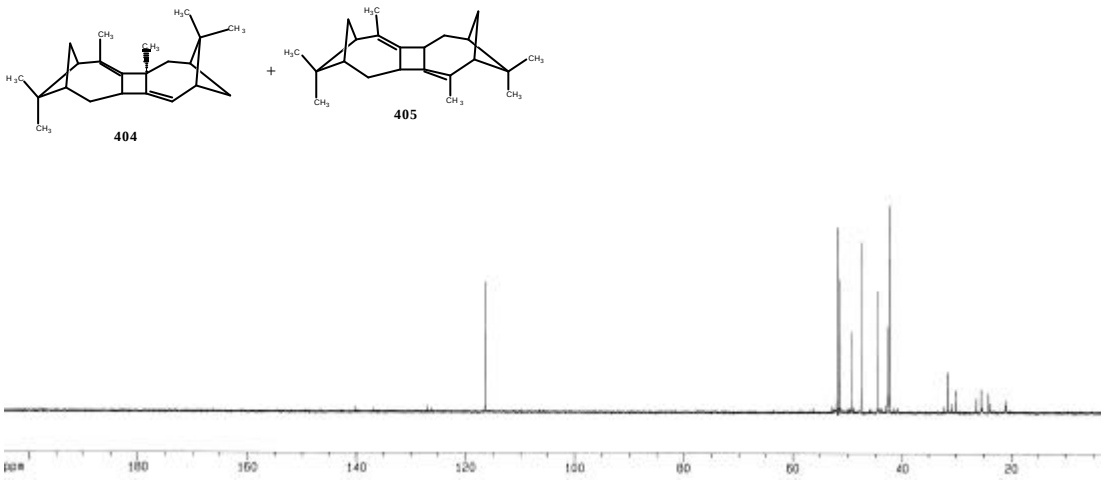

Figure A.37: DEPT-90 spectrum of **404+405**

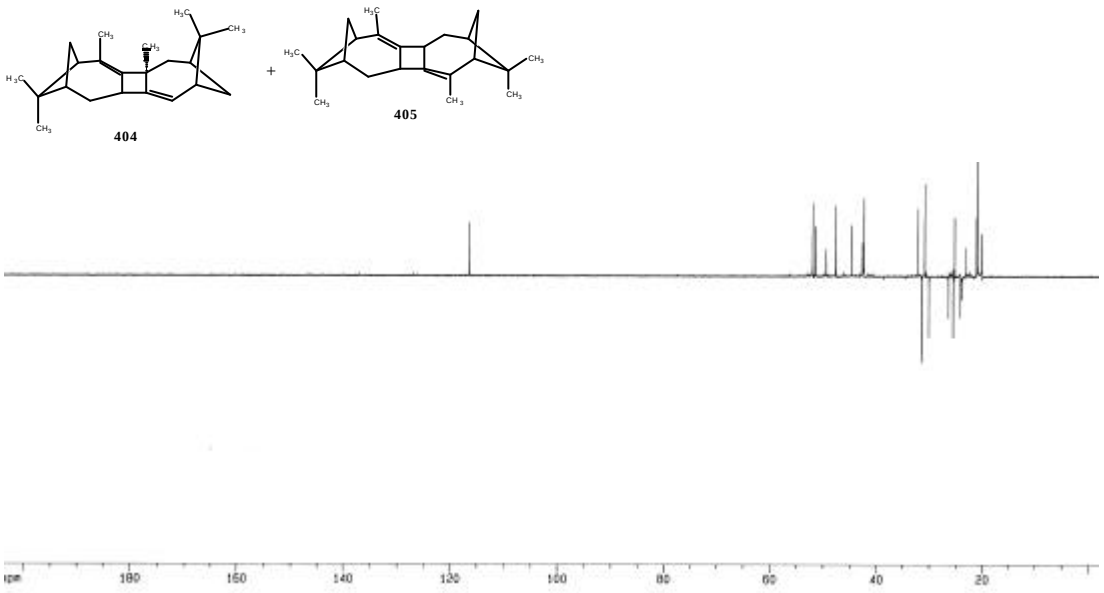

Figure A.38: DEPT-135 spectrum of **404+405**

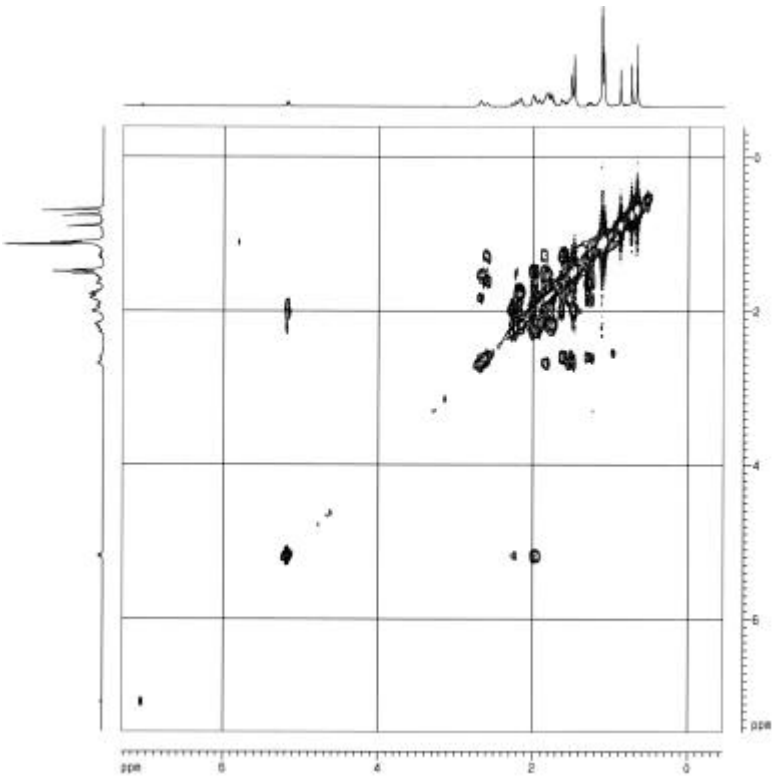

Figure A.39: COSY spectrum of **404+405**

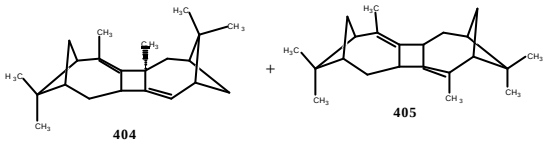

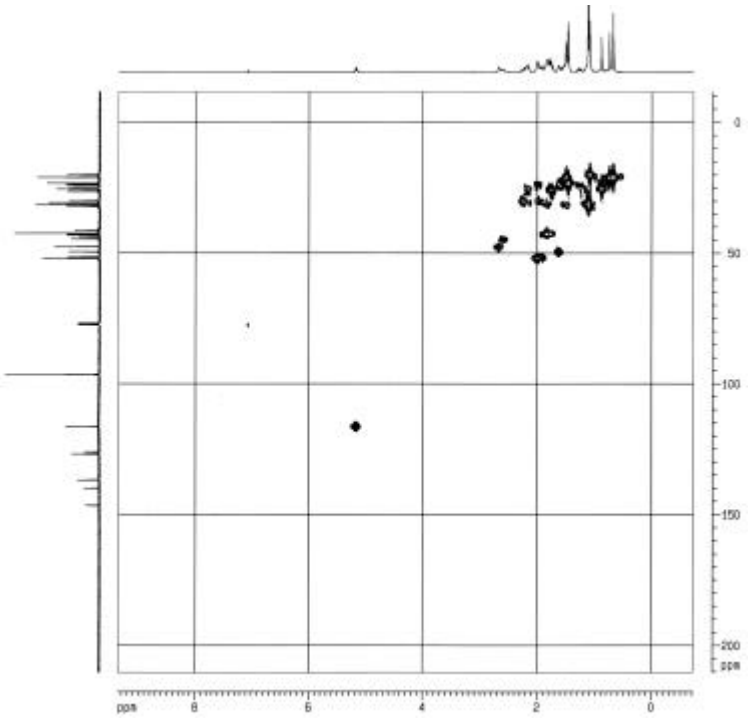

Figure A.40: HMQC spectrum of **404+405**

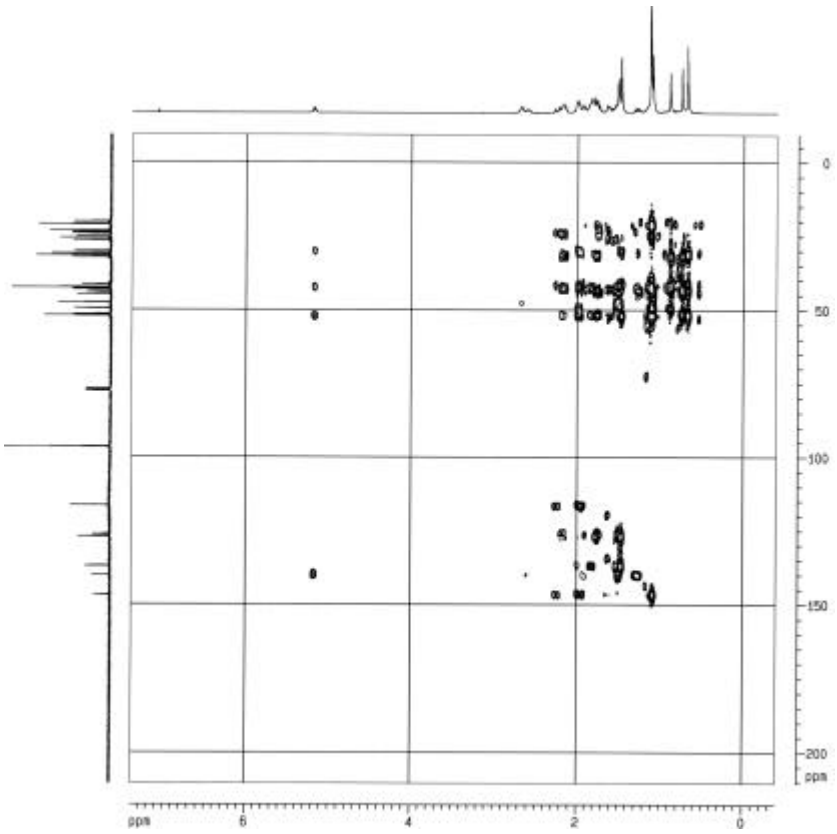

Figure A.41: HMBC spectrum of **404+405**

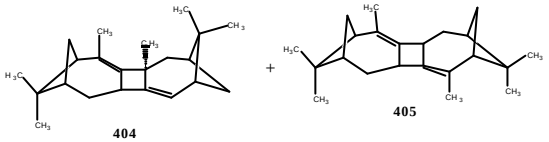

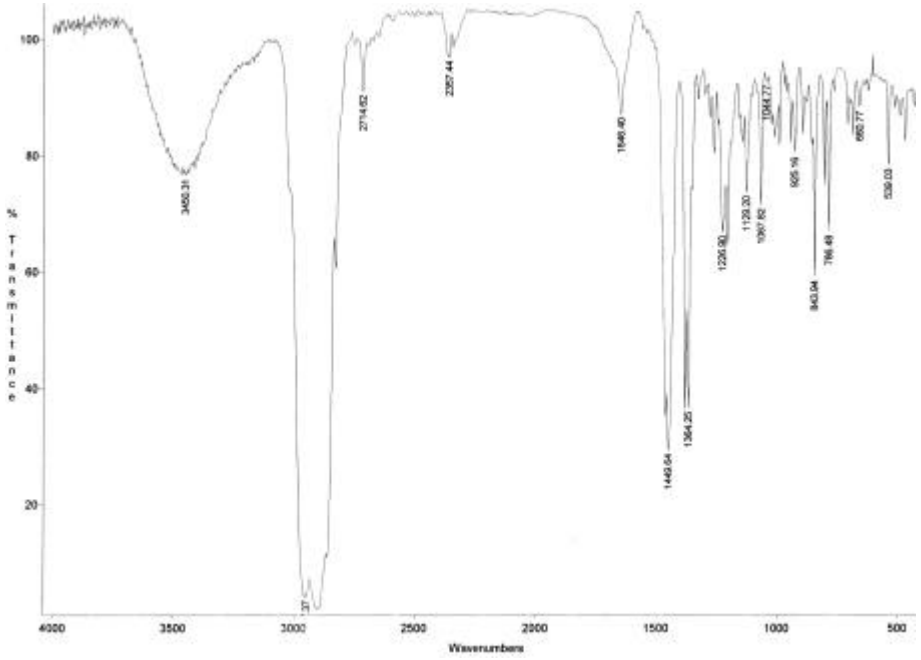

Figure A.42: IR-spectrum of **404+405**

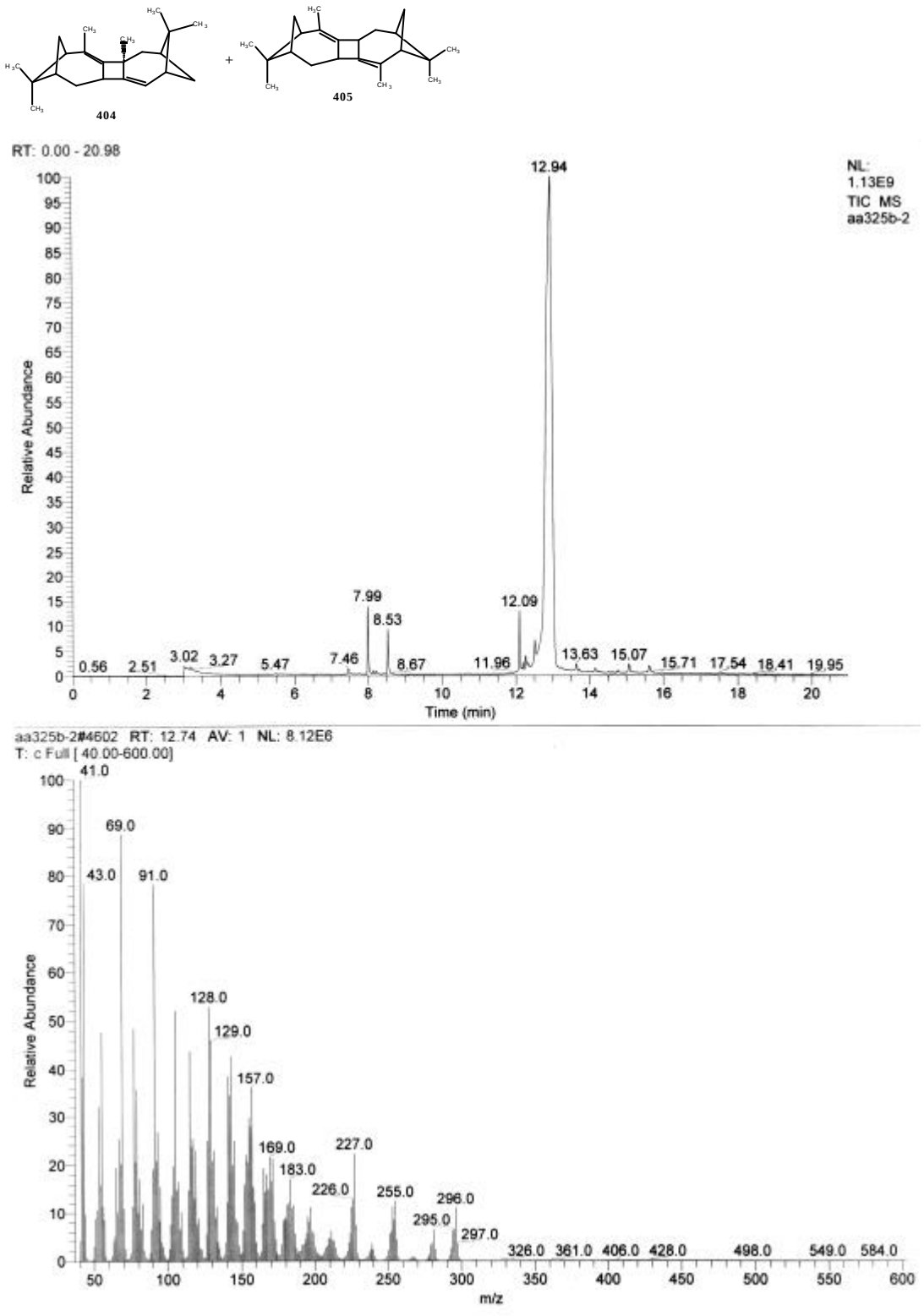

Figure A.43: GC/MS spectrum of **404+405**

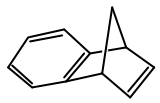

337

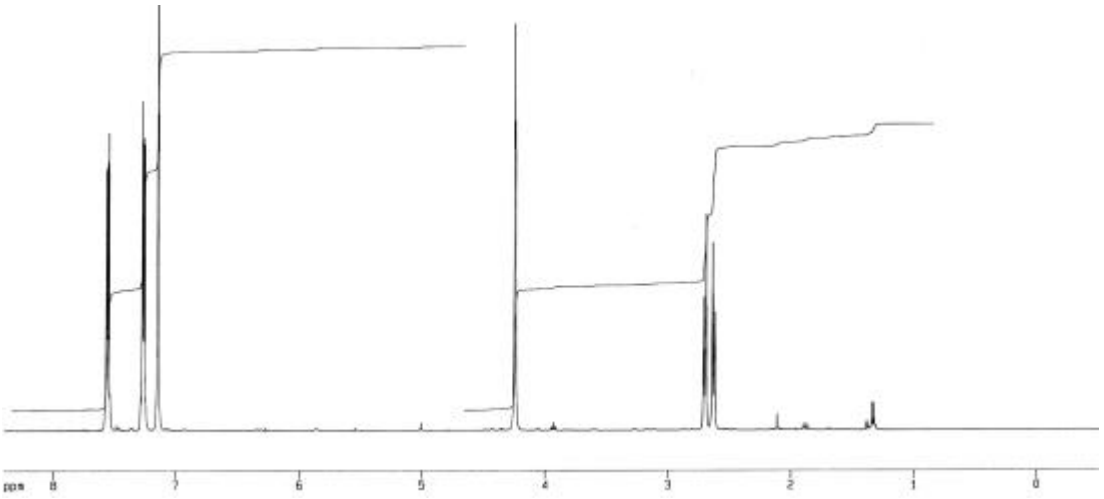

Figure A.44: ^{1}H-NMR spectrum of **337**

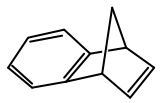

337

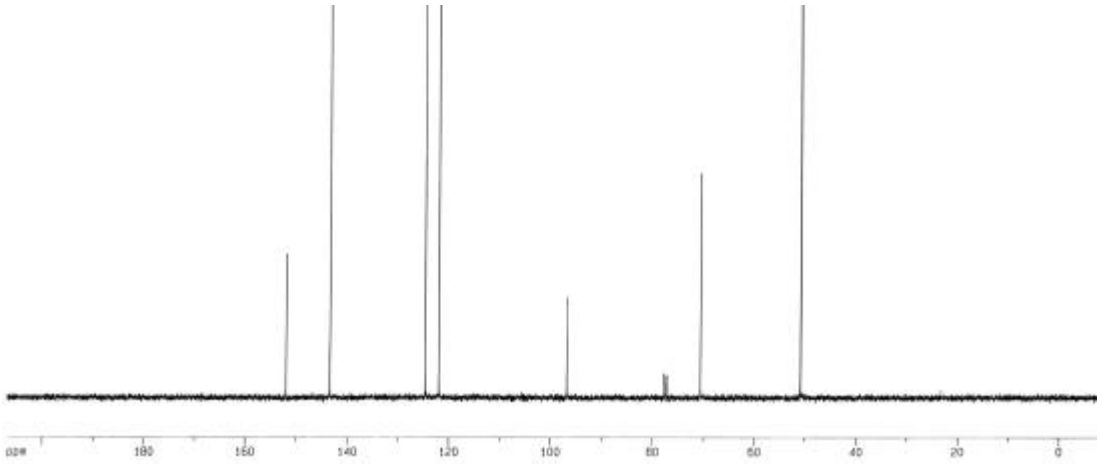

Figure A.45: ^{13}C-NMR spectrum of **337**

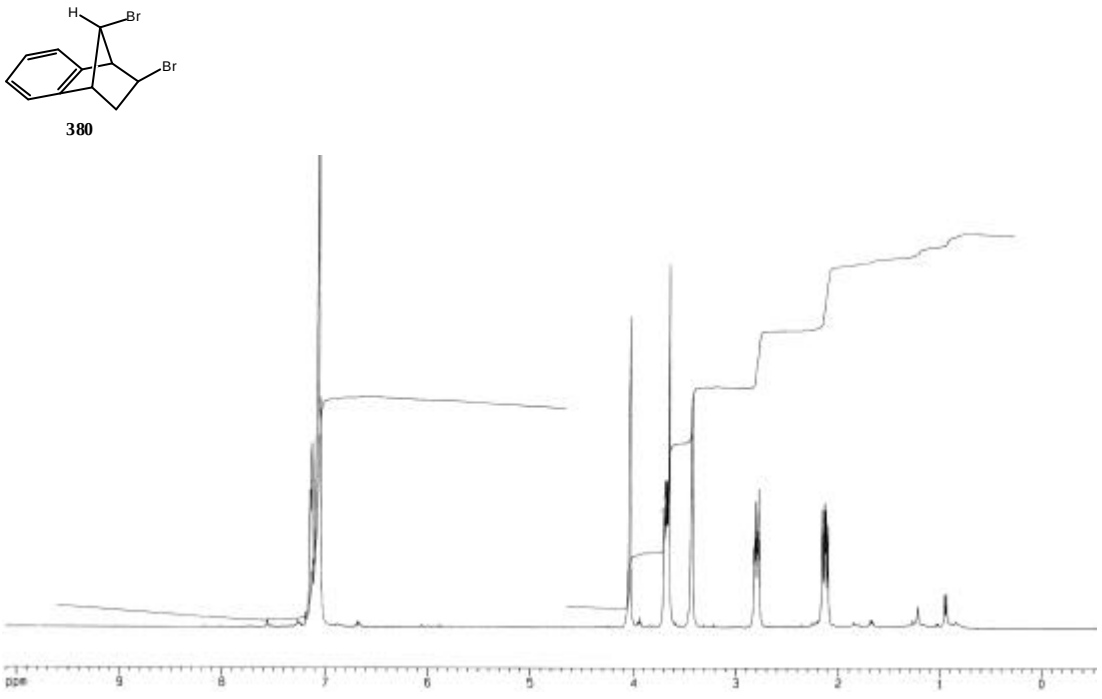

Figure A.46: ^{1}H-NMR spectrum of **380**

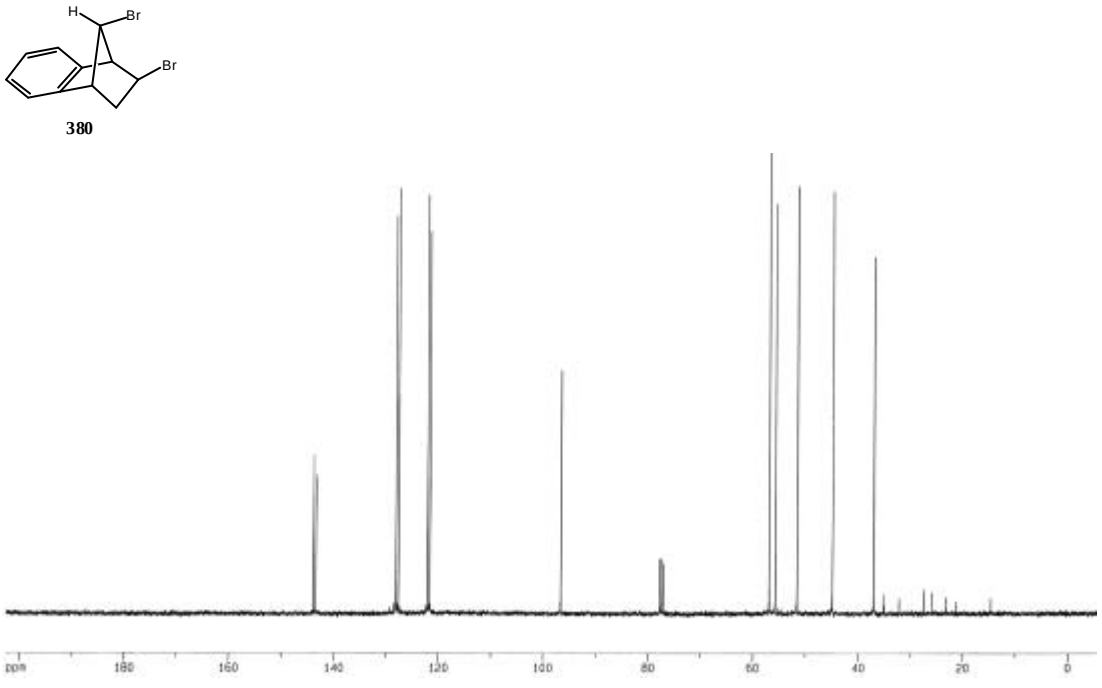

Figure A.47: ^{13}C-NMR spectrum of **380**

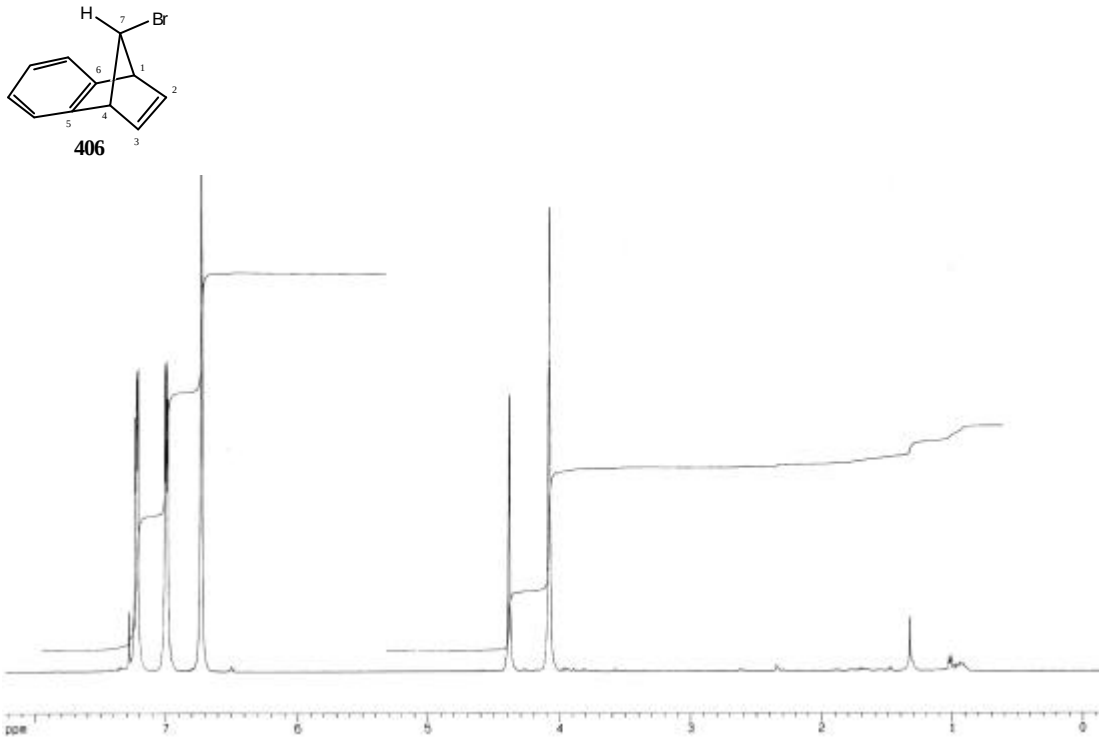

Figure A.48: ^{1}H-NMR spectrum of **406**

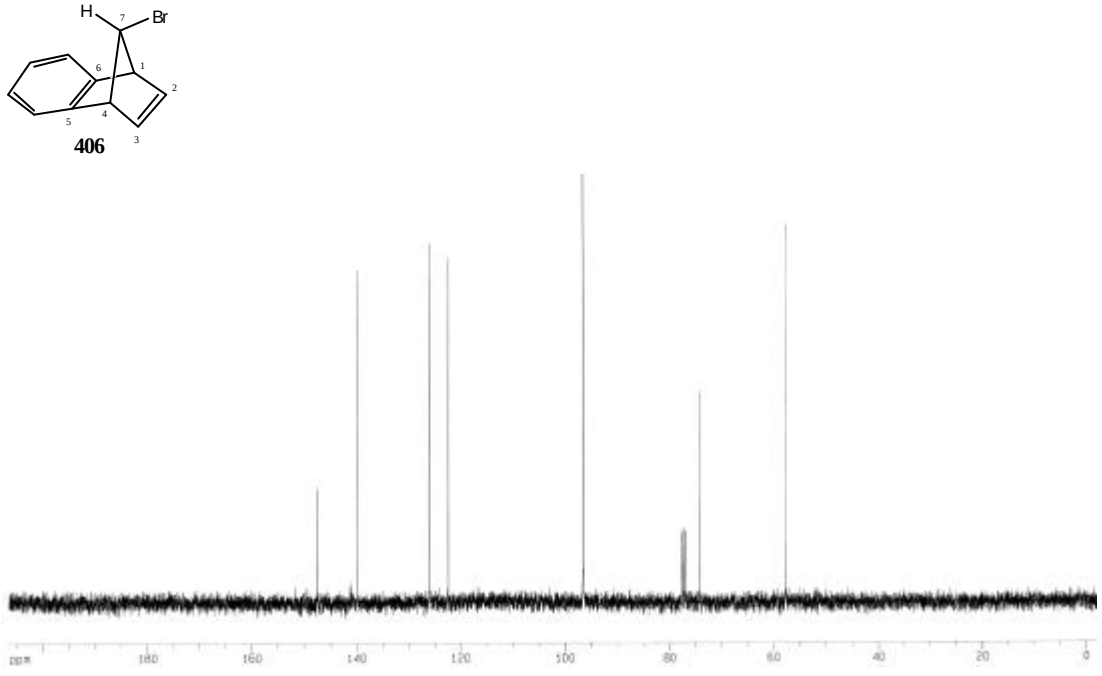

Figure A.49: ^{13}C-NMR spectrum of **406**

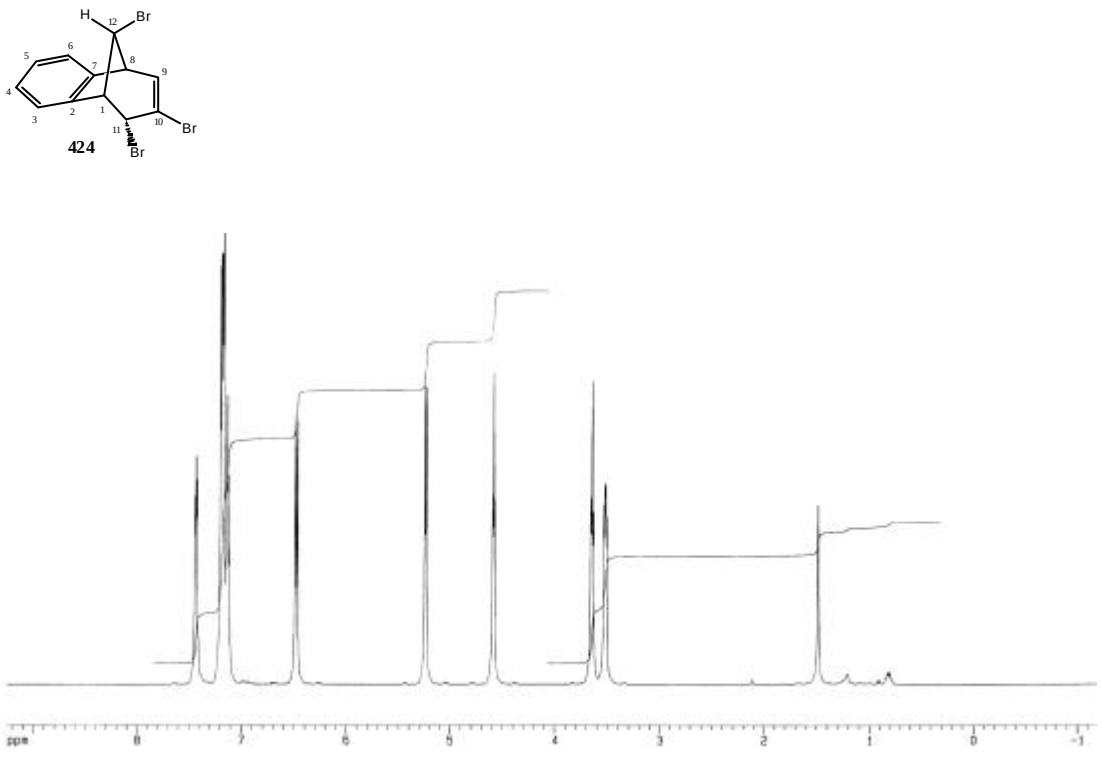

Figure A.50: ^{1}H-NMR spectrum of **424**

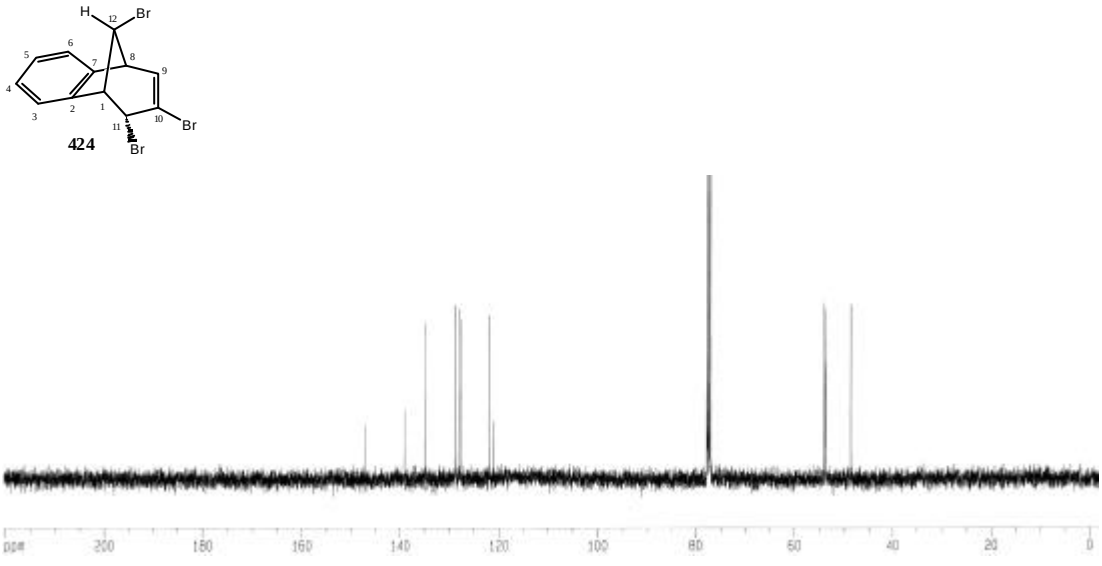

Figure A.51: ^{13}C-NMR spectrum of **424**

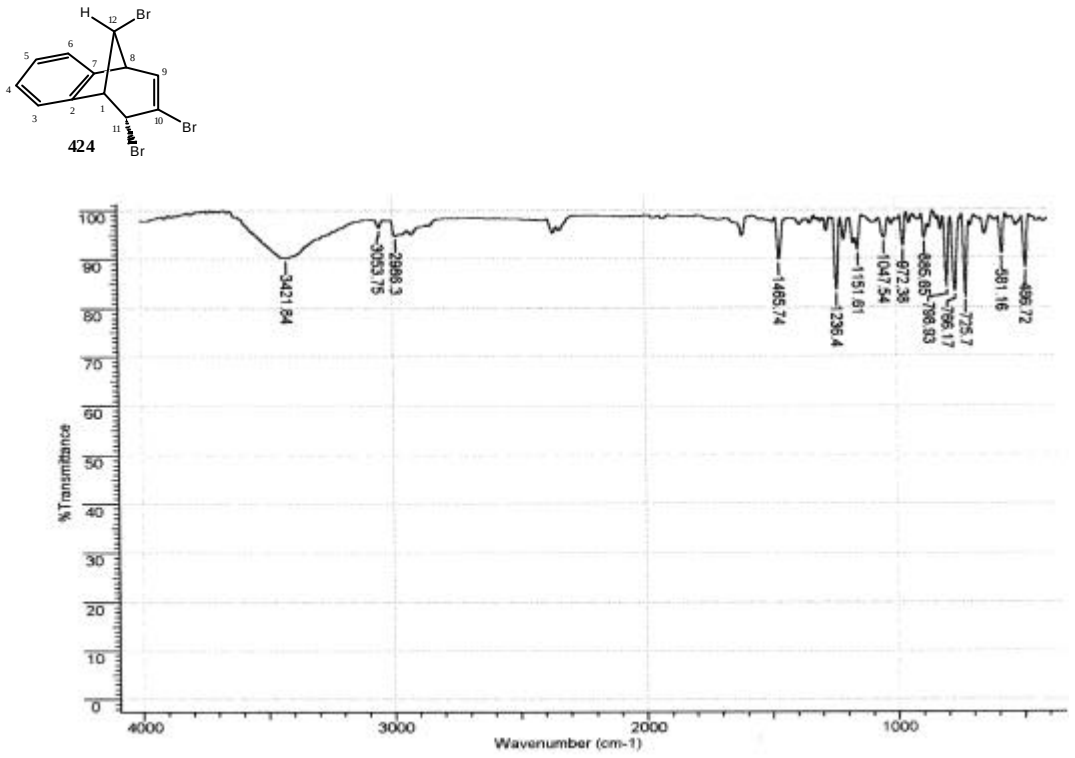

Figure A.52. IR spectrum of **424**

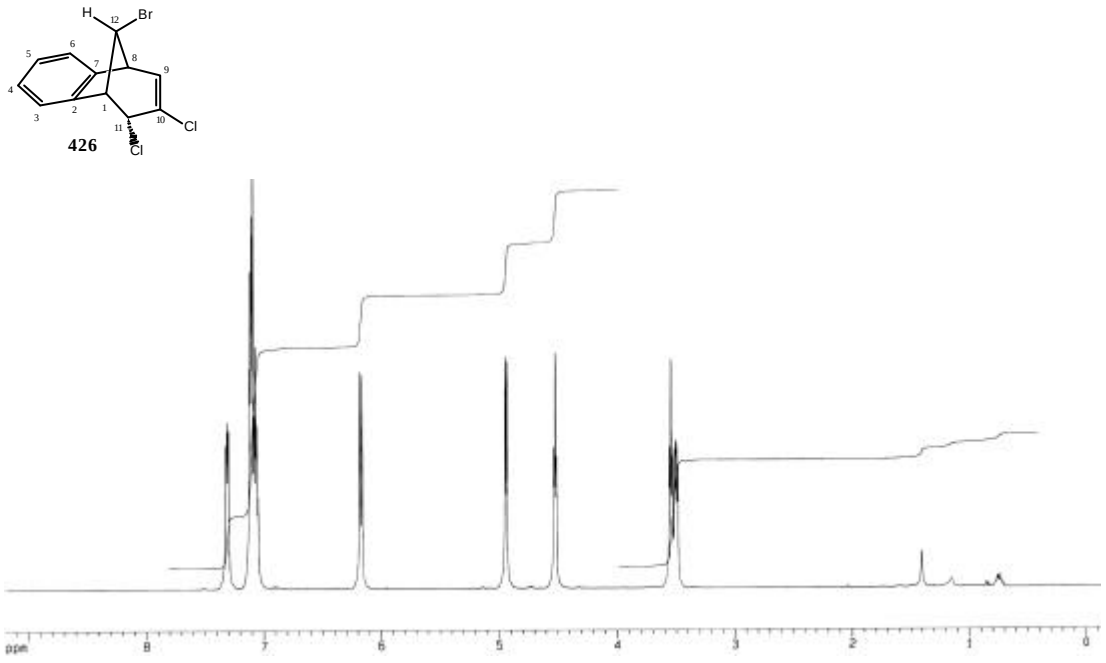

Figure A.53: ^{1}H-NMR spectrum of **426**

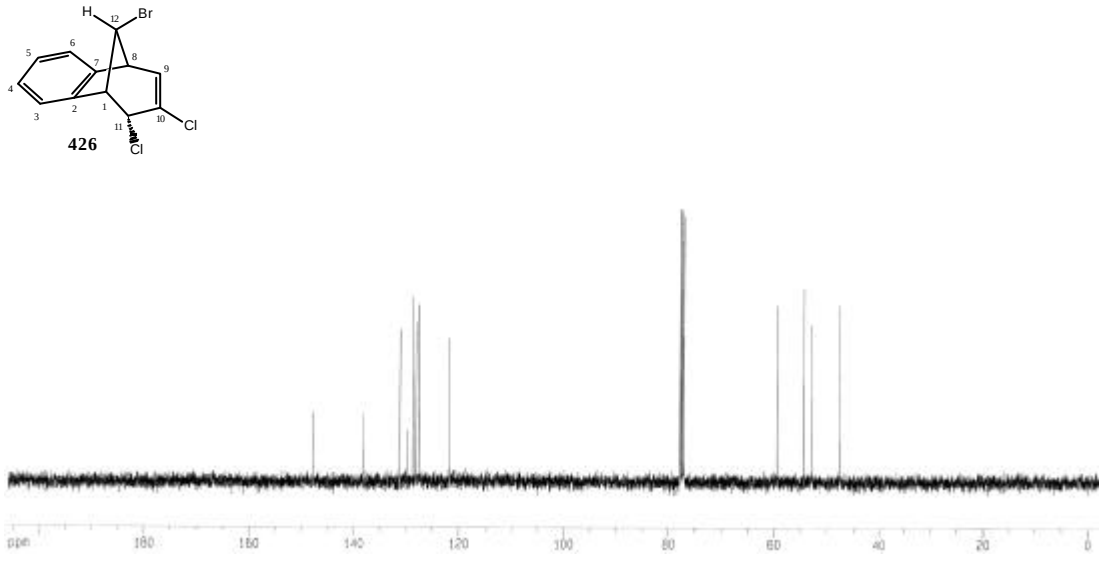

Figure A.54: ^{13}C-NMR spectrum of **426**

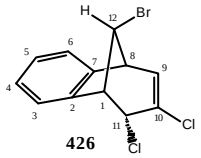

426

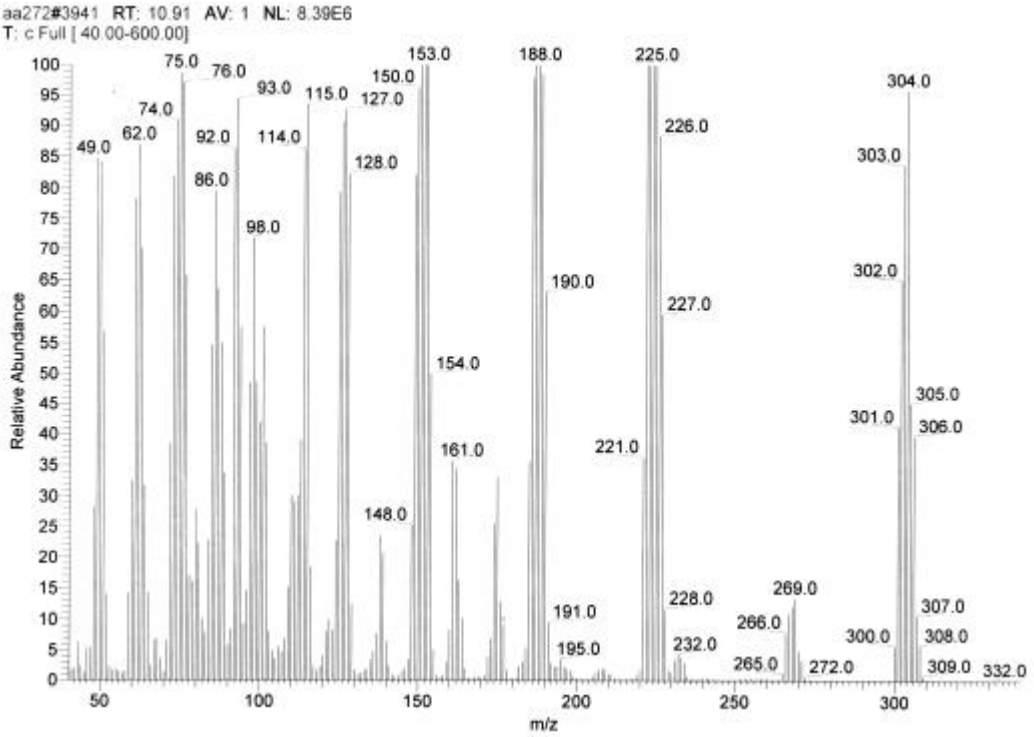

Figure A.55: Mass spectrum of **426**

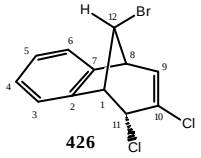

426

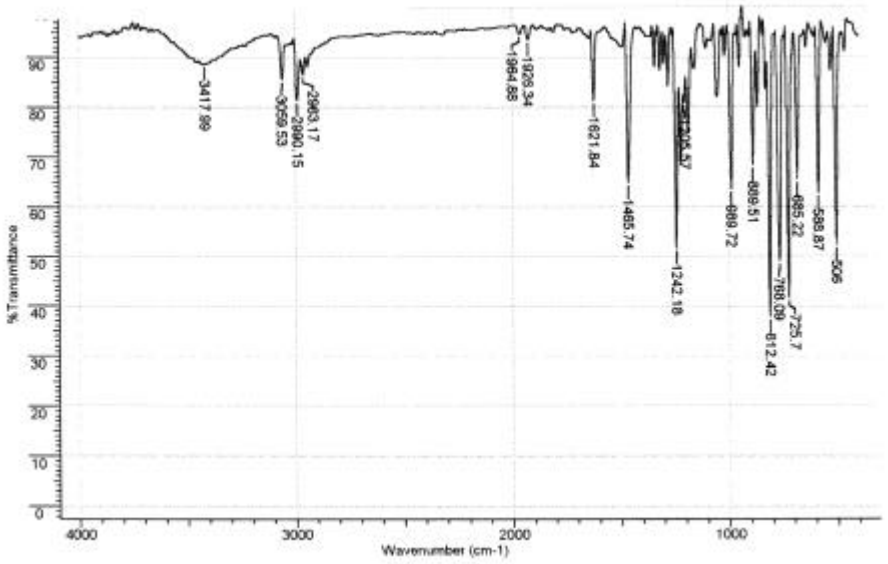

Figure A.56: IR spectrum of **426**

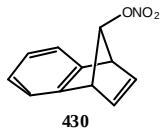

430

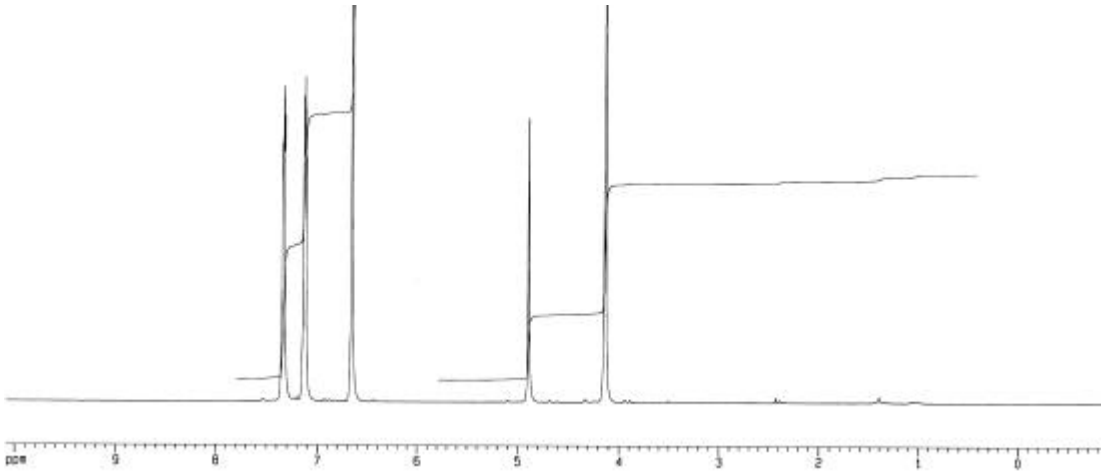

Figure A.57: ^{1}H-NMR spectrum of **430**

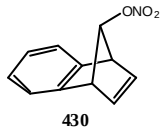

430

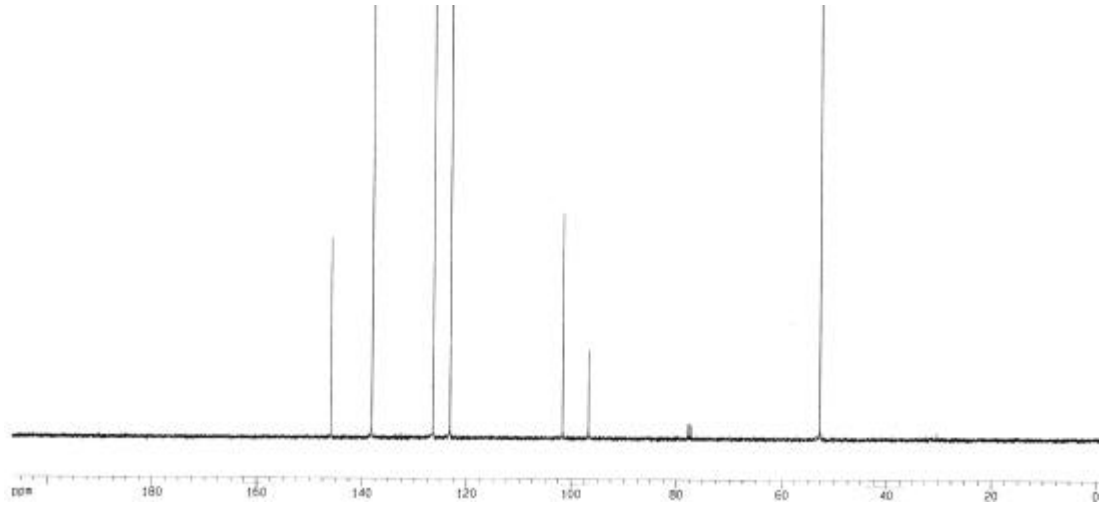

Figure A.58: ^{13}C-NMR spectrum of **430**

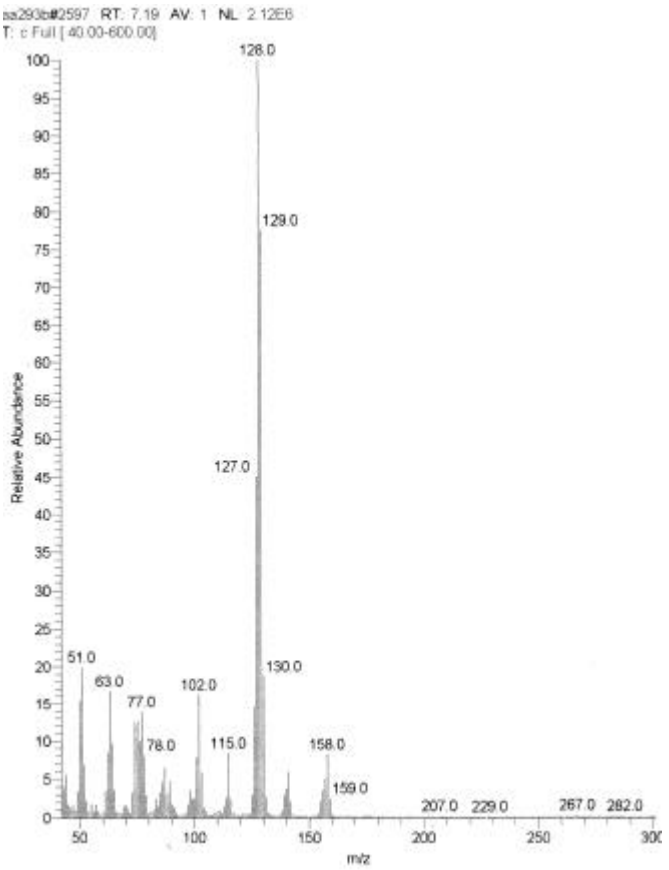

Figure A.59: Mass spectrum of **430**

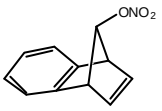

430

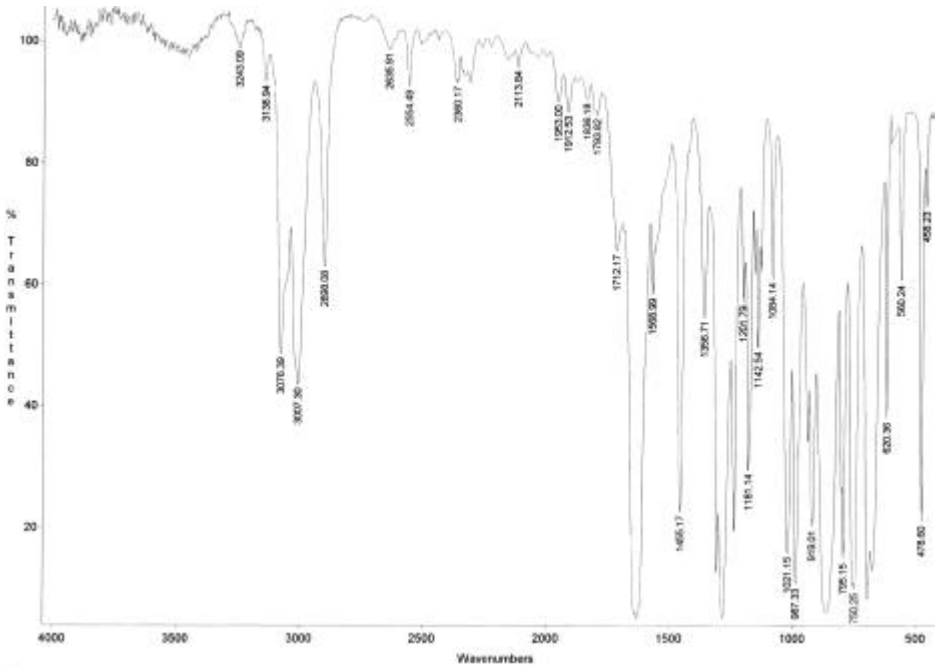

Figure A.60: IR spectrum of **430**

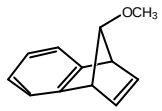

407

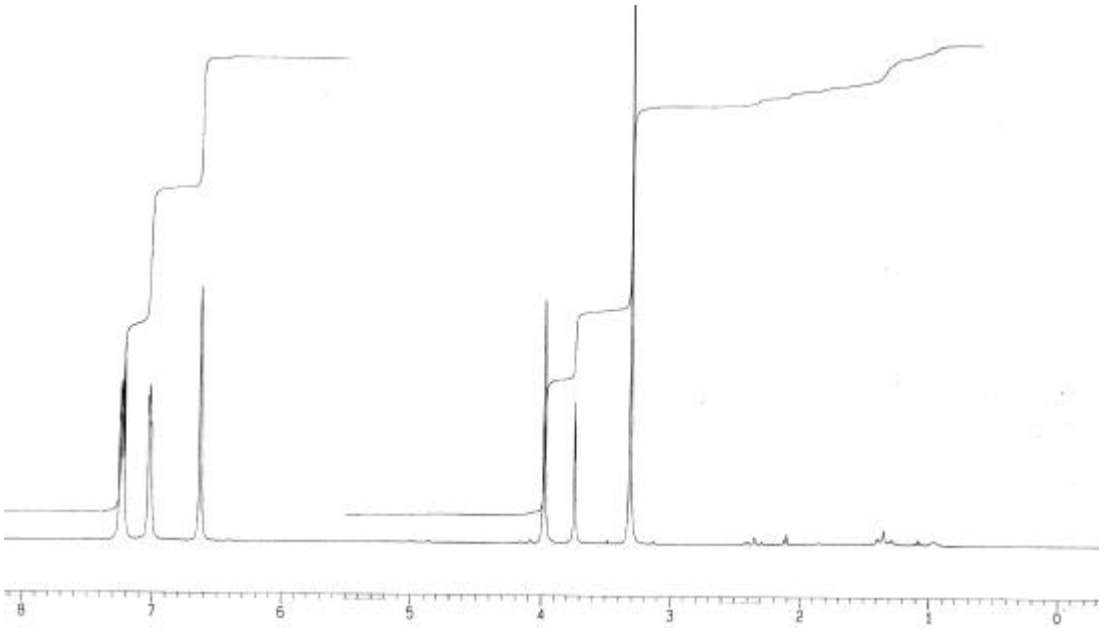

Figure A.61: ^{1}H-NMR spectrum of **407**

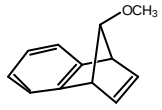

407

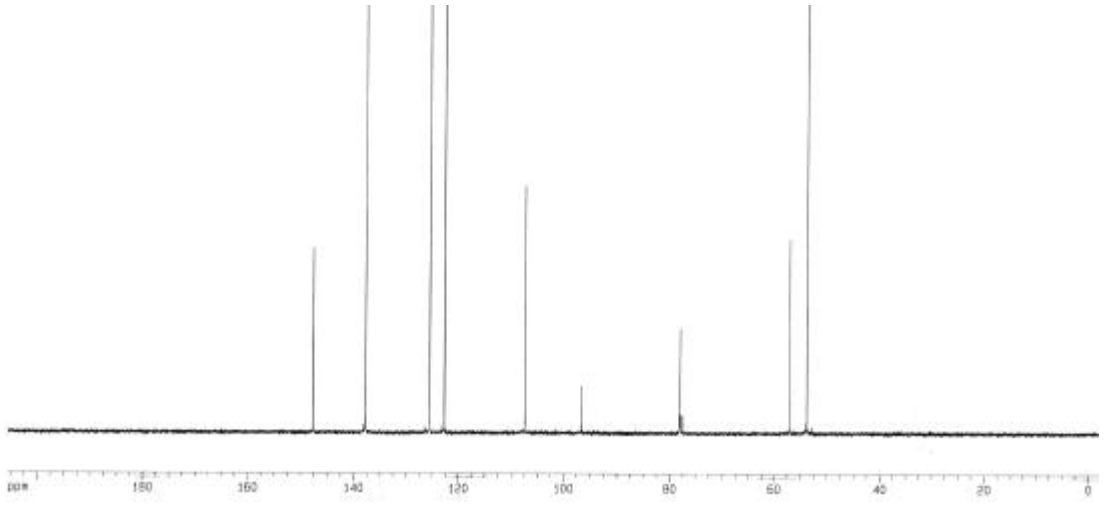

Figure A.62: ^{13}C-NMR spectrum of **407**

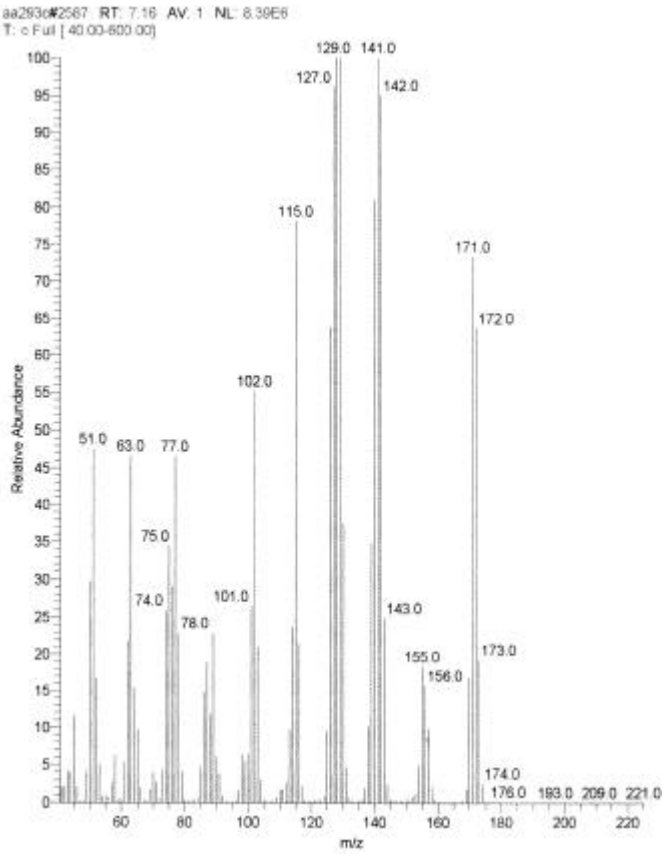

Figure A.63: Mass spectrum of **407**

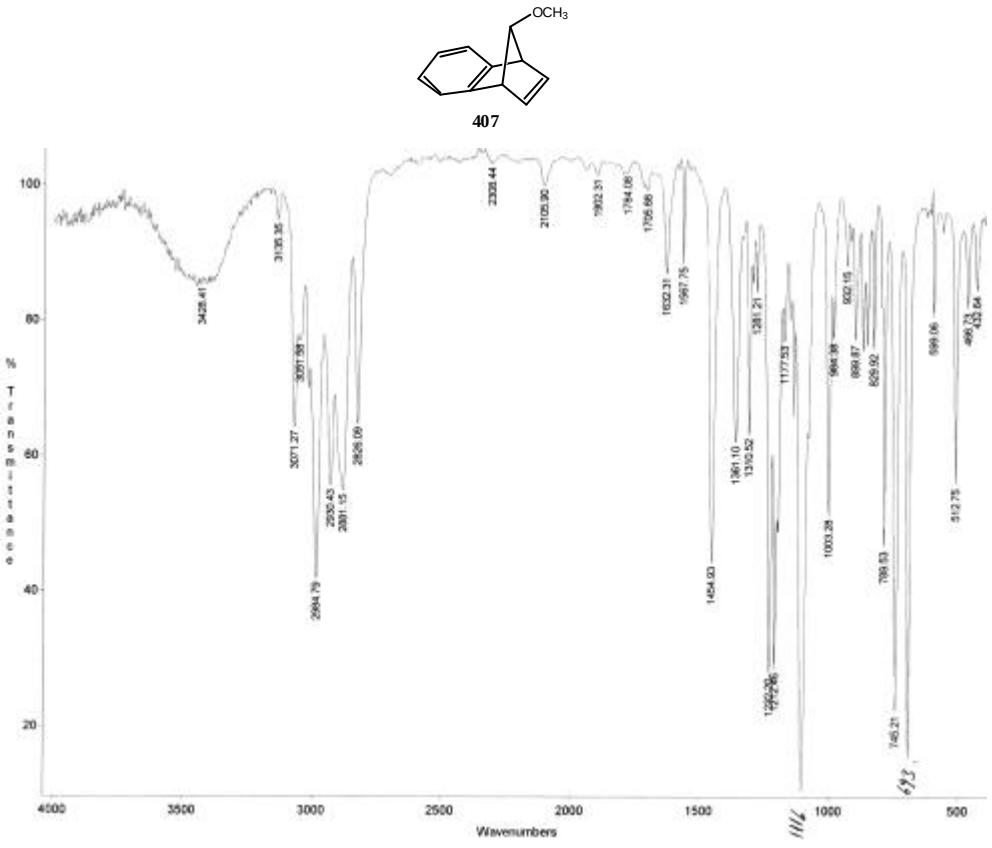

Figure A.64: IR spectrum of **407**

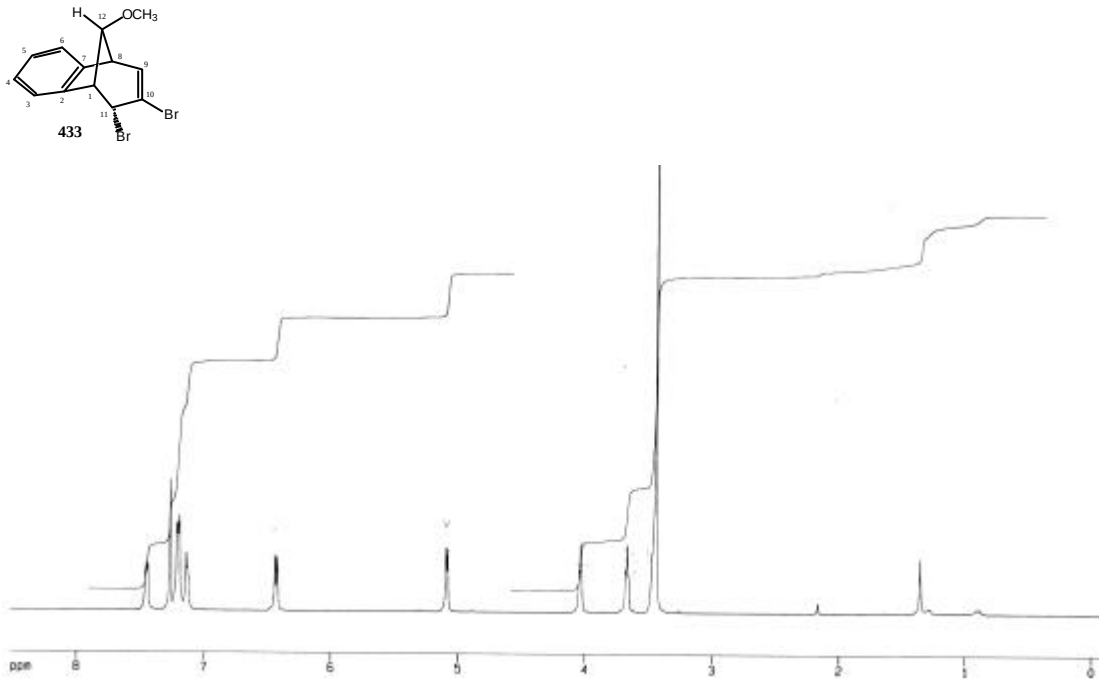

Figure A.65: ^{1}H-NMR spectrum of **433**

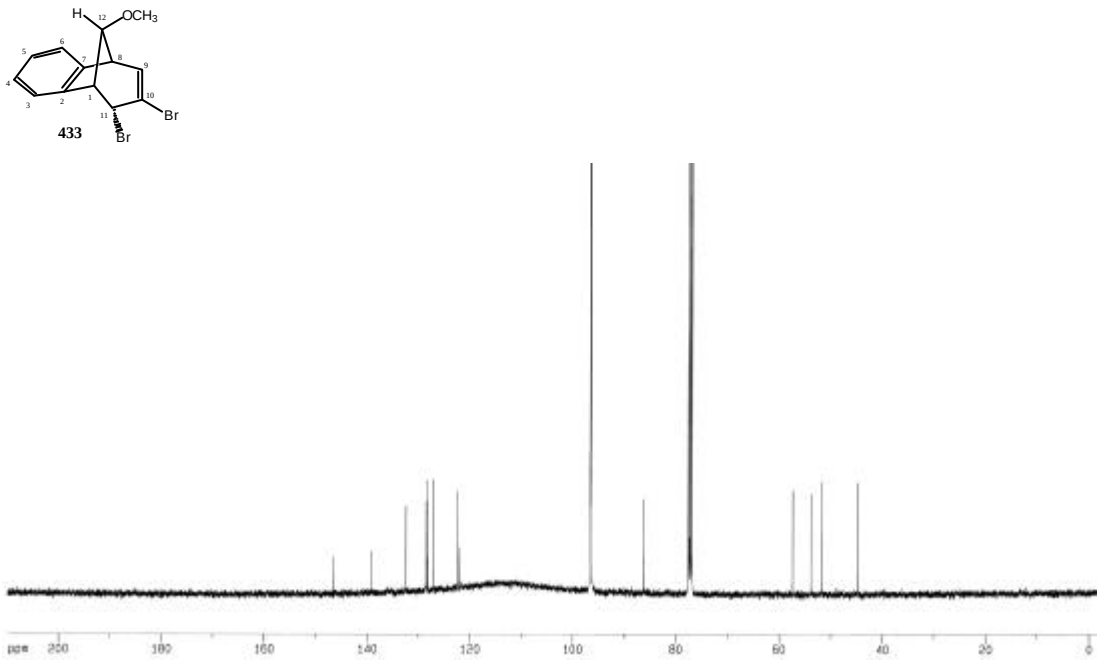

Figure A.66: ^{13}C-NMR spectrum of **433**

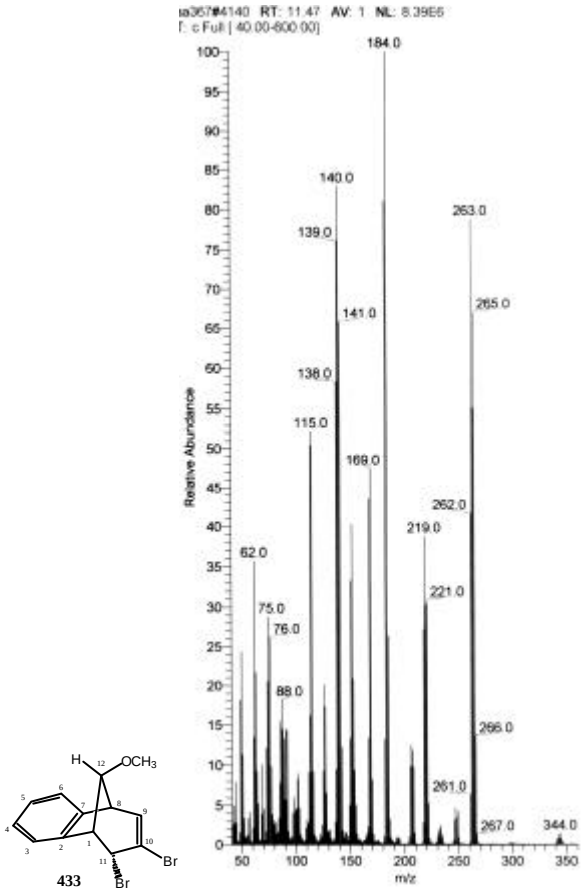

Figure A.67: Mass spectrum of **433**

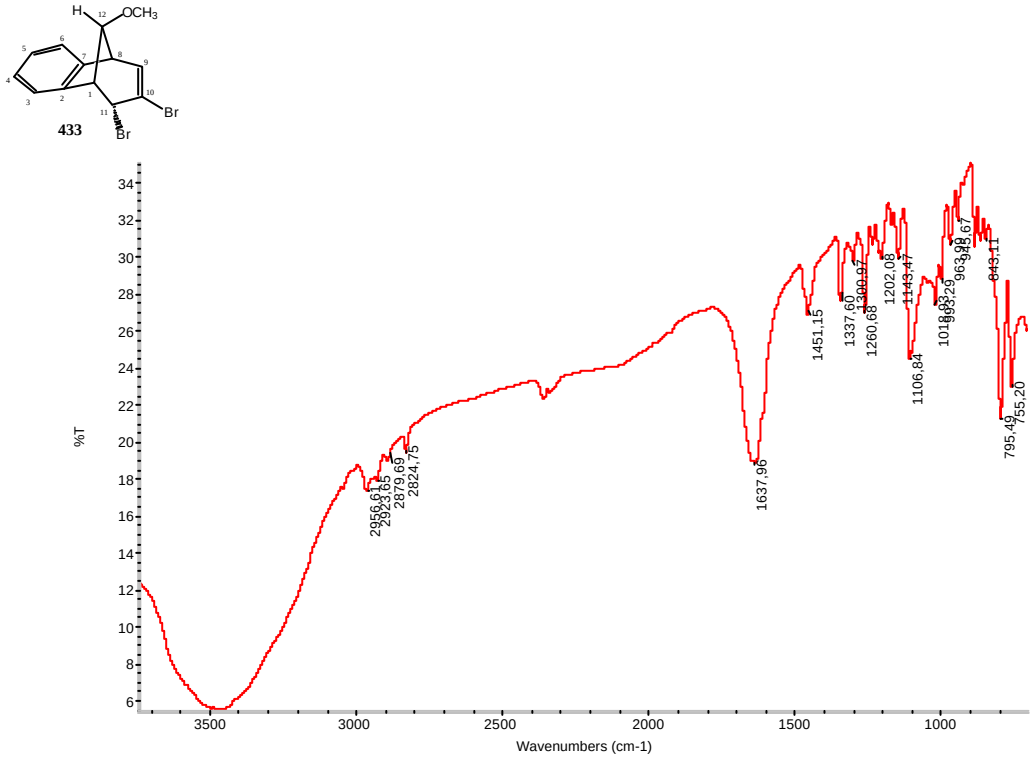

Figure A.68: IR spectrum of **433**

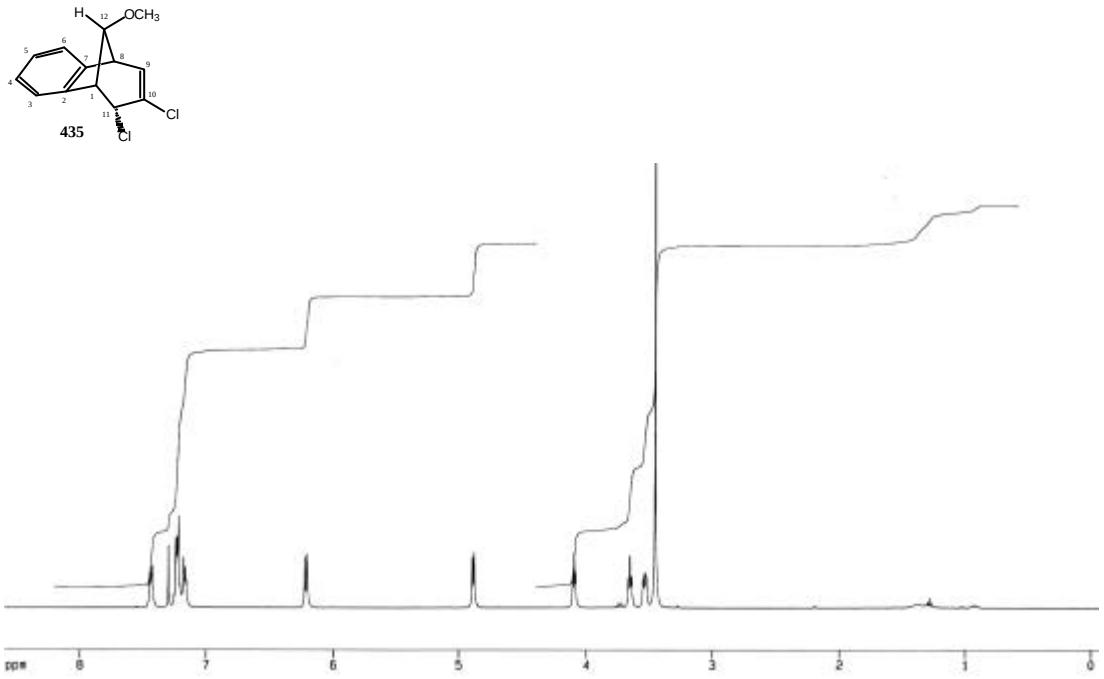

Figure A.69: ^{1}H-NMR spectrum of **435**

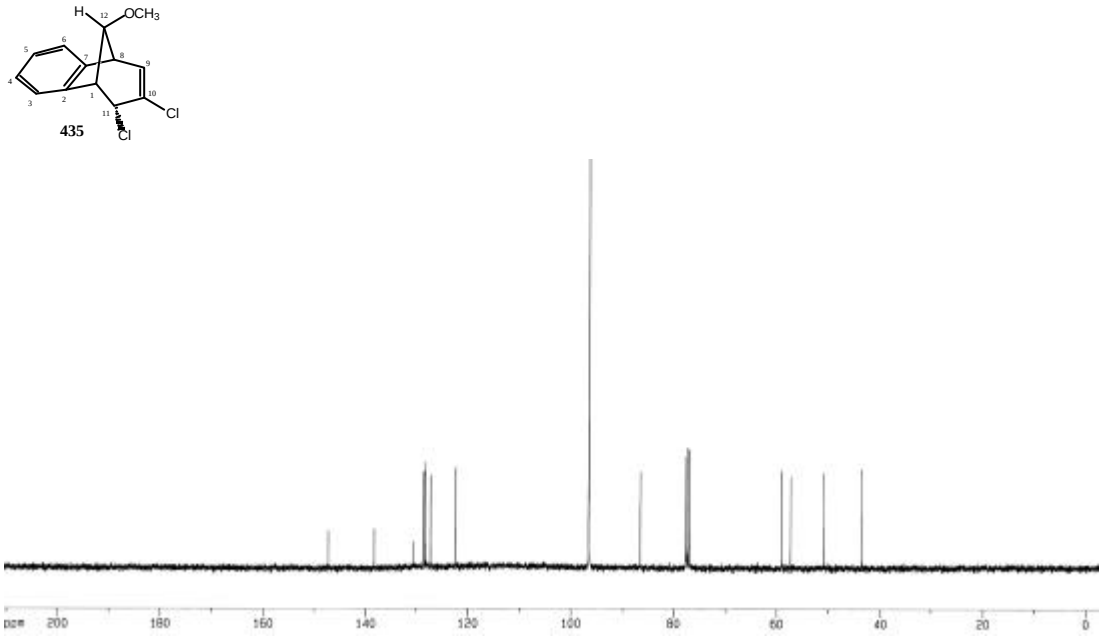

Figure A.70: ^{13}C-NMR spectrum of **435**

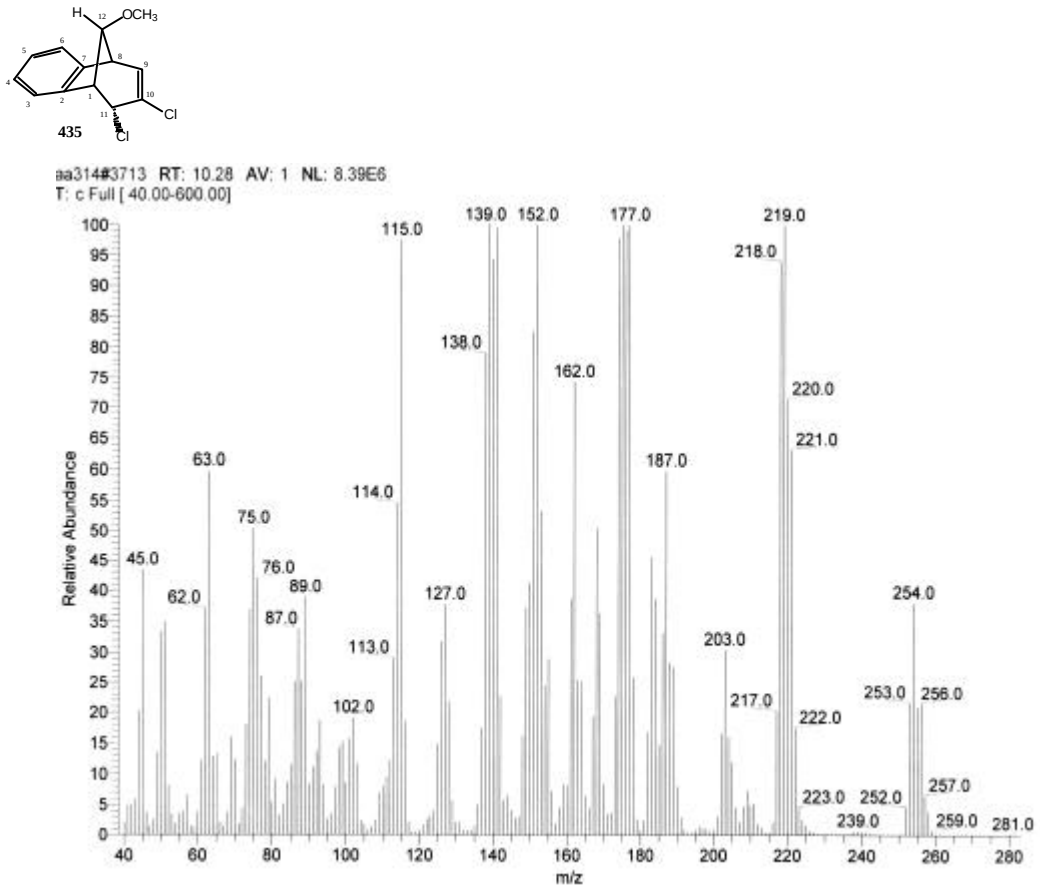

Figure A.71: Mass spectrum of **435**

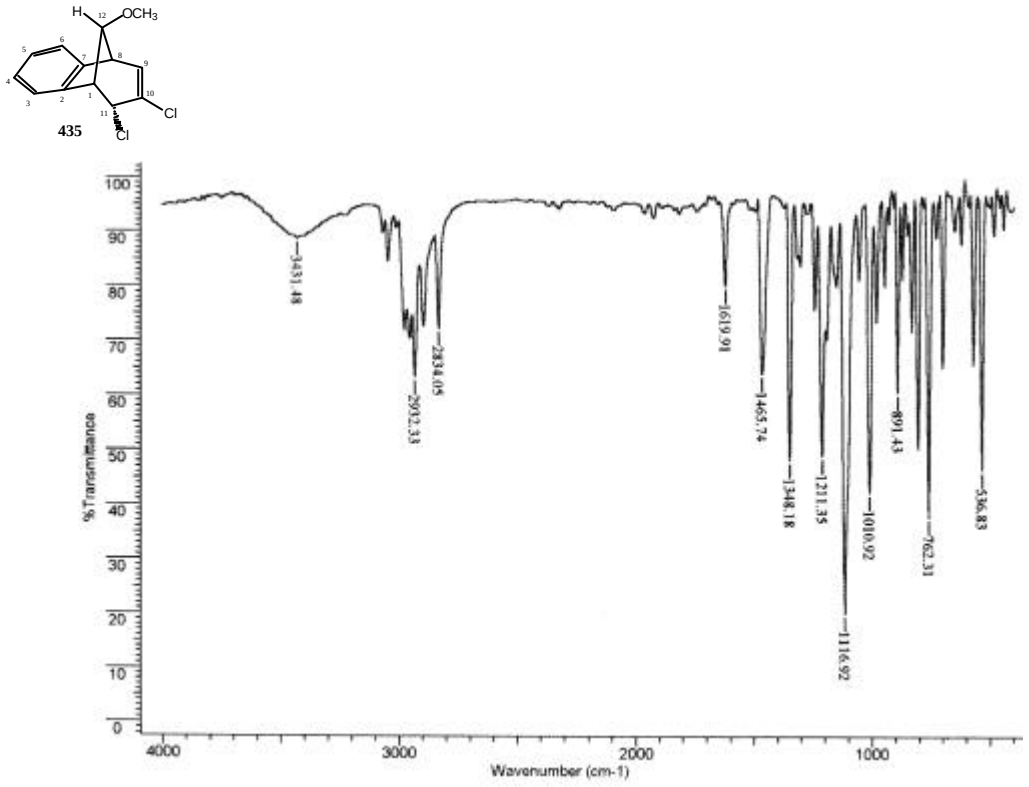

Figure A.72: IR spectrum of **435**

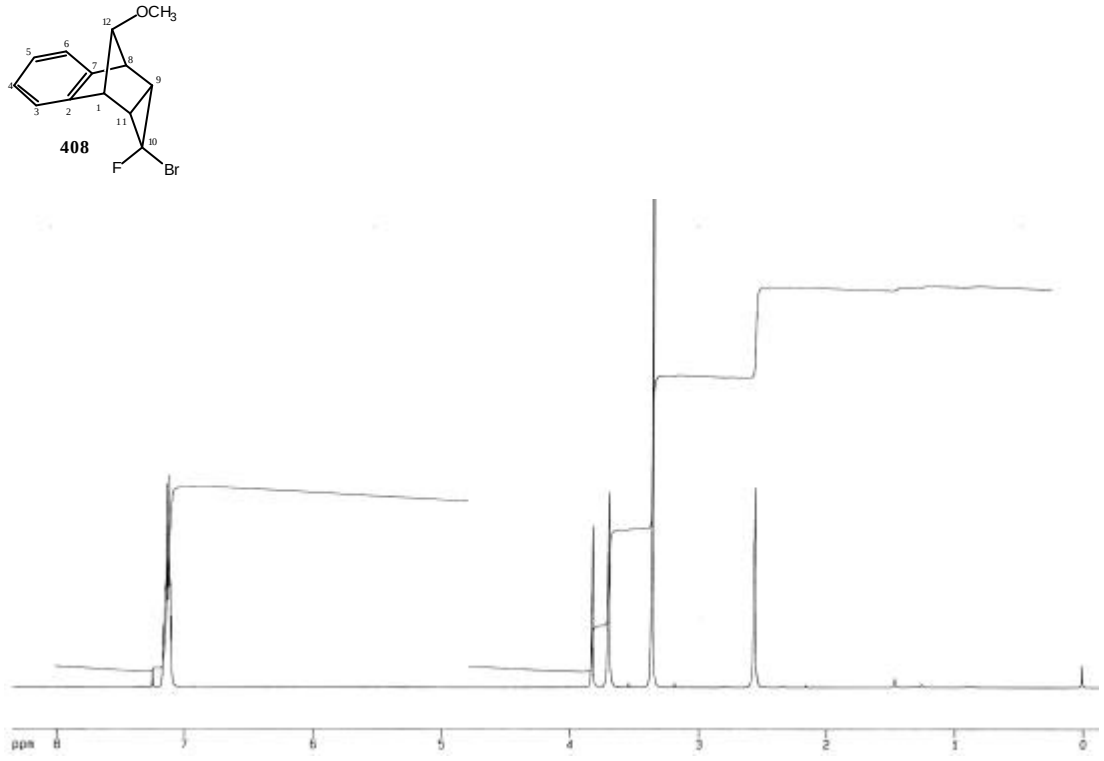

Figure A.73: ^{1}H-NMR spectrum of **408**

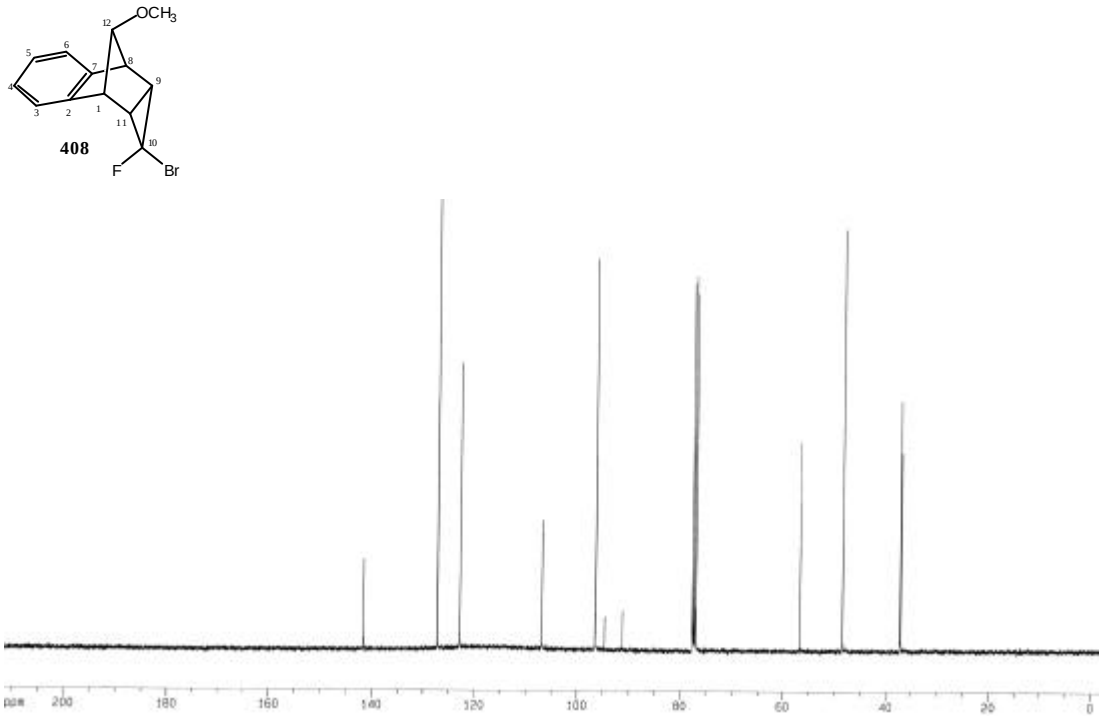

Figure A.74: ^{13}C-NMR spectrum of **408**

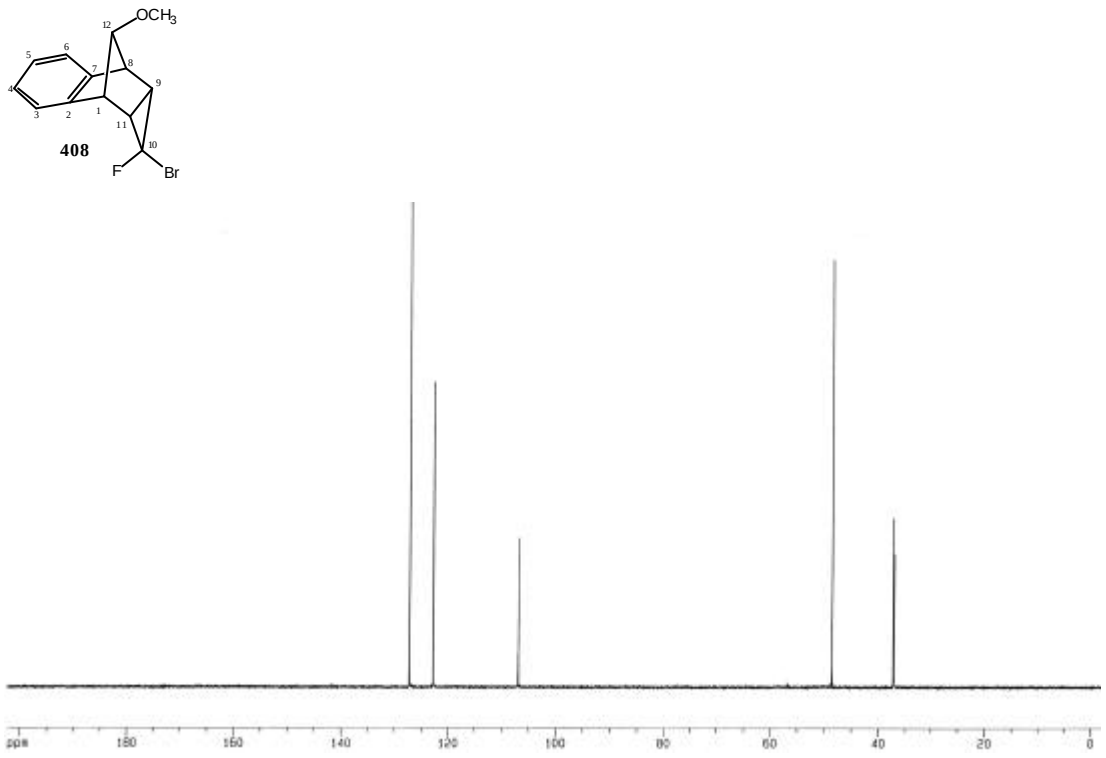

Figure A.75: DEPT-90 spectrum of **408**

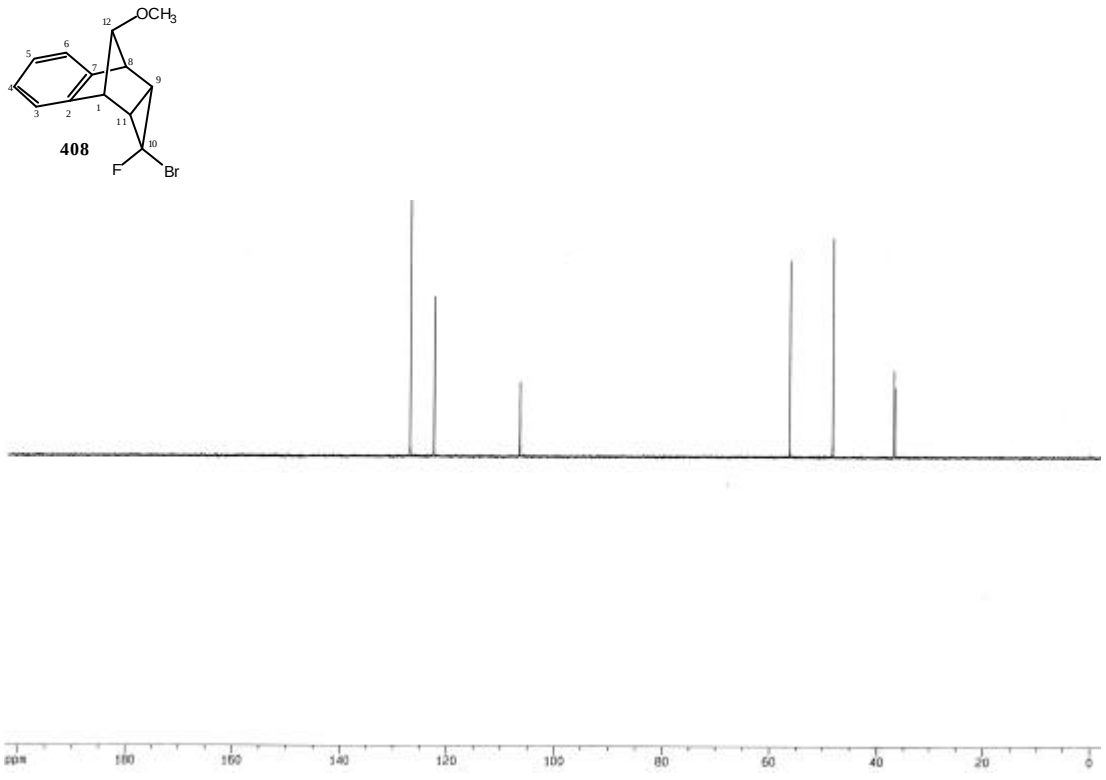

Figure A.76: DEPT-135 spectrum of **408**

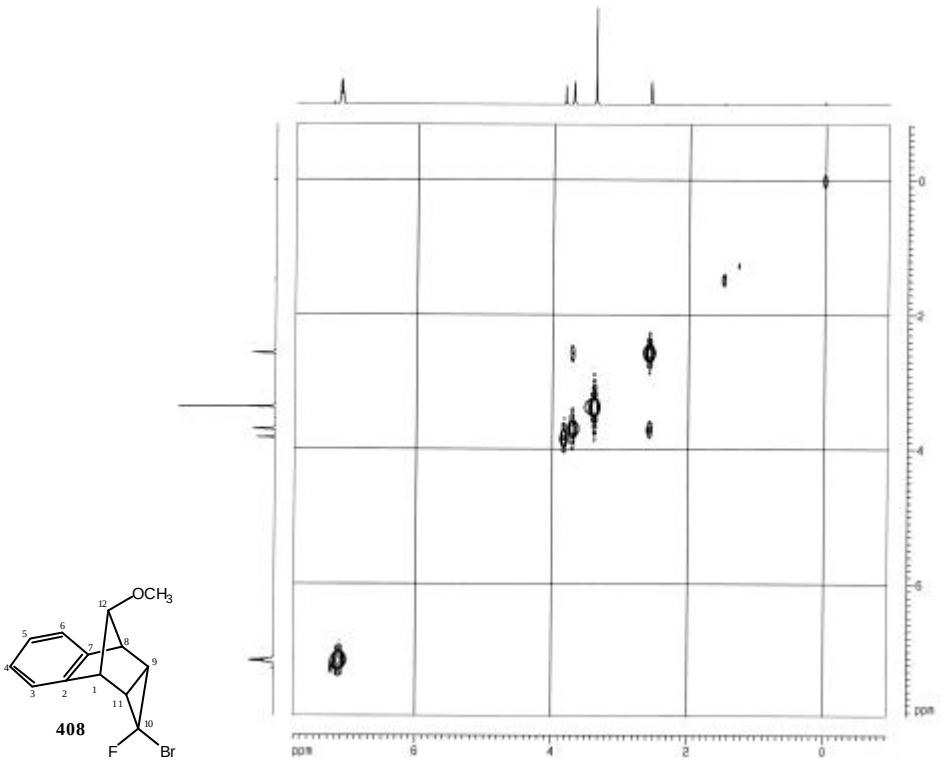

Figure A.77: COSY spectrum of **408**

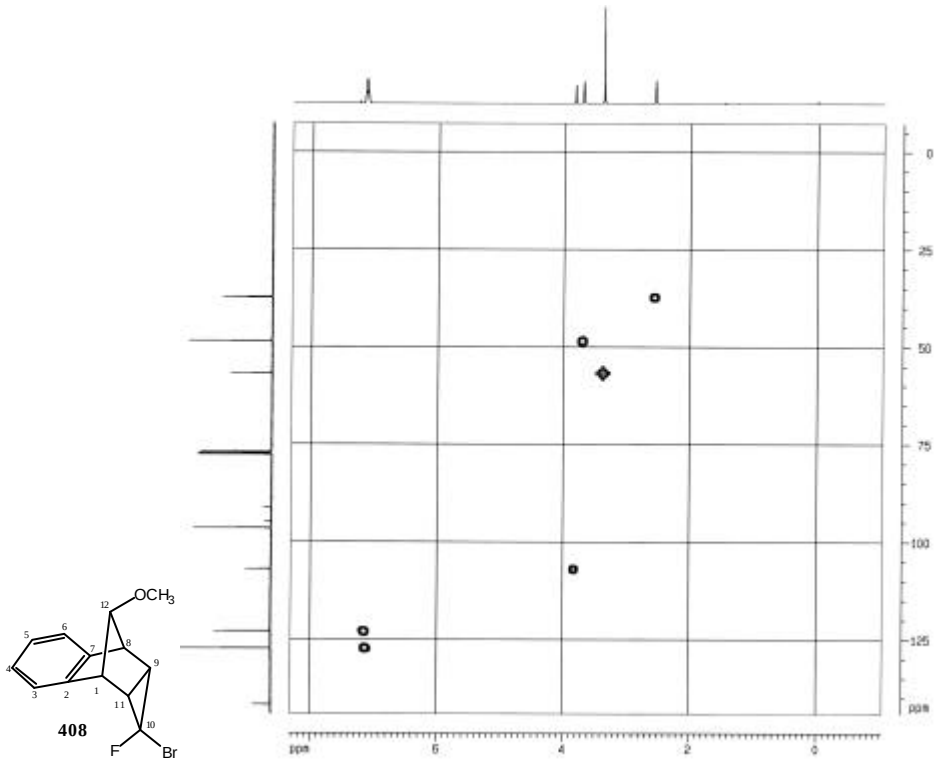

Figure A.78: HMQC spectrum of **408**

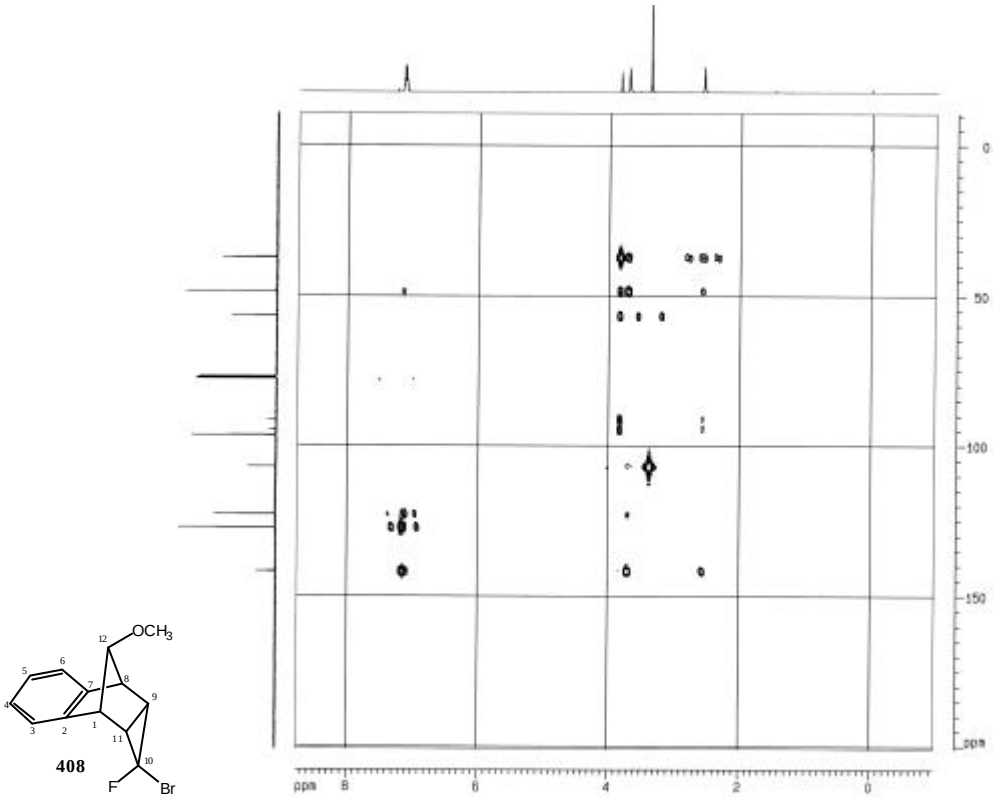

Figure A.79: HMBC spectrum of **408**

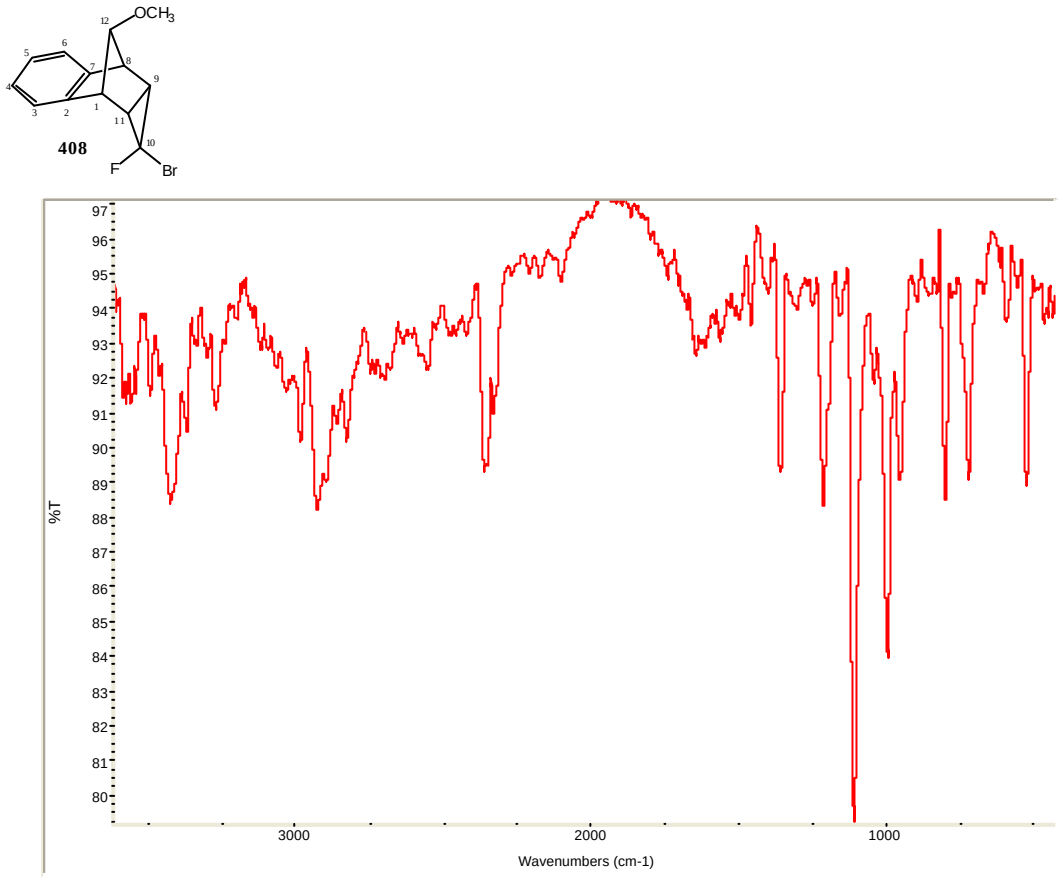

Figure A.80: IR-spectrum of **408**

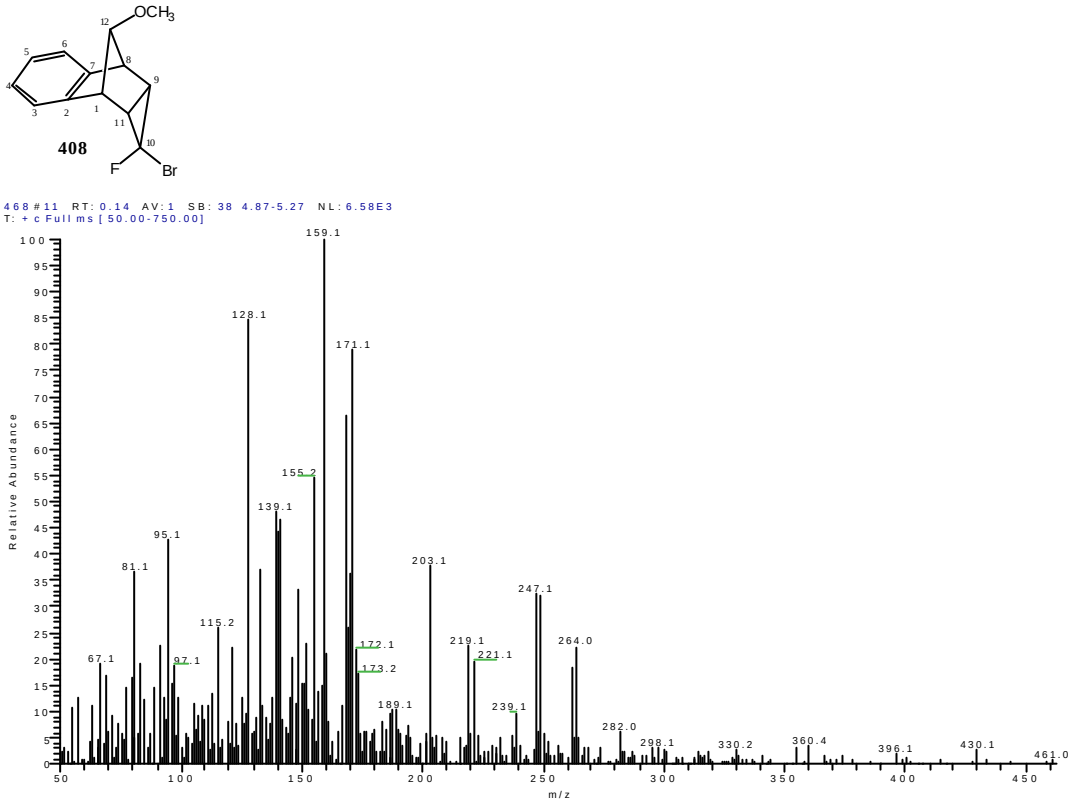

Figure A.81: GC/MS spectrum of **408**

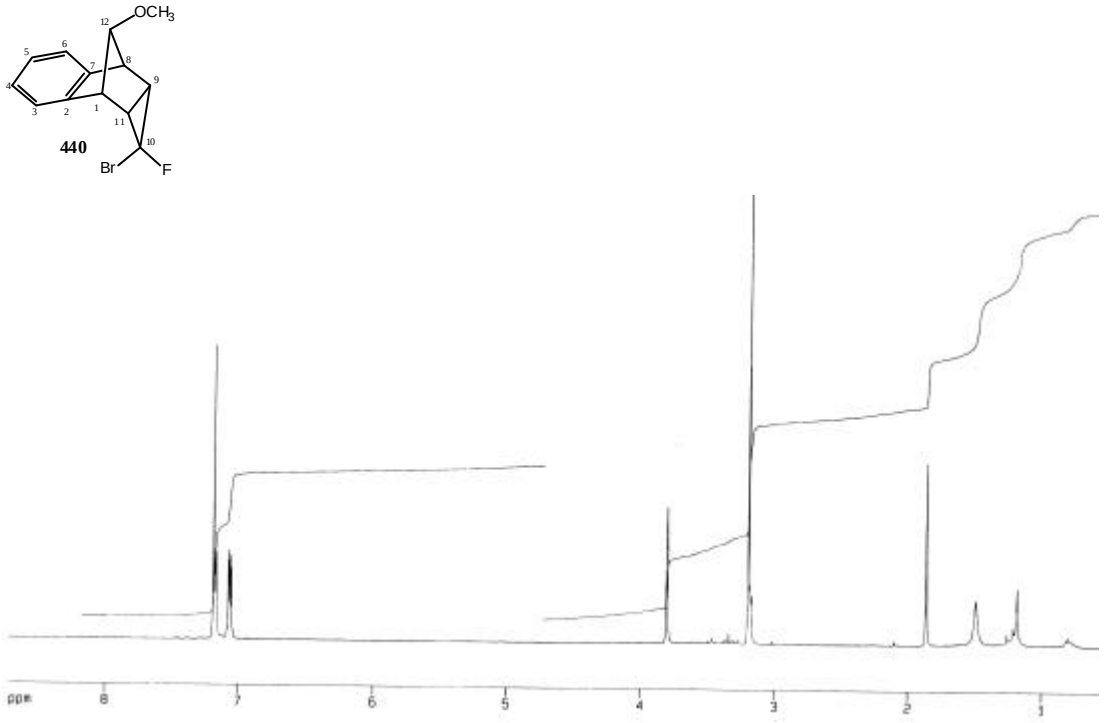

Figure A.82: ^{1}H-NMR spectrum of **440**

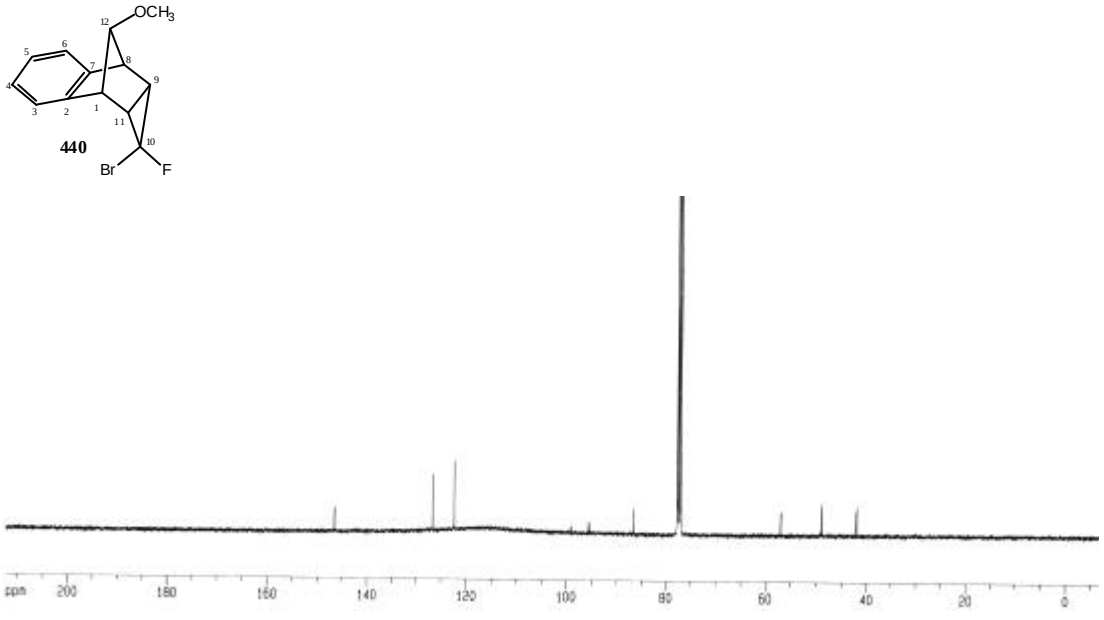

Figure A.83: ^{13}C-NMR spectrum of **440**

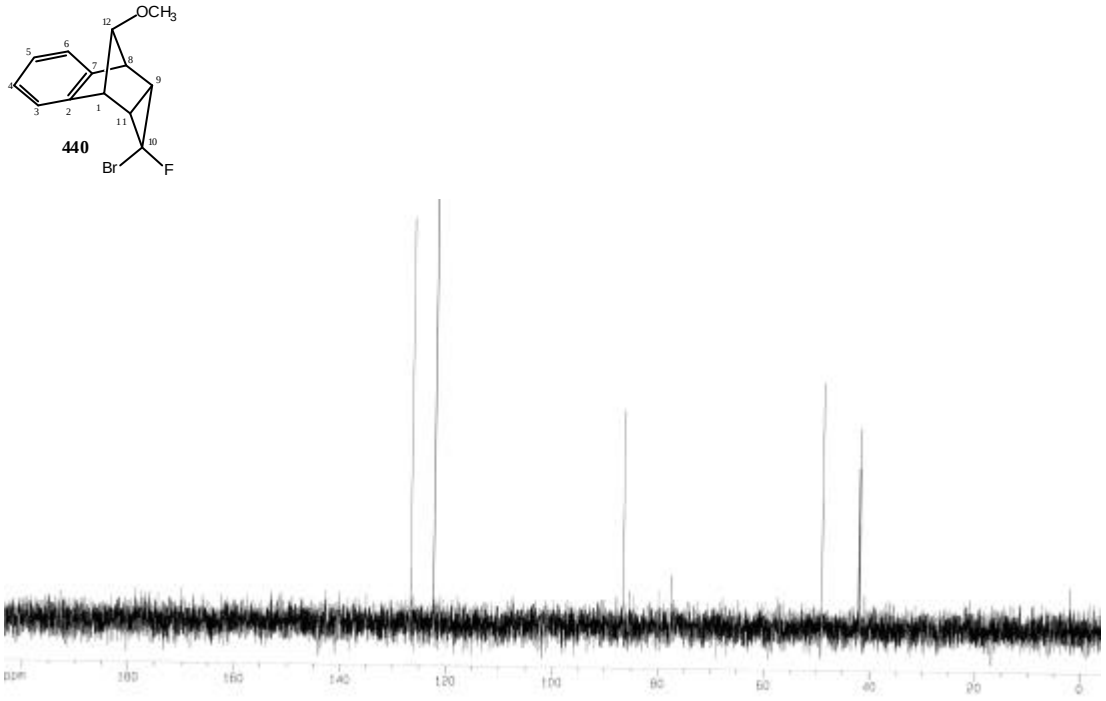

Figure A.84: DEPT-90 spectrum of **440**

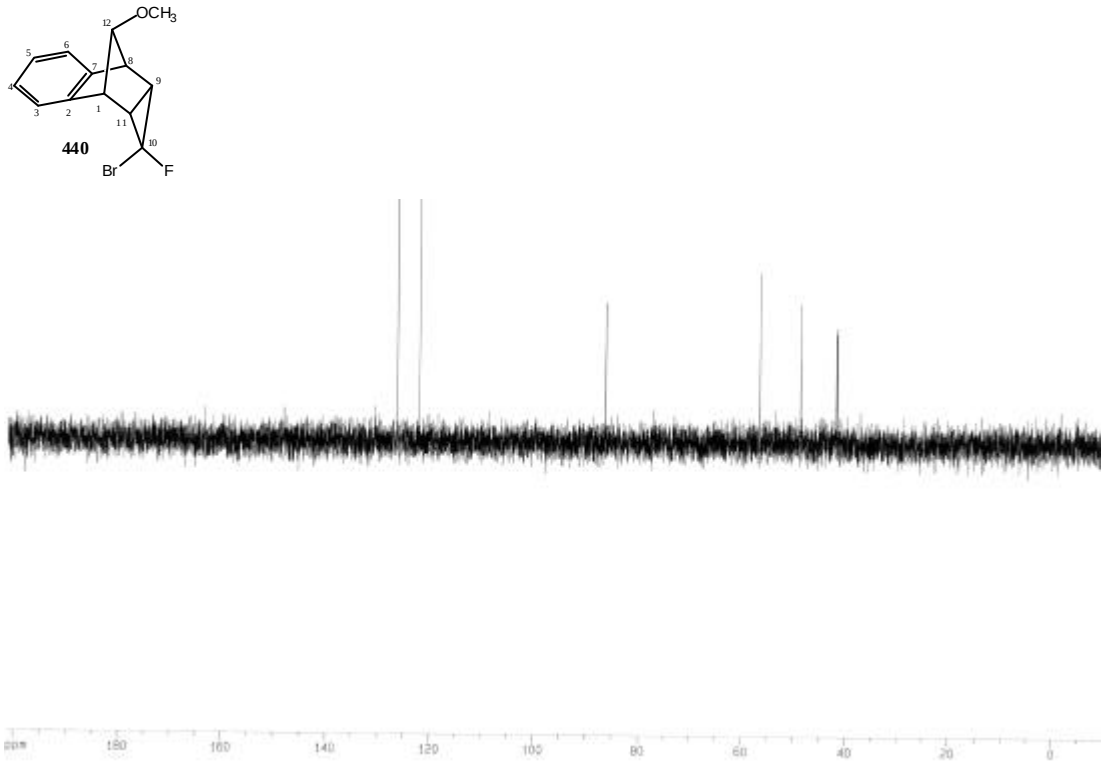

Figure A.85: DEPT-135 spectrum of **440**

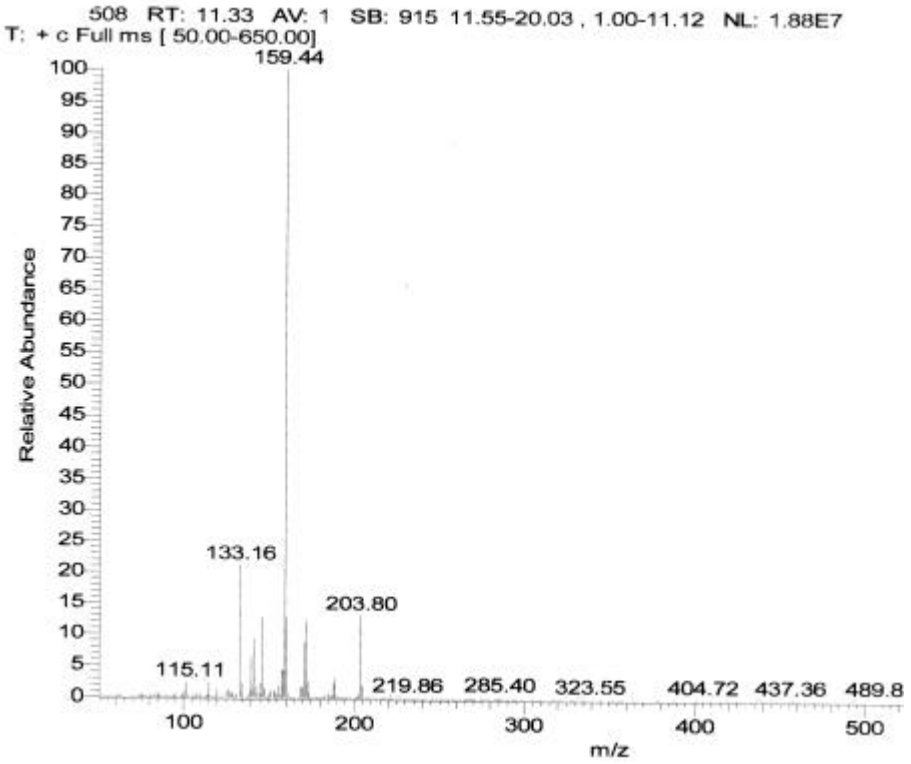

Figure A.86: Mass spectrum of **440**

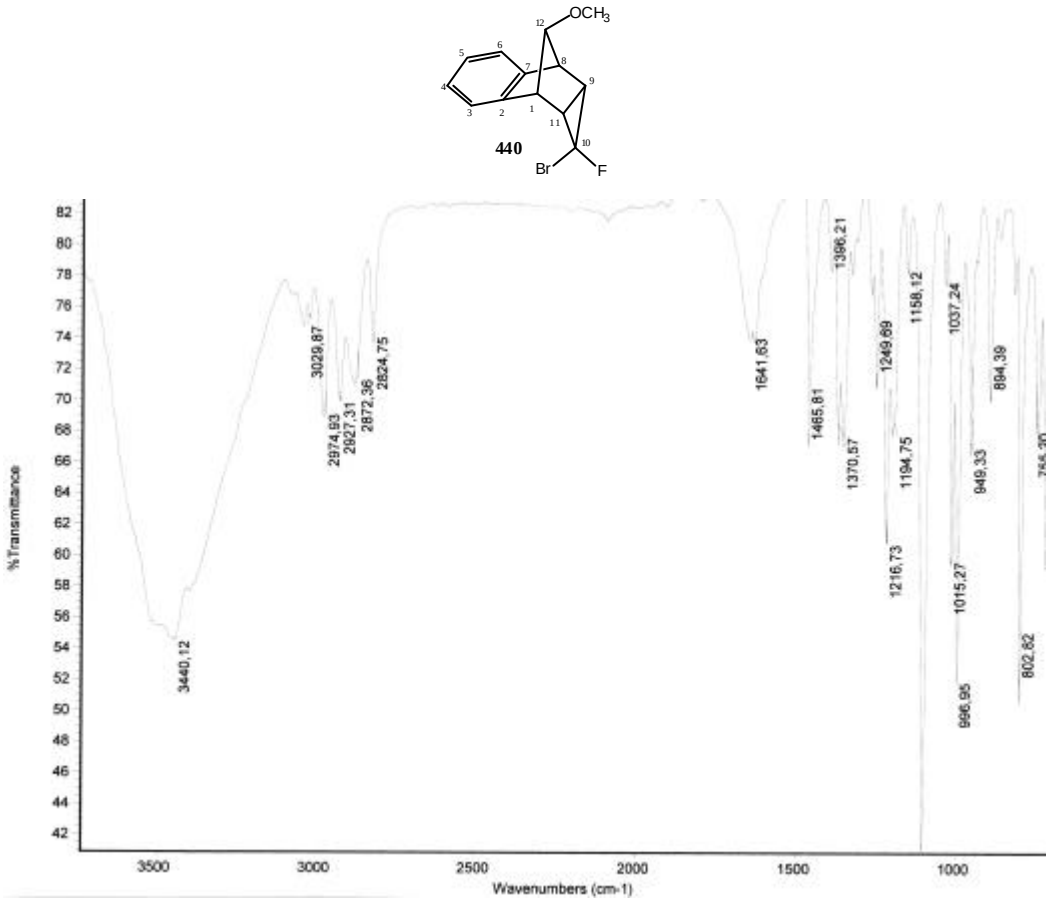

Figure A.87: IR spectrum of **440**

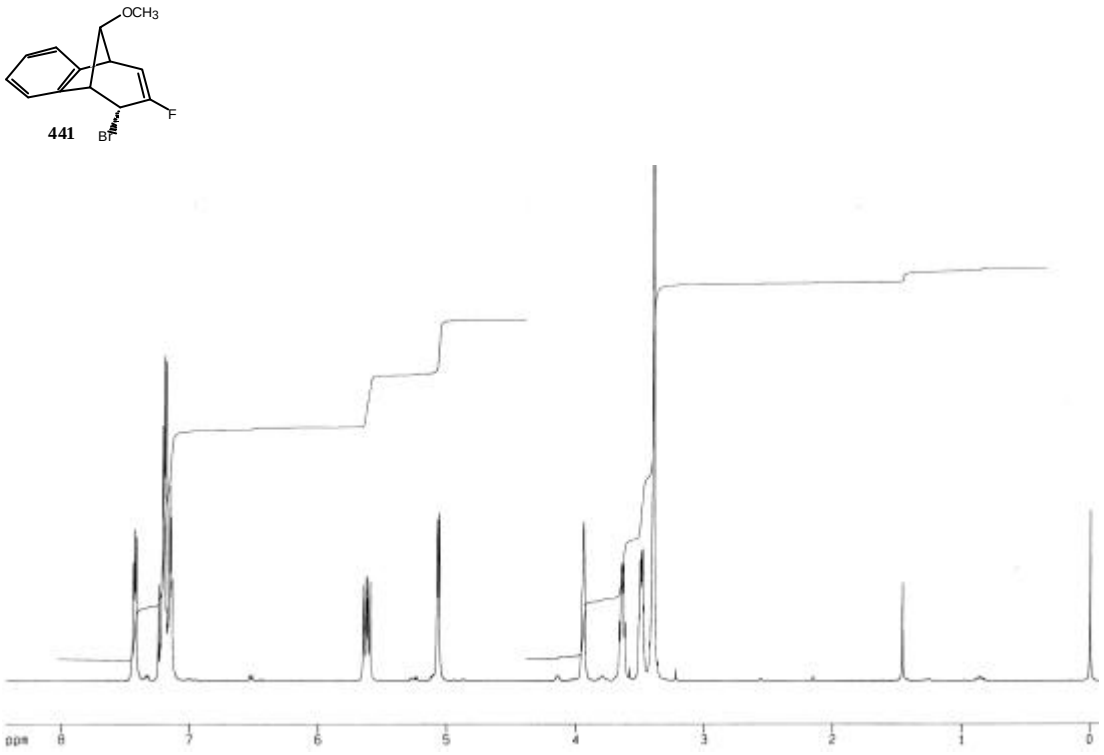

Figure A.88: ^{1}H-NMR spectrum of **441**

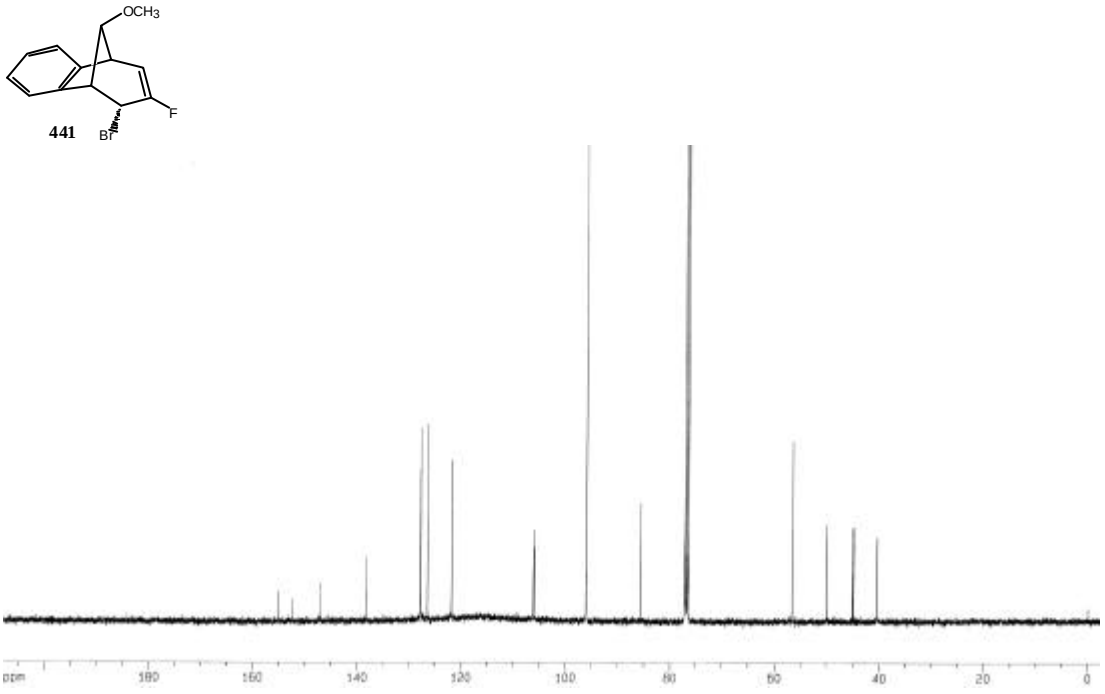

Figure A.89: ^{13}C-NMR spectrum of **441**

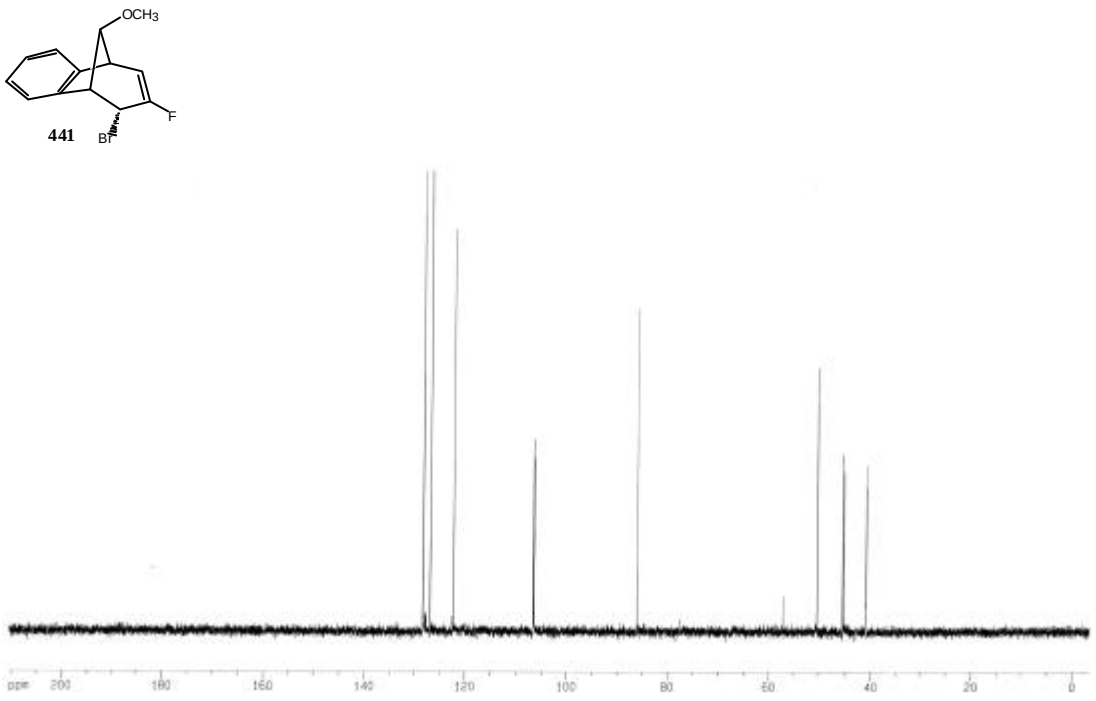

Figure A.90: DEPT-90 spectrum of **441**

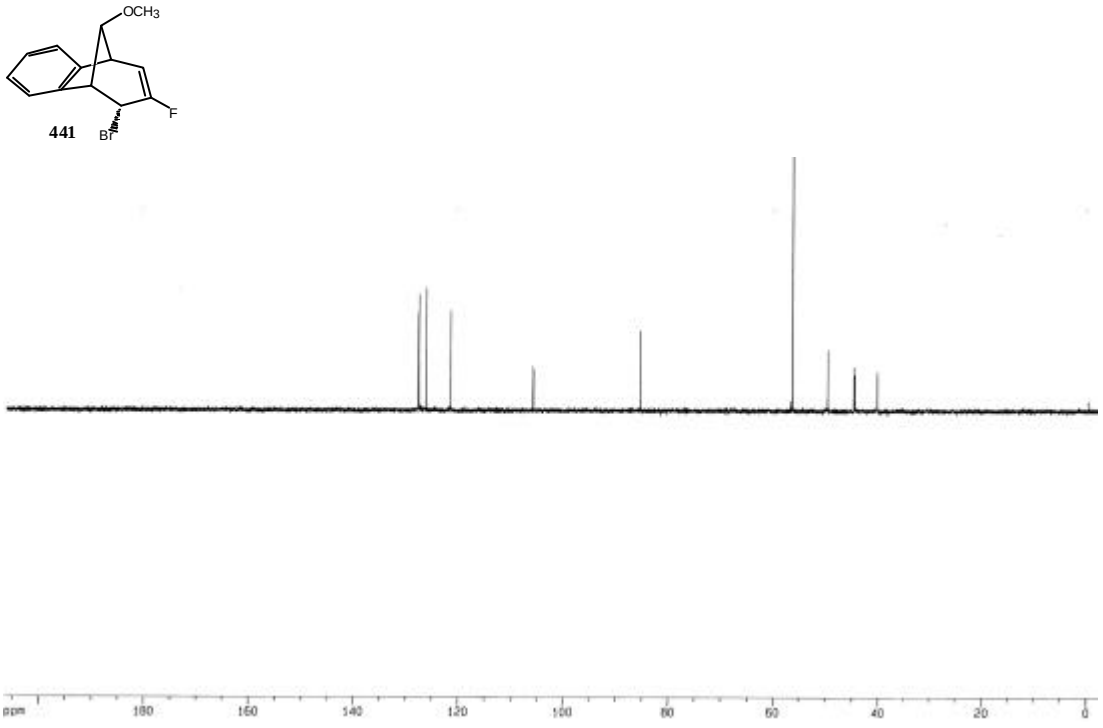

Figure A.91: DEPT-135 spectrum of **441**

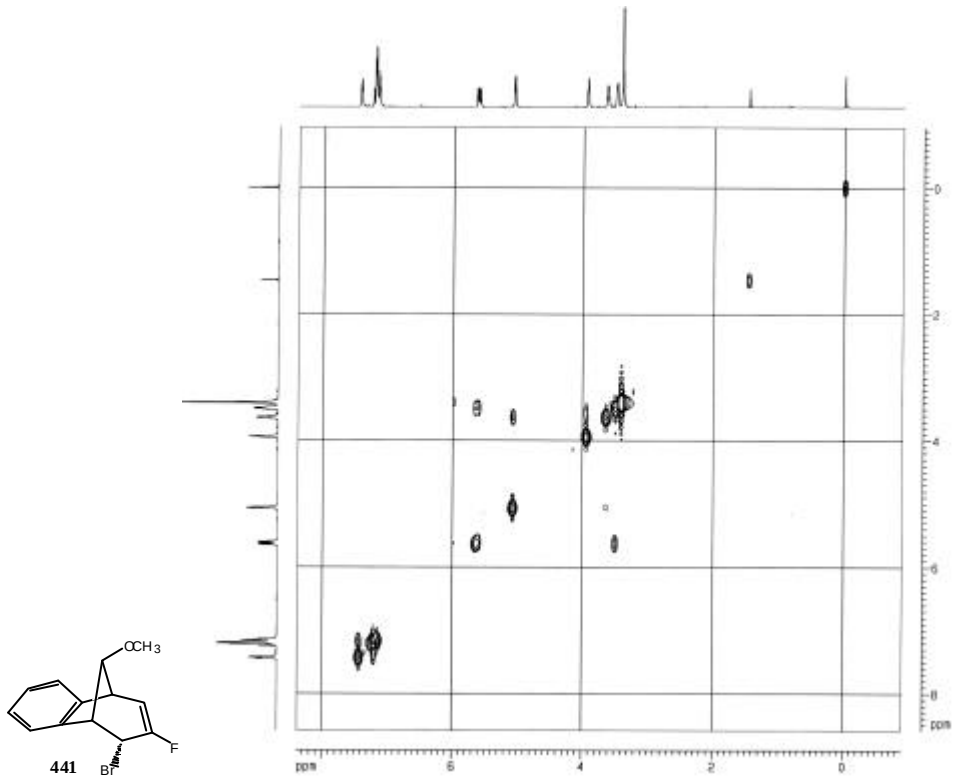

Figure A.92: COSY spectrum of **441**

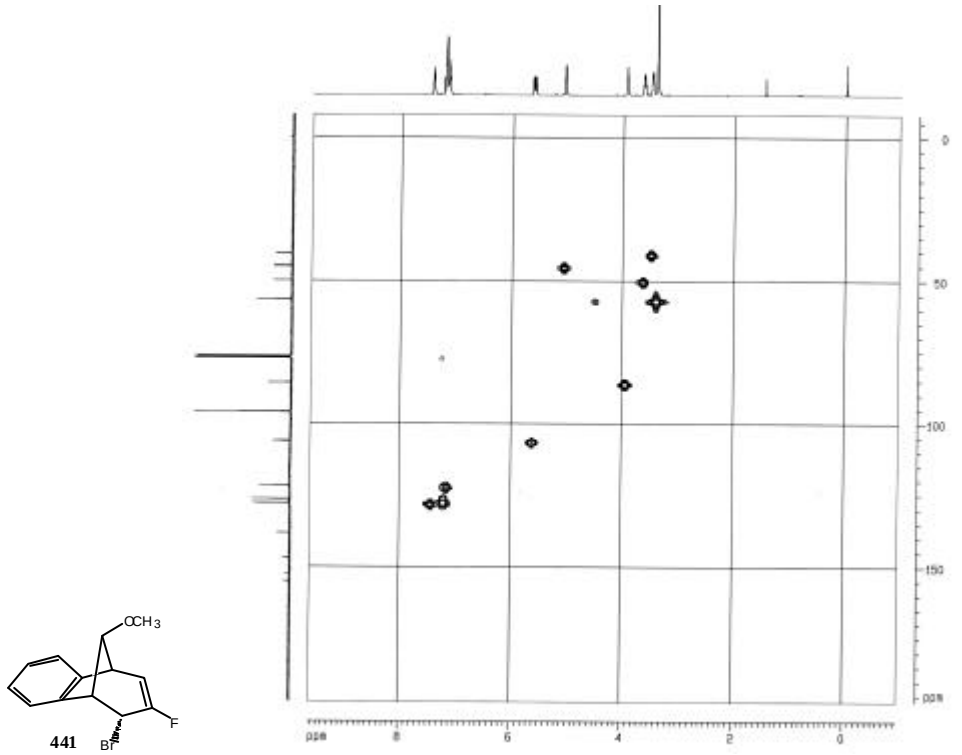

Figure A.93: HMQC spectrum of **441**

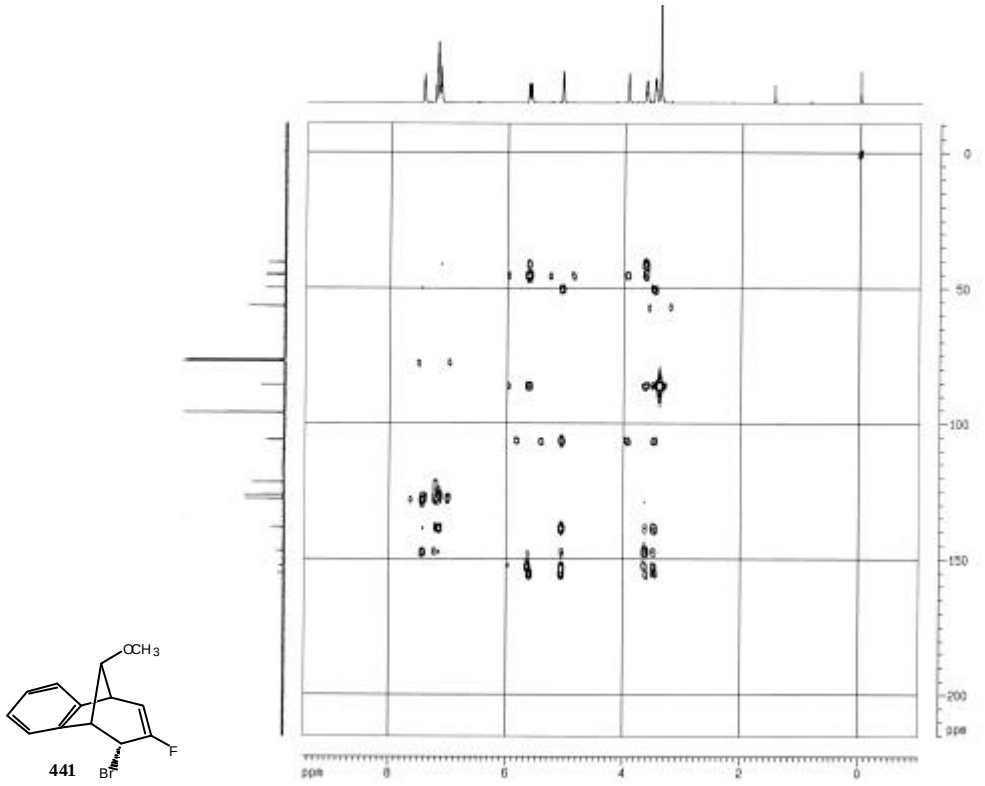

Figure A.94: HMBC spectrum of **441**

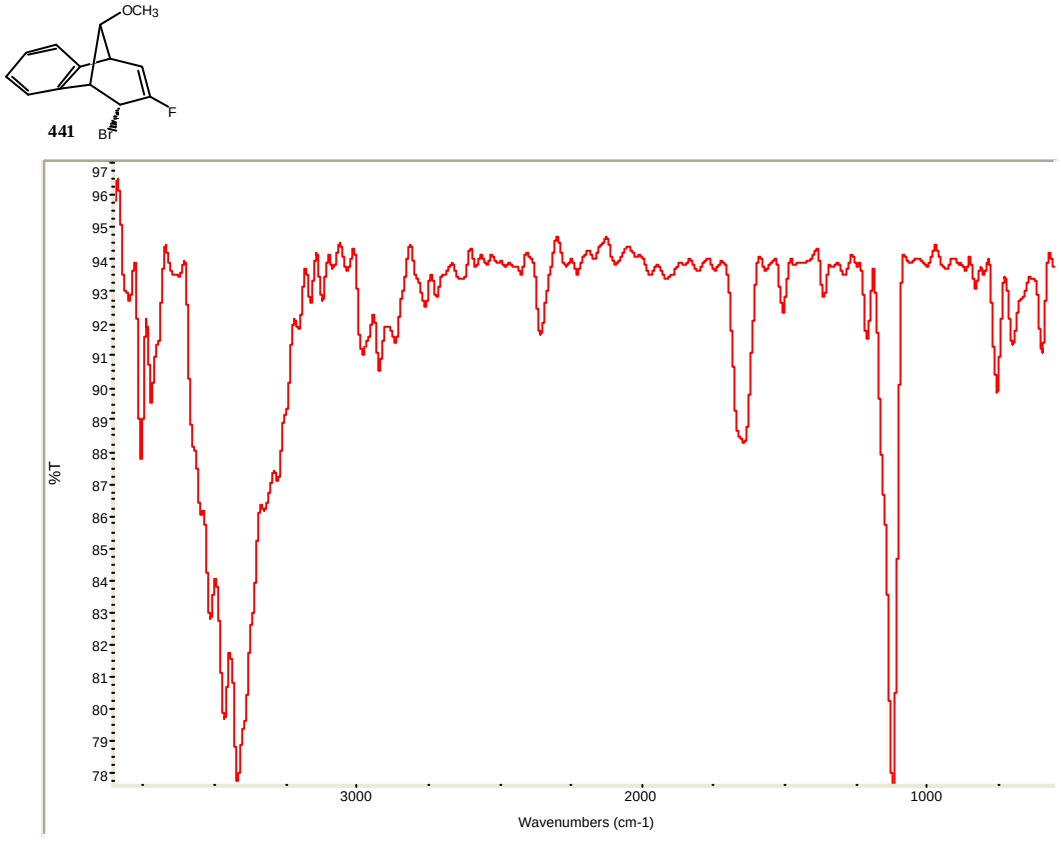

Figure A.95: IR-spectrum of **441**

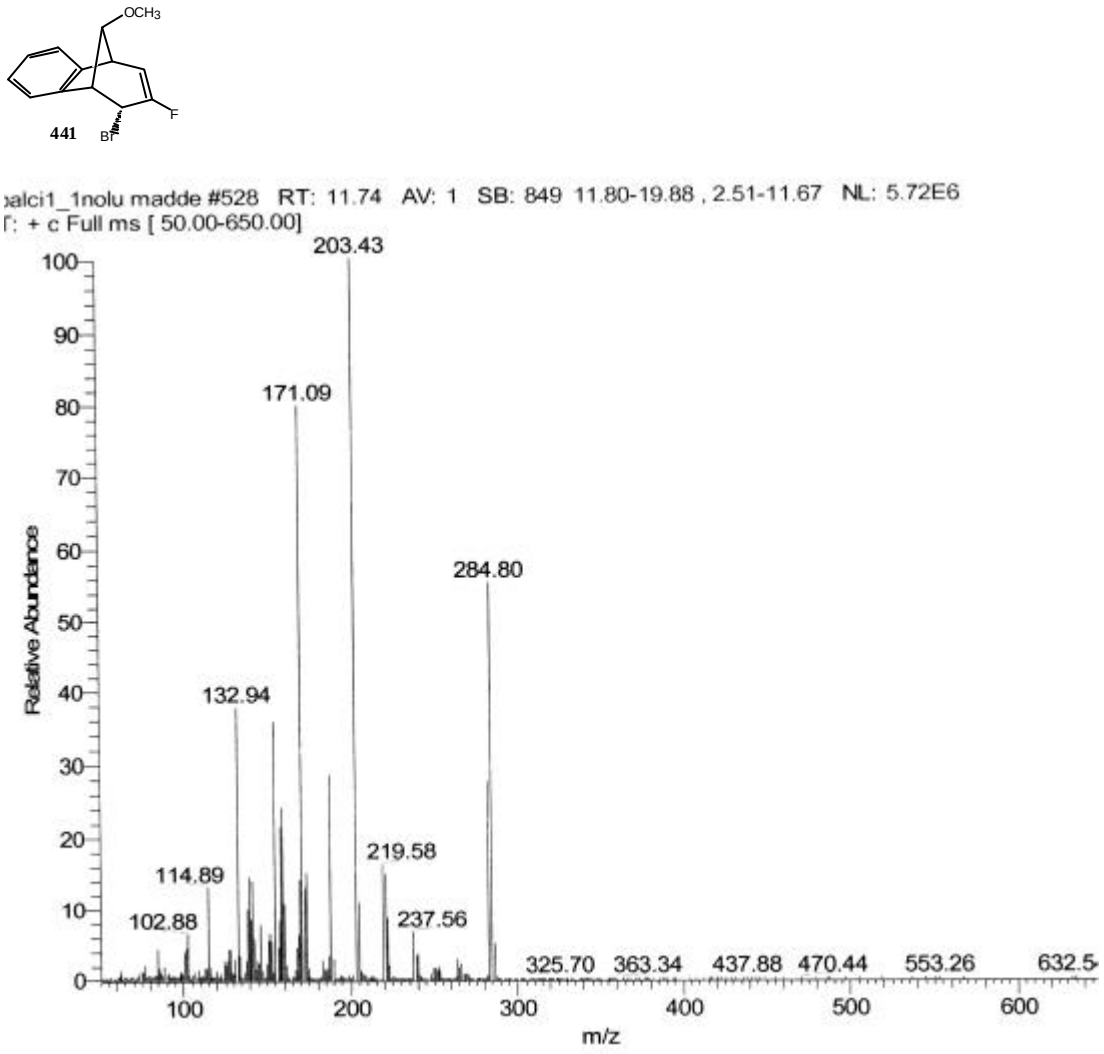

Figure A.96: Mass spectrum of **441**

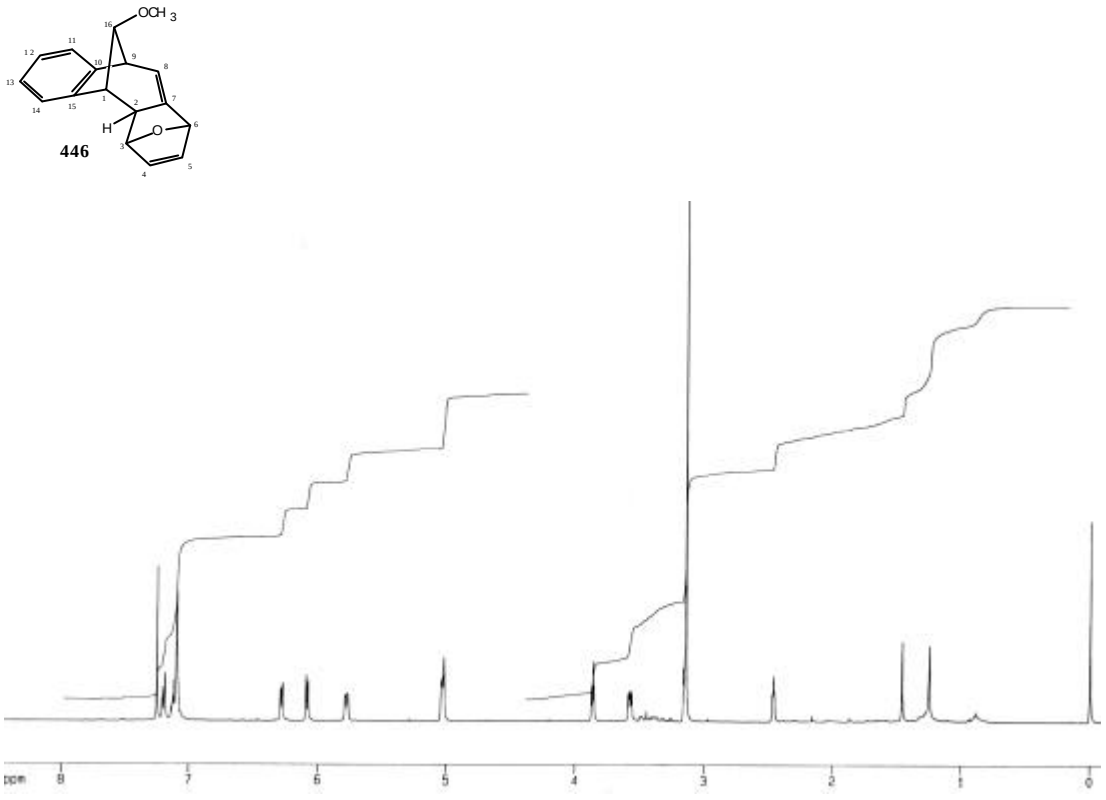

Figure A.97: ^{1}H-NMR spectrum of **446**

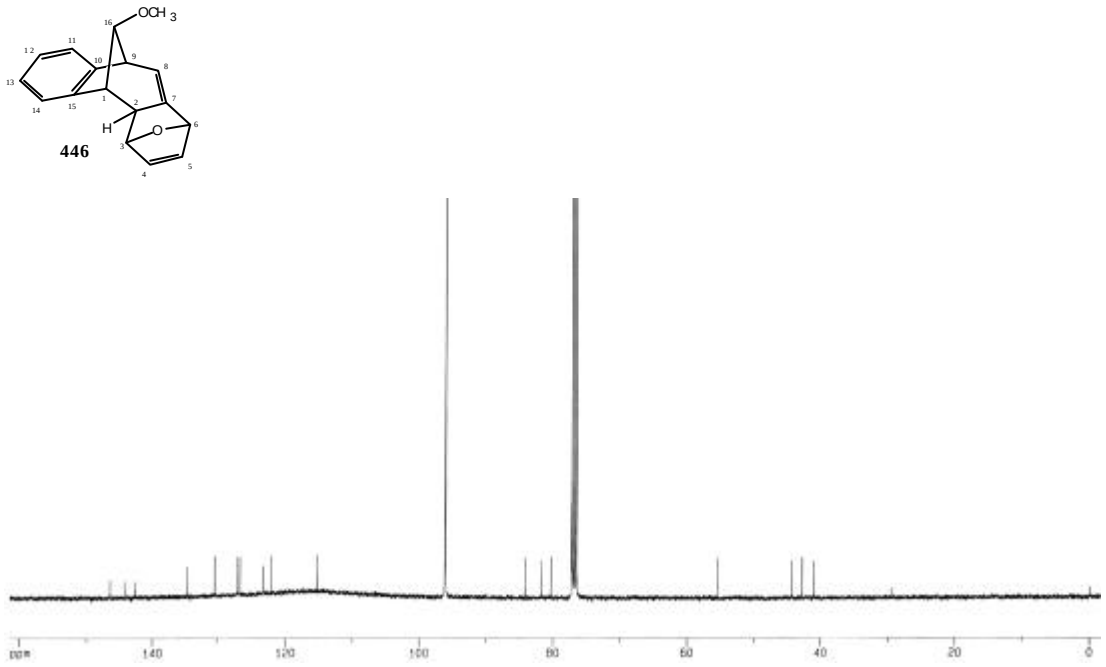

Figure A.98: ^{13}C-NMR spectrum of **446**

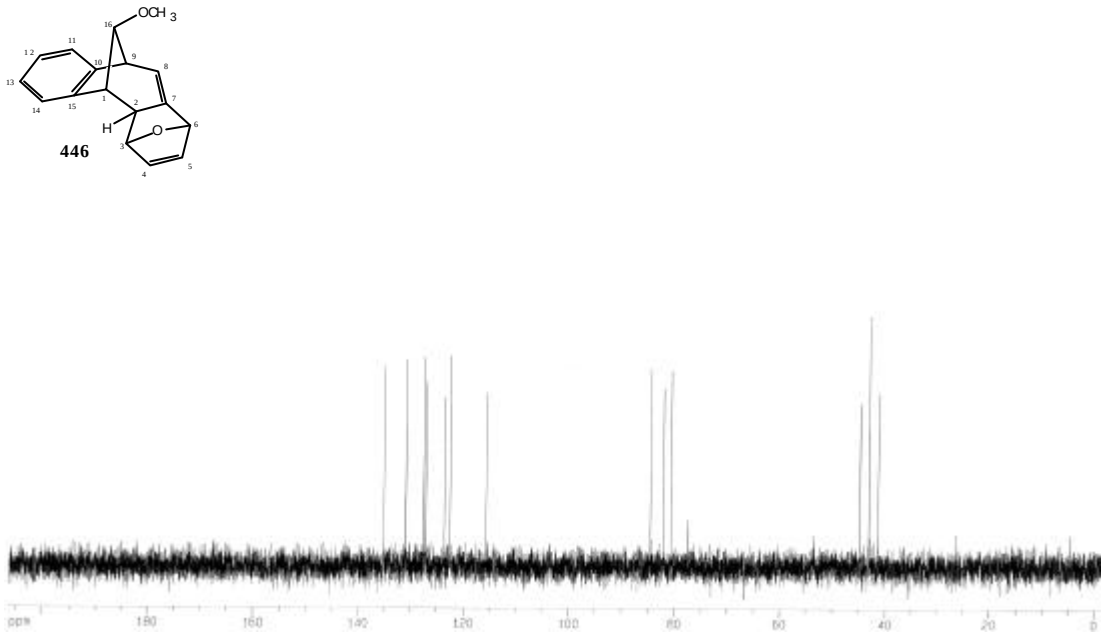

Figure A.99: DEPT-90 spectrum of **446**

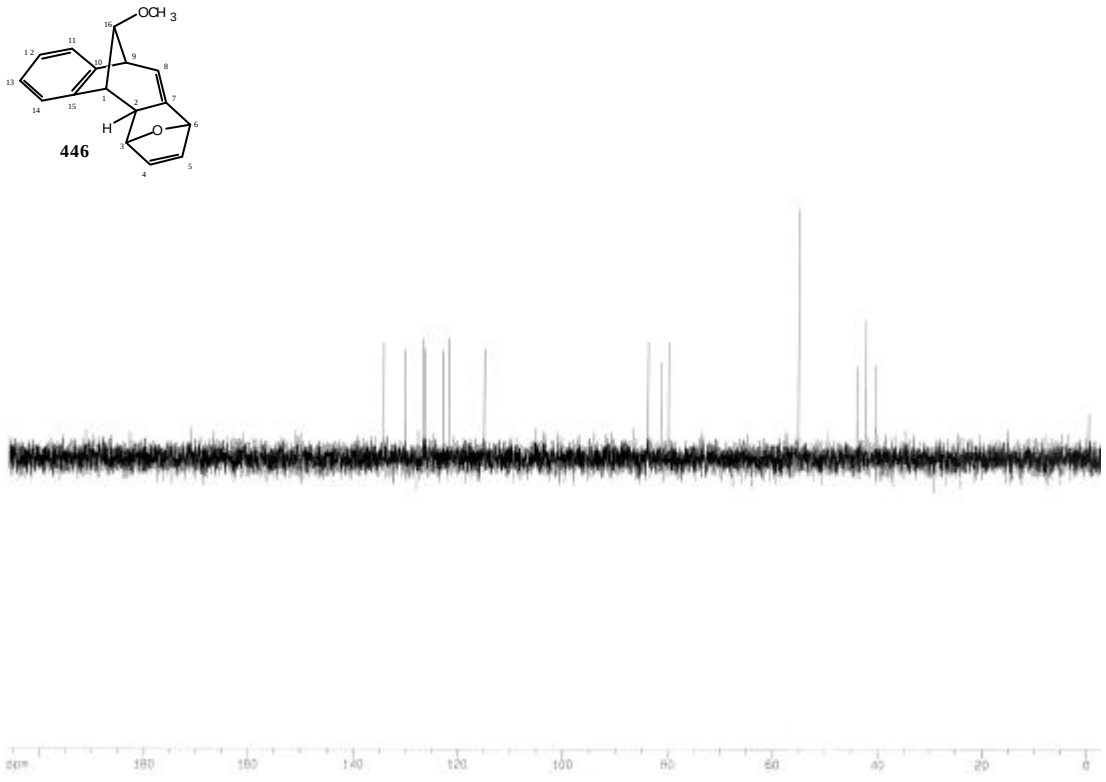

Figure A.100: DEPT-135 spectrum of **446**

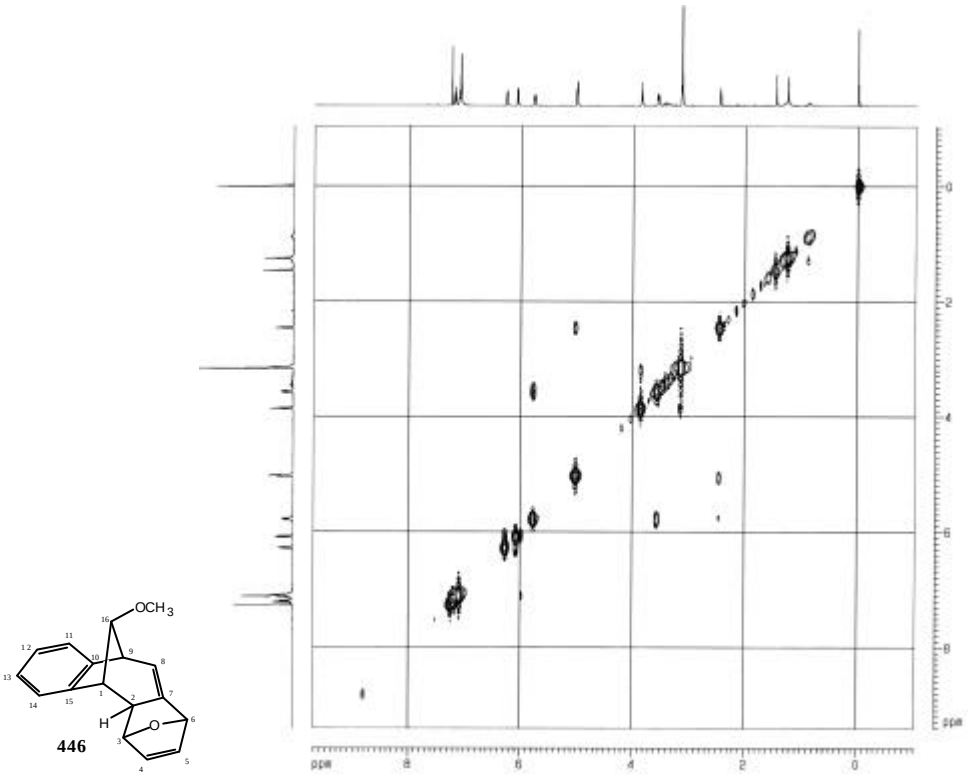

Figure A.101: COSY spectrum of **446**

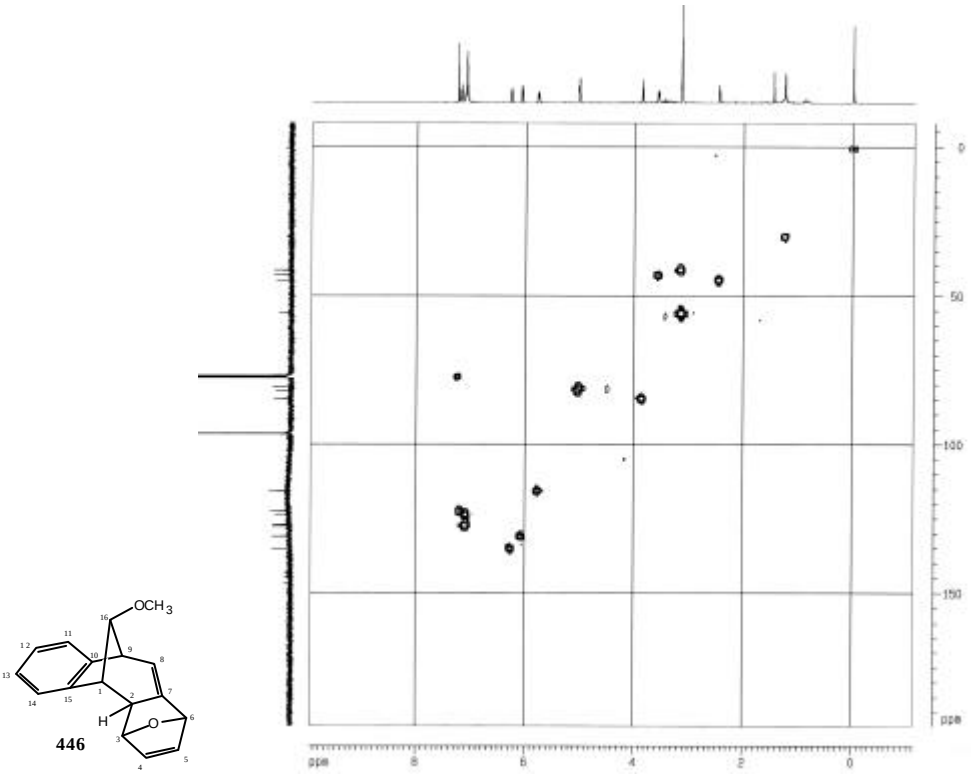

Figure A.102: HMQC spectrum of **446**

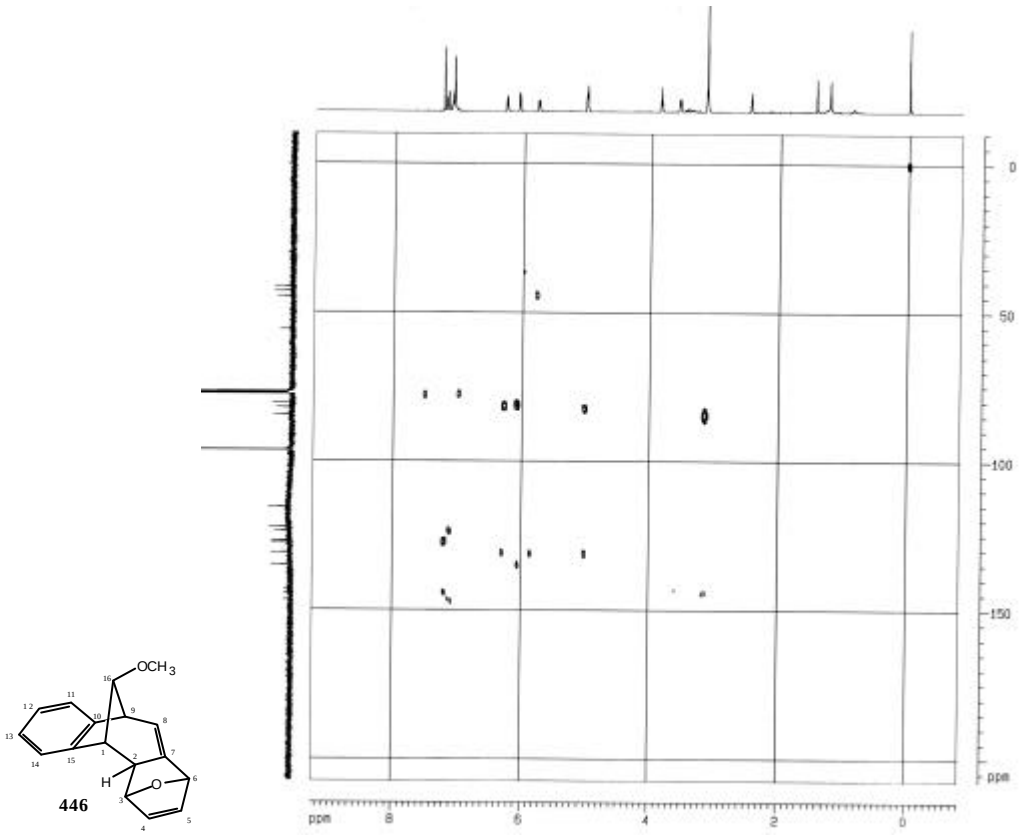

Figure A.103: HMBC spectrum of **446**

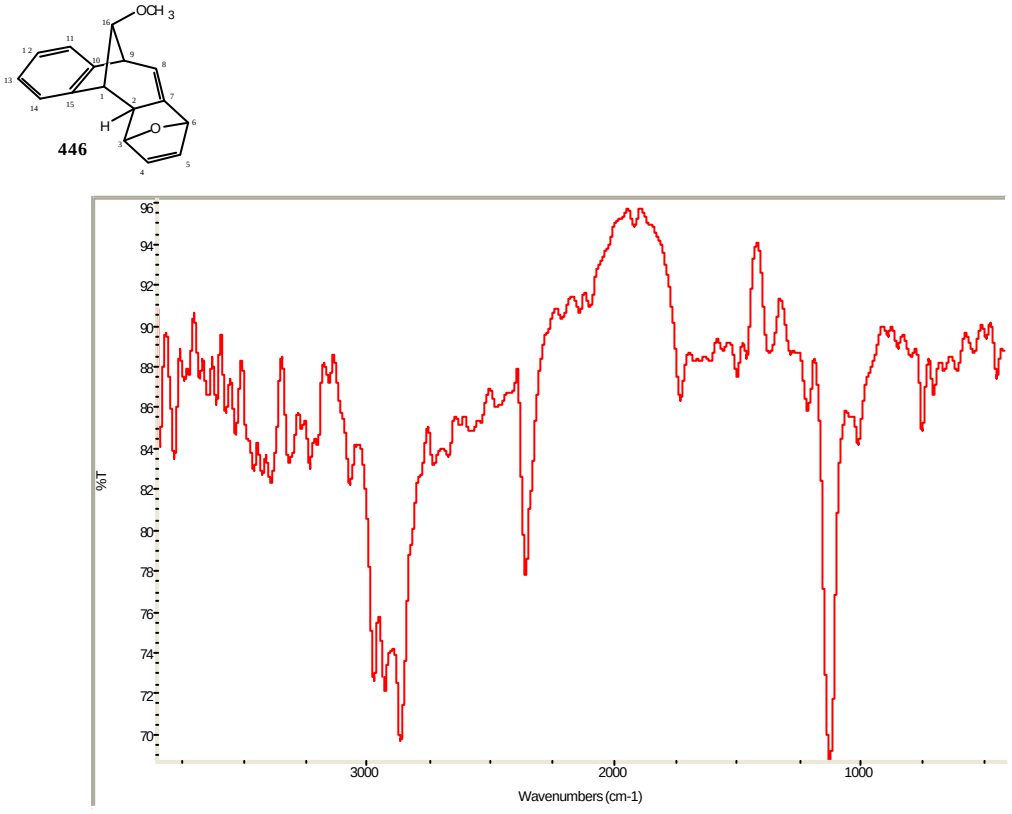

Figure A.104: IR-spectrum of **446**

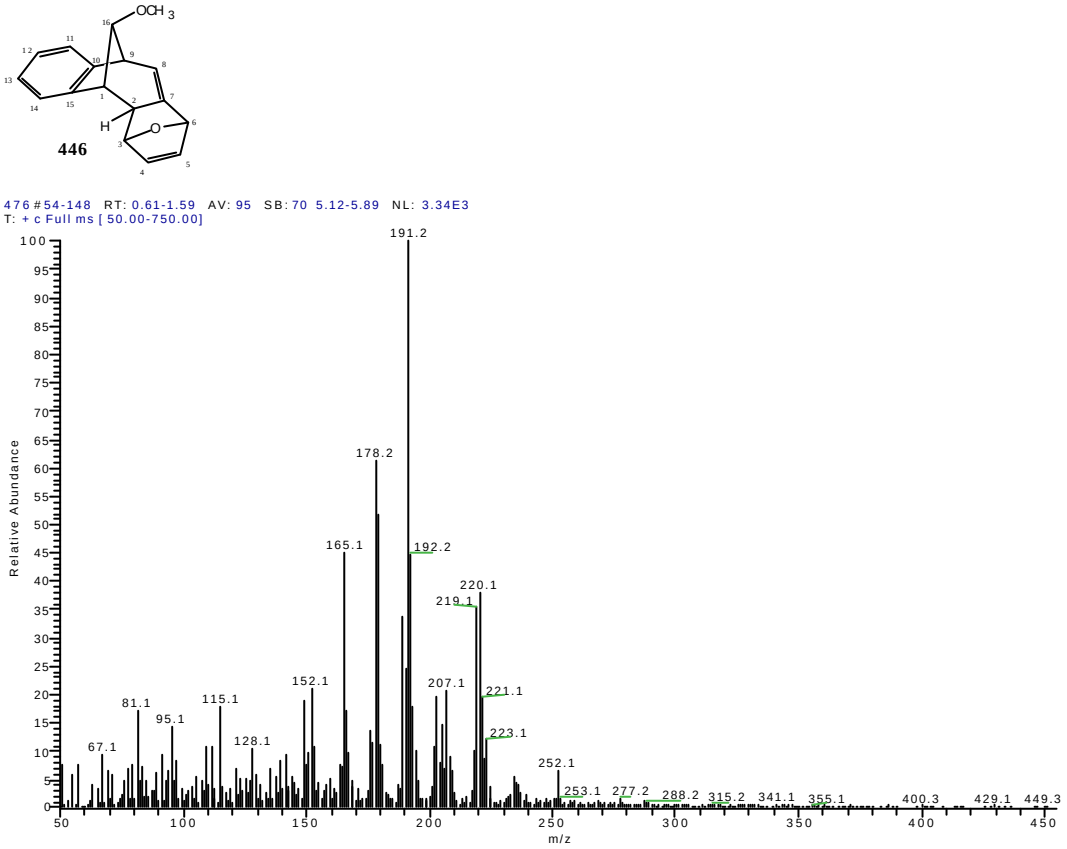

Figure A.105: Mass spectrum of **446**

APPENDIX B

THEORETICAL CALCULATION RESULTS OF THE STUDIED MOLECULES

Table B1: Cartesian Coordinates of the optimized structure and energy values for compound **399** by B3LYP/6-31 (d)

C	-1.220455	0.324497	0.102816
C	-0.064330	0.339990	-0.967156
C	-0.920740	-1.217975	0.205406
C	-0.405717	-1.158704	-1.256113
C	1.315998	0.419217	-0.295029
C	1.485864	-0.667827	0.721873
C	0.269550	-1.512098	1.135116
C	1.993341	1.775013	-0.217378
C	2.145552	-0.798741	-0.630956
C	-2.590903	0.598095	-0.537938
C	-1.097964	1.183532	1.364009
H	-0.132552	1.051254	-1.798288
H	-1.766097	-1.879611	0.430290
H	2.250668	-0.556968	1.497225
H	0.006379	-1.286009	2.175593
H	0.521217	-2.580669	1.091154
H	1.397012	2.486955	0.366190
H	2.979347	1.701475	0.255281
H	2.138099	2.190721	-1.222268
H	-1.187492	-1.280359	-2.007909
H	0.427554	-1.824601	-1.523949
H	-2.761608	0.025846	-1.454691
H	-3.397393	0.345412	0.162323
H	-2.691765	1.661502	-0.788531
H	-1.237177	2.245350	1.123478
H	-1.877626	0.911338	2.087382
H	-0.129741	1.078373	1.858819

E(RB+HF-LYP) = -428.61424 (Hartree/Particle)
Zero-point vibrational energy 629101.7 (Joules/Mol)
150.35890 (Kcal/Mol)
Zero-point correction= 0.239612 (Hartree/Particle)
Sum of electronic and zero-point Energies= -428.374624
Sum of electronic and thermal Energies= -428.363928
Sum of electronic and thermal Enthalpies= -428.362984
Sum of electronic and thermal Free Energies= -428.409169

Table B2: Cartesian Coordinates of the optimized structure and energy values for compound **372** by B3LYP/6-31 (d)

C	0.342921	-0.843101	-1.502259
C	0.097848	0.608136	-1.001048
C	0.809371	-1.255055	-0.070814
C	1.126867	0.272011	0.183790
C	2.565997	0.605902	-0.240695
C	0.895762	0.828560	1.589673
C	-1.275765	0.827707	-0.370794
C	-1.691685	-1.557155	0.293864
C	-0.300309	-1.927249	0.810951
C	-1.690227	2.223762	0.011234
H	1.164673	-0.881639	-2.221970
H	-0.516995	-1.365328	-1.927589
H	0.394394	1.426432	-1.670968
H	1.704874	-1.889292	-0.034077
H	3.285136	0.178452	0.470243
H	2.813652	0.219084	-1.234365
H	2.722393	1.692010	-0.258634
H	-0.125482	0.674979	1.946730
H	1.574739	0.336225	2.298546
H	1.112695	1.903423	1.631459
H	-2.355641	-2.354721	-0.038060
H	-0.187660	-3.017037	0.746640
H	-0.147998	-1.670686	1.866914
H	-0.874790	2.766025	0.505091
H	-1.957399	2.804629	-0.883023
H	-2.558023	2.214495	0.677488
C	-1.888877	-0.289695	-0.016305

E(RB+HF-LYP) = -428.69093 (Hartree/Particle)
Zero-point vibrational energy 634030.2 (Joules/Mol)
151.53685 (Kcal/Mol)
Zero-point correction= 0.241489 (Hartree/Particle)
Thermal correction to Energy= 0.252152
Thermal correction to Enthalpy= 0.253097
Thermal correction to Gibbs Free Energy= 0.206925
Sum of electronic and zero-point Energies= -428.449440
Sum of electronic and thermal Energies= -428.438777
Sum of electronic and thermal Enthalpies= -428.437833
Sum of electronic and thermal Free Energies= -428.484005

Table B3: Cartesian Coordinates of the optimized structure and energy values for compound **398** by B3LYP/6-31 (d)

C	-1.327235	0.296621	0.050141
C	-0.081639	0.612939	-0.817234
C	-0.825951	-1.198207	0.061345
C	0.074199	-0.881745	-1.210734
C	1.317498	0.515758	-0.144574
C	1.432257	-0.746471	0.713231
C	0.179704	-1.468945	1.187829
C	2.256577	1.680596	0.024146
C	1.559080	-0.856027	-0.779512
C	-2.605680	0.420436	-0.789672
C	-1.492339	1.041793	1.374333
H	-0.138342	1.404171	-1.574732
H	-1.605043	-1.962880	-0.025374
H	2.340475	-0.807009	1.310022
H	-0.185239	-1.134708	2.165613
H	0.393210	-2.543814	1.269340
H	2.359177	2.247829	-0.909954
H	1.900132	2.375870	0.796119
H	3.257836	1.344524	0.319919
H	-0.219683	-1.271725	-2.184990
H	-2.513333	-0.096808	-1.752082
H	-3.464083	-0.014062	-0.260982
H	-2.839024	1.472400	-0.998738
H	-1.784912	2.083645	1.189723
H	-2.274785	0.588044	1.997034
H	-0.566020	1.060025	1.956879
H	2.420807	-1.245995	-1.313589

E(RB+HF-LYP) = -428.718273204 (Hartree/Particle)
Zero-point vibrational energy 637249.3 (Joules/Mol)
152.30625 (Kcal/Mol)
Zero-point correction= 0.242715 (Hartree/Particle)
Thermal correction to Energy= 0.252504
Thermal correction to Enthalpy= 0.253448
Thermal correction to Gibbs Free Energy= 0.208927
Sum of electronic and zero-point Energies= -428.475558
Sum of electronic and thermal Energies= -428.465769
Sum of electronic and thermal Enthalpies= -428.464825
Sum of electronic and thermal Free Energies= -428.509346

Table B4: Cartesian Coordinates of the optimized structure and energy values for compound **400** by B3LYP/6-31 (d)

C	-1.285069	-0.262530	0.144310
C	-0.149205	-0.453201	-0.934578
C	-0.815898	1.243304	0.076889
C	-0.470510	0.989166	-1.417972
C	1.259204	-0.407070	-0.254061
C	1.779047	0.986805	0.051870
C	0.541325	1.399085	0.820187
C	2.240791	-1.490463	-0.649869
C	1.301870	0.142035	1.152886
C	-1.216080	-1.034274	1.485223
C	-2.696702	-0.475354	-0.434543
H	-0.235183	-1.290395	-1.638491
H	-1.531674	2.029419	0.344924
H	2.727863	1.473048	-0.135517
H	0.639763	2.234803	1.511330
H	2.430169	-1.476728	-1.730419
H	3.201738	-1.364164	-0.137384
H	1.852908	-2.485824	-0.399169
H	0.362449	1.564910	-1.831265
H	-1.000597	-0.375110	2.331701
H	-2.169961	-1.530932	1.697023
H	-0.444329	-1.810350	1.478028
H	-2.883658	-1.546876	-0.582787
H	-3.451929	-0.108139	0.272437
H	-2.873514	0.022977	-1.390865
H	-1.324384	1.054656	-2.093940
H	1.767701	-0.216313	2.062335

E(RB+HF-LYP) = -428.67802 (Hartree/Particle)
Zero-point vibrational energy 634661.7 (Joules/Mol)
151.68779 (Kcal/Mol)
Zero-point correction= 0.241730 (Hartree/Particle)
Thermal correction to Energy= 0.250974
Thermal correction to Enthalpy= 0.251919
Thermal correction to Gibbs Free Energy= 0.208520
Sum of electronic and zero-point Energies= -428.436286
Sum of electronic and thermal Energies= -428.427041
Sum of electronic and thermal Enthalpies= -428.426097
Sum of electronic and thermal Free Energies= -428.469496

Table B5: Cartesian Coordinates of the optimized structure and energy values for compound **401** by B3LYP/6-31 (d)

C	1.340470	-0.306535	0.075443
C	0.175378	-0.452414	-0.985270
C	0.874108	1.198477	0.165422
C	0.386574	1.057222	-1.304364
C	-1.130856	-0.586629	-0.236219
C	-1.408824	0.311832	0.936862
C	-0.333512	1.400540	1.115621
C	2.731529	-0.438140	-0.567821
C	1.324538	-1.178022	1.335560
C	-2.478136	-1.193563	-0.421636
C	-2.340908	0.296765	-0.239820
H	0.290184	-1.189297	-1.788102
H	1.652240	1.942822	0.375381
H	1.178620	1.238551	-2.034345
H	-0.497071	1.629373	-1.602477
H	-1.778344	-0.128338	1.870684
H	0.013818	1.375065	2.155257
H	-0.750468	2.404639	0.956377
H	2.852566	0.162761	-1.473397
H	3.509886	-0.126696	0.140309
H	2.931040	-1.483549	-0.835530
H	1.556260	-2.220207	1.080414
H	2.093959	-0.838721	2.041392
H	0.365292	-1.172451	1.855238
H	-2.922687	-1.801452	0.374737
H	-2.734278	-1.535377	-1.425274
H	-2.603180	1.085680	-0.933331

E(RB+HF-LYP) = -428.691339079 (Hartree/Particle)
Zero-point vibrational energy 638932.4 (Joules/Mol)
152.70852 (Kcal/Mol)
Zero-point correction= 0.243356 (Hartree/Particle)
Thermal correction to Energy= 0.253014
Thermal correction to Enthalpy= 0.253958
Thermal correction to Gibbs Free Energy= 0.209724
Sum of electronic and zero-point Energies= -428.447983
Sum of electronic and thermal Energies= -428.438325
Sum of electronic and thermal Enthalpies= -428.437381
Sum of electronic and thermal Free Energies= -428.481615

Table B6: Cartesian Coordinates of the optimized transition structure and energy values for **TS 399® 372** by B3LYP/6-31 (d)

C	-1.219038	0.291882	0.156131
C	-0.071702	0.404825	-0.919762
C	-0.963649	-1.248953	0.042271
C	-0.457940	-1.017760	-1.401767
C	1.350390	0.484040	-0.365284
C	1.572603	-0.963102	0.613506
C	0.230738	-1.666988	0.893189
C	1.835706	1.902833	-0.097002
C	2.399037	-0.492660	-0.465208
C	-2.583391	0.699344	-0.422900
C	-1.050676	0.960523	1.521304
H	-0.165052	1.223002	-1.644708
H	-1.817357	-1.916926	0.211170
H	2.219098	-1.120100	1.487912
H	-0.000362	-1.552176	1.959351
H	0.431226	-2.738807	0.742690
H	1.259554	2.388844	0.698973
H	2.891161	1.897680	0.184379
H	1.722223	2.509678	-1.006116
H	-1.256233	-1.003956	-2.146454
H	-2.796972	0.237538	-1.391458
H	-3.390808	0.413446	0.263030
H	-2.634637	1.787310	-0.556530
H	-1.177063	2.047477	1.441910
H	-1.814692	0.595897	2.220217
H	-0.071021	0.771549	1.967966
H	0.348475	-1.664356	-1.759204

E(RB+HF-LYP) = -428.603702347 (Hartree/Particle)
****** 1 imaginary frequencies (negative Signs) ******
Zero-point vibrational energy 628111.1 (Joules/Mol)
150.12215 (Kcal/Mol)
Zero-point correction= 0.239235 (Hartree/Particle)
Thermal correction to Energy= 0.249613
Thermal correction to Enthalpy= 0.250557
Thermal correction to Gibbs Free Energy= 0.204634
Sum of electronic and zero-point Energies= -428.364468
Sum of electronic and thermal Energies= -428.354089
Sum of electronic and thermal Enthalpies= -428.353145
Sum of electronic and thermal Free Energies= -428.399068

Table B7: Cartesian Coordinates of the optimized transition structure and energy values for **TS 399® 398** by B3LYP/6-31 (d)

C	-1.291801	0.311329	0.070582
C	-0.076151	0.503638	-0.893778
C	-0.861611	-1.212336	0.119519
C	-0.147096	-0.991705	-1.226653
C	1.302046	0.477846	-0.229538
C	1.448990	-0.690910	0.727965
C	0.226305	-1.475315	1.176417
C	2.142403	1.725465	-0.091868
C	1.923084	-0.858679	-0.691392
C	-2.620417	0.475881	-0.678663
C	-1.317778	1.108597	1.373728
H	-0.155151	1.247991	-1.694004
H	-1.664924	-1.956065	0.154878
H	2.265004	-0.610940	1.447576
H	-0.113823	-1.193599	2.180799
H	0.461240	-2.548005	1.203587
H	2.240218	2.240113	-1.056476
H	1.708767	2.434096	0.626447
H	3.154483	1.477237	0.248728
H	-0.526463	-1.388418	-2.169063
H	-2.625800	-0.062874	-1.633731
H	-3.456226	0.092826	-0.079167
H	-2.819271	1.533508	-0.892342
H	-1.545132	2.162316	1.168280
H	-2.094120	0.731970	2.052249
H	-0.359847	1.072740	1.899588
H	1.163197	-1.475756	-1.395258

E(RB+HF-LYP) = -428.60140 (Hartree/Particle)
****** 1 imaginary frequencies (negative Signs) ******
Zero-point vibrational energy 621844.9 (Joules/Mol)
148.62451 (Kcal/Mol)
Zero-point correction= 0.236848 (Hartree/Particle)
Thermal correction to Energy= 0.246799
Thermal correction to Enthalpy= 0.247743
Thermal correction to Gibbs Free Energy= 0.203017
Sum of electronic and zero-point Energies= -428.364554
Sum of electronic and thermal Energies= -428.354603
Sum of electronic and thermal Enthalpies= -428.353659
Sum of electronic and thermal Free Energies= -428.398385

Table B8: Cartesian Coordinates of the optimized transition structure and energy values for **TS 399® 400** by B3LYP/6-31 (d)

C	1.274687	0.274340	0.156663
C	0.133336	0.451489	-0.923602
C	0.843265	-1.241782	0.077268
C	0.485380	-0.977823	-1.415301
C	-1.269532	0.411507	-0.261776
C	-2.130307	-0.897684	-0.100045
C	-0.500242	-1.482936	0.815098
C	-2.182402	1.593796	-0.530980
C	-1.389084	-0.288974	1.046356
C	1.228808	1.032569	1.490015
C	2.683840	0.513702	-0.421111
H	0.213800	1.287141	-1.628259
H	1.574370	-2.019405	0.326957
H	-0.526079	-2.214667	1.624379
H	-2.295488	1.764917	-1.607900
H	-3.182400	1.426416	-0.113449
H	-1.781584	2.512325	-0.082057
H	-0.330952	-1.564266	-1.845725
H	2.016292	0.661062	2.158749
H	1.429277	2.098329	1.319575
H	0.281239	0.957421	2.019183
H	2.854645	1.589141	-0.555234
H	3.446660	0.148041	0.278099
H	2.865472	0.032251	-1.384617
H	1.343317	-1.022007	-2.086704
H	-1.768409	0.033524	2.012905
H	-1.206648	-2.019454	-0.031417

E(RB+HF-LYP) = -428.58417 (Hartree/Particle)
****** 1 imaginary frequencies (negative Signs) ******
Zero-point vibrational energy 623472.8 (Joules/Mol)
149.01358 (Kcal/Mol)
Zero-point correction= 0.237468 (Hartree/Particle)
Thermal correction to Energy= 0.247534
Thermal correction to Enthalpy= 0.248478
Thermal correction to Gibbs Free Energy= 0.203251
Sum of electronic and zero-point Energies= -428.346699
Sum of electronic and thermal Energies= -428.336634
Sum of electronic and thermal Enthalpies= -428.335690
Sum of electronic and thermal Free Energies= -428.380917

Table B9: Cartesian Coordinates of the optimized transition structure and energy values for **TS 399® 401** by B3LYP/6-31 (d)

C	1.304447	-0.330418	0.098660
C	0.169020	-0.425138	-0.995605
C	0.909856	1.196719	0.167708
C	0.451792	1.071718	-1.314453
C	-1.178226	-0.457923	-0.301299
C	-1.425443	0.421942	0.873356
C	-0.314465	1.470080	1.077461
C	2.705630	-0.528886	-0.503185
C	1.211252	-1.194827	1.360598
C	-2.354808	-1.355842	-0.353005
C	-2.273720	0.593765	-0.403624
H	0.263592	-1.172947	-1.791834
H	1.717206	1.903803	0.394521
H	1.264048	1.221115	-2.028566
H	-0.414386	1.664258	-1.625382
H	-1.860334	0.004377	1.784228
H	-0.009208	1.440819	2.130162
H	-0.681146	2.488047	0.886944
H	2.875486	0.055372	-1.411756
H	3.476857	-0.240887	0.222499
H	2.868554	-1.584870	-0.753774
H	1.404793	-2.247885	1.117133
H	1.971839	-0.887294	2.090058
H	0.236849	-1.141725	1.848839
H	-2.600976	-1.916482	0.555098
H	-2.519911	-1.887429	-1.291544
H	-3.225283	-0.465406	-0.366306

E(RB+HF-LYP) = -428.59236 (Hartree/Particle)
****** 1 imaginary frequencies (negative Signs) ******
Zero-point vibrational energy 624213.8 (Joules/Mol)
149.19069 (Kcal/Mol)
Zero-point correction= 0.237750 (Hartree/Particle)
Thermal correction to Energy= 0.247476
Thermal correction to Enthalpy= 0.248420
Thermal correction to Gibbs Free Energy= 0.204091
Sum of electronic and zero-point Energies= -428.354612
Sum of electronic and thermal Energies= -428.344886
Sum of electronic and thermal Enthalpies= -428.343942
Sum of electronic and thermal Free Energies= -428.388271

Table B10: Cartesian Coordinates of the optimized structure and energy values for compound **446a** by B3LYP/6-31 (d)

1	6	0	3.434356	-0.574257	-0.971280
2	6	0	3.756337	-0.201576	0.335987
3	6	0	2.161193	-0.311203	-1.492474
4	6	0	1.217959	0.321825	-0.688966
5	6	0	1.553199	0.711940	0.624394
6	6	0	2.815049	0.448221	1.144436
7	6	0	-0.198977	0.760477	-1.004595
8	6	0	0.332174	1.375532	1.254607
9	6	0	-1.322436	-0.193613	-0.538274
10	6	0	-0.292805	1.986960	-0.020678
11	1	0	4.179946	-1.064853	-1.591570
12	1	0	4.750394	-0.406014	0.725395
13	1	0	1.920745	-0.591936	-2.515695
14	1	0	3.074640	0.749226	2.156698
15	1	0	-0.331319	1.035996	-2.057439
16	1	0	0.564191	2.127308	2.014254
17	1	0	0.367432	2.787470	-0.391849
18	8	0	-1.577449	2.507424	0.225783
19	6	0	-2.061446	3.346276	-0.806389
20	1	0	-3.021746	3.743479	-0.468074
21	1	0	-1.373908	4.184901	-0.999217
22	1	0	-2.217621	2.801303	-1.749503
23	6	0	-1.217944	-0.517084	0.943457
24	6	0	-0.525936	0.233468	1.802081
25	6	0	-1.593667	-1.638538	-1.089839
26	6	0	-1.751004	-1.950730	1.034483
27	6	0	-0.540427	-2.778134	0.584373
28	6	0	-0.441232	-2.571498	-0.733179
29	8	0	-2.599102	-2.035313	-0.127682
30	1	0	-2.266140	0.344009	-0.694405
31	1	0	-0.392638	-0.050916	2.844413
32	1	0	-1.998237	-1.689584	-2.101669
33	1	0	-2.282702	-2.253047	1.936462
34	1	0	0.151117	-3.286987	1.245567
35	1	0	0.341903	-2.895632	-1.407044

SCF Done: E(RB+HF-LYP) = -807.786115178 A.U. after 1 cycles
Zero-point vibrational energy 763582.6 (Joules/Mol)
182.50063 (Kcal/Mol)
Zero-point correction= 0.290833 (Hartree/Particle)
Sum of electronic and zero-point Energies= -807.495282
Sum of electronic and thermal Energies= -807.481385
Sum of electronic and thermal Enthalpies= -807.480441
Sum of electronic and thermal Free Energies= -807.535567

Table B11: Cartesian Coordinates of the optimized structure and energy values for compound **446b** by B3LYP/6-31 (d)

1	6	0	3.787918	-1.183663	-0.906847
2	6	0	4.090208	-0.871679	0.420695
3	6	0	2.571042	-0.781773	-1.473152
4	6	0	1.670857	-0.066690	-0.690840
5	6	0	1.978149	0.252427	0.643818
6	6	0	3.185448	-0.145754	1.206117
7	6	0	0.271899	0.447060	-1.007716
8	6	0	0.837052	1.069577	1.231641
9	6	0	-0.724505	-0.646701	-0.507486
10	6	0	0.287026	1.707027	-0.084272
11	1	0	4.504169	-1.738816	-1.507024
12	1	0	5.039376	-1.187577	0.845794
13	1	0	2.341765	-1.023867	-2.508599
14	1	0	3.430191	0.105000	2.235589
15	1	0	0.116326	0.674869	-2.068036
16	1	0	1.172038	1.819937	1.953420
17	1	0	1.036512	2.410257	-0.485753
18	8	0	-0.922358	2.381396	0.143507
19	6	0	-1.439387	3.049764	-0.987617
20	1	0	-2.312434	3.612919	-0.648885
21	1	0	-0.705511	3.750544	-1.418828
22	1	0	-1.759749	2.350758	-1.773628
23	6	0	-1.053442	-0.487199	0.974897
24	6	0	-0.316760	0.250499	1.806175
25	6	0	-2.202906	-0.777777	-1.049155
26	6	0	-2.539277	-0.836397	1.073593
27	6	0	-2.776627	-2.264948	0.584419
28	6	0	-2.590229	-2.226720	-0.738396
29	8	0	-2.982584	-0.064076	-0.073471
30	1	0	-0.642326	0.452091	2.824361
31	1	0	-2.397326	-0.395533	-2.052467
32	1	0	-3.048425	-0.509455	1.980020
33	1	0	-2.958074	-3.124392	1.219219
34	1	0	-2.569781	-3.051186	-1.442374
35	1	0	-0.226007	-1.606443	-0.688339

SCF Done: E(RB+HF-LYP) = -807.777506054
Zero-point vibrational energy 763160.6 (Joules/Mol)
182.39976 (Kcal/Mol)
Zero-point correction= 0.290672 (Hartree/Particle)
Sum of electronic and zero-point Energies= -807.486834
Sum of electronic and thermal Energies= -807.472863
Sum of electronic and thermal Enthalpies= -807.471919
Sum of electronic and thermal Free Energies= -807.527217

Table B12: Cartesian Coordinates of the optimized structure and energy values for compound **446c** by B3LYP/6-31 (d)

1	6	0	3.925690	-0.852964	-0.940897
2	6	0	4.181952	-0.585068	0.405743
3	6	0	2.676665	-0.554672	-1.501233
4	6	0	1.697250	0.012525	-0.693637
5	6	0	1.957726	0.288037	0.661762
6	6	0	3.197082	-0.007455	1.217415
7	6	0	0.251755	0.389471	-1.001867
8	6	0	0.726885	0.939032	1.280652
9	6	0	-0.615365	-0.828437	-0.564467
10	6	0	0.132870	1.588182	-0.006466
11	1	0	4.702632	-1.292974	-1.560647
12	1	0	5.156576	-0.819405	0.825955
13	1	0	2.482898	-0.763358	-2.551011
14	1	0	3.404773	0.209464	2.262616
15	1	0	0.079630	0.662700	-2.048943
16	1	0	0.971779	1.680521	2.046649
17	1	0	0.818122	2.380286	-0.349392
18	8	0	-1.143412	2.137286	0.217117
19	6	0	-1.560800	3.033176	-0.792656
20	1	0	-2.529583	3.433487	-0.482284
21	1	0	-0.852032	3.868252	-0.912633
22	1	0	-1.680161	2.539181	-1.768961
23	6	0	-0.954213	-0.816181	0.916648
24	6	0	-0.311677	-0.053558	1.802614
25	6	0	-2.027677	-1.242079	-1.134797
26	6	0	-2.305110	-1.539715	0.978541
27	6	0	-3.292946	-0.434678	0.582832
28	6	0	-3.107282	-0.248894	-0.727624
29	1	0	-0.601980	-0.010484	2.850089
30	1	0	-2.024377	-1.601668	-2.164825
31	1	0	-2.529739	-2.148981	1.853977
32	1	0	-3.884201	0.152839	1.274965
33	1	0	-3.540843	0.509962	-1.367829
34	8	0	-2.281215	-2.336666	-0.222465
35	1	0	-0.013310	-1.725113	-0.760324

SCF Done: E(RB+HF-LYP) = -807.779517259 A.U. after 1 cycles
Zero-point vibrational energy 763286.5 (Joules/Mol)
182.42986 (Kcal/Mol)
Zero-point correction= 0.290720 (Hartree/Particle)
Sum of electronic and zero-point Energies= -807.488797
Sum of electronic and thermal Energies= -807.474880
Sum of electronic and thermal Enthalpies= -807.473936
Sum of electronic and thermal Free Energies= -807.528998

Table B13: Cartesian Coordinates of the optimized structure and energy values for compound **446d** by B3LYP/6-31 (d)

1	6	0	3.297674	-1.439338	-1.004391
2	6	0	3.743144	-1.119264	0.279796
3	6	0	2.108618	-0.891578	-1.502978
4	6	0	1.372650	-0.030028	-0.697866
5	6	0	1.828264	0.294080	0.596440
6	6	0	3.007590	-0.247203	1.093040
7	6	0	0.094056	0.728738	-0.993528
8	6	0	0.799566	1.218292	1.244852
9	6	0	-1.220498	0.064922	-0.512217
10	6	0	0.302364	1.948744	-0.022241
11	1	0	3.881467	-2.113941	-1.625131
12	1	0	4.671644	-1.546079	0.650305
13	1	0	1.773230	-1.136618	-2.508222
14	1	0	3.359781	0.002049	2.091348
15	1	0	0.011801	1.018967	-2.047803
16	1	0	1.203616	1.898235	2.000140
17	1	0	1.117515	2.579137	-0.412849
18	8	0	-0.827504	2.748116	0.244654
19	6	0	-1.134036	3.662767	-0.790527
20	1	0	-1.974224	4.268284	-0.441074
21	1	0	-0.281393	4.324941	-1.009156
22	1	0	-1.427140	3.156538	-1.722789
23	6	0	-1.138319	-0.293094	0.968285
24	6	0	-0.264199	0.273312	1.801038
25	6	0	-1.705886	-1.327905	-1.060220
26	6	0	-1.810520	-1.662452	1.063903
27	6	0	-3.261185	-1.561890	0.594756
28	6	0	-3.199123	-1.374913	-0.727223
29	1	0	-2.006007	0.810549	-0.680341
30	1	0	-0.125231	-0.096726	2.815657
31	1	0	-1.392526	-1.601378	-2.068529
32	1	0	-1.598418	-2.242847	1.961855
33	1	0	-4.130812	-1.548139	1.241413
34	1	0	-4.007444	-1.160604	-1.417501
35	8	0	-1.172098	-2.257052	-0.096259

SCF Done: E(RB+HF-LYP) = -807.783646183 A.U. after 1 cycles
Zero-point vibrational energy 763633.7 (Joules/Mol)
182.51283 (Kcal/Mol)
Zero-point correction= 0.290853 (Hartree/Particle)
Sum of electronic and zero-point Energies= -807.492794
Sum of electronic and thermal Energies= -807.478886
Sum of electronic and thermal Enthalpies= -807.477942
Sum of electronic and thermal Free Energies= -807.533134

Table B14: Cartesian Coordinates of the optimized structure and energy values for compound **310** by B3LYP/6-31 (d)

Center Number	Atomic Number	Atomic Type	Coordinates (Angstroms) X	Y	Z
1	6	0	-2.770218	-0.563269	-0.175309
2	6	0	-2.679581	0.829104	-0.263471
3	6	0	-1.634395	-1.335463	0.092937
4	6	0	-0.418131	-0.688179	0.291727
5	6	0	-0.321900	0.716585	0.196728
6	6	0	-1.452505	1.477710	-0.079769
7	6	0	0.983838	-1.247874	0.548637
8	6	0	1.097612	1.161038	0.473096
9	6	0	1.469310	-1.245182	-0.930269
10	6	0	2.130843	1.066693	-0.686108
11	6	0	1.583882	-0.065205	1.342707
12	1	0	-3.732361	-1.050106	-0.311383
13	1	0	-3.571277	1.413963	-0.472985
14	1	0	-1.707841	-2.418364	0.159139
15	1	0	-1.388576	2.560937	-0.149946
16	1	0	1.030345	-2.213752	1.058879
17	1	0	1.151921	2.128192	0.981417
18	1	0	0.969347	-1.919480	-1.622193
19	1	0	2.995576	1.726263	-0.652942
20	1	0	1.126774	-0.030158	2.338901
21	1	0	2.671443	-0.111692	1.451363
22	6	0	2.087020	-0.120259	-1.274281

SCF Done: E(RB+HF-LYP) = -463.174935441 A.U. after 1 cycles
Zero-point vibrational energy 475647.9 (Joules/Mol)
113.68258 (Kcal/Mol)
Zero-point correction= 0.181165 (Hartree/Particle)
Thermal correction to Energy= 0.189336
Thermal correction to Enthalpy= 0.190280
Thermal correction to Gibbs Free Energy= 0.148411
Sum of electronic and zero-point Energies= -462.993771
Sum of electronic and thermal Energies= -462.985599
Sum of electronic and thermal Enthalpies= -462.984655
Sum of electronic and thermal Free Energies= -463.026525

Table B15: Cartesian Coordinates of the optimized structure and energy values for compound **445** by B3LYP/6-31 (d)

Center Number	Atomic Number	Atomic Type	Coordinates (Angstroms) X	Y	Z
1	6	0	3.236838	-0.916854	-0.053866
2	6	0	3.316894	0.375520	-0.583141
3	6	0	2.002170	-1.460584	0.314162
4	6	0	0.853026	-0.693582	0.136706
5	6	0	0.931396	0.612874	-0.394009
6	6	0	2.163062	1.146591	-0.760301
7	6	0	-0.604746	-0.990850	0.478714
8	6	0	-0.449585	1.210026	-0.525383
9	6	0	-0.657179	-0.276791	1.856721
10	6	0	-1.109701	1.820839	0.735831
11	6	0	-1.264590	-0.143293	-0.654603
12	6	0	-1.013897	0.998371	1.768206
13	1	0	4.142273	-1.505517	0.068314
14	1	0	4.284750	0.783102	-0.862742
15	1	0	1.943023	-2.466546	0.722680
16	1	0	2.230360	2.148982	-1.176043
17	1	0	-0.885897	-2.047489	0.481792
18	1	0	-0.555635	1.864607	-1.395272
19	1	0	-0.064248	-0.706260	2.661633
20	1	0	-1.894925	2.558163	0.593298
21	1	0	-0.997673	-0.615645	-1.614885
22	8	0	-2.651881	0.063027	-0.598233
23	6	0	-3.416345	-1.080489	-0.926772
24	1	0	-4.463078	-0.766335	-0.940334
25	1	0	-3.148817	-1.476645	-1.919758
26	1	0	-3.299137	-1.885299	-0.186413

SCF Done: E(RB+HF-LYP) = -577.688733958 A.U. after 1 cycles
Zero-point vibrational energy 560772.6 (Joules/Mol)
134.02787 (Kcal/Mol)
Zero-point correction= 0.213587 (Hartree/Particle)
Thermal correction to Energy= 0.224537
Thermal correction to Enthalpy= 0.225481
Thermal correction to Gibbs Free Energy= 0.177155
Sum of electronic and zero-point Energies= -577.475147
Sum of electronic and thermal Energies= -577.464197
Sum of electronic and thermal Enthalpies= -577.463253
Sum of electronic and thermal Free Energies= -577.511579

Table B16: Cartesian Coordinates of the optimized structure and energy values for compound ***endo*-412** by B3LYP/6-31 (d)

Center Number	Atomic Number	Atomic Type	Coordinates (Angstroms) X	Y	Z
1	6	0	2.702627	-0.698094	0.202234
2	6	0	2.702627	0.698094	0.202234
3	6	0	1.519213	-1.416822	-0.024202
4	6	0	0.353643	-0.704770	-0.264509
5	6	0	0.353643	0.704770	-0.264509
6	6	0	1.519213	1.416822	-0.024202
7	6	0	-1.086143	-1.129841	-0.534651
8	6	0	-1.086143	1.129841	-0.534651
9	6	0	-1.964198	-0.756085	0.718207
10	6	0	-1.964198	0.756085	0.718207
11	6	0	-1.510085	0.000000	-1.508889
12	6	0	-1.336368	0.000000	1.850101
13	1	0	3.630867	-1.235247	0.378063
14	1	0	3.630867	1.235247	0.378063
15	1	0	1.524398	-2.503966	-0.016094
16	1	0	1.524398	2.503966	-0.016094
17	1	0	-1.232014	-2.163331	-0.853191
18	1	0	-1.232014	2.163331	-0.853190
19	1	0	-2.781541	-1.431422	0.971350
20	1	0	-2.781541	1.431422	0.971350
21	1	0	-0.925265	0.000000	-2.437742
22	1	0	-2.581146	0.000000	-1.734739

SCF Done: E(RB+HF-LYP) = -463.103156439 A.U. after 1 cycles
Zero-point vibrational energy 470223.8 (Joules/Mol)
112.38619 (Kcal/Mol)
Zero-point correction= 0.179099 (Hartree/Particle)
Thermal correction to Energy= 0.187561
Thermal correction to Enthalpy= 0.188506
Thermal correction to Gibbs Free Energy= 0.145720
Sum of electronic and zero-point Energies= -462.924058
Sum of electronic and thermal Energies= -462.915595
Sum of electronic and thermal Enthalpies= -462.914651
Sum of electronic and thermal Free Energies= -462.957437

Table B17: Cartesian Coordinates of the optimized structure and energy values for compound **449** by B3LYP/6-31 (d)

Center Number	Atomic Number	Atomic Type	Coordinates (Angstroms) X	Y	Z
1	6	0	-0.175788	2.998139	0.698141
2	6	0	-0.175788	2.998139	-0.698141
3	6	0	-0.177321	1.793369	1.416889
4	6	0	-0.192105	0.603252	0.704773
5	6	0	-0.192105	0.603252	-0.704773
6	6	0	-0.177321	1.793369	-1.416889
7	6	0	-0.191571	-0.859862	1.127727
8	6	0	-0.191571	-0.859862	-1.127727
9	6	0	-1.088426	-1.457065	0.000000
10	6	0	-1.294993	-2.966718	0.000000
11	1	0	-0.176156	3.942774	1.235400
12	1	0	-0.176156	3.942774	-1.235400
13	1	0	-0.171987	1.800031	2.504024
14	1	0	-0.171987	1.800031	-2.504024
15	1	0	-0.477082	-1.063630	2.161936
16	1	0	-0.477082	-1.063630	-2.161936
17	1	0	-2.065502	-0.952819	0.000000
18	1	0	-0.342824	-3.507107	0.000000
19	1	0	-1.862605	-3.279918	0.884283
20	1	0	-1.862605	-3.279918	-0.884283
21	6	0	1.206536	-1.480306	0.758292
22	6	0	1.206536	-1.480306	-0.758292
23	6	0	2.204622	-0.664180	0.000000
24	1	0	1.609877	-2.232952	1.436106
25	1	0	1.609877	-2.232952	-1.436106

SCF Done: E(RB+HF-LYP) = -502.418643012 A.U. after 22 cycl
Zero-point Vibrational energy 543464.7 (Joules/Mol)
129.89119 (Kcal/Mol)
Zero-point correction= 0.206995 (Hartree/Particle)
Thermal correction to Energy= 0.217028
Thermal correction to Enthalpy= 0.217972
Thermal correction to Gibbs Free Energy= 0.171939
Sum of electronic and zero-point Energies= -502.211648
Sum of electronic and thermal Energies= -502.201615
Sum of electronic and thermal Enthalpies= -502.200671
Sum of electronic and thermal Free Energies= -502.246704

Table B18: Cartesian Coordinates of the optimized transition structure and energy values for compound **TS6 (*endo*-412 ® 310)** by B3LYP/6-31 (d)

Center Number	Atomic Number	Atomic Type	Coordinates (Angstroms) X	Y	Z
1	6	0	-2.710727	0.698298	0.229527
2	6	0	-2.710727	-0.698298	0.229527
3	6	0	-1.530575	1.417361	-0.011926
4	6	0	-0.369543	0.703819	-0.269998
5	6	0	-0.369543	-0.703819	-0.269998
6	6	0	-1.530575	-1.417361	-0.011926
7	6	0	1.064115	1.124105	-0.550546
8	6	0	1.064115	-1.124105	-0.550546
9	6	0	1.952217	0.778530	0.704111
10	6	0	1.952217	-0.778530	0.704111
11	6	0	1.488340	0.000000	-1.529325
12	6	0	1.518253	0.000000	1.883050
13	1	0	-3.636892	1.235068	0.416989
14	1	0	-3.636892	-1.235068	0.416989
15	1	0	-1.535155	2.504486	-0.002046
16	1	0	-1.535155	-2.504486	-0.002046
17	1	0	1.209461	2.158610	-0.867140
18	1	0	1.209461	-2.158610	-0.867140
19	1	0	2.773519	1.473821	0.890208
20	1	0	2.773519	-1.473821	0.890208
21	1	0	0.911917	0.000000	-2.463368
22	1	0	2.560817	0.000000	-1.749041

SCF Done: E(RB+HF-LYP) = -463.103046701 A.U. after 21 cycle
****** 1 imaginary frequencies (negative Signs) ******
Zero-point vibrational energy 469768.1 (Joules/Mol)
112.27728 (Kcal/Mol)
Zero-point correction= 0.178925 (Hartree/Particle)
Thermal correction to Energy= 0.186739
Thermal correction to Enthalpy= 0.187683
Thermal correction to Gibbs Free Energy= 0.146295
Sum of electronic and zero-point Energies= -462.924121
Sum of electronic and thermal Energies= -462.916308
Sum of electronic and thermal Enthalpies= -462.915364
Sum of electronic and thermal Free Energies= -462.956752

Table B19: Cartesian Coordinates of the optimized transition structure and energy values for compound **TS8 (449® 450)** by B3LYP/6-31 (d)

Center Number	Atomic Number	Atomic Type	Coordinates (Angstroms) X	Y	Z
1	6	0	3.001655	0.698234	-0.173328
2	6	0	3.001624	-0.698230	-0.173646
3	6	0	1.797109	1.416790	-0.176184
4	6	0	0.606580	0.704919	-0.191834
5	6	0	0.606547	-0.704802	-0.192170
6	6	0	1.797046	-1.416732	-0.176832
7	6	0	-0.856516	1.127979	-0.195543
8	6	0	-0.856569	-1.127802	-0.196132
9	6	0	-1.457139	0.000319	-1.088546
10	6	0	-2.985235	0.000313	-1.269049
11	1	0	3.946470	1.235304	-0.172511
12	1	0	3.946415	-1.235342	-0.173070
13	1	0	1.803652	2.503960	-0.171053
14	1	0	1.803544	-2.503905	-0.172188
15	1	0	-1.060628	2.161377	-0.483833
16	1	0	-1.060774	-2.161051	-0.484887
17	1	0	-0.953823	0.000580	-2.065382
18	1	0	-3.451861	0.880824	-0.814361
19	1	0	-3.252162	0.001188	-2.330851
20	1	0	-3.451629	-0.881097	-0.815877
21	6	0	-1.486871	0.754293	1.197738
22	6	0	-1.487155	-0.754764	1.197376
23	6	0	-0.645821	-0.000749	2.183138
24	1	0	-2.239994	1.427052	1.607630
25	1	0	-2.240738	-1.427500	1.606454

SCF Done: E(RB+HF-LYP) = -502.414459117 A.U. after 1 cycles
****** 1 imaginary frequencies (negative Signs) ******
Zero-point vibrational energy 542592.1 (Joules/Mol)
129.68261 (Kcal/Mol)
Zero-point correction= 0.206662 (Hartree/Particle)
Thermal correction to Energy= 0.216097
Thermal correction to Enthalpy= 0.217041
Thermal correction to Gibbs Free Energy= 0.172179
Sum of electronic and zero-point Energies= -502.207797
Sum of electronic and thermal Energies= -502.198362
Sum of electronic and thermal Enthalpies= -502.197418
Sum of electronic and thermal Free Energies= -502.242280

APPENDIX C

X-RAY DATA OF COMPOUND 403

```
data_cad4

_audit_creation_method           SHELXL-97
_chemical_name_systematic
;
 ?
;
_chemical_name_common            ?
_chemical_melting_point          ?
_chemical_formula_moiety         'C22 H32'
_chemical_formula_sum
 'C22 H32'
_chemical_formula_weight         296.48

loop_
 _atom_type_symbol
 _atom_type_description
 _atom_type_scat_dispersion_real
 _atom_type_scat_dispersion_imag
 _atom_type_scat_source
 'C'  'C'   0.0033   0.0016
 'International Tables Vol C Tables 4.2.6.8 and 6.1.1.4'
 'H'  'H'   0.0000   0.0000
 'International Tables Vol C Tables 4.2.6.8 and 6.1.1.4'

_symmetry_cell_setting           monoclinic
_symmetry_space_group_name_H-M    'P 21/c'
_symmetry_space_group_name_Hall   '-P 2ybc'

loop_
 _symmetry_equiv_pos_as_xyz
 'x, y, z'
 '-x, y+1/2, -z+1/2'
 '-x, -y, -z'
 'x, -y-1/2, z-1/2'

_cell_length_a                   14.5155(10)
_cell_length_b                   6.3411(10)
_cell_length_c                   20.7470(10)
_cell_angle_alpha                 90.00
```

```
_cell_angle_beta                108.151(10)
_cell_angle_gamma               90.00
_cell_volume                    1814.6(3)
_cell_formula_units_Z           4
_cell_measurement_temperature   293(2)
_cell_measurement_reflns_used   25
_cell_measurement_theta_min     10
_cell_measurement_theta_max     18

_exptl_crystal_description      'prism'
_exptl_crystal_colour           'colourless'
_exptl_crystal_size_max         0.30
_exptl_crystal_size_mid         0.20
_exptl_crystal_size_min         0.10
_exptl_crystal_density_meas     ?
_exptl_crystal_density_diffrn   1.085
_exptl_crystal_density_method   'not measured'
_exptl_crystal_F_000            656
_exptl_absorpt_coefficient_mu   0.060
_exptl_absorpt_correction_type  none
_exptl_absorpt_correction_T_min ?
_exptl_absorpt_correction_T_max ?
_exptl_absorpt_process_details  ?

_exptl_special_details
;
 ?
;

_diffrn_ambient_temperature     293(2)
_diffrn_radiation_wavelength    0.71073
_diffrn_radiation_type          MoK\a
_diffrn_radiation_source        'fine-focus sealed tube'
_diffrn_radiation_monochromator graphite
_diffrn_measurement_device_type 'Enraf Nonius CAD4'
_diffrn_measurement_method      'non-profiled omega scans'
_diffrn_detector_area_resol_mean ?
_diffrn_standards_number        3
_diffrn_standards_interval_count ?
_diffrn_standards_interval_time 120
_diffrn_standards_decay_%       1
_diffrn_reflns_number           3565
_diffrn_reflns_av_R_equivalents 0.0150
_diffrn_reflns_av_sigmaI/netI   0.0587
_diffrn_reflns_limit_h_min      -17
_diffrn_reflns_limit_h_max      17
_diffrn_reflns_limit_k_min      -7
_diffrn_reflns_limit_k_max      7
_diffrn_reflns_limit_l_min      -25
_diffrn_reflns_limit_l_max      25
```

```
_diffrn_reflns_theta_min         2.89
_diffrn_reflns_theta_max         26.00
_reflns_number_total             3545
_reflns_number_gt                1461
_reflns_threshold_expression     I>2\s(I)

_computing_data_collection       'CAD4 Express (Enraf Nonius, 1994)'
_computing_cell_refinement       'CAD4 Express (Enraf Nonius, 1994)'
_computing_data_reduction        'XCAD4 (Harms & Wocadlo, 1995)'
_computing_structure_solution    'SHELXS-97 (Sheldrick, 1997)'
_computing_structure_refinement  'SHELXL-97 (Sheldrick, 1997)'
_computing_molecular_graphics    'Ortep-3 for windows (Farrugia, 1997)'
_computing_publication_material  'WinGX publication routines (Farrugia, 1999)'

_refine_special_details
;
 Refinement of F^2^ against ALL reflections.  The weighted R-factor wR and
 goodness of fit S are based on F^2^, conventional R-factors R are based
 on F, with F set to zero for negative F^2^. The threshold expression of
 F^2^ > 2sigma(F^2^) is used only for calculating R-factors(gt) etc. and is
 not relevant to the choice of reflections for refinement.  R-factors based
 on F^2^ are statistically about twice as large as those based on F, and R-
 factors based on ALL data will be even larger.
;

_refine_ls_structure_factor_coef  Fsqd
_refine_ls_matrix_type           full
_refine_ls_weighting_scheme      calc
_refine_ls_weighting_details
 'calc w=1/[\s^2^(Fo^2^)+(0.0688P)^2^+0.0733P] where P=(Fo^2^+2Fc^2^)/3'
_atom_sites_solution_primary     direct
_atom_sites_solution_secondary   difmap
_atom_sites_solution_hydrogens   geom
_refine_ls_hydrogen_treatment    mixed
_refine_ls_extinction_method     none
_refine_ls_extinction_coef       ?
_refine_ls_number_reflns         2815
_refine_ls_number_parameters     315
_refine_ls_number_restraints     0
_refine_ls_R_factor_all          0.1075
_refine_ls_R_factor_gt           0.0447
_refine_ls_wR_factor_ref         0.1300
_refine_ls_wR_factor_gt          0.1057
_refine_ls_goodness_of_fit_ref   1.013
_refine_ls_restrained_S_all      1.013
_refine_ls_shift/su_max          0.000
_refine_ls_shift/su_mean         0.000

loop_
 _atom_site_label
```

_atom_site_type_symbol
_atom_site_fract_x
_atom_site_fract_y
_atom_site_fract_z
_atom_site_U_iso_or_equiv
_atom_site_adp_type
_atom_site_occupancy
_atom_site_symmetry_multiplicity
_atom_site_calc_flag
_atom_site_refinement_flags
_atom_site_disorder_assembly
_atom_site_disorder_group
C4 C 0.2875(2) 0.8973(5) 0.3057(2) 0.0658(9) Uani 1 1 d . . .
C16 C 0.2567(2) 0.1281(5) 0.0487(2) 0.0675(9) Uani 1 1 d . . .
C8 C 0.4147(3) 0.4200(5) 0.36173(19) 0.0643(9) Uani 1 1 d . . .
C19 C 0.1216(3) 0.5966(5) -0.00625(19) 0.0628(9) Uani 1 1 d . . .
C20 C 0.1294(2) 0.2934(6) -0.07889(14) 0.0843(11) Uani 1 1 d . . .
H20A H 0.1564 0.1557 -0.0802 0.126 Uiso 1 1 calc R . .
H20B H 0.1494 0.3863 -0.1086 0.126 Uiso 1 1 calc R . .
H20C H 0.0600 0.2842 -0.0934 0.126 Uiso 1 1 calc R . .
C10 C 0.0981(2) 0.5331(8) 0.2582(2) 0.0692(10) Uani 1 1 d . . .
C7 C 0.4067(3) 0.7238(7) 0.43360(17) 0.0734(10) Uani 1 1 d . . .
C14 C 0.0943(2) 0.1249(6) 0.14438(18) 0.0613(9) Uani 1 1 d . . .
H21 H 0.4703(18) 0.704(4) 0.2515(12) 0.062(8) Uiso 1 1 d . . .
H191 H 0.128(2) 0.655(5) 0.0394(16) 0.083(11) Uiso 1 1 d . . .
H141 H 0.1076(18) 0.152(4) 0.1966(15) 0.072(9) Uiso 1 1 d . . .
H71 H 0.380(2) 0.871(6) 0.4344(16) 0.100(12) Uiso 1 1 d . . .
H161 H 0.301(2) 0.094(4) 0.0967(15) 0.077(10) Uiso 1 1 d . . .
H143 H 0.111(2) -0.024(6) 0.1376(16) 0.098(12) Uiso 1 1 d . . .
H41 H 0.249(2) 0.940(4) 0.2599(15) 0.074(10) Uiso 1 1 d . . .
H11 H 0.3789(16) 0.424(4) 0.2173(11) 0.045(7) Uiso 1 1 d . . .
H31 H 0.4457(17) 0.912(4) 0.3344(11) 0.051(7) Uiso 1 1 d . . .
H22 H 0.383(2) 0.870(5) 0.2121(16) 0.106(12) Uiso 1 1 d . . .
H101 H 0.063(2) 0.499(5) 0.2091(16) 0.078(10) Uiso 1 1 d . . .
H51 H 0.2244(16) 0.684(4) 0.3616(12) 0.059(8) Uiso 1 1 d . . .
H151 H 0.1021(17) 0.112(4) 0.0243(12) 0.051(7) Uiso 1 1 d . . .
H211 H 0.396(2) 0.419(4) 0.1042(13) 0.070(9) Uiso 1 1 d . . .
H102 H 0.077(3) 0.664(6) 0.2700(18) 0.119(15) Uiso 1 1 d . . .
H171 H 0.3136(18) 0.341(4) -0.0126(13) 0.069(8) Uiso 1 1 d . . .
H221 H 0.2586(14) 0.705(4) 0.1219(10) 0.037(6) Uiso 1 1 d . . .
H142 H 0.023(2) 0.139(4) 0.1217(13) 0.071(9) Uiso 1 1 d . . .
H81 H 0.388(2) 0.350(5) 0.3203(16) 0.076(10) Uiso 1 1 d . . .
H73 H 0.380(2) 0.636(5) 0.4637(15) 0.090(11) Uiso 1 1 d . . .
H82 H 0.489(3) 0.430(6) 0.3766(18) 0.136(15) Uiso 1 1 d . . .
H192 H 0.048(3) 0.593(5) -0.0345(16) 0.104(11) Uiso 1 1 d . . .
H193 H 0.153(2) 0.695(6) -0.0297(16) 0.106(12) Uiso 1 1 d . . .
H72 H 0.482(2) 0.720(5) 0.4534(13) 0.089(10) Uiso 1 1 d . . .
H42 H 0.2912(19) 1.013(5) 0.3421(14) 0.078(9) Uiso 1 1 d . . .
H83 H 0.401(2) 0.336(5) 0.3980(17) 0.098(12) Uiso 1 1 d . . .
H103 H 0.086(2) 0.430(5) 0.2888(16) 0.096(12) Uiso 1 1 d . . .

H212 H 0.354(2) 0.617(5) 0.0601(14) 0.081(10) Uiso 1 1 d . . .
H162 H 0.255(2) 0.022(5) 0.0119(16) 0.096(11) Uiso 1 1 d . . .
C11 C 0.24336(17) 0.4985(4) 0.21960(12) 0.0425(7) Uani 1 1 d . . .
C12 C 0.20682(17) 0.4252(4) 0.14812(12) 0.0426(7) Uani 1 1 d . . .
C1 C 0.34016(18) 0.5531(4) 0.20956(12) 0.0439(7) Uani 1 1 d . . .
C6 C 0.37286(18) 0.6405(4) 0.36105(13) 0.0488(7) Uani 1 1 d . . .
C22 C 0.28496(17) 0.5584(4) 0.13226(13) 0.0442(7) Uani 1 1 d . . .
C9 C 0.20496(17) 0.5528(4) 0.26748(12) 0.0456(7) Uani 1 1 d . . .
C18 C 0.16551(19) 0.3795(4) -0.00618(13) 0.0521(7) Uani 1 1 d . . .
C3 C 0.3889(2) 0.8139(4) 0.31207(14) 0.0513(8) Uani 1 1 d . . .
C15 C 0.1535(2) 0.2065(4) 0.04432(14) 0.0527(8) Uani 1 1 d . . .
C2 C 0.4011(2) 0.7424(5) 0.24499(14) 0.0579(8) Uani 1 1 d . . .
C13 C 0.15074(17) 0.2700(4) 0.11319(13) 0.0455(7) Uani 1 1 d . . .
C21 C 0.3341(2) 0.4930(6) 0.08029(15) 0.0558(8) Uani 1 1 d . . .
C17 C 0.2770(2) 0.3468(5) 0.02327(15) 0.0554(8) Uani 1 1 d . . .
C5 C 0.2617(2) 0.6779(5) 0.32875(15) 0.0549(8) Uani 1 1 d . . .

loop_
 _atom_site_aniso_label
 _atom_site_aniso_U_11
 _atom_site_aniso_U_22
 _atom_site_aniso_U_33
 _atom_site_aniso_U_23
 _atom_site_aniso_U_13
 _atom_site_aniso_U_12
C4 0.069(2) 0.043(2) 0.079(2) -0.0050(18) 0.0138(19) 0.0062(16)
C16 0.083(2) 0.046(2) 0.075(2) -0.0038(19) 0.028(2) 0.0015(17)
C8 0.074(2) 0.054(2) 0.058(2) 0.0084(19) 0.0107(19) 0.0067(18)
C19 0.067(2) 0.050(2) 0.064(2) 0.0139(19) 0.0094(19) -0.0030(17)
C20 0.101(3) 0.090(3) 0.057(2) -0.0101(18) 0.0180(18) -0.033(2)
C10 0.052(2) 0.092(3) 0.068(2) 0.001(2) 0.0254(18) -0.002(2)
C7 0.081(3) 0.083(3) 0.054(2) -0.008(2) 0.0181(19) -0.009(2)
C14 0.054(2) 0.056(2) 0.069(2) 0.0166(18) 0.0128(17) -0.0101(17)
C11 0.0420(15) 0.0399(15) 0.0460(16) 0.0066(12) 0.0143(12) -0.0036(12)
C12 0.0364(14) 0.0426(16) 0.0486(16) 0.0075(13) 0.0130(12) -0.0018(13)
C1 0.0412(15) 0.0431(18) 0.0479(17) 0.0000(14) 0.0146(13) -0.0057(14)
C6 0.0524(16) 0.0464(17) 0.0464(16) -0.0026(13) 0.0137(13) -0.0010(13)
C22 0.0432(15) 0.0414(17) 0.0481(16) 0.0015(14) 0.0145(13) -0.0062(13)
C9 0.0402(15) 0.0477(17) 0.0500(16) 0.0086(14) 0.0158(13) 0.0011(13)
C18 0.0608(18) 0.0471(18) 0.0462(16) -0.0003(14) 0.0135(14) -0.0097(14)
C3 0.0527(18) 0.0466(17) 0.0511(17) -0.0017(15) 0.0109(14) -0.0104(15)
C15 0.0576(19) 0.0403(17) 0.0583(19) -0.0023(15) 0.0152(15) -0.0123(15)
C2 0.054(2) 0.065(2) 0.0524(19) -0.0012(17) 0.0134(15) -0.0191(17)
C13 0.0417(15) 0.0400(16) 0.0533(17) 0.0111(14) 0.0125(13) -0.0049(13)
C21 0.0495(18) 0.066(2) 0.0539(19) -0.0005(17) 0.0193(15) -0.0090(17)
C17 0.0644(19) 0.0516(18) 0.0561(18) -0.0059(15) 0.0273(16) -0.0063(15)
C5 0.0544(18) 0.0553(19) 0.0592(19) -0.0056(15) 0.0240(15) -0.0001(15)

_geom_special_details
;

All esds (except the esd in the dihedral angle between two l.s. planes)
are estimated using the full covariance matrix. The cell esds are taken
into account individually in the estimation of esds in distances, angles
and torsion angles; correlations between esds in cell parameters are only
used when they are defined by crystal symmetry. An approximate (isotropic)
treatment of cell esds is used for estimating esds involving l.s. planes.
;

loop_
_geom_bond_atom_site_label_1
_geom_bond_atom_site_label_2
_geom_bond_distance
_geom_bond_site_symmetry_2
_geom_bond_publ_flag
C4 C3 1.531(4) . ?
C4 C5 1.554(4) . ?
C4 H41 0.98(3) . ?
C4 H42 1.04(3) . ?
C16 C17 1.544(4) . ?
C16 C15 1.554(4) . ?
C16 H161 1.02(3) . ?
C16 H162 1.01(3) . ?
C8 C6 1.522(4) . ?
C8 H81 0.94(3) . ?
C8 H82 1.02(4) . ?
C8 H83 0.99(3) . ?
C19 C18 1.517(4) . ?
C19 H191 1.00(3) . ?
C19 H192 1.04(3) . ?
C19 H193 0.98(4) . ?
C20 C18 1.535(4) . ?
C20 H20A 0.9600 . ?
C20 H20B 0.9600 . ?
C20 H20C 0.9600 . ?
C10 C9 1.507(4) . ?
C10 H101 1.01(3) . ?
C10 H102 0.95(4) . ?
C10 H103 0.97(3) . ?
C7 C6 1.525(4) . ?
C7 H71 1.01(3) . ?
C7 H73 1.00(3) . ?
C7 H72 1.04(3) . ?
C14 C13 1.505(4) . ?
C14 H141 1.05(3) . ?
C14 H143 0.99(4) . ?
C14 H142 1.00(3) . ?
C11 C9 1.327(3) . ?
C11 C12 1.486(3) . ?
C11 C1 1.523(3) . ?
C12 C13 1.338(3) . ?

C12 C22 1.530(3) . ?
C1 C2 1.536(4) . ?
C1 C22 1.554(3) . ?
C1 H11 0.98(2) . ?
C6 C5 1.560(4) . ?
C6 C3 1.563(4) . ?
C22 C21 1.524(4) . ?
C22 H221 1.00(2) . ?
C9 C5 1.507(4) . ?
C18 C17 1.555(4) . ?
C18 C15 1.564(4) . ?
C3 C2 1.525(4) . ?
C3 H31 1.02(2) . ?
C15 C13 1.497(4) . ?
C15 H151 0.95(2) . ?
C2 H21 1.00(2) . ?
C2 H22 1.04(3) . ?
C21 C17 1.528(4) . ?
C21 H211 1.00(3) . ?
C21 H212 0.98(3) . ?
C17 H171 1.04(3) . ?
C5 H51 0.99(2) . ?

loop_
 _geom_angle_atom_site_label_1
 _geom_angle_atom_site_label_2
 _geom_angle_atom_site_label_3
 _geom_angle
 _geom_angle_site_symmetry_1
 _geom_angle_site_symmetry_3
 _geom_angle_publ_flag
C3 C4 C5 88.9(2) . . ?
C3 C4 H41 115.2(17) . . ?
C5 C4 H41 115.0(17) . . ?
C3 C4 H42 110.5(15) . . ?
C5 C4 H42 111.7(15) . . ?
H41 C4 H42 113(2) . . ?
C17 C16 C15 88.6(2) . . ?
C17 C16 H161 113.1(16) . . ?
C15 C16 H161 114.9(16) . . ?
C17 C16 H162 107.7(18) . . ?
C15 C16 H162 111.4(16) . . ?
H161 C16 H162 117(2) . . ?
C6 C8 H81 112.1(18) . . ?
C6 C8 H82 109(2) . . ?
H81 C8 H82 114(3) . . ?
C6 C8 H83 109.2(19) . . ?
H81 C8 H83 108(3) . . ?
H82 C8 H83 104(3) . . ?
C18 C19 H191 115.2(17) . . ?

C18 C19 H192 109.5(18) . . ?
H191 C19 H192 109(2) . . ?
C18 C19 H193 108(2) . . ?
H191 C19 H193 108(3) . . ?
H192 C19 H193 106(3) . . ?
C18 C20 H20A 109.5 . . ?
C18 C20 H20B 109.5 . . ?
H20A C20 H20B 109.5 . . ?
C18 C20 H20C 109.5 . . ?
H20A C20 H20C 109.5 . . ?
H20B C20 H20C 109.5 . . ?
C9 C10 H101 109.0(16) . . ?
C9 C10 H102 108(2) . . ?
H101 C10 H102 110(3) . . ?
C9 C10 H103 111.4(19) . . ?
H101 C10 H103 112(3) . . ?
H102 C10 H103 106(3) . . ?
C6 C7 H71 109.1(19) . . ?
C6 C7 H73 110.9(18) . . ?
H71 C7 H73 106(3) . . ?
C6 C7 H72 110.9(16) . . ?
H71 C7 H72 112(3) . . ?
H73 C7 H72 107(2) . . ?
C13 C14 H141 113.0(15) . . ?
C13 C14 H143 109.1(19) . . ?
H141 C14 H143 109(2) . . ?
C13 C14 H142 111.4(16) . . ?
H141 C14 H142 108(2) . . ?
H143 C14 H142 106(2) . . ?
C9 C11 C12 136.5(2) . . ?
C9 C11 C1 131.6(2) . . ?
C12 C11 C1 89.56(19) . . ?
C13 C12 C11 137.6(2) . . ?
C13 C12 C22 131.0(2) . . ?
C11 C12 C22 89.07(18) . . ?
C11 C1 C2 122.0(2) . . ?
C11 C1 C22 86.85(17) . . ?
C2 C1 C22 120.8(2) . . ?
C11 C1 H11 107.3(13) . . ?
C2 C1 H11 111.0(13) . . ?
C22 C1 H11 105.8(13) . . ?
C8 C6 C7 107.7(3) . . ?
C8 C6 C5 120.0(2) . . ?
C7 C6 C5 110.1(3) . . ?
C8 C6 C3 120.8(2) . . ?
C7 C6 C3 109.3(3) . . ?
C5 C6 C3 87.6(2) . . ?
C21 C22 C12 122.9(2) . . ?
C21 C22 C1 121.3(2) . . ?
C12 C22 C1 86.83(18) . . ?

C21 C22 H221 109.4(12) . . ?
C12 C22 H221 107.4(12) . . ?
C1 C22 H221 106.3(12) . . ?
C11 C9 C10 122.5(3) . . ?
C11 C9 C5 121.4(2) . . ?
C10 C9 C5 115.0(3) . . ?
C19 C18 C20 107.9(3) . . ?
C19 C18 C17 120.5(2) . . ?
C20 C18 C17 109.5(2) . . ?
C19 C18 C15 120.2(2) . . ?
C20 C18 C15 109.5(2) . . ?
C17 C18 C15 87.9(2) . . ?
C2 C3 C4 113.9(3) . . ?
C2 C3 C6 117.8(2) . . ?
C4 C3 C6 88.0(2) . . ?
C2 C3 H31 106.8(13) . . ?
C4 C3 H31 116.7(13) . . ?
C6 C3 H31 113.2(13) . . ?
C13 C15 C16 110.0(2) . . ?
C13 C15 C18 119.5(2) . . ?
C16 C15 C18 87.5(2) . . ?
C13 C15 H151 109.7(15) . . ?
C16 C15 H151 115.9(14) . . ?
C18 C15 H151 112.8(14) . . ?
C3 C2 C1 117.1(2) . . ?
C3 C2 H21 110.2(15) . . ?
C1 C2 H21 106.2(15) . . ?
C3 C2 H22 106.9(18) . . ?
C1 C2 H22 107.7(17) . . ?
H21 C2 H22 109(2) . . ?
C12 C13 C15 121.5(2) . . ?
C12 C13 C14 122.5(3) . . ?
C15 C13 C14 115.2(2) . . ?
C22 C21 C17 116.9(2) . . ?
C22 C21 H211 109.0(15) . . ?
C17 C21 H211 106.8(15) . . ?
C22 C21 H212 110.2(18) . . ?
C17 C21 H212 108.5(17) . . ?
H211 C21 H212 105(2) . . ?
C21 C17 C16 113.3(3) . . ?
C21 C17 C18 118.1(2) . . ?
C16 C17 C18 88.2(2) . . ?
C21 C17 H171 107.5(14) . . ?
C16 C17 H171 113.8(15) . . ?
C18 C17 H171 115.1(14) . . ?
C9 C5 C4 109.4(2) . . ?
C9 C5 C6 120.2(2) . . ?
C4 C5 C6 87.3(2) . . ?
C9 C5 H51 109.1(14) . . ?
C4 C5 H51 114.3(15) . . ?

C6 C5 H51 115.0(14) . . ?

loop_
 _geom_torsion_atom_site_label_1
 _geom_torsion_atom_site_label_2
 _geom_torsion_atom_site_label_3
 _geom_torsion_atom_site_label_4
 _geom_torsion
 _geom_torsion_site_symmetry_1
 _geom_torsion_site_symmetry_2
 _geom_torsion_site_symmetry_3
 _geom_torsion_site_symmetry_4
 _geom_torsion_publ_flag
C9 C11 C12 C13 -54.8(5) . . . . ?
C1 C11 C12 C13 142.0(3) . . . . ?
C9 C11 C12 C22 142.0(3) . . . . ?
C1 C11 C12 C22 -21.18(19) . . . . ?
C9 C11 C1 C2 -18.9(4) . . . . ?
C12 C11 C1 C2 145.7(3) . . . . ?
C9 C11 C1 C22 -143.7(3) . . . . ?
C12 C11 C1 C22 20.86(19) . . . . ?
C13 C12 C22 C21 -18.4(4) . . . . ?
C11 C12 C22 C21 146.5(3) . . . . ?
C13 C12 C22 C1 -144.2(3) . . . . ?
C11 C12 C22 C1 20.77(19) . . . . ?
C11 C1 C22 C21 -147.4(3) . . . . ?
C2 C1 C22 C21 86.7(4) . . . . ?
C11 C1 C22 C12 -20.27(19) . . . . ?
C2 C1 C22 C12 -146.1(3) . . . . ?
C12 C11 C9 C10 5.0(5) . . . . ?
C1 C11 C9 C10 162.3(3) . . . . ?
C12 C11 C9 C5 -162.5(3) . . . . ?
C1 C11 C9 C5 -5.2(4) . . . . ?
C5 C4 C3 C2 98.2(3) . . . . ?
C5 C4 C3 C6 -21.6(2) . . . . ?
C8 C6 C3 C2 29.2(4) . . . . ?
C7 C6 C3 C2 154.9(3) . . . . ?
C5 C6 C3 C2 -94.6(3) . . . . ?
C8 C6 C3 C4 145.3(3) . . . . ?
C7 C6 C3 C4 -89.0(3) . . . . ?
C5 C6 C3 C4 21.5(2) . . . . ?
C17 C16 C15 C13 -99.7(2) . . . . ?
C17 C16 C15 C18 20.9(2) . . . . ?
C19 C18 C15 C13 -33.5(4) . . . . ?
C20 C18 C15 C13 -159.2(2) . . . . ?
C17 C18 C15 C13 90.9(3) . . . . ?
C19 C18 C15 C16 -145.2(3) . . . . ?
C20 C18 C15 C16 89.1(3) . . . . ?
C17 C18 C15 C16 -20.8(2) . . . . ?
C4 C3 C2 C1 -64.4(4) . . . . ?

C6 C3 C2 C1 36.6(4) . . . . ?
C11 C1 C2 C3 26.8(4) . . . . ?
C22 C1 C2 C3 134.2(3) . . . . ?
C11 C12 C13 C15 -161.1(3) . . . . ?
C22 C12 C13 C15 -3.8(4) . . . . ?
C11 C12 C13 C14 8.2(5) . . . . ?
C22 C12 C13 C14 165.6(3) . . . . ?
C16 C15 C13 C12 61.0(3) . . . . ?
C18 C15 C13 C12 -37.8(4) . . . . ?
C16 C15 C13 C14 -109.0(3) . . . . ?
C18 C15 C13 C14 152.1(3) . . . . ?
C12 C22 C21 C17 25.8(4) . . . . ?
C1 C22 C21 C17 134.3(3) . . . . ?
C22 C21 C17 C16 -64.1(4) . . . . ?
C22 C21 C17 C18 36.8(4) . . . . ?
C15 C16 C17 C21 98.9(3) . . . . ?
C15 C16 C17 C18 -21.0(2) . . . . ?
C19 C18 C17 C21 29.5(4) . . . . ?
C20 C18 C17 C21 155.4(3) . . . . ?
C15 C18 C17 C21 -94.6(3) . . . . ?
C19 C18 C17 C16 145.1(3) . . . . ?
C20 C18 C17 C16 -89.0(3) . . . . ?
C15 C18 C17 C16 20.9(2) . . . . ?
C11 C9 C5 C4 62.7(3) . . . . ?
C10 C9 C5 C4 -105.7(3) . . . . ?
C11 C9 C5 C6 -35.7(4) . . . . ?
C10 C9 C5 C6 155.9(3) . . . . ?
C3 C4 C5 C9 -99.5(3) . . . . ?
C3 C4 C5 C6 21.6(2) . . . . ?
C8 C6 C5 C9 -34.8(4) . . . . ?
C7 C6 C5 C9 -160.6(3) . . . . ?
C3 C6 C5 C9 89.8(3) . . . . ?
C8 C6 C5 C4 -145.7(3) . . . . ?
C7 C6 C5 C4 88.5(3) . . . . ?
C3 C6 C5 C4 -21.2(2) . . . . ?

_diffrn_measured_fraction_theta_max 1.000
_diffrn_reflns_theta_full 26.00
_diffrn_measured_fraction_theta_full 1.000
_refine_diff_density_max 0.135
_refine_diff_density_min -0.195
_refine_diff_density_rms 0.037

VITA

Akýn Azizoðlu was born in Balýkesir on June 25, 1975. He was graduated in 1992 from High School of Balýkesir Lisesi. He received his B.S. degrees (Double-Major Program) in Faculty of Education, Department of Chemistry Education and in Faculty of Arts and Sciences, Department of Chemistry from Middle East Technical University in June 1997. He became a research assistant at Chemistry Department of Balýkesir University in 1997. Then, he began his M.S. study under the supervision of Prof. Dr. Okan Tarhan and Prof. Dr. Lemi Türker at Middle East Technical University, Chemistry Department. After receiving his M.S. degree in 1999, he began his Ph.D. study under the supervision of Prof. Dr. Metin Balcý. He has four international publications, one of which relates with his Ph.D. study. He had three oral presentations in National Congresses.